Investigating and exploiting fungal natural products in *Aspergillus spp*.

Lara Manzanares Miralles BSc

Thesis submitted to

Maynooth University

for the degree of

Doctor of Philosophy

October 2015

Supervisor:

Prof. Sean Doyle,

Department of Biology,

University of Maynooth,

Co. Kildare.

Head of Department:

Prof. Paul Moynagh

Table of Contents

Declaration of authorship

This thesis has not previously been submitted in whole or in part to this or any other University for any other degree. This thesis is the sole work of the author, with the exception of the generation of Section 5.2.5.1.

_____

Lara Manzanares Miralles, BSc

Acknowledgments

First I would like to thank my supervisor Professor Sean Doyle for all these years of mentoring, support and encouragement. Thanks for the opportunities I have had in the lab, for saying I am getting Irish accent and for making the experience an amazing journey. Thanks to the John and Pat Hume Scholarship for funding my PhD and to the HEA and SFI for LC-MS (12/RI/2346) and qRT-PCR (SFI/07/RFP/GEN/F571/ECO7) facilities necessary for the completion of this project. Aspergillus research in the Doyle laboratory was funded by SFI (P1/11/1188) and IvP/12/1695. I would also like to thanks Dr Gary W. Jones, Dr Özgür Bayram and Dr Özlem Sarikaya-Bayram for all the advice received through this PhD and especially for their support during the writing process. My sincere thanks to Caroline Batchelor for all the assistance received on LC-MS, which was a lot!

Special thanks to Grainne, Rebecca and Cindy for answering all my annoying questions about mass spec, for introducing me to those tea breaks and for helping me all these years and making this PhD a great experience. It has been a pleasure working with the three of you! Thanks to all the Biotech and Yeast Genetics Lab. Thanks to Niamh, Nicola and Stephen for all the support during good and bad moments, for been there, for trying salsa and climbing and for been great friends. To Kevin, Elisabeth, Eoin, Darragh, Rose and Linan, for great chats, laughs and epic ping pong games.

Thanks to Nick for those climbing sessions, for your help fixing the HPLC and for been a great person to talk to. To Nuria for those Erasmus and salsa days and for your good humour. Special thanks to Eddie, for these two fantastic years and your support and help during the writing isolation process, you are a very patient and wonderful man!

Mostly I would like to thank my parents Agustin y Mercedes, for their support during this PhD and in every step I have done in life. Thanks for being there.

Esta tesis la dedico a mis padres, Agustin y Mercedes, por su apoyo no solo durante este doctorado sino en todas las decisiones que he tomado en mi vida. Gracias por estar ahi.

Publications and Presentations

Research Publications

Manzanares-Miralles, L., Sarikaya-Bayram, Ö., Smith E.B., Dolan, S.K., Bayram, O., Jones, G.W. and Doyle, S. (2016). Quantitative proteomics reveals the mechanism and consequence of gliotoxin-mediated dysregulation of the methionine cycle in Aspergillus niger. *J. Proteomics* 131, 149-162. doi:10.1016/j.prot.2015.10.024.

Oral Presentations

A proteomic and metabolomic investigation of the response of *Aspergillus niger* to gliotoxin. Irish Fungal Society Meeting. Trinity College Dublin, 11-12th June 2015.

Exploring thiomethylation in fungi by mass spectrometry. Annual Irish Mass Spectrometry Society Meeting. Dublin, 13th May 2015.

S-methylation of gliotoxin by *Aspergillus niger*: Identification and characterization of a S-methyltransferase. Departmental Symposium. Maynooth University, Ireland, 14th April 2015.

S-methylation of exogenous gliotoxin by *Aspergillus niger*. Departmental Symposium. Maynooth University, Ireland, 29th July 2014.

Immunoassay for the detection of Fusarinine C produced by *Aspergillus spp*. Annual Biology Research Day. Maynooth University, Ireland, 7th June 2013.

Why does gliotoxin inhibit the growth of *Aspergillus niger*? Departmental Symposium. Maynooth University, Ireland, 30th April 2013.

Poster Presentations

A proteomic and metabolomic investigation of the response of *Aspergillus niger* to gliotoxin. Irish Fungal Society Meeting. Trinity College Dublin, 11-12th June 2015.

Comparative proteomic and metabolomics analysis of *Aspergillus niger* following exposure to *Aspergillus fumigatus* secondary metabolite gliotoxin. Annual Biology Research Day. Maynooth University, Ireland, 12th June 2015.

Characterizing the response of *Aspergillus niger* to gliotoxin. Applications of Proteomics in Human Clinical and Infectious Disease. Dublin City University, Ireland, 16th September 2014.

How does gliotoxin inhibit the growth of *Aspergillus niger*? 12th European Conference on Fungal Genetics (ECFG12). Seville, Spain, 24th March 2014.

How does gliotoxin inhibit the growth of *Aspergillus niger*? The Eleventh International Aspergillus Meeting (Asperfest11). Seville, Spain, 22nd March 2014.

Immunoassay for the detection of Fusarinine C produced by *Aspergillus spp*. The Eleventh International Aspergillus Meeting (Asperfest11). Seville, Spain, 22nd March 2014.

Immunoassay for the detection of Fusarinine C produced by *Aspergillus spp*. Annual Biology Research Day. Maynooth University, Ireland, 7th June 2013.

Why does gliotoxin inhibit the growth of *Aspergillus niger*? Irish Fungal Society Meeting. Maynooth University, Ireland, 20th-21st June 2013

Proteomic response and assessment of redox status in *Aspergillus niger* and *Candida albicans* after gliotoxin exposure. Irish Fungal Society Meeting. Belfast City Hospital, UK, 21st-22nd June 2012.

Abbreviations

2D-PAGE	2-Dimensional Polyacrylamide Gel Electrophoresis
ACL	ATP-citrate lyase
Ado	Adenosine
AMM	*Aspergillus* Minimum Media
ALS	Acetolactate synthase
APS	Ammonium Persulphate
APS	Adenosine 5-phosphosulfate
APS Kinase	Adenosine 5-phosphosulfate kinase
ATPS	ATP sulfurylase
BAL	Bronchoalveolar Lavage
BCAA	Branched-chain amino acid
BCKA	Branched-chain keto acid
BDG	1,3 β-D-glucan
BmGT	Bisdethiobis(methylthio)gliotoxin
BSA	Bovine serum albumin
CAS	Chrome Azurol S
CAZymes	Carbohydrate-active enzymes
CBL	Cystathionine β-lyase
CBM	Carbohydrate binding module
CBS	Cystathionine β-synthase
cBSA	Cationised BSA
CGL	Cystathionine γ-lyase
CGS	Cystathionine γ-synthase
ChIP	Chromatin Immunoprecipitation
CMC	Carboxymethylcellulose
CMT	Cysteine methyltransferase
CS	Cysteine synthase
DAB	3,3’-Diaminebenzidine
DAO	D-amino acid oxidase

dcSAM	Decarboxylated *s*-adenosylmethionine
DTNB	5,5’-dithio-bis(2-nitrobenzoic acid)
DTT	Dithiothreitol
EDTA	Ethylenediaminetetraacetic Acid
EGT	Ergothioneine
EIC	Extracted Ion Chromatogram
ELISA	Enzyme-linked Immunosorbent Assay
ER	Endoplasmic Reticulum
ERAD	Endoplasmic Reticulum Associated Degradation
ERQC	Endoplasmic Reticulum Quality Control
ETP	Epipolythiodioxopiperazine
FA	Fatty Acid
FAE	Feruloyl esterases
FDR	False Discovery Rate
FunCat	Functional Catalogue
FusC	Fusarinine
GAAC	General Amino Acid Control
GH	Glycoside hydrolases
GM	Galactomannan
GRAS	Generally regarded as safe
GR	Glutathione Reductase
GSH	Glutathione
GSSG	Glutathione disulphide (oxidized)
GST	Glutathione *s*-transferase
GT	Gliotoxin
HAT	Histone acetyltransferase
HCD	Higher-energy collisional dissociation
Hcy	Homocysteine
HP	Hydroxypyrazines
HRP	Horseradish peroxidase
HSDH	Homoserine dehydrogenase

IA	Invasive Aspergillosis
IAA	Iodoacetamide
IBTS	Irish Blood Transfusion Service
IEF	Isoelectric Focusing
IL	Interleukin
Ile	Isoleucine
IPTG	Isopropyl β-D-Thiogalactopyranoside
I.V.	Index values
IVD	Isovaleryl-CoA dehydrogenase
KLH	Keyhole Limpet Hemocyanin
LB	Luria-Bertani
LC-MS	Liquid Chromatography Mass Sepctrometry
Leu	Leucine
LFQ	Label-free quantitative
Met	Methionine
MEA	Malt Extract Agar
MM	Minimal media
MmGT	*Mono*-thiomethylgliotoxin
MP	Methoxypyrazine
MTA	5'-methylthioadenosine
MTase	Methyltransferase
NADPH	β-nicotinamide adenine dinucleotide 2'-phosphate reduced tetrasodium salt hydrate
NCP	Nitrocellulose Paper
NPMT	Natural product methyltransferase
NRPS	Non-ribosomal peptide synthase
OAA	Oxaloacetate
OE	Overexpressed
OPA	*O*-phthaldialdehyde
ORF	Open Reading Frame
PAPS	3'-phosphoadenosine 5'-phosphosulfate
PBS	Phosphate Buffer Saline

PBST	Phosphate Buffer Saline Tween
PCR	Polymerase Chain Reaction
PDB	Potato Dextrose Broth
PDA	Potato Dextrose Agar
PGC	Porous Graphitized Carbon
Phe	Phenylalanine
PMSF	Phenylmethylsulfonyl fluoride
PPi	Pyrophosphate
PPP	Pentose Phosphate Pathway
PKS	Polyketide synthase
PZN	Plantazolicin
qPCR	Quantitative Polymerase Chain Reaction
qRT-PCR	Quantitative reverse transcriptase PCR
rGT	Dithiol Gliotoxin
ROS	Reactive Oxygen Species
RP-HPLC	Reverse-Phase High Performance Liquid Chromatography
RT	Room Temperature
SAM	*S*-adenosylmethionine
SAM-MTases	SAM dependent methyltransferases
SAH	*S*-adenosylhomocysteine
SAHase	*S*-adenosylhomocysteinase
SATA	N-succinimidyl-S-acetylthioacetate
SDS	Sodium Dodecyl Sulfate
SDS-PAGE	Sodium Dodecyl Sulfate Polyacrylamide Gel Electrophoresis
sGFP	Synthetic Green Fluorescent Protein
sHSAB	N-hydroxysulfosuccinimidyl-4-aziobenzoate
SM	Secondary Metabolites
SMCC	Succinimidyl 4-[N-maleimidomethyl] cyclohexane -1- carboxylate
SOD	Superoxide dismutase

SP	Signal peptide
SSA	5’5-sulfosalicilic Acid
ST	Sterigmatocystin
TAE	Tris-Acetate
TAFC	Triacetylfusarinine
TAP	Tandem Affinity Purification
TB	Terrific Broth
TCA	Trichloroacetic Acid
TCA Cycle	Tricarboxylic acid cycle
TF	Transcription Factor
TFA	Trifluoroacetic Acid
Thr	Threonine
TM	Tunicamycin
TM	Transformation Media
TMB	Tetramethylbenzidine
TMT	Thiomethyltransferase
TPS	Trehalose-6-phosphate synthase
TR	Transcriptional Regulator
UPR	Unfolded Protein Response
UPREs	Unfolded Protein Response Elements
Val	Valine

Summary

Gliotoxin (GT) is a redox-active natural product produced by some fungal species that contributes to the virulence of the human pathogen *Aspergillus fumigatus*. It contains a characteristic disulphide bridge responsible for the deleterious effects of this molecule. GT also displays antifungal properties, however the mechanisms of cytotoxicity behind it has not been fully characterised. The work presented here investigates *A. niger* as a model organism to understand GT cytotoxicity and reveal new metabolic systems, as it does not produce GT.

Comparative proteomics revealed that exposure of *A. niger* to exogenous GT resulted in a significant ($p < 0.05$) dysregulation of hundreds of proteins involved in several cellular processes, especially metabolism. Two putative *S*-adenosylmethionine (SAM)-dependent methyltransferases showed de novo abundance under GT conditions. In addition an increase in abundance of proteins involved in the methionine cycle was also observed. Analysis of methionine-related metabolites revealed significant increases in the levels of methionine and adenosine, in correlation with proteomic data. Moreover, proteomic data revealed a significant increase in the abundance of hydrolytic enzymes, including glycoside hydrolases ($n = 22$) and peptidases ($n = 16$) which have important applications in the biotechnology industry. A significant dysregulation of proteins involved in amino acid metabolism coupled to an increase in the levels of selected amino acids appeared to occur in *A. niger* under GT conditions. Furthermore this thesis reveals a novel protection mechanism in *A. niger* against GT which is mediated by one the methyltransferases (MTases) identified on the proteomic data. This MTase (referred as MT-II) is responsible for bisthiobis(methylthio)gliotoxin (BmGT) formation and deletion of MT-II led to increased GT sensitivity in *A. niger*.

The applications of other fungal natural products like siderophores (Fusarinine C), are also evaluated herein. The development and validation of a Fusarinine C based enzyme-linked immunosorbent assay (ELISA) was carried out. Results showed the potential applications of this ELISA in the diagnosis of aspergillus related diseases. Overall, this work highlights the different roles and applications fungal natural products have.

Chapter 1

Introduction

1 Introduction

1.1 General characteristics of *Aspergillus niger*

Aspergillus niger is a filamentous ascomycete, ubiquitous in nature that can grow in many ecological habitats like decaying vegetation, compost piles and stored grain. It is a saprophytic fungus member of the genus *Aspergillus* which play a role in carbon and nitrogen recycling (Dagenais and Keller, 2009). Phenotypically, it is distinguished from other *Aspergillus spp*. through the production of black or dark brown spores (Raper and Fennel, 1965). It exhibits a complex endomembrane trafficking system that is specialized for high secretion of both organics and hydrolytic enzymes (Andersen et al., 2008). This capacity has been extensively exploited by the biotechnology industry and it is considered a "secretion factory". Though some isolates have been associated with pathogenicity it is mostly found as a terrestrial strain (Person et al., 2010; Roehrl et al., 2007).

1.1.1 Life cycle

The genus *Aspergillus* comprise both known asexual and sexual species (Lee et al., 2010; O'Gorman et al., 2009; Paoletti et al., 2007; Pel et al., 2007a). *A. niger* reproduces asexually by forming conidia (asexual spores) and multicellular structures such as spores-bearing hyphae and fruiting bodies, which perform specific biological functions (Priegnitz et al., 2015).

The life cycle of *A. niger* starts with the germination of a spore (conidium) under appropriate environmental conditions such as light, carbon and nitrogen availability which are signals that break spores dormancy (Meyer et al., 2015). Upon germination, spores swell and a polarity axis is established which leads to the

formation of a germ tube that will eventually form a hypha (Figure 1.1). Lateral and apical branch formation of the hypha extend away from the point of germination and result in an interconnected network known as the mycelium (Harris et al., 2009; Rokas, 2013). As the mycelium expands, superficial hyphae start a number of developmental changes that lead to the formation of spore-bearing structures known as conidiophores (or fruiting bodies) (Etxebeste et al., 2010; Sewall et al., 1990). This process involves the formation of a foot cell followed by appearance of the stem, vesicle, metulae, philiades and conidia (Figure 1.1) (Sewall et al., 1990). The release of the conidia from the conidiophores, a process known as sporulation, can then occur through several atmospheric conditions.

A

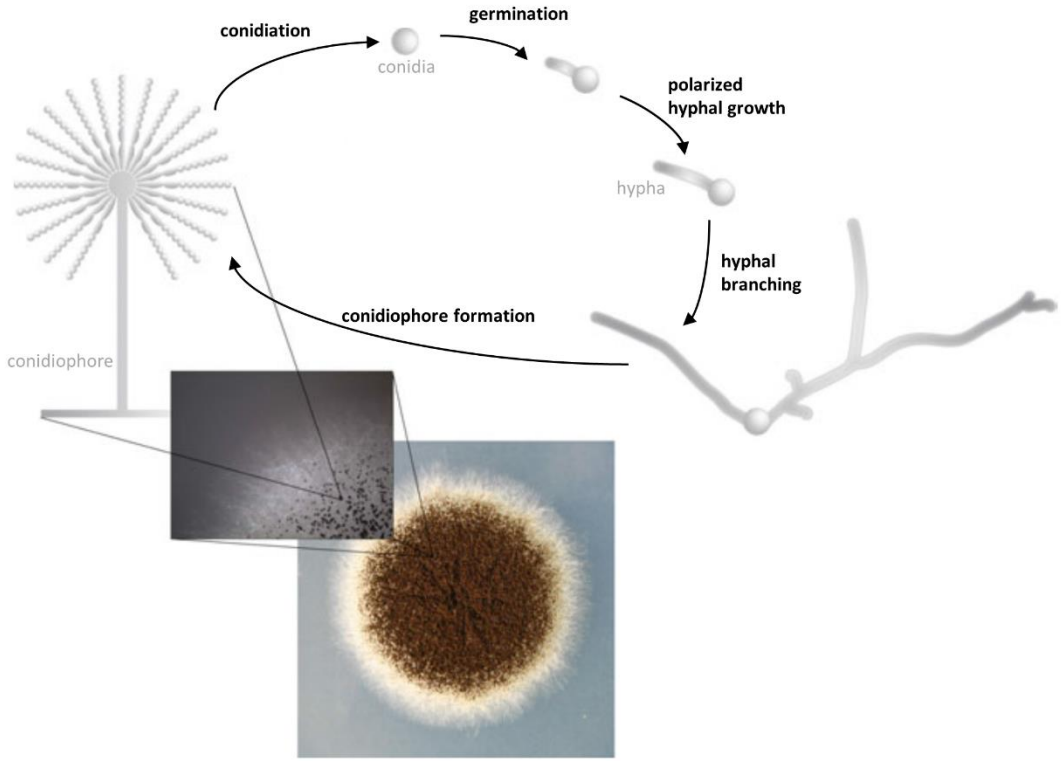
conidiation
germination
conidia
polarized
hyphal growth
hypha
hyphal
branching
conidiophore formation
conidiophore

B

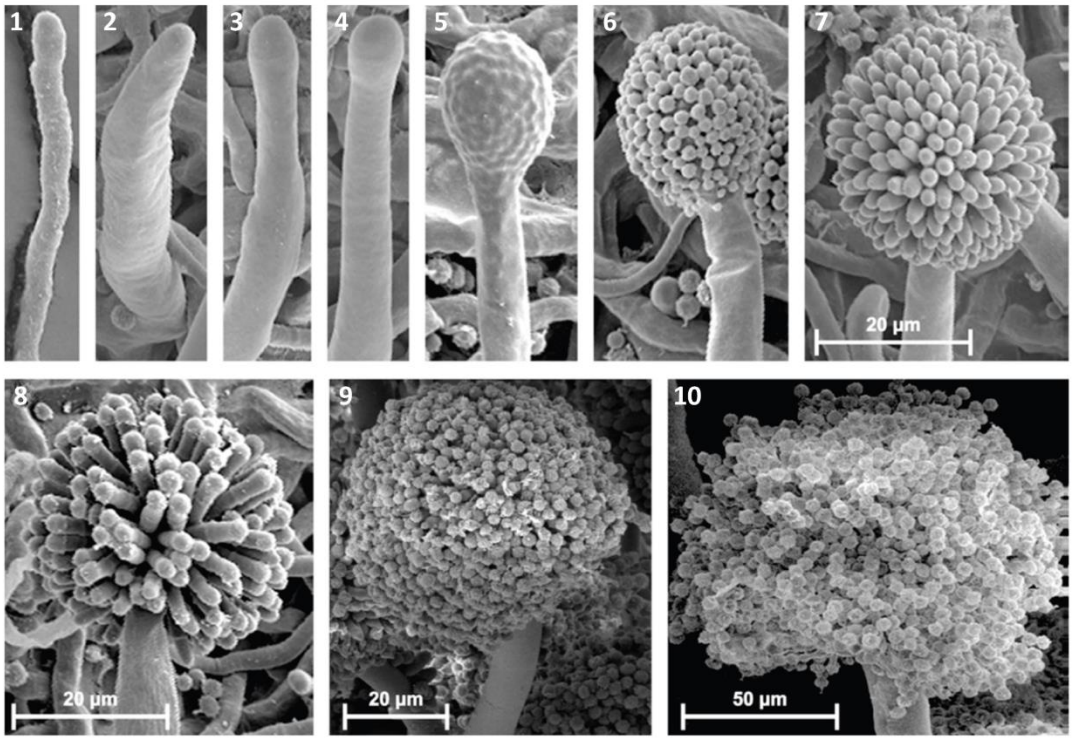
1
2
3
4
5
6
7
20 µm
8
20 µm
9
20 µm
10
50 µm

Figure 1.1: (A) Life cycle of *A. niger* adapted from (Meyer et al., 2015). **(B)** Developmental stages of *A. niger* visualised under electron microscopy. (1-4) Competent hyphae become thicker and begin to swell at the tip forming a vesicle. (5) Buds form on the vesicle which (6,7) develops into metulae. (8) Philiades grow on top of the metulae, which (9, 10) will result in chains of conidia. Image obtained from Krijgsheld et al. (2013).

Aspergillus sexual reproduction is controlled by a genetic locus known as the MAT locus (mating type), which encodes transcription factors that direct fungal developmental fate (Lee et al., 2010). Genome sequencing of *A. niger* showed the presence of a *mat-1* gene (alpha domain mating-type) that is required for normal sexual development in heterothallic species and a pheromone-precursor gene *pro1* (Pel et al., 2007a). Despite the presence of both *mat1* and *pro1* in the genome of *A. niger*, during fed-batch fermentations of the fungus, these genes are not expressed, which could suggest that they require particular environmental conditions for induction (Pel et al., 2007a). Sexual reproduction has been demonstrated in *A. fumigatus*, thought to be exclusively asexual (O'Gorman et al., 2009) and *A. nidulans* (Paoletti et al., 2007) where expression of MAT genes was a requirement for sexual development and ascospore production.

1.1.2 Genome

The complete sequence of the *A. niger* genome was published in 2007, and the sequenced strain was *A. niger* CBS 513.88, which is industrially used for large scale enzyme production (Pel et al., 2007a). This sequencing project revealed that the genome was 33.9 Mb in size, comprising 8 chromosomes, on which 14,165 protein coding genes were present (Table 1.1) (Pel et al., 2007a). In 2011, a second strain of *A. niger*, ATCC 1015, was sequenced and was used to improve the CBS 513.88 (Andersen et al., 2011). The ATCC 1015 strain is widely used for the production of citric acid, thus, comparison between the genome of both strains was carried out in order to gain insights of both phenotypes. In contrast to other filamentous fungi, *A. niger* contains a large number of genes encoding proteins for C-compound metabolism, carbohydrate and fatty acid metabolism and secondary metabolism which potentiate the use of this organism as a cell factory (Pel et al., 2007a). Comparison of both strains showed that the CBS 513.88 strains contain several unique genes including two α-amylases and three possible polyketide synthases that can account for a high amylase producing phenotype and a unique secondary metabolism (Andersen et al., 2011). On the other hand, no obvious cause of high citric acid production was elucidated from the genome.

As of October 2015, of the total ORFs (14,058) of *A. niger* CBS 513.88, only 245 (1.74 %) have a verified function (www.aspergillusgenome.org). Table 1.1 presents the genome characteristics of *A. niger* CBS 513.88 obtained from Pel et al. (2007).

Table 1.1: Key features of the *A. niger* CBS 513.88 genome (Pel et al., 2007a).

Genome	**Value**
Size (Mb)	33.9
GC content (%)	50.4
Protein coding genes	14,165
Average gene length (bp)	1,572
Average number of introns per gene	2.57
Number of tRNA genes	269

1.2 Industrial applications of *A. niger*

The genus *Aspergillus* is widely used by the Biotechnology industry as a cell factory for the production of food ingredients, pharmaceuticals and enzymes (Meyer et al., 2010). There are several advantages associated to the use of these fungi in industrial processes which include (i) the high secretion capacity (ii) the ability to express eukaryotic proteins that require post-translational modifications and (iii) the high tolerance to cultivation conditions where they can withstand a broad range of temperatures, pH and salinity (van den Hombergh et al., 1997; Meyer et al., 2010). Ultimately most industrial processes involving *Aspergillus spp*., specially *A. niger*, *A. oryzae* and *A. terreus* have been certified as generally regarded as safe (GRAS) by the Food and Drug Administration (USA) and the World Health Organisation (van den Hombergh et al., 1997; Schuster et al., 2002). *A. niger* is mainly used for the production of homologous and heterologous proteins and primary and secondary metabolites (Archer, 2000). *A. oryzae* has great importance in the Asian market where it is used to ferment soybeans and rice into soy sauce and sake while *A. terreus* produces lovastatin

which is a cholesterol-lowering drug. Other filamentous fungi like *A. fumigatus* can cause human infections (Dagenais and Keller, 2009; De Lucca, 2007), while *A. flavus* and *A. parasiticus* can contaminate crops by releasing a highly toxic carcinogen, aflatoxin, that if ingested can cause illness or death (Wild, 2007).

Within the *Aspergillus spp*, *A. niger* is of great interest due to its versatile metabolic capacities, which position this fungus as a major industrial workhouse. The applications of *A. niger* extend to the production of bulk chemical derived from primary metabolism like citric acid and glutamic acid and also to the production of hydrolytic enzymes and heterologous enzymes like human interferon or chymosin (Dunn-Coleman et al., 1991; Punt et al., 2002).

1.2.1 Bulk chemicals

Two major bulk chemicals produced at a global scale by *A. niger* are citric acid and gluconic acid. The first one is used in the food, pharmaceutical and cosmetic industry as an acidulant, preservative, antioxidant and emulsifier. Gluconic acid and its derivatives are also used in the food and pharma industry and in the textile and photographic industry. Both biochemicals are produced naturally by *A. niger* through fermentation processes where citric acid is an intermediate of the tricarboxylic acid (TCA) cycle and gluconic acid is generated by a dehydrogenation reaction from glucose (Znad et al., 2004). To satisfy the high demand of these biochemicals, specific strains of *A. niger* have been engineered to increase the yields as much as possible.

Using a citric acid producer strain, of the total sugar supplied in batch fermentations approximately 95 % will be directed towards citric acid production, resulting in an almost complete conversion (Karaffa and Kubicek, 2003). Similarly, a

98 % yield of gluconic acid is produced by *A. niger* when glucose is used as the main carbohydrate source (Singh and Kumar, 2007).

1.2.2 Lignocellulose degradation for biofuel production

Due to its role as a saprophyte, *A. niger* secretes a broad spectrum of lignocellulosic enzymes which degrade plant material and release sugars that are consumed by the fungus (De Souza, 2013). This hydrolytic potential is exploited for the production of bioethanol whereby feedstocks like sugarcane, grains and lignocellulosic materials are treated with a cocktail of enzymes derived from several microorganisms (e.g. *Trichoderma reesei* and *A. niger*) that degrade the cellulosic biomass (Talebnia et al., 2009). The worldwide production of ethanol estimated for 2015 is over 115 billion liters (Talebnia et al., 2010), thus bioethanol is one of the most important biofuels used. Additionally, it represents a potential green energy source to replace the use of dwindling fossil fuels (Fitzpatrick et al., 2014).

Feedstock for bioethanol production like wheat straw and sugarcane are composed of cellulose (40 – 50 %), hemicellulose (25 – 35 %) and lignin (15 – 25 %) (Ragauskas et al., 2006; de Souza et al., 2011, 2013). Cellulose is a β-(1,4)-linked glucose polymer while hemicellulose is an heteropolymer composed of sugars like xylose, mannose, galactose, rhamnose and arabinose. For ethanol production, these polymers have to be hydrolysed into the sugar monomers (Talebnia et al., 2010). The hydrolysis of cellulose is carried out by the action of three types of glycoside hydrolases (GHs) also referred as cellulases which include endoglucanases, cellobiohydrolases and β-glucosidases (Elkins et al., 2010). These enzymes are majorly produced by two filamentous fungi, *Trichoderma reesei* and *A. niger*. Endoglucanases and cellobiohydrolases are mainly produced by *T. reesei* and are

involved in the depolymerzation of cellulose by exposing new side chain ends that are subsequently cleaved to release cellobiose (Asztalos et al., 2012). β-glucosidase is produced by *A. niger* and breaks cellobiose to release glucose (Talebnia et al., 2010). Enzymatic hydrolysis can be improved by the combination of cellulases and hemicellulases. The most utilized hemicellulases include xylanases, feruloyl esterases (FAE) and laccases (Talebnia et al., 2010). After hydrolysis, utilization of the released sugars (hexoses and pentoses) in fermentation processes is required for the generation of bioethanol.

Currently, cocktails of hydrolytic enzymes are been developed to improve catalytic activity and thermostability (Mohanram et al., 2013). Novozymes Cellic® CTec2 is a commercially available cocktail composed of a blend of cellulases, hemicellulases and high levels of β-glucosidases (bioenergy.novozymes.com).

The mechanisms involved in hydrolase production in fungi like *A. niger* and *T. reesei* have been and are subject to extensive research. Elucidating these mechanisms can improve the development of fungal strains with a high production capacity of polysaccharide degrading enzymes (de Souza et al., 2013).

1.2.3 Heterologous protein expression

Genes encoding for proteins or metabolites of interest are expressed under the control of promoters, which can have different strengths. *A. niger* is a preferred host organism as it has GRAS approval and an active metabolism (Punt et al., 2002). Most promoters available for high yield protein production are either constitutively active (e.g. *A. niger* glyceraldehyde-3-phosphate dehydrogenase promoter (*PgpdA*)) or dependent on the carbon or nitrogen source present in the medium (e.g. *A. niger* glucoamylase promoter (*PglaA*)) (Meyer et al., 2010, 2011; Punt et al., 2002).

A recent expression system (Tet-on system) was developed to provide a tight, tunable and carbon-source independent control mechanism, that becomes induced with the addition of doxycycline (Dox) (Vogt et al., 2005). This system is able to respond fast to the inducer and allows for gene control in a concentration-dependent manner. It is also a strong system capable of competing with the *gpdA* promoter (Meyer et al., 2010, 2011).

Most proteins expressed in *A. niger* are from closely related organisms, like other *Aspergillus spp*., due to the high yields obtained (similar to native protein yields like hydrolases) (g/L). However, proteins or metabolites of animal or other fungal organisms have been expressed in *A. niger* at lower quantities (mg/L) (Valkonen et al., 2003). Currently there is a great interest in increasing the yields of heterologous proteins in this fungus.

Punt et al. (2002) investigated the secretion of human interleukin 6 (IL-6) and fungal manganese peroxidase (MnP) in *A. niger*, under the control of different promoters and growth conditions to optimize production. MnP from *Phanerochaete chrysosporium* is a heme-containing peroxidase that degrades lignin. Under the control of a glucoamylase promoter yields ranged from 5 – 10 mg/L compared to 25 mg/ml when placed under the control of a pH-independent *gpdA* promoter (Punt et al., 2002). The production of human IL-6 in *A. niger* strains under the control of the *gpdA* promoter and the *glaA* promoter was also investigated. Initially, an *A. niger* AB1.13 (protease deficient) strain was used, with a production of 2 mg/L. The remaining proteolytic activity (against IL-6) in the culture medium was dependent on pH and absent in non-acidic pH. Thus a new strain of *A. niger* D15 (protease deficient, non-

acidifying) using the same *gpdA* promoter showed improved yields of 50-150 mg/l, with highest yields at pH 7 (Punt et al., 2002).

A. niger was also a host for the expression of secondary metabolite enniantin from *Fusarium oxysporum*. The gene encoding for this metabolite, *esyn1*, was placed under the control of the Tet-on system and it was observed that production rates were very high. Yields of 4.5 g/L were obtained after *A. niger* DS3.1 was grown for 66 h (Richter et al., 2014). This was the first demonstration showing that *A. niger* was a suitable host for the production of secondary metabolites and that high yields can be obtained when genes are placed under the Tet-on control system (Richter et al., 2014).

1.2.4 Bottlenecks

Several bottlenecks or factors that negatively affect protein expression include mRNA instability, inefficient translation, mis-folding and degradation of the protein of interest (Guillemette et al., 2007; Sharma et al., 2009; Valkonen et al., 2003). In order to improve protein yields, some approaches have been used, which include the deletion of certain genes (proteases) and the use of strong promoters (Carvalho et al., 2012). Additionally, bottlenecks associated with problems in the secretory pathway of *A. niger* have been proposed and investigated (Carvalho et al., 2012; Guillemette et al., 2007; MacKenzie and Guillemette, 2005).

Endogenous protease production during growth conditions can lead to the degradation of the protein of interest and significantly lower the yields. As a result, protease-deficient strains have been developed and are currently used in commercial processes (van den Hombergh et al., 1997; Mattern et al., 1992). Though these strains have improved the problem, some proteins under certain conditions can still result in losses of protein yield (Punt et al., 2002).

Large-scale proteome and genome analysis of *A. niger* have been carried out mimicking batch fermentation processes to understand the overall response of the fungus under industrial stress conditions. These efforts might provide an opportunity to further improve strain manipulations (Carvalho et al., 2011; Guillemette et al., 2007; Lu et al., 2010; MacKenzie and Guillemette, 2005; van Munster et al., 2014, 2015; Nitsche et al., 2012; Sharma et al., 2009; de Souza et al., 2011).

1.3 Fungal systems biology

The availability of fungal genome sequences led *Aspergillus* research into a new era known as systems biology (Meyer et al., 2010). Analysis methods in systems biology provide a comprehensive understanding of complex interactions in the organism of study. An integration of several omic techniques like genomics, transcriptomics, proteomics and metabolomics increases the understanding of interactions at gene and protein level and also metabolic fluxes (Zhang et al., 2010).

Transcriptomic and proteomics are frequent tools utilised in fungal species to investigate the fitness and productivity of Aspergillus industrial strains (*A. niger*) and to identify important factors involved in the pathogenicity of clinical aspergilli (*A. fumigatus*) (Meyer et al., 2010). Comparative studies using these tools on *A. niger* in response to stress agents has been the approach to understand the stress response this fungus has under industrial fermentations. On the other hand comparative omics on gene deletion mutants in *A. fumigatus* have aided assessment of the role played in infection.

1.4 Gliotoxin

Fungal toxins are usually secondary metabolites (SM) varying from immuno-suppressive metabolites to antibiotics. SM are low molecular mass molecules that are dispensable for the normal growth of the fungus but aid in the adaptation to hostile environments like under nutrient limitation or in the presence of competitors (Sheridan et al., 2015). *Aspergillus spp*. secrete a broad range of SM such as polyketides (e.g. cyclic peptides, alkaloids, sesquiterpenoids) and epipolythiodioxopiperazines (ETPs) (Frisvad et al., 2009; Gardiner et al., 2005). This last class of SM (ETPs) contains an internal disulphide bridge within a diketopiperazine ring that confers cytotoxicity to the molecule (Figure 1.2) (Müllbacher et al., 1986). The best characterised ETP is gliotoxin (GT) (326 Da) (Figure 1.2), which has a discontinuous distribution within different fungal species whereby ascomycetes like *A. fumigatus*, *A. terreus*, *A. flavus* and *Gliocladium virens* will produce the toxin but *A. nidulans* and *A. niger* will not (Fox and Howlett, 2008; Patron et al., 2007).

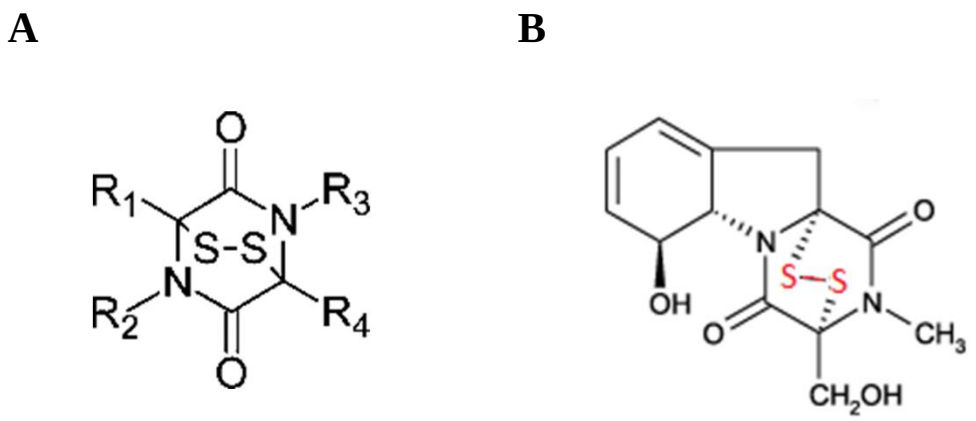

Figure 1.2: (A) Generic structure of an ETP formed by the diketopiperazine ring and the disulphide bridge (Gardiner et al., 2005). **(B)** Gliotoxin structure.

A. fumigatus causes severe disease and mortality in immunosuppressed patients (Tekaia and Latgé, 2005) and it is the main GT producer within the *Aspergillus spp*. (Lewis et al., 2005). GT has been established as a virulence factor of *A. fumigatus* (Sugui et al., 2007) and multiple studies have focused on the effect this toxin has on animal cells (Müllbacher et al., 1988; Nouri et al., 2015).

Toxicity of GT can be mediated by the disulphide bridge that (i) can cross-link with proteins containing cysteine residues leading to their inactivation and (ii) can generate reactive oxygen species through redox cycling (Figure 1.3) (Gardiner et al., 2005; Rodriguez and Carrasco, 1992). Formation of the disulphide bridge can be repressed by the addition of cellular reductants like glutathione (GSH) and dithiothreitol (DTT). These agents will inhibit the production of redox species and impede the formation of the disulphide bridge (Figure 1.3) (Gardiner et al., 2005).

A

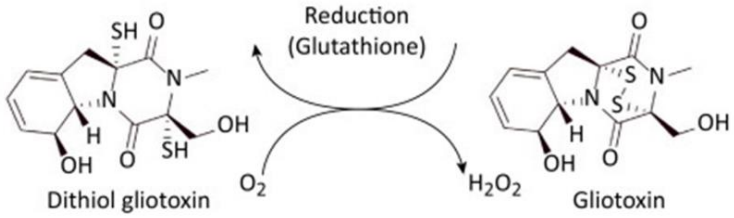

B

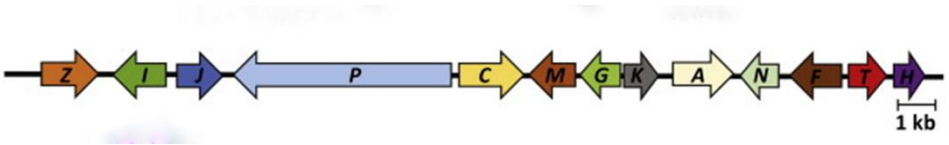

Figure 1.3: (A) Redox cycling of GT between the reduced (dithiol) and oxidised (disulphide) forms. **(B)** Gliotoxin biosynthetic gene cluster. Images adapted from (Dolan et al., 2015)

Recent studies on the GT biosynthetic pathway have revealed that GT is encoded by a 13 gene cluster in *A. fumigatus* (known as the *gli* cluster) (Figure 1.3) and that it requires of an oxidoreductase (GliT) to protect the organism against exogenous GT (Scharf et al., 2010; Schrettl et al., 2010b). Genes encoding enzymes for the biosynthesis of fungal SM are normally clustered within the genome of the organism (Bok and Keller, 2004; Brown et al., 1996).

Figure 1.4 shows current knowledge about the GT biosynthetic mechanism in *A. fumigatus*. This process starts with the assembly of phenylalanine and serine by GliP to form cyclo-phenylalanyl-serine, which, by the action of GliC and GliG is converted to a bis-glutathionylated intermediate (Balibar and Walsh, 2006; Chang et

al., 2013; Davis et al., 2011; Scharf et al., 2011). The next step is catalysed by GliK which removes the γ-glutamyl moieties from GSH (Gallagher et al., 2012). Subsequent reactions will yield an intermediate which, by the action of a N-methyltransferase (GliN), is N-methylated (Scharf et al., 2014). Ultimately, GliT will close the disulphide bridge (Scharf et al., 2010; Schrettl et al., 2010b). Secretion of GT from the cell will be carried out by GliA, MFS transporter (Wang et al., 2014).

Recently, a regulatory mechanism of GT biosynthesis was identified by Dolan et al. (2014), whereby a gliotoxin *bis*-thiomethyltransferase (GtmA) was observed to *bis*-methylate dithiol GT to form a *bis*-methyl GT derivative. This would prevent disulphide closure by GliT during GT biosynthesis (Figure 1.4) (Dolan et al., 2014).

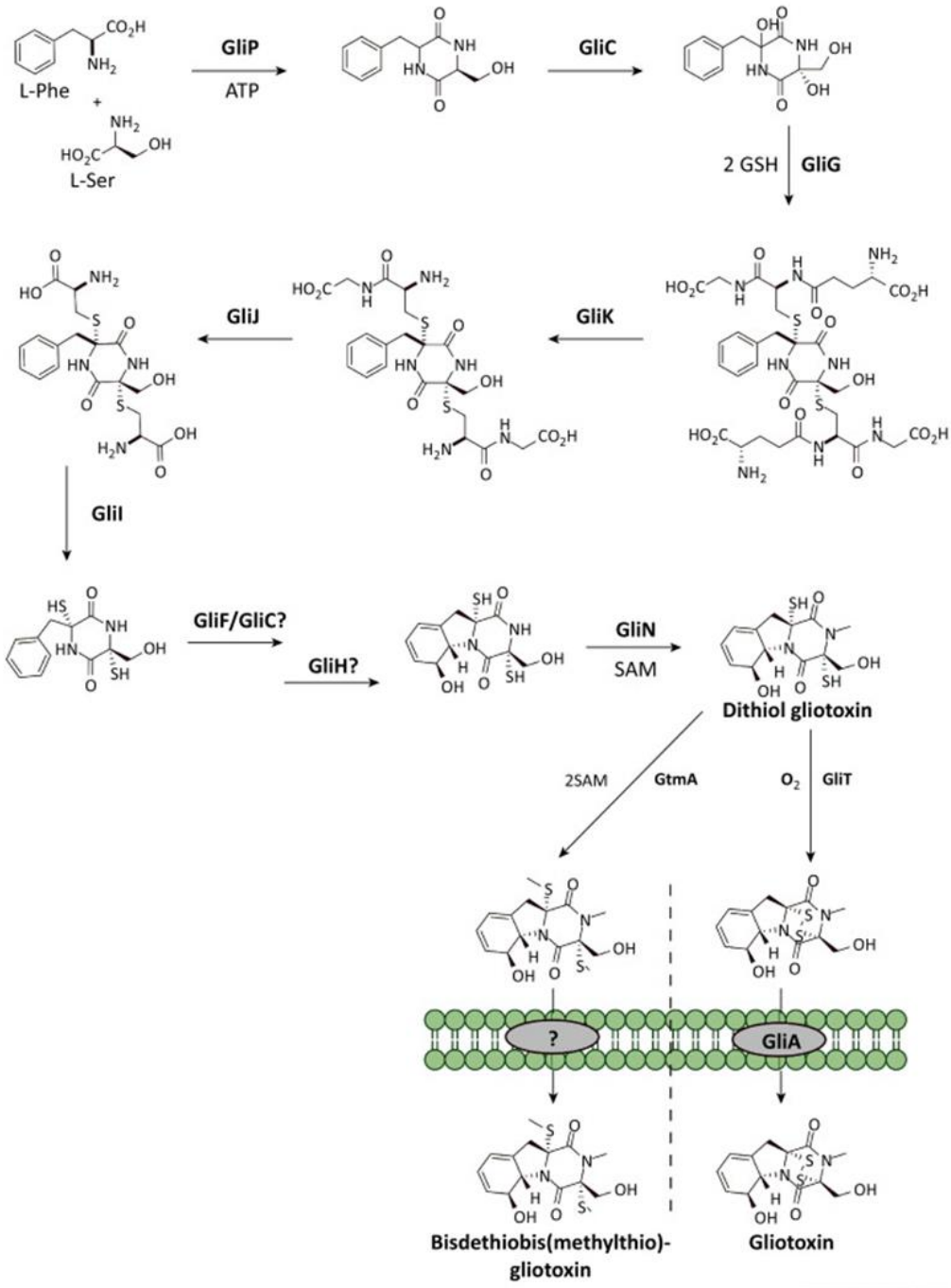

Figure 1.4: Gliotoxin biosynthesis and secretion. Figure obtained from Dolan et al. (2015).

The work described above has aimed to dissect the GT biosynthetic pathway of *A. fumigatus* and understand how the biosynthesis of this molecule is controlled to

avoid its deleterious affects. Oxidoreductase (GliT) and MFS transporter (GliA), have been shown to be part of a self-protection mechanism whereby dithiol GT is oxidised and secreted outside the cell thereby attenuating the intracellular toxicity of the dithiol form (Owens et al., 2015; Scharf et al., 2010; Schrettl et al., 2010b; Wang et al., 2014). Recently, an RNA-seq analysis of *A. fumigatus* Δ*gliT* compared to wild-type has aimed to elucidate the cellular processes involved in self-protection against GT (O'Keeffe et al., 2014). It is surprising to note that most studies on GT are carried out on the producing fungus (*A. fumigatus*) and on mammalian model organisms like *Saccharomyces cerevisiae* (Chamilos et al., 2008), while research on the response of GT-naïve fungi to this molecule is practically non-existent. Phenotypic assays have been carried out on *A. niger*, *A. nidulans*, *Candida albicans* and *Cryptococcus neoformans* in the presence of exogenous GT, and growth inhibition has been observed. Despite the antifungal capacity of GT on these organisms, no insights into the cellular processes involved have been carried out until the present thesis.

1.5 Sulphur metabolism

As mentioned earlier, comparative transcriptomic, proteomic and metabolomics, are powerful tools to elucidate the overall state of the cell under different conditions like stress. The interconnectivity of the different cellular processes is exemplified in any –omics study where adaptation to an environmental alarm triggers multiple responses. In *A. niger*, most –omics investigations have aimed to mimic industrial fermentations where the fungus can encounter stress conditions such as nutrient deficiency (e.g. carbon starvation). Studies carried out under carbon limitation have aimed to understand the effect on hydrolytic enzyme production (van Munster et al.,

2014, 2015; Nitsche et al., 2012). Though carbon is an essential nutrient, there are other elements, like sulphur required for growth and adaptation that haven't received as much attention.

In fungi, organosulphur compounds are involved in protein biosynthesis (methionine and cysteine), stress response (glutathione, ergothioneine) (Fahey, 2013; Pócsi et al., 2004), iron metabolism (Fe-S clusters) (Amich et al., 2013), secondary metabolism (ETP toxins) (Davis et al., 2011; Sheridan et al., 2015) and methylation reactions (SAM) (Attieh et al., 2000b; Dolan et al., 2014; Scharf et al., 2014). *Aspergillus spp*. can acquire sulphur from inorganic sulphate and sulphur-containing amino acids through different metabolic pathways.

1.5.1 Assimilation of inorganic sulphur

Inorganic sulphate (SO_4^{2-}) is transported into the cell by sulphate permease (encoded by *sB* gene in *A. nidulans*). Once in the cell, ATP sulfurylase (*sC*) yields adenosine 5-phophosulfate (APS) which will be phosphorylated by an APS kinase encoded by *sD* that will generate 3'-phosphoadenosine 5'-phosphosulfate (PAPS) (Figure 1.5) (Marzluf, 1997). The next step in the assimilation of sulphur is carried out by PAPS reductase (*sA* in *A. nidulans*) releasing sulphite (SO_3^{2-}) that subsequently will be reduced by a sulphite reductase to produce sulphide (S^{2-}) (Figure 1.5). In filamentous fungi, sulphide can be condensed to (i) *O*-acetylserine to form cysteine by cysteine synthase (*cysB* gene) or to (ii) *O*-acetylhomoserine to generate homocysteine through homocysteine synthase (*cysD* gene) (Figure 1.6) (Brzywczy et al., 2007).

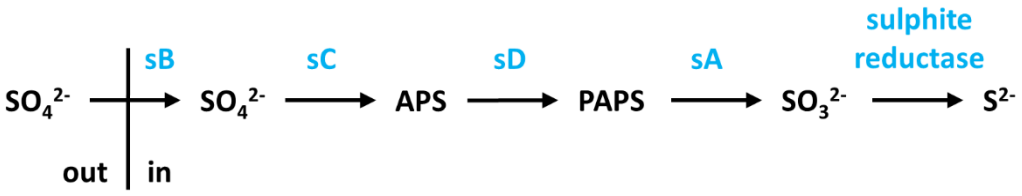

Figure 1.5: Sulphur assimilation in *A. nidulans*. Inorganic sulphur (SO_4^{2-}) is transformed into sulphide (S^{2-}) through a series of enzymes (shown in blue). Sulphate permease (sB), ATP sulphurilase (sC), APS kinase (sD), PAPS reductase (sA) and sulphite reductase.

Homocysteine and cysteine can interconvert through the forward and reverse transsulfuration pathways (Sohn et al., 2014). The reverse pathway involves the conversion of homocysteine to cystathionine and cysteine by the action of cystathionine β-synthase (CBS) (encoded by *mecA* in *A. nidulans*) and cystathionine γ-lyase (CGL) (*A. nidulans mecB* gene) (Sieńko et al., 2009). The forward pathway requires cystathionine γ-synthase (CGS) (*metB* gene in *A. nidulans*) and cystathionine β-lyase (CBL) (*A. nidulans metG*) to convert cysteine to homocysteine (Figure 1.6) (Brzywczy et al., 2007; Sieńko et al., 2014). Though filamentous fungi like *A. nidulans* and *Neurospora crassa* can incorporate sulphide through cysteine synthase and homocysteine synthase, and can use both the reverse and forward transsulfuration pathway, yeasts like *S. cerevisiae*, *Schizosaccharomyces pombe* and *Hansenula polymorpha* do not contain some of the enzymes required to catalyse the aforementioned reactions. *S. cerevisiae* lacks cysteine synthase thus the last step of the sulphur assimilation pathway is dependent on homocysteine synthase (*met25* or *met17*) (Figure 1.6) (Thomas and Surdin-Kerjan, 1997). *S. pombe* is unable to perform

the reverse transsulfuration pathway due to the absence of cystathionine β-synthase and cystathionine γ-lyase (Brzywczy et al., 2002) and *H. polymorpha* lacks homocysteine synthase activity (Figure 1.6) (Sohn et al., 2014).

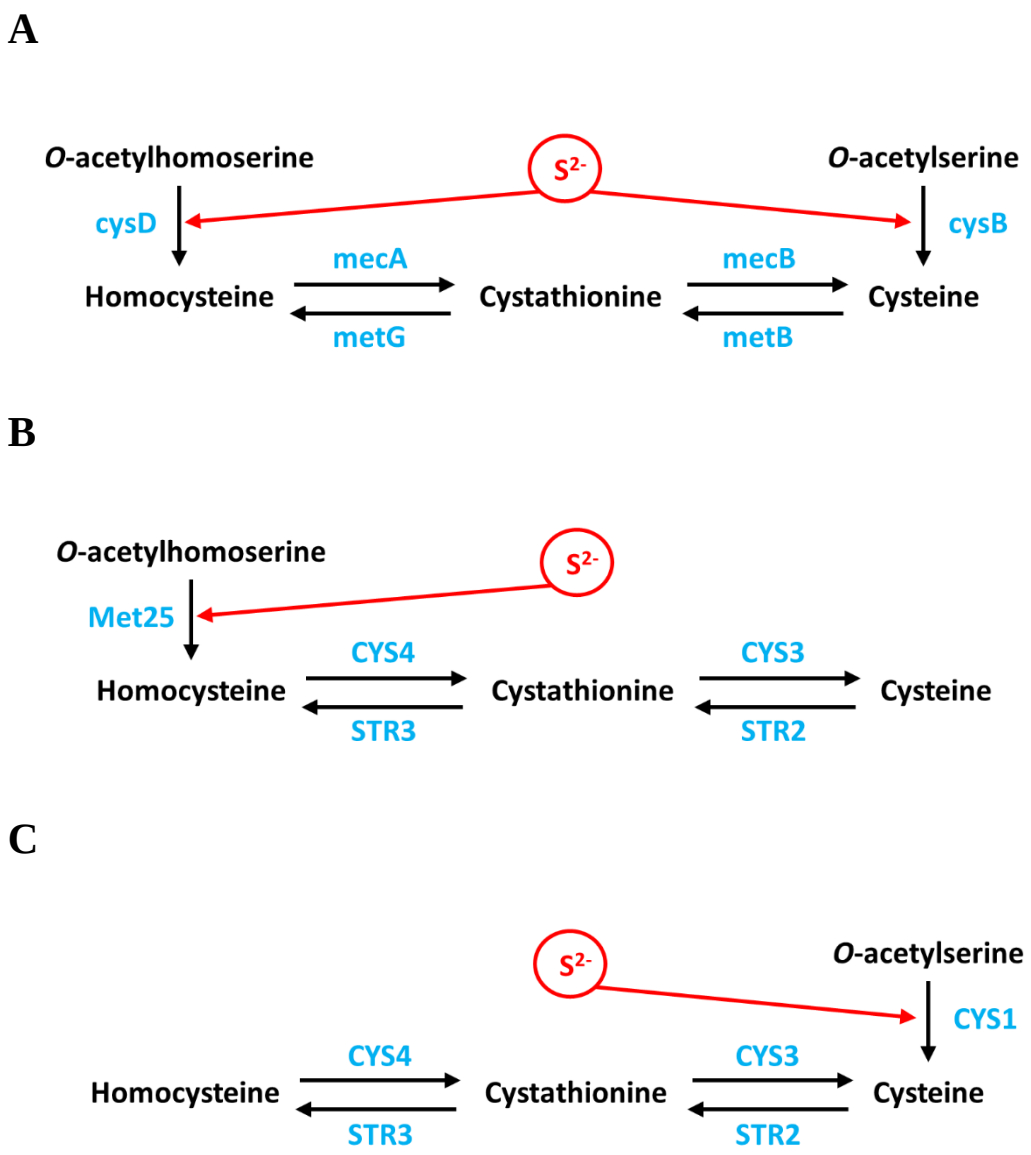

Figure 1.6: Sulphur incorporation into amino acids in **(A)** *A. nidulans* **(B)** *S. cerevisiae* and **(C)** *H. polymorpha*. Image adapted from Sohn et al. (2014).

It was observed that *S. cerevisiae met25* mutant (deletions between nucleotide 320 – 270) required organic sulphur sources like Cys, Met and Hcy for growth (Thomas and Surdin-Kerjan, 1997). Contrary to this observation, deletion of its homolog in *A. nidulans* (*cysD*) had the same nutritional requirement as to wild type and could assimilate sulphate using cysB (Brzywczy et al., 2002; Sieńko et al., 2014). Thus is appears that filamentous fungi have a larger set of enzymes employed for sulphur assimilation.

1.5.2 Biosynthesis of sulphur-containing amino acids

Methionine (Met) is a sulphur-containing amino acid required for protein synthesis as well as other cellular processes like methylation and polyamine biosynthesis (Sauter et al., 2013). In fungi, *S*-adenosylmethionine (SAM) synthetase catalyzes the formation of SAM from methionine and ATP (Figure 1.7) (Gerke et al., 2012). SAM synthetase is encoded by only one gene in most *Aspergillus* species (*SasA* in *A. nidulans*) however two independent coding genes are found in *S. cerevisiae* (*SAM1* and *SAM2*) (Gerke et al., 2012). SAM is the main donor of methyl groups in cells. It is involved in the transmethylation of proteins, DNA, RNA, polysaccharides and phospholipids, whereby methyltransferases transfer the methyl group of SAM to the different substrates (Kanai et al., 2013). This leads to the formation of *S*-adenosylhomocysteine (SAH), which behaves as a substrate for the next reaction in the methionine cycle. SAH hydrolase (*sah1*) catalyses the hydrolysis of SAH to homocysteine (Hcy) and adenosine (Ado). The last reaction in the cycle involves the methylation of Hcy by a cobalamin-independent methionine synthase (*Met6* in *A. niger*) that uses 5-methyl-tetrahydrofolate (CH_3-THF) as the methyl donor (Figure 1.7) (Saint-Macary et al., 2015). The generation of methionine from Hcy, independent of

Met6, have also been described in fungi. In *S. cerevisiae* a SAM-Hcy methyltransferase (SAM4) and an *S*-methylmethionine (SMM)-Hcy methyltransferase (MHT1) were characterised and found to play a major role in the control of Met/SAM equilibrium (Thomas et al., 2000). Additionally, this balance can also be regulated by the methionine salvage cycle, also known as the Yang cycle. In this pathway SAM is decarboxylated to form dcSAM (decarboxylated SAM) which donates aminopropyl groups to putrescine and in a reaction catalysed by spermidine synthase, it generates spermidine and 5'-methylthioadenosine (MTA). MTA is then metabolized in the Yang cycle to generate more methionine (Figure 1.7) (Sauter et al., 2013). These pathways aid in the maintenance of cytosolic Met and SAM levels and corroborate the importance these metabolites have within the cell.

Met biosynthesis converges with the reverse transsulfuration pathway whereby its precursor, Hcy, can be converted to cysteine using cystathionine β-synthase and cystathionine γ-lyase (Figure 1.7) (Sieńko et al., 2009). From cysteine, the action of γ-glutamylcysteine synthetase (encoded by *GSH1* in *S. cerevisiae*) and glutathione synthetase (*GSH2* in *S. cerevisiae*) will lead to the synthesis of glutathione (Ljungdahl and Daignan-Fornier, 2012). In *S. cerevisiae* and *S. pombe*, deletion of γ-glutamylcysteine synthase produces GSH auxotrophy and only upon GSH supplementation in the medium growth can be restored (Chaudhuri et al., 1997). GSH is a non-protein thiol that has an important role in the response to oxidative stress in the cell. It also exists in an oxidised form (GSSG) where the thiol group (-SH) of its cysteine is oxidised. GSH behaves as a potent antioxidant, thus, when reactive oxygen species (ROS) (superoxide [$O_2^{\cdot-}$], hydrogen peroxide [H_2O_2] and hydroxyl radicals [·OH]) and xenobiotics are produced, if not removed properly, they can cause the

oxidative obliteration of cell (Pócsi et al., 2004). In this scenario, GSH donates electrons to a glutathione peroxidase that reduces H_2O_2 to produce H_2O.

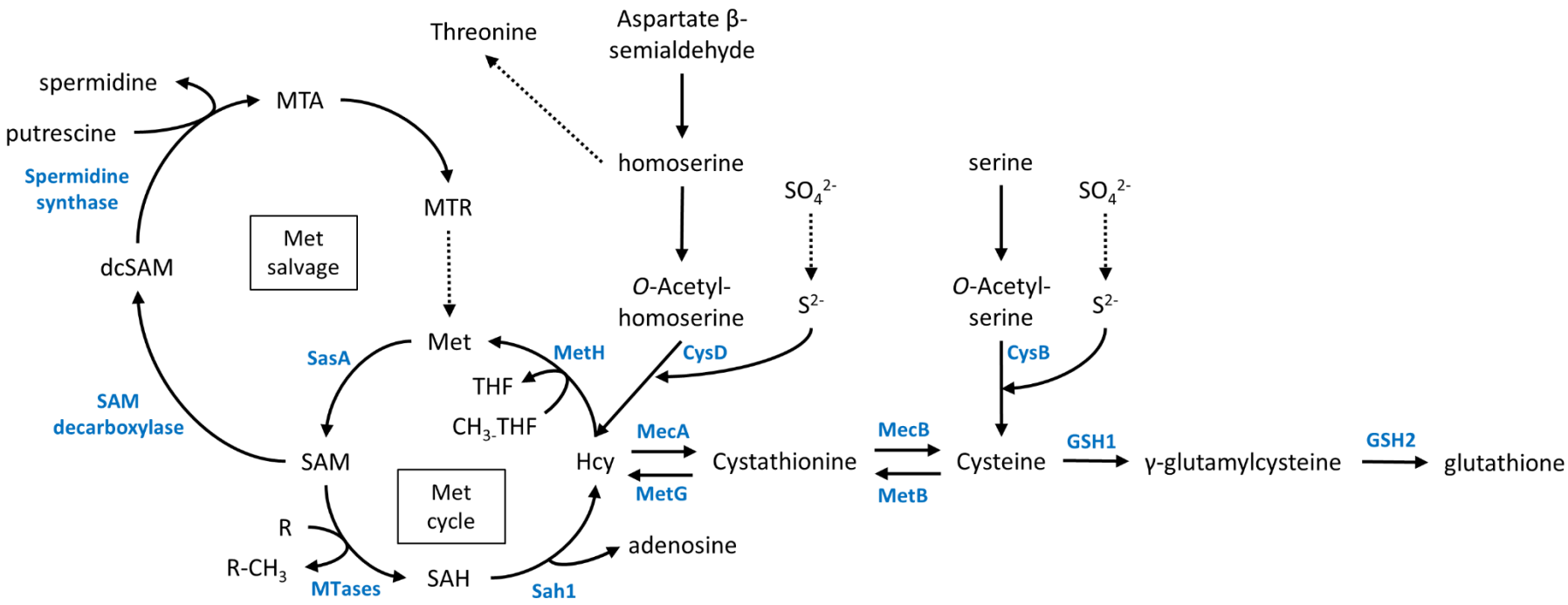

Figure 1.7: Methionine metabolism in *A. nidulans*. Enzymes involved in the methionine cycle (SAM synthetase, **SasA**; methyltransferases, **MTases**; SAH hydrolase, **Sah1**; methionine synthase, **MetH**), transsulphuration pathway (cystathionine γ-synthase, **MetB**; cystathionine β-liase, **MetG**), reverse transsulphuration pathway (cystathionine β-synthase, **MecA**; cystathionine γ-liase, **MecB**), sulphur assimilation pathway (homocysteine synthase, **CysD**; cysteine synthase, **CysB**) and glutathione biosynthesis (γ-glutamylcysteine synthetase, **GSH1**;

glutathione synthetase, **GSH2**) are shown. Metabolites appear as: dcSAM (decarboxylated SAM), MTA (5'-methylthioadenosine), MTR (5'-methylthioribose), THF (tetrahydrofolate) and CH_3-THF (5-methyl-tetrahydrofolate).

1.5.3 Transcriptional regulation of sulphur metabolism

Control of sulphur assimilation and metabolism at the transcriptional level is carried out by catabolite repression which involves positive and negative regulatory proteins. In *A. nidulans*, *metR* gene encodes for a transcriptional activator of sulphur metabolism genes (Natorff et al., 2003) while *scon* (*A, B, C* and *D*) genes encode for negative-acting regulatory proteins (Natorff et al., 1993). SconB shows high similarity with Met30 in *S. cerevisiae*. Both proteins contain a F-box motif that binds to a Skp1 protein, which is a subunit of multiprotein ubiquitin ligases (SCF complexes) (Natorff et al., 1998). In *S. cerevisiae*, SCF^{Met30} complex targets Met4 (MetR ortholog) for degradation by the 26S proteasome when intracellular SAM increases (Rouillon et al., 2000). Similarly, SCF^{SconB} complex represses MetR activity when excess cysteine is present in *A. nidulans* (Natorff et al., 1998). SconC belongs to the Skp1 family proteins and was proposed to interact with SconB (Piotrowska et al., 2000). SCF complexes also contain a scaffold protein (Cdc53/cullin), a RING finger protein and a ubiquitin conjugating enzyme (Figure 1.8) (Sieńko et al., 2014).

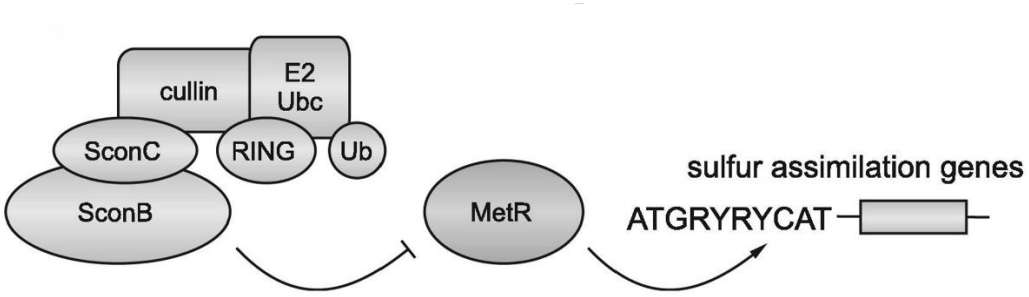

Figure 1.8: Regulation of sulphur metabolism in *A. nidulans* by catabolite repression (Image from Sienko et al., 2014).

Genes regulated by MetR include *sB* (sulphate permease), *sC* (ATP sulphurylase), *cysB* (cysteine synthase) and *cysD* (homocysteine synthase) (Natorff et al., 2003). Deletion of *cysB* and *scon* genes (*sconB* and *sconC*) cause a shortage of cysteine and a derepression of MetR-dependent genes in *A. nidulans* (Sieńko et al., 2014). All three mutants have shown an overproduction of sulphide and an up-regulation of sulphide:quinone reductase which is involved in sulphide detoxification. Additionally, functional categories overrepresented in the mutants compared to wild-type strain included genes from the carbohydrate and energy metabolism, particularly trehalose synthesis and degradation, which is known to occur in response to stress (Sieńko et al., 2014). Overall Sienko et al. (2014) observed that the dysregulation of genes in Δ*cysB*, Δ*sconB* and Δ*sconC* overlapped in most functional categories and hypothesised that despite each mutation have a different defect in sulphur metabolism, all of them lead to elevated sulphide production and activation of the stress response.

In *A. fumigatus*, MetR is required for assimilation of inorganic sulphur sources as a Δ*metR* mutant was unable to grow in the presence of sulphate (SO_4^{2-}) as a sole source of sulphur or any other inorganic sulphur source (S^{2-}, SO_3^{2-}, thioSO_3^{2-} and nitrophenylSO_4^{2-}) (Amich et al., 2013). On the contrary, *A. fumigatus* wt and Δ*metR* grew at a similar rate on medium containing organic sulphur sources like methionine, cysteine or glutathione (Amich et al., 2013). This group also observed that MetR was required for the utilisation of volatile sulphur compounds derived from methionine catabolism as a source of sulphur (Amich et al., 2013). An interesting regulatory crosstalk between sulphur assimilation and iron homeostasis was observed whereby in *A. fumigatus* Δ*metR* several genes involved in iron acquisition (*sidA*, *mirB*, *amcA* and *hapX*) were up-regulated despite enough iron was present in the media, thus confirming Δ*metR* strain has a defect in iron regulation (Amich et al., 2013).

A new transcriptional regulator has been identified and characterised in *A. nidulans* by Pilsyk et al. (2015). It was named MetZ and it contains a bZIP domain similar to that from MetR. Overexpression of *metZ* in a Δ*metR* mutant strain appeared to partially complement the phenotype of Δ*metR* by activating genes encoding for sulphate permeases and homocysteine synthase (Piłsyk et al., 2015).

Gerke et al. (2012) observed that overexpression of *sasA* in *A. nidulans* results in altered sterigmatocystin (fungal secondary metabolite) production. Moreover, protein interaction studies of SasA were carried out using tandem affinity purification (TAP) technology which revealed double tagged VelB-VeA as a putative partner. Both of these proteins are involved in the regulation of secondary metabolism in fungi thus these observations are indicative of a crosstalk between sulphur metabolism and secondary metabolism (Gerke et al., 2012).

In the bacterium *Saccharopolyspora spinosa*, *metE* encodes for a cobalamin-independent methionine synthase and it produces a secondary metabolite known as spinosad. When spinosad accumulates in fermentation broths, proteomic analysis has shown the increased abundance of MetE (Yang et al., 2014). Another association between methionine biosynthesis and secondary metabolism was established and from there, comparative proteomic studies of Δ*metE* and wild-type have been carried out to elucidate how the metabolic network of *S. spinosa* adapts to *metE* absence (Yang et al., 2015). These studies revealed an enrichment of functional categories involved in primary metabolism and genetic information processing in the Δ*metE* mutant strain compared to the wild-type and prove the importance of MetE in the overall regulation of the cell (Yang et al., 2015).

Deletion of another cobalamin-independent methionine synthase (*met6*) was performed by Saint-Macary et al. (2015) in the pathogenic fungus *Magnaporthe oryzae*. *M. oryzae* is the causative agent of several crop related diseases (rice) and analysis on this mutant (Δ*met6*) were carried out to establish the influence of this enzyme in the pathogenicity of the fungus. It was observed that the mutant strain was non-pathogenic and that upon addition of exogenous methionine and SAM, the pathogenic phenotype was restored (Saint-Macary et al., 2015). In addition, the levels of SAM related metabolites (cysteine, cystathione, Hcy, SAM and SAH) were increased in *M. oryzae* Δ*met6*, which could be explained by an increased activity of the transsulphuration pathway (Saint-Macary et al., 2015).

1.6 SAM dependent Methyltransferases (SAM-MTases)

Methylation is a process where a methyl group (-CH_3) replaces a hydrogen atom from strong nucleophiles like R-OH, R-OOH, R-NH_2 and R-SH, among others (Bauerle et al., 2015) (Figure 1.9). In most reactions, SAM is the source of methyl groups whereby the transfer of -CH_3 generates SAH that can be recycled in the methionine cycle (Figure 1.7). This process is catalysed by SAM-MTases which depending on the atomic target they are classified into *C*-, *N*-, *O*- and *S*-MTases. These enzymes act in a wide range of substrates such as proteins (including histones), DNA and RNA, thus they are involved in many important cellular functions like signal transduction, protein repair, chromatin regulation and gene silencing (Schubert et al., 2003). SAM MTases are also involved in the methylation of natural products derived from primary of secondary metabolism (Liscombe et al., 2012).

A

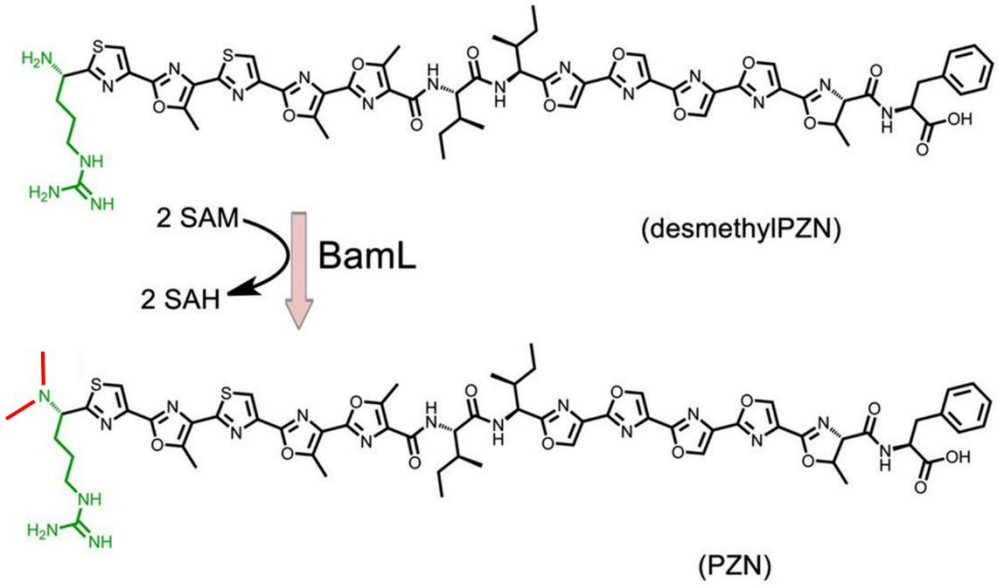

B

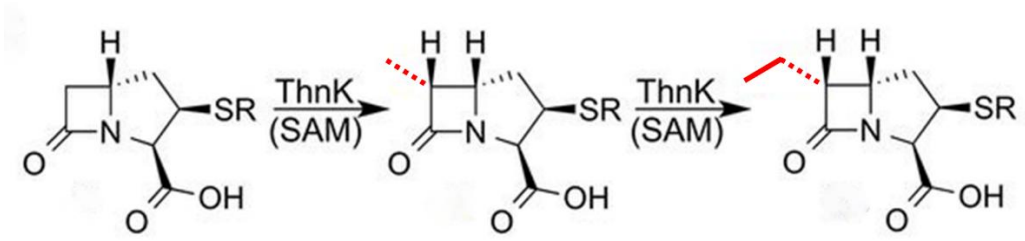

C

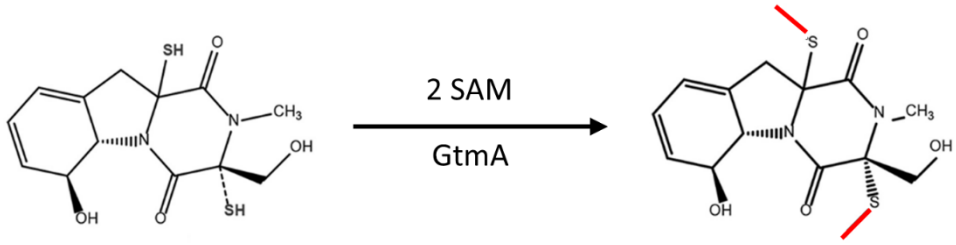

Figure 1.9: *N*-, *C*- and *S*- methylations of natural products. Methyl groups (-CH_3) are represented in red. **(A)** *N*-methylation of dimethylplantazolizin by BamL to form plantazolicin (Lee et al., 2013). **(B)** Consecutive methylations at a C-residue of a carpabenem intermediate by ThnK (Marous et al., 2015). **(C)** *S*-methylation of GT by GtmA to form a bis-methylated product in *A. fumigatus* (Dolan et al., 2014).

1.6.1 Natural product methyltransferases

Natural product methyltransferases (NPMTs) can catalyse the methylation of small molecules like cofactors, pigments, antibiotics and signalling compounds. Thus methylation has an important role in the functionality of cellular metabolism. The most abundant NPMTs are *O*-MTases (54 %), followed by *N*-MTases (23 %), *C*-MTases (18 %) and *S*-MTases (3 %) (Liscombe et al., 2012).

Several *O*-, *N*- and *C*- methyltransferases are part of the biosynthetic machinery of secondary metabolites (SM). Coenzyme A (CoA) esters and carboxylic acids of phenylpropanoids, flavonoids and alkaloids constitute the most common substrates for *O*-MTases in plants (Lam et al., 2007). Two *O*-MTases (VvOMT1 and VvOMT2) isolated from Cabernet Sauvignon grapes have been shown to methylate hydroxypyrazines (HP). As HP is the precursor of methoxypyrazines (MPs), which are synthesised as a SM during amino acid metabolism and confer herbaceous properties to some wines, these MTases can have important applications in conferring flavour to wine (Dunlevy et al., 2010).

The biosynthetic pathway of thienamycin, a carbapenem antibiotic produced by *Streptomyces cattleya*, has remained largely unknown. Only two enzymes (ThnE and ThnM) have been identified and are known to catalyse the first two steps of this pathway. Recently, a third enzyme (ThnK) was shown to perform the SAM-dependent

methylation of a biosynthetic substrate intermediate ((2R,3R,5R)-carbapenam) at C6 (Marous et al., 2015). Interestingly, ThnK appeared to carry out two sequential methylations ultimately generating an ethyl chain at C6 (Marous et al., 2015) (Figure 1.9).

Another SAM-dependent methyltransferase (BamL) was identified and characterized in *Bacillus amyloliquefaciens*. BamL catalyses the SAM dependent double methylation of *N*-terminal arginine residues of dimethylplantazolizin to form plantazolicin (PZN) and SAH (Lee et al., 2013) (Figure 1.9). PZN is a polyheterocyclic antibiotic with bactericidal activity towards anthrax causative agent (*B. anthracis*). The enzyme was highly selective to desmethylPZN or very similar substrates. The importance of BamL was confirmed by the observation that deletion of the MTase gene yielded an intermediate (desmethylPZN) lacking antibiotic activity (Lee et al., 2013). As mentioned in Section 1.4, SAM-dependent MTase, GliN, is part of the gliotoxin biosynthetic machinery of *A. fumigatus*, where it methylates an amide residue which confers stability to the ETP (Scharf et al., 2014).

S-methylation is a less common type of modification mainly associated with the detoxification of xenobiotic thiols in bacteria, plants and mammals (Li et al., 2012a; Zhao et al., 2012). Carried out by *S*-MTases, also known as Thiol MTases (TMT), they can detoxify a broad range of reactive thiols through the formation of less reactive thiomethyl derivatives (Attieh et al., 2000b; Dolan et al., 2014).

The bacterium *Streptomyces clavuligerus*, produces a dithiolopyrrolone class of antibiotic known as holomycin. The biosynthesis of this natural product requires of a dithiol oxidase (HlmI) that closes the disulphide bridge of dihydroholomycin (holomycin precursor) to form the bicyclic oxidised form (holomycin). Deletion of

hlmI would presumably lead to the accumulation of the toxic intermediate dihydroholomycin, however, a methylated form of this metabolite (*S*-methylated-dihydroholomycin) was identified. Thus, it was hypothesised that a SAM-dependent MTase was methylating the free thiols in order to deal with the toxicity of dihydroholomycin (Li et al., 2012a). However, so far, the identification of this enzyme has remained elusive.

A novel role of a fungal *S*-MTase (GtmA) was found by Dolan et al. (2014). GtmA was identified and characterized in *A. fumigatus* to behave as a negative regulator of gliotoxin biosynthesis whereby Δ*gtmA* resulted in an increase in gliotoxin production. This was the first demonstration of a *S*-MTase from *A. fumigatus* involved in the regulation of secondary metabolite GT, and not self-protection (Figure 1.9) (Dolan et al., 2014).

The *S*-methylation of small molecules will be discussed in more detail in Chapter 5.

1.6.2 Secondary metabolism regulators: role in methylation

Biosynthetic and regulatory genes encoding for fungal secondary metabolites (SM) appear clustered within the genome of the organism. LaeA, a putative SAM-MTase, is the global regulator of secondary metabolism and it is responsible for the control of several SM clusters including sterigmatocystin (ST), penicillin, lovastatin and gliotoxin in several *Aspergillus spp*. (Bok and Keller, 2004). Deletion of *laeA* in *A. nidulans*, *A. fumigatus* and *A. flavus* have demonstrated that this enzyme was regulating a significant amount of SM clusters (~50 %) (Bok and Keller, 2004; Kale et al., 2008; Perrin et al., 2007). A SAM-binding site mutant of LaeA was generated and resulted in loss of functionality. Due to the location of this regulator in the nucleus

it has been hypothesised to behave as a histone MTase (Bok and Keller, 2004; Bok et al., 2006). Biochemical identification of methylation substrates for LaeA have not been described so far. A novel automethylation reaction was observed at a methionine residue situated close to the SAM binding site of LaeA in *A. nidulans* which could indicate that this process occurs due to the absence of appropriate substrates or as a self-regulatory mechanism (Patananan et al., 2013).

LaeA is part of the velvet complex composed of LaeA, VeA and VelB that couples differentiation (asexual and sexual) and secondary metabolism in fungi (Figure 1.10) (Bayram et al., 2008). In addition, LaeA regulates another velvet complex (VelB-VosA) which takes part in the repression of asexual development (Sarikaya Bayram et al., 2010). Several interacting partners have been identified for VeA, most of them are SAM-MTases with high homology to LaeA. These include LlmF (LaeA-like MTase F), VipC (velvet interacting protein), and VapB (VipC associated protein B (Palmer et al., 2013; Sarikaya-Bayram et al., 2014, 2015).

LlmF was found to negatively regulate ST production, and despite its SAM motif is required for functionality, no methylation substrate has been identified yet (Palmer et al., 2013). VipC and VipD form a heterodimer complex that interacts with VeA resulting in decreased secondary metabolism. Moreover, VapB was observed to play a role in heterochromatin regulation (Figure 1.10) (Sarikaya-Bayram et al., 2014).

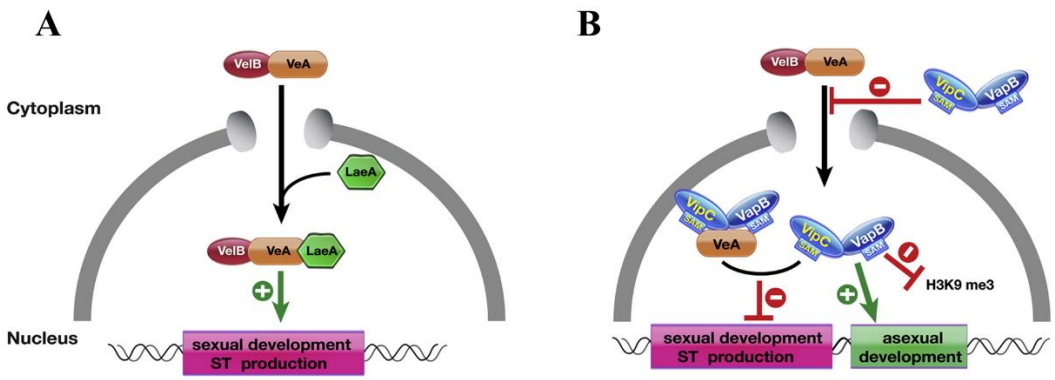

Figure 1.10: SAM-MTases regulate fungal secondary metabolism **(A)** VelB-VeA-LaeA trimetic complex positively regulates secondary metabolism (sterigmatocystin (ST) production) and sexual development. **(B)** VeA recruits MTases VipB-VipC thereby reducing SM production and activating asexual genes. The complex also affects histone posttranslational modifications (H3K9me3) (Sarikaya-Bayram et al., 2014).

1.7 Epigenetic regulation in filamentous fungi

DNA within the nucleus of an organism interacts with a number of proteins to form chromatin. The fundamental unit of chromatin is the nucleosome, which consist on DNA wrapped around a core of histones (two copies of H2A, H2B, H3 and H4). The nature of chromatin can be regulated by posttranslational modifications on histones and interactions with other proteins (Goto and Nakayama, 2012). Loosely packed chromatin is termed euchromatin and it is accessible for transcription while heterochromatin is referred to the tightly packed chromatin which is not available for transcription (Figure 1. 11). Histones have long tails that extend from the nucleosomes that can be covalently modified at different amino acid residues through modifications

such as methylation, acetylation or phosphorylation. These posttranslational modifications are heritable and do not require changes in the DNA sequence, thus they are denoted as epigenetic modifications. Most posttranslational modifications are found in H3 tails, specially at lysine 4 (H3K4) and lysine 9 (H3K9). Typical histone modifications associated with active transcription (euchromatin) include the hyperacetylation of lysine 4 and 9 residues (K4 and H9) of H3 and the trimethylation of H3K4 (H3K4me3) (Figure 1.11). Gene silencing (heterochromatin) occurs when H3K9 is trimethylated and other K residues are hypoacetylated (Goto and Nakayama, 2012).

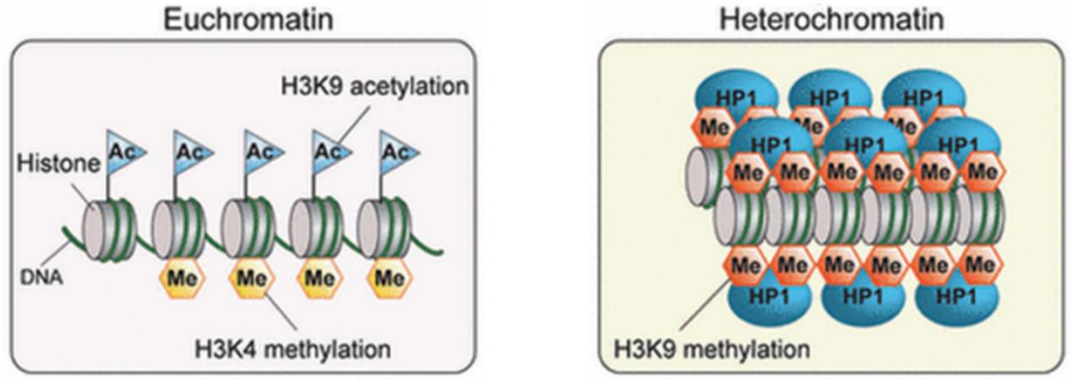

Figure 1.11: Most common histone modifications. Two stages of chromatin. Image adapted from (Goto and Nakayama, 2012).

The field of fungal epigenetics is currently attracting a lot of attention as a tool to improve fungal strains. A recent review by Aghcheh and Kubicek, (2015) discussed potential applications of chromatin regulation on secondary metabolites and hydrolytic enzyme production (Aghcheh and Kubicek, 2015).

1.7.1 Crosstalk of sulphur and secondary metabolism in chromatin regulation

As mentioned earlier efforts towards the identification of LaeA methylation substrates, rather than itself, have been unsuccessful. Its nuclear localisation and function as a regulator of SM gene clusters has led to speculate of an epigenetic control through modifications of chromatin structure (Reyes-Dominguez et al., 2010; Strauss and Reyes-Dominguez, 2011). Recently, two groups have observed the influence of LaeA on histone methylation. In *A. nidulans,* Reyes-Dominguez et al. (2010) deleted *hepA* and *clrD* genes involved in heterochromatin formation which encode for an heterochromatin protein and a H3K9 histone methyltransferase, respectively, and found that mutant strains displayed an overexpression of genes involved in secondary metabolite biosynthesis, especially, sterigmatocystin (ST) biosynthetic genes and the general regulator *laeA* (Reyes-Dominguez et al., 2010). Moreover, they showed that in *A. nidulans* Δ*laeA*, HepA occupancy at the promoter region of ST increased and so did the levels of H3K9 methylation. Thus, they hypothesised towards a role of LaeA in reversing heterochromatin formation by the HepA/ClrD complex (Reyes-Dominguez et al., 2010).

Sarikaya-Bayram et al. (2014) observed that overexpression of nuclear MTase, VapB, caused a decrease in H3K9me3 (gene silencing). Deletion of *vapB* in *A. nidulans* resulted in an increase of H3K9me3 marks at the promoter regions of several genes involved in asexual conidiation regulation, thus it was proposed that VapB played a role in active transcription by interfering with ClrD activity or by increasing demethylase activity at H3K9 residues (Sarikaya-Bayram et al., 2014).

SasA catalyses the biosynthesis of SAM, which is the methyl donor of LaeA and several other MTases. TAP analysis of SasA identified histone-2B as a putative

interaction partner and it was proposed that SasA might affect LaeA function and consequently histone-2B (Gerke et al., 2012).

SAHase is another key enzyme in the maintenance of methylation homeostasis whereby it catalyses the hydrolysis of SAH to Hcy and Ado. SAH is the by-product of methylation reactions, which, if not removed by SAHase, can interfere with MTases and competitively inhibit their activity. Such scenario was described in *Arabidopsis* where a missense mutation of the *SAH* gene resulted in reduced methylation of non-GC sequences that are under the control of CMT3 DNA MTase (Mull et al., 2006). These authors described that, the susceptibility of the methylation process by SAH perturbations was due to the requirement of a CMT3 pathway that uses of two enzymes, SUVH H3 K9 MTase and CMT3 cytosine MTase, which guide DNA methylation to the cytosine residue. This work led the authors to propose that controlled SAH downregulation could be a useful tool for dissecting regions in the genome controlled by the interplay between histone and DNA methylations (Mull et al., 2006).

1.7.2 Epigenetics of hydrolytic enzyme production

Genome sequence analysis of *T. reesei* showed that many genes encoding carbohydrate-active enzymes (CAZymes) are clustered in discrete (non-continuous) regions with genes encoding non-ribosomal polypeptide synthases (NRPS) and polyketide synthases (PKS) (Martinez et al., 2008). Due to the regulatory control of LaeA on SM gene clusters, deletion of *T. reesei lae1* (*A. nidulans laeA* homolog), was carried out by Seiboth et al. (2012). It was found that Δ*lae1* mutant strains showed complete loss of cellulase production (Seiboth et al., 2012). On the other hand, overexpression of *lae1* lead to an increased expression of cellulase gene transcription

(Seiboth et al., 2012). XYR1 is the general regulator of cellulase production, and so the relationship between LAE1 and XYR1 was investigated in *T. reesei*. It was shown that both LAE1 and XYR1 depend on each other as no cellulase production was observed when *xyr1* was overexpressed (OE) in a Δ*lae1* strain or vice-versa (Seiboth et al., 2012). As LAE1 is part of the velvet complex, *vel1*, an homolog of *A. nidulans veA*, was deleted in *T. reesei*. A similar response to that observed in *T. reesei* Δ*lae1* was seen in Δ*xyr1*, whereby expression of cellulases, xylanases and *xyr1* was impaired when grown on lactose or sophorose (Karimi Aghcheh et al., 2014).

Owing to the hypothesis that SM genes are regulated by LaeA at the level of chromatin structure by reversing heterochromatin formation (Reyes-Dominguez et al., 2010; Strauss and Reyes-Dominguez, 2011), histone methylation was investigated in the CAZy coding regions (Aghcheh and Kubicek, 2015; Kubicek, 2013; Seiboth et al., 2012). Chromatin immunoprecipitation in combination with high-throughput sequencing (ChIP-seq) with antibodies against H3K4me2 and H3K4me3 (associated with transcription) and H3K9me3 (associated with gene silencing) was carried out in *T. reesei* wild-type and Δ*lae1*. Though it was observed that some transcribed genes had H3K4me2 and H3K4me3 enrichment and H3K9me9 absence, there was no histone change observed for any of the CAZyme genes affected by LAE1 (Kubicek, 2013; Seiboth et al., 2012). In 2013, the same group published a ChIP-seq analysis on the *T. reesei* wild-type, OE*lae1* (overexpressed *lae1*) and Δ*lae1* where (i) 13 genes exhibited H3K9 methylation in the Δ*lae1* strain but where independent of LAE1 and (ii) 74 genes showed H3K4 methylation and a correlation with LAE1 regulation but no direct implication of LAE1 on epigenetic control in OE*lae1* and Δ*lae1* strains (Karimi-Aghcheh et al., 2013). Thus this authors concluded that the theory proposed for *A.*

nidulans where LaeA counteracts H3K9me3 is somehow unlikely for *T. reesei* (Karimi-Aghcheh et al., 2013).

Recently, an interesting observation was made by Mello-de-Sousa et al. (2015) where in *T. reesei* Δ*xyr1*, chromatin appeared more compact compared to the wild-type strain at the promoter regions of some CAZymes. They determined that XYR1 was required for chromatin loosening of two cellobiohydrolases (*cbh1* and *cbh2*) and two xylanases (*xynI* and *xynII*) genes, when grown on sophorose (inducing conditions) (Mello-de-Sousa et al., 2015).

The impact of secondary metabolite regulators (velvet complex) on CAZymes production has also been observed in *Aspergillus spp*. Targeted studies on cell wall polysaccharides, have revealed that in the absence of *velB* or *vosA* there is an increase in the up-regulation of *gelA*, *gelB* and *fksA*, which are involved in β-1,3-glucan biosynthesis. Additionally, chromatin-immuno-precipitation (ChIP) studies indicated that tagged proteins VelB and VosA accumulated at the promoter region of *fksA* (β-1,3-glucan synthase). A model was proposed whereby the VosA-VelB complex represses β-glucan synthesis through its binding to promoter regions of cell wall biosynthetic genes (Park et al., 2015). It is noteworthy that in *A. nidulans* Δ*vosA* there is an increase in the expression of genes associated to ST biosynthesis compared to wild-type. Due to the variability of the velvet complexes, the authors suggested the formation of the VelB-VeA-LaeA instead of VosA-VelB (Park et al., 2015).

Comparative proteomic analysis of *A. flavus* wild-type and Δ*veA* grown on starch, revealed a production of glucose in the wild-type but an accumulation of maltose and maltotriose in the mutant (Duran et al., 2014). This was corroborated by a high glucoamylase activity (which cleaves α-(1,6) and α-(1,4)-glycosidic bonds of

amylose and amylopectin, releasing glucose) in the wild-type compared to Δ*veA*. Additionally, an increase in expression of α-amylase was observed in the mutant strain which could compensate for the reduction of glucoamylase activity and account for the observed accumulation of maltose and maltotriose (Duran et al., 2014). Deletion of *laeA* in *A. flavus* resulted in a similar response to that observed for Δ*veA* with a reduction of glucoamylase activity. These results clearly suggest a key role for the velvet complex on amylase production (Duran et al., 2014).

In *A. nidulans*, mRNA levels of an α-mutanase (α-1,3 glucanase) encoding gene, *mutA*, were significantly reduced in a Δ*laeA* strain compared to wild type. It was observed that sGFP (synthetic green fluorescent protein) labelling of MutA showed a signal during the late stages of vegetative growth and development in wild type while there was no signal detected for Δ*laeA* (Sarikaya Bayram et al., 2010).

Work investigating a cellulase gene of *Magnaporthe oryzae* (*MoCel7C*) when grown in different substrates indicated an up-regulation of the cellulase gene when grown in carboxymethylcellulose (CMC) compared to the growth on standard medium (Vu et al., 2013). It was observed a H3K4 methylation at the locus of *MoCel7C* occurred under CMC addition (Vu et al., 2013).

An interesting regulatory crosstalk between sulphur metabolism and cellulase gene expression was shown in *H. jecorina*, whereby a putative E3 ubiquitin ligase (LIMPET) (homolog of *S. cerevisiae Met30*) was identified as a binding protein to the promoter region of the cellobiohydrolase (*cbh2*) gene (Gremel et al., 2008). *limpet* was also responsive to growth on cellulase inducing conditions (sophorose as the carbon source) and sulphur limitation (Gremel et al., 2008).

1.8 Endoplasmic Reticulum Quality Control (ERQC) System

As previously mentioned, *A. niger* is a natural cell factory for secretory proteins. Both secreted and membrane proteins fold in the lumen of the endoplasmic reticulum (ER) where they reach their native and functional conformation (Deng et al., 2013). The Sec61 complex (translocon) is responsible for the translocation of nascent polypeptides into the lumen where protein folding is started (Rapoport, 2007). Here, various molecular chaperones and enzymes (e.g. foldases), some of which are members of the ER quality control (ERQC), assist protein folding (Thibault and Ng, 2012). Chaperones maintain nascent protein solubility to prevent their aggregation and ease folding (Deng et al., 2013). Many proteins can become glycosylated, after which they are placed into COPII coated vesicles and are delivered to the Golgi, where further modifications can take place. From here the vesicles are transported to the tip of the growing hyphae where they fuse with the plasma membrane and the proteins are released extracellularly (Taheri-Talesh et al., 2008). If the balance between protein folding capacity and demand is altered, unfolded and misfolded proteins accumulate in the ER, causing ER stress (Carvalho et al., 2006; Deng et al., 2013). The ER folding capacity can be compromised by spontaneous errors during transcription and translation as well as cellular stresses like hypoxia, oxidative stress, nutrient limitation or increased temperature (Vembar and Brodsky, 2008). Since the accumulation of unfolded or misfolded proteins are toxic to the cell, their occurrence activates a series of responses kown as unfolded protein response (UPR), which produces factors that aid in protein folding (Deng et al., 2013; Krishnan and Askew, 2014). If the UPR is not enough to relieve stress, proteins are targeted for destruction by the ER-associated degradation (ERAD) pathway (Carvalho et al., 2011).

1.8.1 Unfolded Protein Response (UPR)

The UPR stress response was best characterised in *Saccharomyces cerevisiae* but it is now been studied in a number of filamentous fungi including *A. niger* (Krishnan and Askew, 2014; Mulder et al., 2004). This response is aimed towards maintaining the fidelity of the protein folding activities of the ER and its main aspects are conserved from yeast to mammals (Krishnan and Askew, 2014).

In *S. cerevisiae* Ire1 (inositol-requiring protein-1) is an ER-localised transmembrane protein with a cytosolic domain linked to an endoribonuclease (RNase) and a stress sensing luminal domain (Korennykh and Walter, 2012). Under normal conditions, Ire1 (IreA in *A. niger*) is bound to BiP (a Hsp70 type chaperone) which maintains Ire1 in an inactive state (Figure 1.12). When the ER is stressed, BiP dissociates from Ire1 allowing for Ire1 dimerization and activation of the cytoplasmic domain by transautophosphorylation which activates the RNase domain (Krishnan and Askew, 2014). RNase activity splices an unconventional intron from *hac1* mRNA that allows for translation into a bZIP transcription factor Hac1 (Figure 1.12) (Krishnan, 2014). Hac1 then migrates into the nucleus where it binds to UPR elements (UPREs) and other sequences in the promoter region of target genes inducing their expression (Figure 1.12) (Vembar and Brodsky, 2008).

In *A. niger*, HacA (Hac1 ortholog) targets the promoters of genes encoding for ER-localised chaperones and foldases as well as the *hacA* gene itself (Mulder et al., 2004). Recently, a $HacA^{CA}$ mutant (^{CA} stands for constitutively active) was generated in *A. niger* and compared transcriptionally to a wild type strain to identify HacA responsive genes (Carvalho et al., 2012). Up-regulation of genes involved in protein

glycosylation, intracellular protein transport, exocytosis and protein complex assembly was observed in the $HacA^{CA}$ mutant (Carvalho et al., 2012).

Importantly, the UPR can be induced by agents like tunicamycin (TM) or DTT under laboratory conditions. In *A. niger*, the UPR has been widely studied as it is induced when ER stress occurs in the cell. This type of stress in a known bottleneck for the expression of homologous and heterologous proteins (Carvalho et al., 2012; Guillemette et al., 2007; MacKenzie and Guillemette, 2005).

Despite UPR activation, some proteins will fail to attain their proper conformation (Krishnan et al., 2013). These abnormal proteins can form aggregates in the ER which can cause stress in the lumen and are disposed through ER-associated degradation (ERAD), a pathway that directs unfolded proteins to the proteasome (Krishnan and Askew, 2014).

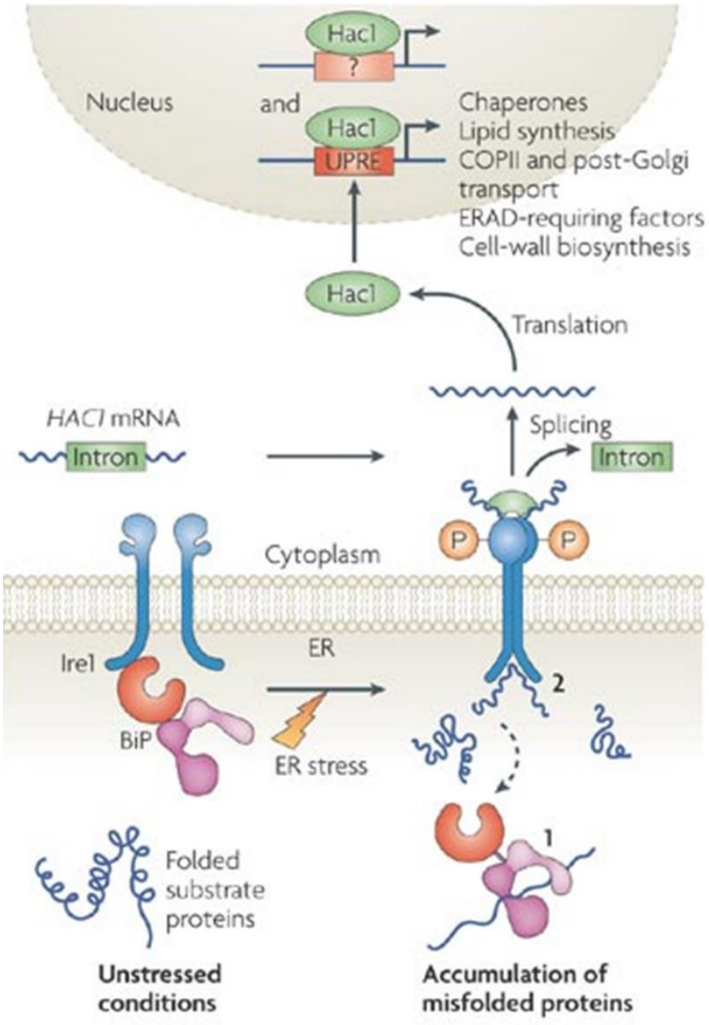

Figure 1.12: The yeast unfolded protein response. Image from Vembar et al., 2008.

1.8.2 Endoplasmic Reticulum Associated Degradation (ERAD)

Misfolded or unassembled proteins can be targeted for proteasomal degradation through the ERAD pathway, where substrates are polyubiquitinated and transferred to the cytosol (Figure 1.13). In *S. cerevisiae*, it was observed that location of a lesion in a protein dictates the type of ERAD pathway the substrate is going to use. When the misfolded domain is located in the cytoplasmic side of the ER, in the lumen or in the membrane of the ER they follow the ERAC-C, ERAC-L and ERAC-

M, respectively (Figure 1.13) (Carvalho et al., 2006; Huyer et al., 2004; Vashist and Ng, 2004). ERAD-L and ERAD-M require a complex embedded in the ER membrane, known as the Hrd1 complex, while ERAD-C requires of the Doa10 complex (Figure 1.13) (Thibault and Ng, 2012). These complexes bear receptors which recognise misfolded substrates and constitute the ERAD degradation signal (Ruggiano et al., 2014).

A

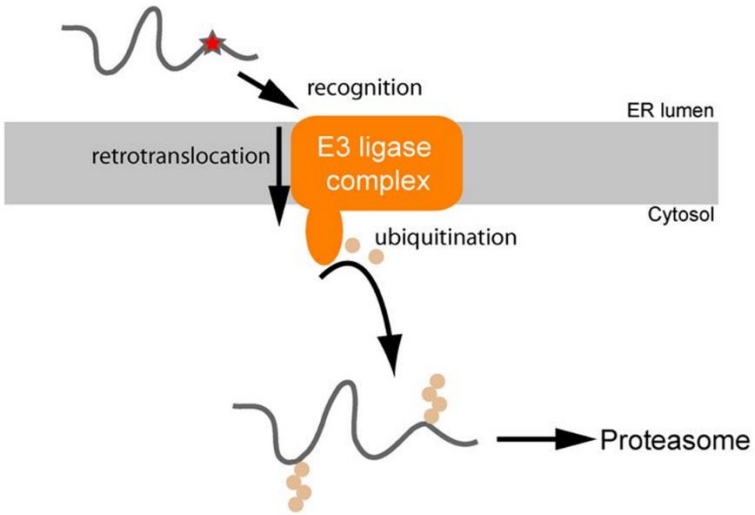

B

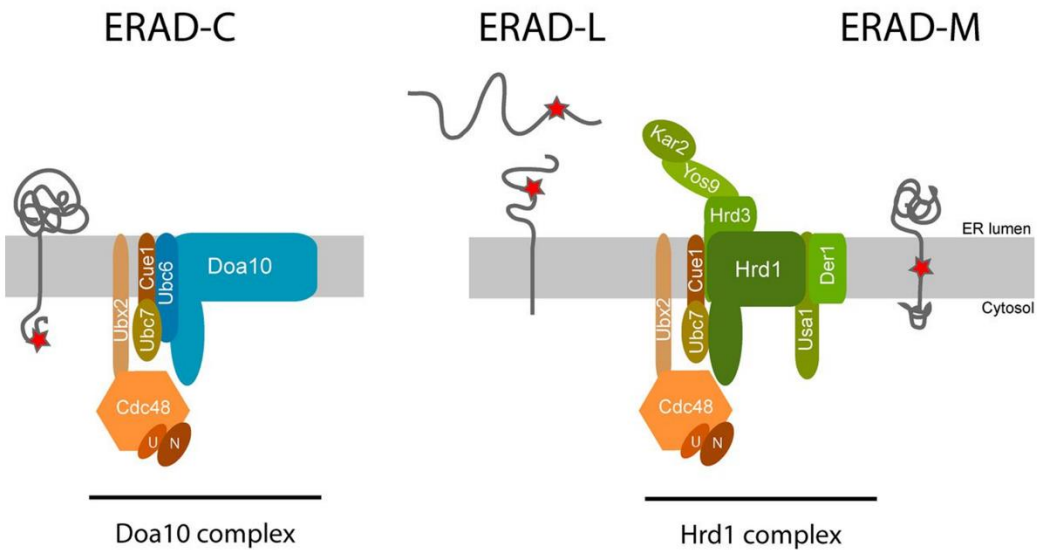

Figure 1.13: ERAD pathway **(A)** Schematic of protein degradation through ERAD. **(B)** Different ERAD pathways based on the location of the misfolded domain (shown in red). Proteins with a misfolded domain in the cytoplasm are degraded through the Doa10 complex while proteins with abnormal domains in the lumen or membrane region use the Hrd1 complex. Both complexes are named based on a ubiquitin ligase (Doa10 and Hrd1 ubiquitin ligase). Figure obtained from Fuggiano et al. (2014).

Once luminal proteins are selected by ERAD, they need to be fully retrotranslocated across the ER membrane into the cytoplasm where the proteasome is located. In the case of membrane substrates, only certain domains of the polypeptide require transport into the cytosol (Ruggiano et al., 2014). Thus, ubiquitination of substrates, will occur at late stages of retrotranslocation for luminal proteins while it will be generally simultaneous in the case of membrane proteins (Burr et al., 2013). A model was proposed in which Hdr1 induces ubiquitination of substrates at the cytoplasmic side of the ER membrane that signals the recruitment of the ATPase

complex (Figure 1.13). In yeast, this complex is composed of Cdc48 and cofactors Ufd1 and Npl4 that hydrolyse ATP and provide the mechanical force to move the ubiquitinated substrates fully out of the membrane into the cytosol (Ye, 2003). Ultimately, polyubiquitinated substrates are transferred to the proteasome where they are degraded (Figure 1.13).

The ERAD pathway has been studied in fungi, particularly in *A. niger* protein overproducing strains in terms of its impact on heterologous protein production. In work carried out by Carvalho et al. (2011), certain genes of the ERAD pathway, including *derA*, *doaA*, *hrdC*, *mifA* and *mnsA*, were deleted and compared to their parental strain under ER-stress conditions (Tunicamycin and DTT). Surprisingly, although it was expected that deletion of these genes would cause significant ER-stress, no apoptotic phenotype was observed and authors concluded that alternative pathways besides ERAD might be playing a role in the removal of misfolded proteins (Carvalho et al., 2011).

In *A. fumigatus*, deletion of *hrdA* (*hrd1* homolog) was shown to activate of the UPR response and conferred resistant to voriconazole (Krishnan et al., 2013).

1.9 Thesis Rationale and objectives

GT is an ETP class of toxin majorly produced by *A. fumigatus* that has redox-cycling capacity, antifungal activity and it has been established as a virulence factor in Aspergillus-related infections affecting immunocompromised individuals (Carberry et al., 2012; Coleman et al., 2011; Dagenais and Keller, 2009; Gardiner et al., 2005; Sugui et al., 2007). Research on GT has mainly focused on deciphering the mechanism

of biosynthesis of this toxin and several deletion strategies have been performed on genes within the *gli* cluster (Davis et al., 2011; Gallagher et al., 2012; Scharf et al., 2010; Schrettl et al., 2010b; Wang et al., 2014). These investigations have considerably dissected this biosynthetic machinery and shown a fundamental self-protection strategy present in *A. fumigatus* against the deleterious effects of its own toxin (Scharf et al., 2010; Schrettl et al., 2010b; Wang et al., 2014). Work carried out by O'Keeffe et al. (2014) was the first large scale transcriptomic approach performed on *A. fumigatus* Δ*gliT* targeted to understand cellular processes involved in self-protection against GT.

Other fungal organisms like *S. cerevisiae* have been used to screen genes linked with GT resistance and sensitivity as mammalian model systems (Chamilos et al., 2008). The effect GT has on other fungi has considerably lacked attention as only phenotypic studies have been carried out to prove the antifungal properties of GT, with no focus on the cellular processes affected in the organism (Carberry et al., 2012; Coleman et al., 2011).

It thus appears that the mechanism of GT cytotoxicity is mostly studied in *Aspergillus spp*. (*A. fumigatus*) producing this toxin, where self-protection mechanisms (e.g. GliT and GliA) are operating and not in GT-naïve fungi.

Therefore, the objectives of this thesis are as follows;

1. To use *A. niger* as an alternative model for the study of GT cytotoxicity as it does no produce GT.
2. Perform Label-free quantitative (LFQ) proteomic analysis of *A. niger* exposed to GT coupled to comparative metabolite analysis of selected metabolic

pathways under the same conditions to determine the response of *A. niger* to exogenous GT.

3. Characterise a putative SAM-dependent methyltransferase identified from the proteomic analysis and assess functionality within *A. niger* exposed to GT.
4. To assess if the response of A. niger to GT can inform on recombinant protein overexpression.
5. To exploit fungal natural products like siderophores as biomarkers of infection. Develop an enzyme-linked immunosorbent assay (ELISA) system for the quantification of siderophore (FusC) and evaluate this peptide as an indicator of fungal infection.

Chapter 2

Materials and Methods

2 Materials and Methods

2.1 Materials

All chemicals were purchased from Sigma-Aldrich Chemical Co. Ltd. (UK), unless otherwise stated.

2.1.1 Solutions for pH Adjustment

2.1.1.1 5 M Hydrochloric Acid (HCl)

Hydrochloric acid (43.64 ml) was added to deionised water (40 ml) in a glass graduated cylinder. The final volume was adjusted to 100 ml with deionised water. The solution was stored at room temperature.

2.1.1.2 5 M Sodium Hydroxide (NaOH)

NaOH (20 g) was added to deionised water (80 ml). The solution was mixed and brought to a final volume of 100 ml with deionised water. The solution was stored at room temperature.

2.1.2 *Aspergillus* Media and Agar

2.1.2.1 Potato Dextrose Broth (PDB)

Potato dextrose broth (24 g) was added to 800 ml distilled water, mixed and made up to 1L. The solution was autoclaved at 121 ºC for 15 min and stored at 4 ºC.

2.1.2.2 Potato Dextrose Agar (PDA)

Agar (9 g) (Fisher Chemical) was added to 500 ml Potato Dextrose Broth (Section 2.1.2.1). The solution was autoclaved at 121 ºC for 15 min and allowed to

cool to ~50 ºC before being poured into 90 mm Petri dishes under sterile conditions. The plates were allowed to set and were stored at 4 ºC.

2.1.2.3 Malt Extract Agar (MEA)

Malt extract agar (50 g) (Oxoid Ltd, Hants, England) was dissolved in 1 L of distilled water. The solution was autoclaved at 115 ºC for 10 min and allowed to cool to ~50 ºC before being poured into 90 mm Petri dishes under sterile conditions.

2.1.2.4 *Aspergillus* Minimal Media (AMM)

2.1.2.4.1 *Aspergillus* Trace Elements

$Na_2B_4O_7.10H_2O$ (40 mg), $CuSO_4.5H_2O$ (400 mg), $FeSO_4.7H_2O$ (800 mg), $Na_2MoO.2H_2O$ (800 mg), $ZnSO_4.H_2O$ (8 g) were dissolved in order in 800 ml distilled water, allowing each to dissolve completely before addition of the next component. The solution was brought to a final volume of 1 L with distilled water. The solution was filter sterilised into 50 ml aliquots and stored at -20 ºC.

2.1.2.4.2 50 X *Aspergillus* Salt Solution

KCl (26 g), $MgSO_4.7H_2O$ (26 g) and KH_2PO_4 (76 g) were dissolved in 800 ml distilled water. The solution was brought to 1 L with distilled water and autoclaved at 121 ºC for 15 min. The solution was stored at room temperature.

2.1.2.4.3 100 X Ammonium Tartrate

Ammonium tartrate (92 g) was dissolved in 1 L distilled water and autoclaved. The solution was stored at room temperature.

2.1.2.4.4 AMM Liquid Media

Aspergillus Trace Elements (1 ml) (Section 2.1.2.4.1), 50 X *Aspergillus* Salt Solution (20 ml) (Section 2.1.2.4.2), 100 X Ammonium tartrate (10 ml) (Section 2.1.2.4.3) and glucose (10 g) were added to 800 ml distilled water and dissolved. The pH of the solution was adjusted to 6.8 and made up to a final volume of 1 L with distilled water. The solution was autoclaved at 105 ºC for 30 min and stored at room temperature.

2.1.2.4.5 AMM Agar

Agar (9 g) (Fisher Chemical) was added to 500 ml of AMM Liquid media (Section 2.1.2.4.4) before it was autoclaved at 105 ºC for 30 min. The solution was allowed to cool to ~60 ºC before being poured (25 ml) into 90 mm sterile Petri dishes, under sterile conditions. The plates were allowed to set and stored at 4 ºC.

2.1.2.5 Transformation Media

2.1.2.5.1 Trace Elements

$FeSO_4.7H_2O$ (5 g) and EDTA (50 g) were dissolved in 400 ml of distilled water and pH was adjusted to approximately pH 5.5. To this solution $ZnSO_4.7H_2O$ (22 g), H_3BO_3 (11 g), $MnCl_2.4H_2O$ (5 g), $CoCl_2.6H_2O$ (1.6 g), $CuSO_4.5H_2O$ (1.6 g) and $(NH_4)_6Mo_7)_{24}.4H_2O$ (1.1 g) were added in the order described. The solution was adjusted to pH 6.5 and brought to 1 L with distilled water. The solution was filter sterilised into 50 ml aliquots and stored at 4 ºC.

2.1.2.5.2 50 X Nitrate Salts

$NaNO_3$ (300 g), KCl (26 g), KH_2PO_4 (76 g) and $MgSO_4.7H_2O$ (26 g) were dissolved in 800 ml of distilled water. The solution was adjusted to pH 5.5 with KOH.

2.1.2.5.3 5 % Uridine

Uridine (1.25 g) was dissolved in 25 ml of distilled water. Solution was filter sterilised and stored at 4 ºC.

2.1.2.5.4 Transformation Liquid Media

50 X Nitrate Salts (20 ml) (Section 2.1.2.5.2), glucose (20 g), yeast extract (5 g), casamino acids (2 g) and uracil (1 g) were added to 800 ml distilled water and dissolved. The pH of the solution was adjusted to 6 and made up to a final volume of 1 L with distilled water. The solution was autoclaved at 105 ºC for 30 min and stored at room temperature. After autoclave, trace elements (1 ml) (Section 2.1.2.5.1) and uridine (5 ml) (Section 2.1.2.5.3) were added to 1 L of autoclaved media. The solution was stored at room temperature.

2.1.2.5.5 Transformation Agar

Agar (9 g) (Fisher Chemical) was added to 500 ml liquid media (Section 2.1.2.5.4) before it was autoclaved at 105 ºC for 30 min. The solution was allowed to cool to ~50 ºC before pouring (25 ml) into 90 mm sterile Petri dishes, under sterile conditions. The plates were allowed to set and stored at 4 ºC.

2.1.3 Plate Assays

Plate assays on AMM (Section 2.1.2.4.5) and Transformation Agar (Section 2.1.2.5.5) were used at range of gliotoxin concentrations (Table 2.1).

Table 2.1: Gliotoxin concentration used in plate assays to test for phenotypic alterations in *A. niger*.

Reagent	Stock Concentration	Concentration range used
Gliotoxin	1 mg/ml in Methanol	0 – 10 µg/ml

2.1.4 *E. coli* Media and Agar

2.1.4.1 Luria-Bertani Broth (LB)

LB Broth (25 g) (Difco, Maryland, USA) was dissolved in 1 L distilled water. The solution was autoclaved at 121 ºC for 15 min and stored at 4 ºC.

2.1.4.2 Luria-Bertani Agar (LB Agar)

Agar (9 ml) (Fisher Chemical) was added to 500 ml of LB (Section 2.1.4.1) before it was autoclaved at 121 ºC for 15 min. The solution was allowed to cool to ~50 ºC before pouring (25 ml) into 90 mm sterile Petri dishes, under sterile conditions. The plates were allowed to set and stored at 4 ºC.

2.1.4.3 Terrific Broth (TB)

Terrific Broth (47.6 g) (Difco, Maryland, USA) and glycerol (4 ml) were dissolved in 1 L distilled water. The solution was autoclaved at 121 ºC for 15 min and stored at 4 ºC.

2.1.5 Reagents for *E. coli* protein extraction

2.1.5.1 Leupeptin (1 mg/ml)

Leupeptin (10 mg) was dissolved in distilled water (10 ml). The solution was split into 1 ml aliquots and stored at -20 ºC.

2.1.5.2 Lysozyme (10 mg/ml)

Lysozyme (100 mg) was dissolved in distilled water (10 ml). The solution was split into 1 ml aliquots and stored at -20 ºC.

2.1.5.3 *E. coli* Lysis Buffer

Trizma-base (3.02 g), EDTA (0189 mg), NaCl (2.92 g) and glycerol (50 ml) were dissolved in 400 ml deionised water and adjusted to pH 8. The final volume was brought up to 500 ml with deionised water and stored at 4 ºC. Before use, the solution was brought to 4 µg/ml Leupeptin, 1 mM PMSF and 90 µg/ml Lysozyme by addition of appropriate amounts of the stock solutions (Section 2.1.5.1, 2.1.10.2 and 2.1.5.2).

2.1.5.4 Sodium Deoxycholate (5 % (w/v))

Sodium Deoxycholate (1 g) was dissolved in deionised water (20 ml). The solution was split into aliquots and stored at -20 ºC.

2.1.5.5 0.15 M Sodium Chloride (NaCl)

NaCl (0.9 g) was dissolved in deionised water (100 ml). The solution was stored at -4 ºC.

2.1.5.6 Deoxyribonuclease I (DNase I) (5 KU/ml)

DNase I (15 KU) was dissolved in 0.15 M NaCl (3 ml) (Section 2.1.5.5). The solution was split into aliquots and stored at -20 ºC.

2.1.5.7 2 M Magnesium Chloride

Magnesium Chloride (1.9 g) was dissolved in deionised water (10 ml) and stored at 4 ºC.

2.1.6 Ampicillin (100 mg/ml)

Ampicillin was prepared as stock solution (100 mg/ml) in deionised water and filter sterilised. Prior to use, the stock solution was diluted to a final working concentration of 100 µg/ml.

2.1.7 1 M Isopropyl β-D-Thiogalactopyranoside (IPTG) Stock Solution

IPTG (238 mg) was dissolved in 1 ml deionised water. The solution was filter sterilised using a 0.2 µm filter (Millipore, USA) and stored at -20 ºC.

2.1.8 Phosphate Buffer Saline (PBS)

Ten PBS tablets (Oxoid) were dissolved in 1 L distilled water. The solution was autoclaved at 121 ºC for 15 min and stored at room temperature.

2.1.9 Phosphate Buffer Saline –Tween 20 (0.05 % (v/v)) (PBST 0.05 %)

Tween-20 (500 µl) was added to 1 L PBS (Section 2.1.7). The solution was mixed and stored at room temperature.

2.1.10 Lysis Reagents

2.1.10.1 Pepstatin A (1 mg/ml)

Pepstatin A (10 mg) was dissolved in distilled water (10 ml). The solution was split into 1 ml aliquots and stored at -20 ºC.

2.1.10.2 200 mM Phenylmethylsulfonyl fluoride (PMSF)

PMSF (34.8 mg) was dissolved in methanol (1 ml). The solution was stored at -20 ºC.

2.1.10.3 *A. niger* Mycelial Lysis Buffer; reducing

Tris-HCl (15.7 g), NaCl (2.9 g), EDTA (5.8 g), 10 % glycerol (100 ml) was added to 800 ml deionised water before adjusting the pH to 7.5. The solution was brought to 1 L with deionised water. The solution was stored at 4 ºC. Before use, the solution was brought to 30 mM DTT, 1 mM PMSF and 1 µg/ml Pepstatin A by addition of appropriate amounts of the stock solutions (Section 2.1.10.1 and 2.1.10.2).

2.1.10.4 *A. niger* Mycelial Lysis Buffer; non-reducing

Tris-HCl (15.7 g), NaCl (2.9 g), EDTA (5.8 g), 10 % glycerol (100 ml) was added to 800 ml deionised water before adjusting the pH to 7.5. The solution was brought to 1 L with deionised water. The solution was stored at 4 ºC. Before use, the solution was brought to 1 mM PMSF and 1 µg/ml Pepstatin A by addition of appropriate amounts of the stock solutions (Section 2.1.10.1 and 2.1.10.2).

2.1.11 0.1 M Hydrochloric Acid (HCl)

5 M HCl (4 ml) (Section 2.1.1.1) was added to deionised water (196 ml). Solution was stored at room temperature.

2.1.12 SDS-PAGE Reagents

2.1.12.1 1.5 M Tris-HCl, pH 8.3

Tris-HCl (47.3 g) was dissolved in deionised water (160 ml). The pH was adjusted to pH 8.3. The final volume was brought to 200 ml with deionised water. The solution was stored at 4 ºC.

2.1.12.2 0.5 M Tris-HCl, pH 6.8

Tris-HCl (15.8 g) was dissolved in deionised water (160 ml). The pH was adjusted to pH 6.8. The final volume was brought to 200 ml with deionised water. The solution was stored at 4 ºC.

2.1.12.3 Sodium Dodecyl Sulfate (SDS) (10 % (w/v))

SDS (10 g) was added to distilled water (80 ml) and dissolved. The solution was adjusted to 100 ml with distilled water and stored at room temperature.

2.1.12.4 Ammonium Persulphate (APS) (10 % (w/v))

Ammonium persulphate (50 mg) was added to deionised water (500 µl) and mixed. The solution was stored at 4 ºC and used within 8 h.

2.1.12.5 Bromophenol Blue (1 % (w/v))

Bromophenol blue (0.2 g) was added to distilled water (20 ml). The solution was stored at 4 ºC.

2.1.12.6 Bromophenol Blue (0.5 % (w/v))

Bromophenol blue (0.1 g) was added to distilled water (20 ml). The solution was stored at 4 ºC.

2.1.12.7 5 X Solubilization Buffer

Glycerol (8 ml) was added to deionised water (4 ml), containing 1.6 ml of 10 % SDS (Section 2.1.12.3) and 1 ml of 0.5 M Tris-HCl, pH 6.8 (Section 2.1.12.2). 2-mercaptoethanol (0.4 ml) was added to the solution with 0.2 ml of 0.5 % (w/v) bromophenol blue solution (Section 2.1.12.5). Stored in 1 ml aliquots at -20 ºC.

2.1.12.8 5 X Electrode Running Buffer

Trizma base (30 g), glycine (144 g) and SDS (10 g) were dissolved in deionised water (1600 ml). The final volume was adjusted to 2 L. The solution was stored at room temperature.

2.1.12.9 1 X Electrode Running Buffer

5 X Electrode running Buffer (200 ml) (Section 2.1.11.8) was added to 800 ml distilled water. The solution was stored at room temperature.

2.1.12.10 Coomassie® Blue Stain Solution

Coomassie® Brilliant Blue R (1 g), glacial acetic acid (100 ml), methanol (300 ml) and deionised water (100 ml) were added to a 1 L glass bottle and mixed. The solution was brought to a final volume of 1 L with deionised water and stored at room temperature.

2.1.12.11 Destain Solution

Glacial acetic acid (100 ml) was added to distilled water (600 ml) and methanol (300 ml). The solution was stored at room temperature.

2.1.12.12 Colloidal Coomassie® Stain Solutions

2.1.12.12.1 Fixing Solution

Ethanol (500 ml) and phosphoric acid (30 ml) were added to distilled water (470 ml). The solution was mixed and used within the day.

2.1.12.12.2 Incubation Buffer

Ammonium sulphate (170 g), methanol (340 ml) and phosphoric acid (30 ml) were added to deionised water (400 ml). The solution was mixed and brought to 1 L with deionised water. The solution was made up fresh on the day.

2.1.13 Western Blot Reagents

2.1.13.1 Towbin Electrotransfer Buffer

Trizma base (6.06 g) and glycine (28.8 g) were added to 200 ml methanol and 600 ml distilled water. The solution was brought to 1 L with distilled water and stored at room temperature.

2.1.13.2 Blocking solution

Marvel® (Powdered milk) (1 g) was added to PBST 0.05 % (v/v) (20 ml) (Section 2.1.9).

2.1.13.3 Antibody Buffer

Marvel® (Powdered milk) (200 mg) was added to PBST 0.05 % (v/v) (20 ml) (Section 2.1.9).

2.1.13.4 3,3'-Diaminibenzidine (DAB) Substrate Buffer

Tris-HCl (3.15 g) was added to distilled water (150 ml) and dissolved. The pH of the solution was adjusted to pH 7.6. The final volume was brought to 200 ml and stored at 4 ^{o}C.

2.1.14 Bradford Solution

Bradford Reagent (BioRad) was diluted 1/5 in PBS. This was stored at 4 ºC for up to one week.

2.1.15 DNA Electrophoresis Reagents

2.1.15.1 50 X Tris-Acetate Buffer (TAE)

Trizma base (242 g) was added to deionised water (700 ml) and mixed until dissolved. Glacial acetic acid (57.1 ml) and 0.5 M EDTA (pH 8) (100 ml) were added and mixed. The volume was adjusted to 1 L with distilled water. The solution was stored at room temperature.

2.1.15.2 1 X Tris Acetate Buffer (TAE)

50 X TAE (20 ml) (Section 2.1.15.1) was added to distilled water (980 ml). The solution was stored at room temperature.

2.1.15.3 Ethidium Bromide

Ethidium bromide was supplied at 10 mg/ml, of which 3 µl was used per 100 ml agarose gel.

2.1.15.4 6X DNA Loading Dye

Loading dye (New England BioLabs) was used at the concentration supplied.

2.1.16 Reagents for GST-Protein Purification by Gel Filtration Chromatography

2.1.16.1 Glutathione Agarose

Glutathione agarose was provided as a lyophilised powder. Powder was swollen in 50 ml water and left overnight at 4 ºC for 100 % swelling to occur.

Subsequently, agarose beads were washed with 10 volumes of water or PBS according to manufacturer's instructions.

2.1.16.2 Cleansing Buffer 1

Boric acid (6.2 g) and NaCl (29.2 g) were dissolved in deionised water (800 ml), adjusted to pH 8.5 and brought to 1 L with deionised water. Solution was filter sterilised and stored at room temperature.

2.1.16.3 Cleansing Buffer 2

Sodium acetate (8.2 g) and NaCl (29.2 g) were dissolved in deionised water (800 ml), adjusted to pH 4.5 and brought to 1 L with deionised water. Solution was filter sterilised and stored at room temperature.

2.1.16.4 Elution Buffer

Tris-HCl (3.9 g) and reduced glutathione (1.5 g) were dissolved in deionised water (400 ml), pH adjusted to pH 9 and brought to 500 ml. Solution was filter sterilised, stored at room temperature and used within a day.

2.1.16.5 Storage Buffer

NaCl (58.4 g) and sodium azide (500 mg) were dissolved in deionised water (400 ml). Solution was mixed and brought to 500 ml.

2.1.17 Glycerol (40 % (v/v))

Glycerol (40 ml) was added to deionised water (60 ml). The solution was autoclaved and stored at 4 ºC.

2.1.18 Glycerol (80 % (v/v))

Glycerol (80 ml) was added to deionised water (20 ml). The solution was autoclaved and stored at 4 ºC.

2.1.19 Reverse-Phase High Performance Liquid Chromatography (RP-HPLC) Solvents

2.1.19.1 Solvent A1

NaH_2PO_4 (3 g) and 1-octanesulfonic acid (0.5 g) were added to HPLC grade water (1 L) (pH 4.5). Solution was prepared fresh on day of use.

2.1.19.2 Solvent A2

Trifluoroacetic acid (TFA) (1 ml) was added to 999 ml of HPLC grade water to yield a solution of 1.1 % (v/v) of TCA and water.

2.1.19.3 Solvent B1

HPLC grade acetonitrile (100 %)

2.1.19.4 Solvent B2

Trifluoroacetic acid (1 ml) (TCA) was added to 999 ml of HPLC grade acetonitrile to yield a solution of 0.1 % (v/v) of TCA and acetonitrile.

2.1.20 Intracellular Glutathione Measurement

2.1.20.1 125 mM Sodium Phosphate Monobasic

Sodium phosphate monobasic (1.5 g) was dissolved in distilled water (100 ml). It was stored at 4 ºC until required for use.

2.1.20.2 125 mM Sodium Phosphate Dibasic

Sodium phosphate dibasic (1.77 g) was dissolved in distilled water (100 ml). It was stored at 4 ºC until required for use.

2.1.20.3 GSH/GSSG Assay Buffer (125 mM Sodium phosphate (pH 7.5), 6.3 mM EDTA)

125 mM sodium phosphate monobasic (Section 2.1.20.1) was added, dropwise, to 125 mM sodium phosphate dibasic (100 ml) (Section 2.1.20.2), until the pH was adjusted to 7.5. EDTA (235 mg) was dissolved in 100 ml of this sodium phosphate buffer. It was stored at 4 ºC until ready for use.

2.1.20.4 5'5-sulfosalicilic acid (5 % (w/v)) (5 % SSA)

SSA (0.5 g) was dissolved in GSH/GSSG Assay Buffer (10 ml) (Section 2.1.20.3). The solution was stored on ice.

2.1.20.5 Triethanolamine (50 % (v/v))

Triethanolamine (250 µl) was mixed with GSH/GSSG Assay Buffer (250 µl) (Section 2.1.20.3). Solution was used within a day.

2.1.20.6 2-Vinylpyridine (20 % (v/v))

2-vinylpyridine (20 µl) was mixed with GSH/GSSG Assay Buffer (80 µl) (Section 2.1.20.3).

2.1.20.7 10 mM 5,5'-dithio-bis(2-nitrobenzoic acid) (DTNB)

DTNB (7.927 mg) was dissolved in GSH/GSSG Assay Buffer (2 ml) (Section 2.1.20.3). This was covered in tinfoil and stored on ice.

2.1.20.8 DTNB containing 1 U Glutathione Reductase

For every sample to be assayed, 1 U of glutathione reductase was added to 42 µl of 10 mM DTNB (Section 2.1.20.7).

2.1.20.9 30 mM β-nicotinamide adenine dinucleotide 2'-phosphate reduced tetrasodium salt hydrate (NADPH)

NADPH (25 mg) was dissolved in GSH/GSSG Assay Buffer (1 ml) (Section 2.1.20.3). This was aliquoted into smaller volumes, covered in tinfoil and stored at –20 ºC until required for use.

2.1.20.10 5 mM NADPH

1 volume of 30 mM NADPH (Section 2.1.20.9) was added to 5 volumes of GSH/GSSG Assay Buffer (Section 2.1.20.3). This was covered in tinfoil and stored on ice.

2.1.20.11 1 mg/ml Glutathione; reduced

Reduced glutathione (1 mg) was dissolved in GSH/GSSG Assay Buffer (1 ml) (Section 2.1.20.3). This was covered in tinfoil and stored on ice.

2.1.20.12 2 mg/ml Glutathione; oxidised

Oxidised glutathione (2 mg) was dissolved in GSH/GSSG Assay Buffer (1 ml) (Section 2.1.20.3). This was covered in tinfoil and stored on ice.

2.1.21 2D-PAGE Reagents

2.1.21.1 Trichloroacetic Acid (100 % (w/v)) (100 % TCA)

TCA (100 g) was dissolved in water (45.5 ml). The solution was stored in the dark at 4 ºC.

2.1.21.2 Trichloroacetic Acid (10 % (w/v)) (10 % TCA)

100 % TCA (Section 2.1.21.1) (10 ml) was added to water (90 ml).

2.1.21.3 Isoelectric Focusing Buffer (IEF)

Urea (24 g), thiourea (7.6 g), CHAPS (2 g), Triton X-100 (0.50 ml) and Trizma base (60 mg) were brought to 50 ml with distilled water. The solution was split into 1 ml aliquots which were stored at -20 ºC until use. After thawing, DTT (5 mg) and appropriate Ampholytes (GE Healthcare) (8 µl) were added to a 1 ml aliquot immediately prior to use.

2.1.21.4 IPG Strip Equilibration Buffer

Glycerol (150 ml), SDS (10 g), urea (180 g), and Trizma base (3 g) were added to 400 ml deionised water. The pH was adjusted to pH 6.8. The final volume was adjusted to 500 ml. The solution was frozen in 50 ml aliquots at -20 ºC until use.

2.1.21.5 Reduction Buffer

DTT (400 mg) was added to IPG Strip Equilibration Buffer (20 ml) (Section 2.1.21.4). This volume was adequate for two strips. The solution was made up fresh on the day.

2.1.21.6 Alkylation Buffer

Iodoacetamide (500 mg) was added to IPG Strip Equilibration Buffer (20 ml) (Section 2.1.20.4). This volume was adequate for two strips. Trace amounts of bromophenol blue was added to the solution. The solution was made up fresh on the day.

2.1.21.7 Agarose Sealing Solution (0.5 % Agarose)

Trizma base (1.5 g), glycine (7.2 g) and SDS (0.5 g) were dissolved in deionised water (80 ml). Agarose (0.5 g) and bromophenol blue (200 µl of 1 % (w/v) solution) (Section 2.1.12.5) were added and the solution was adjusted to 100 ml with deionised water.

2.1.22 Mass Spectrometry Reagents

2.1.22.1 Liquid Chromatography Mass Spectrometry Reagents (LC-MS/MS)

2.1.22.1.1 100 mM Ammonium Bicarbonate (NH_4HCO_3)

NH_4HCO_3 (400 mg) was dissolved in HPLC-grade water (50 ml). The solution was made up fresh on the day.

2.1.22.1.2 100 mM Ammonium Bicarbonate/ Acetonitrile (1:1 (v/v))

100 mM ammonium bicarbonate (5 ml) (Section 2.1.22.1.1) was added to acetronitrile (5 ml). The solution was made up fresh on the day.

2.1.22.1.3 10 mM Ammonium Bicarbonate containing Acetonitrile (10 % (v/v))

100 mM ammonium bicarbonate (1 ml) (Section 2.1.22.1.1) and acetonitrile (1 ml) was added to deionised water (8 ml). The solution was made up fresh on the day.

2.1.22.1.4 Trypsin Solution for in-gel digestion (13 ng/µl)

10 mM ammonium bicarbonate containing acetonitrile (10 % (v/v)) (1.5 ml) (Section 2.1.22.1.3) was added to 20 µg of Sequencing Grade Trypsin (Promega) and briefly vortexed until dissolved.

2.1.22.1.5 Formic Acid (0.1 % (v/v))

Formic acid (1 ml) was added to LC-MS grade water (1 L).

2.1.22.1.6 Formic Acid (0.1 % (v/v)) in LC-MS Grade Acetonitrile (90 % (v/v))

LC-MS grade water (100 ml) was added to LC-MS grade acetonitrile (900 ml) in a darkened bottle. Formic acid (1 ml) was added to this using a glass pipette.

2.1.22.2 Reagents for analysis by Q-Exactive

2.1.22.2.1 Resuspension Buffer

Urea (36 g), thiourea (14.4 g) and tris-HCl (1.6 g) were dissolved in 40 ml deionised water and pH was adjusted to pH 8. Solution was brought to a final volume of 100 ml with deionised water and stored at 4 ºC.

2.1.22.2.2 50 mM Ammonium Bicarbonate (NH_4HCO_3)

NH_4HCO_3 (200 mg) was dissolved in HPLC-grade water (50 ml). The solution was made up fresh on the day.

2.1.22.2.3 50 mM Dithiothreitol (DTT)

DTT (77 mg) was dissolved in 50 mM ammonium bicarbonate (1 ml) (Section 2.1.22.2.2). The solution was made up fresh on the day.

2.1.22.2.4 55 mM Iodoacetamide (IAA)

IAA (101.7 mg) was dissolved in 50 mM ammonium bicarbonate (1 ml) (Section 2.1.22.2.2). The solution was made up fresh on the day.

2.1.22.2.5 ProteaseMAX (1 % (w/v))

ProteaseMAX (1 mg) (Promega) was resuspended in 50 mM ammonium bicarbonate (100 µl) (Section 2.1.22.2.2) immediately before use. Solution was made into 20 µl aliquots, snap frozen and stored at -20 ºC until use.

2.1.22.2.6 Trypsin Solution (1 µg/µl)

Sequencing grade trypsin (20 µg) (V5111, Promega) was resuspended in trypsin resuspension buffer (20 µl) (V542A, Promega). Solution was kept on ice until ready for use. Snap-freeze any remaining trypsin and store at -20 ºC for later use.

2.1.22.2.7 Reagents for Millipore ZipTip$_{C18}$ tips

2.1.22.2.7.1 Resuspension Solution

Trifluoroacetic acid (TFA) (5 µl) was added to LC-MS grade water (995 µl).

2.1.22.2.7.2 Equilibration and Washing Solutions

TFA (1 µl) was added to LC-MS grade water (999 µl).

2.1.22.2.7.3 Wetting Solution

TFA (1 µl) was added to LC-MS grade water (199 µl) and LC-MS grade acetonitrile (800 µl).

2.1.22.2.7.4 Elution Solution

TFA (1 µl) was added to LC-MS grade water (399 µl) and LC-MS grade acetonitrile (600 µl).

2.1.22.2.7.5 Loading Buffer

Acetonitrile (20 ml) and TFA (0.5 ml) were added to deionised water (980 ml).

2.2 Methods

2.2.1 Microbiological Culture Methods

Fungal and bacterial strains used in this study are listed in Table 2.2

2.2.1.1 *Aspergillus niger* growth, maintenance and storage

A. niger strains were maintained on PDA (Section 2.1.2.2), MEA (Section 2.1.2.3) or AMM agar (Section 2.1.2.4.5) (Section 2.1.2.5.5). A sterile inoculation loop was used to seed conidia onto agar plates from conidial stocks. Plates were incubated at 30 ºC for 5-7 days with periodic checking until fully grown. Conidia were harvested from agar plates by adding sterile PBST (Section 2.1.9) onto the plate and rubbing the surface with an inoculation loop to dislodge the conidia. Harvested conidia were filtered through sterile Miracloth (filtration cloth, Millipore) to remove any hyphal elements, washed with sterile PBS (Section 2.1.8) and collected. The conidia were centrifuged at 3000 g for 15 min and washed again with sterile PBS (10 ml) (Section 2.1.8). Harvested conidia were stored at 4 ºC until required. Aliquots of the conidial suspensions (500 µl) were added to 500 µl of sterile 80 % glycerol (Section 2.1.18). The tubes were vortexed and snap-frozen in liquid nitrogen before transferring to -70 ºC for long-term storage.

2.2.1.2 *Aspergillus nidulans* growth, maintenance and storage

As mentioned in Section 2.2.1.1, but incubated at 37 ºC.

Table 2.2: Fungal and bacterial strains used in this study, including antibiotics used.

Species	**Strain**	**Antibiotics**	**Reference**
A. niger	CBS 513.88	N/A	ATCC collection
A. niger	N593	N/A	Gift from Dr. Arthur F.J. Ram (Leiden University)
A. niger	Δ*MT-II*^{N593}	Hygromycin (200 μg/ml)	This study
A. niger	Environmental Isolate	N/A	Carberry et al. (2012)
A. nidulans	FGSCA4	N/A	Carberry et al. (2012)
E. coli	BL21	Ampicillin (100 μg/ml)	N/A

2.2.1.3 *E. coli* growth, maintenance and storage

E. coli strains were grown on LB agar (Section 2.1.4.2) overnight at 37 ºC or LB broth (Section 2.1.4.1) overnight at 37 ºC with shaking at 200 rpm. Both media were supplemented with ampicillin (100 µg/ml, final concentration) (Section 2.1.6). Bacterial strains were stored at 4 ºC for short term storage. For long term storage, 500 µl of freshly grown liquid culture was mixed with 500 µl of 40 % (v/v) glycerol (Section 2.1.17). Tubes were snap-frozen in liquid nitrogen before transferring to -70 ºC. To regenerate bacterial strains, tubes were thawed on ice. A sterile inoculation loop was used to streak the culture onto a LB agar plate containing 100 µg/ml ampicillin.

2.2.2 Protein Characterization Methods

2.2.2.1 Bradford Protein Assay

Bio-Rad protein assay dye was diluted 1/5 in PBS (Section 2.1.8) prior to use. The sample to be assayed was also diluted appropriately. 20 µl sample was added to 980 µl of the diluted Bio-Rad protein assay dye and mixed thoroughly. The final sample (1 ml) was transferred to a 1 ml plastic cuvette and incubated for 5 min at room temperature. The A_{595} was read relative to a blank and the protein concentration was determined based on values obtained from a standard curve. All samples were prepared and analysed in duplicate.

2.2.2.2 Sodium Dodecyl Sulphate Polyacrylamide Gel Electrophoresis (SDS-PAGE)

SDS-PAGE gels, both stacking and separating, were prepared according to Table 2.3 and 2.4, respectively. The gels were cast using the Mini-Protean II gel casting apparatus (BioRad, CA, USA) according to the manufacturer's guidelines.

Samples were prepared by adding one volume of 5 X Solubilisation Buffer (Section 2.1.12.7) to every 4 volumes of sample. Samples were boiled for 5 min and centrifuged briefly, before loading onto the gel with a Hamilton syringe. Electrophoresis for 1D separation was carried out initially at 80 V for 30 min, increasing to 120 V until the sample reached the bottom of the separating gel, using 1 X Electrode Running Buffer (Section 2.1.12.9)

Table 2.3: Reagents composition for SDS-PAGE Separating Gels

% Acrylamide	**12 %**	
Number of Minigels	**2**	**5**
1.5 M Tris-HCl pH 8.3	2.8 ml	7 ml
10 % SDS	112 µl	280 µl
30 % Acrylamide, 0.8 % Methylene bis Acrylamide	4.52 ml	11.3 ml
Distilled Water	3.72 ml	9.3 ml
10 % Ammonium Persulfate	40 µl	100 µl
TEMED	9.2 µl	23 µl

Table 2.4: Reagents composition for SDS-PAGE Stacking Gel

% Acrylamide	**4 %**	
Number of Minigels	**2**	**5**
0.5 M Tris-HCl pH 6.8	1.25 ml	3.12 ml
10 % SDS	20 µl	50 µl
30 % Acrylamide, 0.8 % Methylene bis Acrylamide	650 µl	1.62 ml
Distilled Water	3.05 ml	7.62 ml
10 % Ammonium Persulfate	100 µl	250 µl
TEMED	10 µl	25 µl

2.2.2.3 Isoelectric Focusing (IEF) and 2D-PAGE

Protein samples were prepared to the appropriate concentration and volume for the IPG strip size according to Table 2.5. Bromophenol blue was added to the protein samples, which were then centrifuged at 12,000 x g for 5 min. Protein samples were loaded into the positive end of the ceramic IPG strip holders. The IPG strip was added, gel-side down, using a forceps, while the holder was tilted slightly to evenly distribute the sample along the holder. Care was taken to prevent the trapping of air bubbles underneath the strip. The strips were overlaid with Plus One Drystrip Coverfluid (Amersham) (1 – 1.5 ml) and subjected to IEF on an IPGphor II IEF Unit using the following programme;

Step	50 V	12 h
Step	250 V	0.15 h
Gradient	5000 V	2 h
Step	5000 V	5 h
Gradient	8000 V	2 h
Step	8000 V	1 h
Step	250 V	1 h

Following IEF, the IPG strips were equilibrated in Reduction Buffer (Section 2.1.21.5) for 20 min, followed by equilibration in Alkylation Buffer (Section 2.1.21.6) for 20 min. The IPG strips were rinsed in 1 X Electrode Running Buffer (Section 2.1.12.9) and placed on top of 12 % SDS-PAGE gels (Table 2.6) using a forceps. The gels were overlaid with Agarose Sealing Solution (Section 2.1.21.7). Once set, the gels were placed in the PROTEAN Plus Dodeca Cell (BIO-RAD) as per manufacturer's instructions. The gels were electrophoresed in 1 X Electrode Running Buffer (Section 2.1.12.9) overnight at 1.5 W per gel. In the morning, the voltage was increased to 5 W per gel until the dye-front was 2 cm from the end of the gels. The gels were stained with Colloidal Coomassie® Blue (Section 2.2.12.10).

Table 2.5: Protein amounts and volumes for different length IPG Strips

Strip Length	**Protein Amount**	**Volume of IEF Buffer**
7 cm	125 µg	125 µl
13 cm	300 µg	250 µl

Table 2.6: Reagents composition for Large SDS-PAGE Separating Gels

% Acrylamide	**12 %**	
Number of Minigels	**2**	**10**
1.5 M Tris-HCl pH 8.3	31.5 ml	157.5 ml
10 % SDS	1.21 ml	6.05 ml
30 % Acrylamide, 0.8 % Methylene bis Acrylamide	50.7 ml	253.5 ml
Distilled Water	41.7 ml	208.5 ml
10 % Ammonium Persulfate	405 µl	2.25 ml
TEMED	105 µl	525 µl

2.2.2.4 Colloidal Coomassie® Staining

Following SDS-PAGE, gels were incubated for 3 h – overnight in Fixing Solution (Section 2.1.12.12.1) with gentle rocking. This was poured off and the gels were washed 3 X 20 min with deionised water. The gels were then pre-incubated in Incubation Buffer (Section 2.1.12.12.2) for 1 h before a quantity of Colloidal Coomassie® Blue G-250 (Serva Electrophoresis, Germany) was scattered over each gel to attain a concentration of approximately 350 µg/ml. Gels were incubated, with stain, for 5 days and washed repeatedly with deionised water.

2.2.2.5 Western Blot Analysis

Nitrocellulose paper (NCP), and 6 sheets of filter paper, of appropriate size, were pre-soaked in Towbin Buffer (Section 2.1.13.1) for 15 min. The SDS-PAGE gels were removed carefully from the electrophoresis unit. They were assembled on the

transfer unit as follows; 3 sheets of soaked filter paper, soaked NCP, SDS-PAGE gel, and 3 sheets of soaked filter paper. Transfer occurred at 18 V for 30 min. The NCP was blocked in Western Blocking Buffer (Section 2.1.13.2) for 1 h at room temperature with gentle rocking. The Western blocking buffer was poured off and the primary antibody, diluted in Antibody Buffer (Section 2.1.13.3), was added to the blots for 1 h at room temperature with gentle rocking. The antibody was removed and the blots were washed 3 X 5 min with PBST 0.05 % (Section 2.1.9). The secondary antibody, diluted in Antibody buffer, was added to the blots for 1 h at room temperature with gentle rocking. The secondary antibody was removed and the blots were washed 3 X 5 min in PBST 0.05 %. The blots were developed dissolving DAB (10 mg) in DAB Substrate Buffer (Section 2.1.13.4) (15 ml). Hydrogen peroxide (7 µl) was added to the substrate solution which was then applied to blots. Blots were allowed to develop for 10 min and distilled water was applied to stop the reaction and reduce background staining.

2.2.3 Protein Extraction from *A. niger*

2.2.3.1 Whole Protein Extraction using Lysis Buffer

Mycelia from *A. niger* liquid cultures (CBS 513.88; 48 h; 30 ^{o}C) in PDB (Section 2.1.2.1) were harvested by filtering through miracloth, dried on tissue paper and snap frozen in liquid N_2. The mycelia were ground into a fine powder using a pestle and mortar under liquid N_2. The ground mycelia (500 mg) were weighed into a 2 ml Eppendorf tube and Lysis Buffer (Section 2.1.10.3) (900 µl) was added. Samples were then sonicated with a sonication probe (Bandelin Sonopuls, Bandelin Electronic, Berlin) at 10 % power, cycle 6 for 10 s. This was repeated twice more with the sample been cooled on ice between each sonication. The sample was then subjected to bead-

beating at 30 Hz for 5 min in a bead beater (MM300, Retsch®). Samples were incubated on ice for 1 h. The lysate was centrifuged at 13,000 x g for 10 min at 4 ^{o}C and the supernatant was removed to a clean microcentrifuge tube. Aliquots were stored at – 20 ^{o}C until required for use.

2.2.3.2 Whole Protein Extraction using 0.1 M HCl

Mycelia from *A. niger* liquid cultures (CBS 513.88; 48 h; 30 ^{o}C) in PDB (Section 2.1.2.1) were harvested by filtering through miracloth, dried on tissue paper and snap frozen in liquid N_2. The mycelia were ground into a fine powder using a pestle and a mortar under liquid N_2. The ground mycelia (100 mg) were weighed into a 2 ml Eppendorf tube and 0.1 M HCl (Section 2.1.11) (250 µl) was added. Samples were then vortexed and incubated on ice for 1 h. After incubation, samples were centrifuged at 13,000 x g for 10 min at 4 ^{o}C and the HCl-supernatants were removed to a clean microcentrifuge tube and used within the day.

2.2.3.3 Whole Protein Extraction for 2D-PAGE

Mycelia from *A. niger* liquid cultures (Environmental Isolate; 48 h; 30 ^{o}C) in AMM were harvested through miracloth and washed with cold deionised water. The mycelia were dried in tissue, snap frozen in liquid N_2 and ground into a fine powder using a pestle and a mortar under liquid N_2. The ground mycelia (250 mg) was added to 10 % (w/v) TCA (1.5 ml) (Section 2.1.21.2) and incubated on ice for 30 min. The samples were sonicated with a sonication probe (Bandelin Sonopuls, Bandelin electronic, Berlin) for 10 s at 10 % power on cycle 6. This was carried out 4 times in total with cooling on ice between each step. The lysed samples were incubated on ice for a further 30 min before centrifugation at 12,000 x g for 10 min at 4 ^{o}C. The supernatants were discarded. 60 µl of H_2O was added to the samples and vortexed. Ice-

cold acetone (1 ml) was added to each sample and the pellets were re-suspended as much as possible by pipetting and vortexing. The samples were stored at – 20 ºC and were vortexed every 10 min for 1 h. They were then stored overnight at – 20 ºC. The samples were centrifuged at 12,000 g for 10 min. The supernatants were discarded and ice-cold acetone (500 µl) was added to each sample. The samples were vortexed before being centrifuged at 12,000 g for 10 min at 4 ºC. The supernatants were discarded and the pellets were left to air-dry for 5 min. IEF Buffer (Section 2.1.21.3) (500 µl) was added to the pellets which were re-suspended as much as possible by pipetting and vortexing. The samples were incubated at room temperature for 1 h before centrifuging at 13,000 x g for 3 min in a benchtop microfuge. The supernatants were removed to clean microcentrifuge tubes and aliquots were stored at – 20 ºC until required for use.

2.2.3.4 Protein Extraction for Q-Exactive Analysis

2.2.3.4.1 Extraction of Supernatant Proteins from *A. niger*

Supernatant, frozen at – 70 ºC (50 ml) was defrosted and centrifuged at 4,500 rpm (4 ºC) for 30 min. The supernatant was removed to a clean container and passed through 0.2 µm filters. 100 % (w/v) TCA stock solution (Section 2.1.21.1) was added to the filtered supernatant so that it comprised 10 % (v/v) of the final solution. This was mixed and incubated on a daisy wheel overnight at 4 ºC. Samples were centrifuged at 12,000 x g (4 ºC) for 30 min and supernatant was removed. Remaining pellet was washed with ice-cold acetone (1 ml) and was centrifuged for 10 min at 13,000 x g (4 ºC). The wash step was repeated twice with 5 min centrifugation each time. Acetone was removed after the final wash and the pellet was allowed to dry for no more than 5 min before re-suspension with appropriate volume of Re-suspension Buffer (Section 2.1.22.2.1). Final concentration of protein should be approximately 3 mg/ml.

2.2.3.4.2 Extraction of Mycelial Proteins from *A. niger*

A. niger protein lysates (Section 2.2.2.1) were assayed (Section 2.2.2.1) to quantify the protein concentration in each sample. Samples were brought to 15 % TCA by addition of the appropriate volume of cold 100 % TCA solution, vortexed briefly and incubated on ice for 30 min. Ice-cold acetone (500 µl) was added to the TCA/protein suspension, vortexed briefly and incubated at – 20 ^{o}C for 1 h. Samples were centrifuged at 12,000 x g, 10 min, 4 ^{o}C and the supernatant was discarded. Pellets were washed twice with 500 µl of ice-cold acetone. Acetone was removed after the final wash and the pellet was allowed to dry for no more than 5 min before re-suspension with appropriate volume of Re-suspension Buffer (Section 2.1.22.2.1). Final concentration of protein should be approximately 3 mg/ml.

2.2.4 In-Gel Digestion of Protein Spots from 2D-PAGE gels

In-Gel digestion was carried out according to Shevchenko et al. (2007). The samples were excised from the gel and placed in 1.5 ml microcentrifuge tubes. The gel pieces were de-stained by adding 100 mM Ammonium Bicarbonate/Acetonitrile (1:1 (v/v)) (Section 2.1.22.1.2) (100 µl) for 1 h at room temperature with vortexing at intervals. The liquid was removed and 500 µl of acetonitrile was added to shrink the gel pieces. The liquid was removed before addition of trypsin solution (Section 2.1.22.1.4) (50 µl) to each gel piece. The samples were incubated at 4 ^{o}C for 30 min, checked to ensure the gel piece was covered with trypsin solution, before incubation for a further 2. 5 h at 4 ^{o}C. It required, 10 mM Ammonium bicarbonate was added to cover the gel pieces. The gel pieces were incubated overnight at 37 ^{o}C. The gel pieces were sonicated in a sonication bath for 10 min. They were then centrifuged at 12,000 x g for 10 min and supernatants were removed to a clean microcentrifuge tube.

2.2.5 Digestion of *A. niger* extracted proteins for analysis by Q-Exactive

Samples (15 µl; 50 µg) in Resuspension Buffer (Section 2.1.22.2.1) were brought to room temperature for 10 min to ensure urea was in solution. Ammonium bicarbonate (78.5 µl; 50 mM) was added to the samples. DTT (1 µl) (Section 2.1.22.2.3) was added to the samples followed by incubation at 56 ºC for 20 min. Samples were allowed to cool at room temperature and 2.7 µl of IAA (Section 2.1.22.2.2) was added, followed by incubation at room temperature for 15 min in the dark. Following reduction and alkylation, 1 µl Protease MAX stock (Section 2.1.22.2.5) and 1.8 µl of trypsin (Section 2.1.22.2.6) were added to each of the samples, followed by incubation at 37 ºC overnight. The next day, samples were spun briefly to collect any condensate and acidified by adding 1 µl TFA, vortexed briefly, and incubated at room temperature for 5 min. Samples (15 µg) were added into a new tube and were then reduced to dryness using a Thermo Scientific DNA120 Speed Vac concentrator. Samples were then stored at – 20 ºC until Q-Exactive analysis was performed.

2.2.6 Zip Tip Protocol

To purify the trypsin-digested peptides (Section 2.2.5) for analysis by Q-Exactive, the ZipTip procedure was used (Millipore). In brief, trypsin digested peptides were re-suspended in 20 µl Re-suspension Buffer (Section 2.1.22.2.7.1). The peptide samples were sonicated for 2 min to help re-suspend the pellet, followed by a brief centrifugation. The peptide samples were then processed using Zip-tips according to the manufacturer's instructions. The peptide samples were then reduced to dryness using a ThermoScientific DNA120 Speed Vac concentrator and re-suspended in 12 µl of loading buffer (Section 2.1.22.2.7.5).

2.2.7 Organic Extraction of *A. niger* and *A. nidulans* Culture Supernatants

A. niger and *A. nidulans* liquid cultures were grown for 45 h in PBD and AMM. Gliotoxin (2.5 µg/ml final concentration) and MeOH control were added to the liquid cultures after 45 h growth and 2 ml aliquots of supernatant were extracted from the cultures every 30 min for 4 h. Culture supernatants (2 ml) were added to chloroform (2 ml) in a 15 ml tube and agitated vigorously for 3 min, with regular venting of the tube. The mixtures were centrifuged at 3000 x g, 10 min at room temperature to separate the organic layer from the aqueous layer. The lower organic layer (2 ml approximately) was retained and reduced to dryness using a Thermo Scientific DNA120 Speed Vac concentrator. The dried extract retained in the tube, was re-suspended in HPLC grade methanol (20 µl). The re-suspended extract was then transferred to a clean glass vial and stored at – 20 ^{o}C.

2.2.8 Reverse-Phase – High Performance Liquid Chromatography (RP-HPLC) Analysis

2.2.8.1 RP-HPLC detection of S-adenosylhomocysteinease activity

To analyse SAH enzymatic breakdown, *A. niger* CBS 513.88 was grown (*n* = 3 biological replicates) at 30 ^{o}C for 48 h in PDB and mycelia extracted as per Section 2.2.3.2). SAH (50 µg/ml final concentration) was spiked into the *A. niger* lysates and samples were analysed using reverse-phase high-performance liquid chromatography (RP-HPLC; C_{18} column (Agilent Zorbax Eclipse XDB-C18, 4.6 x 150 mm) (Agilent 1200 System) after 0, 35, 70 and 105 min post-spiking. Gradient elution (Table 2.7) was performed with Solvent A consisting in 25 mM NaH_2PO_4 and 2.3 mM octane sulfonic acid, pH 4.5, in HPLC grade water (Sigma-Aldrich) and Solvent B consisting

of 100 % acetonitrile (Uthus, 2003; Zhou et al., 2002). All cultures were grown up in triplicate and each one was compared to a standard curve (6.25 – 400 µg/ml SAH).

Table 2.7: RP-HPLC Gradient for SAH degradation

Time	**% B**
0	5
2	5
13	20
14	20
15	100
18	5
25	5

2.2.8.2 Detection and quantification of amino acids by RP-HPLC

Intracellular methionine (Met), valine (Val), phenylalanine (Phe) and leucine/isoleucine (Leu/Ile) were measured using the method of (Sun et al., 2005), with modifications. *A. niger* CBS 513.88 (*n* = 3 biological replicates) was cultured for 45 h in PDB at 30 ^{o}C prior addition of gliotoxin (2.5 µg/ml final) and methanol solvent control for 3 h. Mycelia were harvested through miracloth and snap frozen in liquid N_2. Mycelia (500 mg) in lysis buffer (900 µl) (Section 2.1.10.3) were sonicated, bead-beaten and clarified using centrifugation. Protein concentrations were quantified by Bradford Assay and brought to the same concentration. *O*-phthaldialdehyde (OPA) (50 µl) was added to *A. niger* lysates (10 µl; 1/5 in 50 mM sodium phosphate pH 7.6) to

effect amino acid derivatization. All samples were incubated for 90 s at room temperature and immediately loaded (20 µl) on the HPLC C_{18} column (Agilent Zorbax Eclipse XDB-C18, 4.6 x 150 mm). Gradient elution was performed with Solvent A consisting of 0.1 % (v/v) trifluoroacetic acid in 99.9% HPLC grade water (Sigma-Aldrich) and Solvent B consisting of 0.1 % (v/v) trifluoroacetic acid in 99.9 % acetonitrile (Sigma-Aldrich) (Table 2.8). Quantification was enabled using commercially available Met obtained from Sigma-Aldrich. Statistical analyses were carried out using Student's t-test.

Table 2.8: RP-HPLC Gradient for Amino Acid Analysis

Time	**% B**
0	40
4.50	40
11.50	54.1
16.50	54.8
21.50	100
26.50	100
27.50	40
35	40

2.2.8.3 RP-HPLC detection of gliotoxin and BmGT

Organic extracts from *A. niger* (Section 2.2.7) were loaded (60 µl) on a C_{18} RT-HPLC column (Agilent Zorbax Eclipse XDB-C18, 9.4 x 250 mm). Gradient elution

was performed with Solvent A consisting of 0.1 % (v/v) trifluoroacetic acid in 99.9% HPLC grade water (Sigma-Aldrich) and Solvent B consisting of 0.1 % (v/v) trifluoroacetic acid in 99.9 % acetonitrile (Sigma-Aldrich) (Table 2.9).

Table 2.9: RP-HPLC Gradient for Amino Acid Analysis.

Time	**% B**
0	30
20	100
23	100
25	20

2.2.9 Gliotoxin Thiomethyltransferase Activity

A. niger CBS 513.88 mycelial lysates were obtained following 48 h growth in PDB media (45 h culture followed by supplementation with gliotoxin (2.5 µg/ml) (Induced) or methanol (Uninduced) for 3 h. Mycelia were snap-frozen and ground in liquid N_2, and lysed by sonication and bead-beating in lysis buffer A. Protein lysates were clarified by centrifugation prior to use in assays. Reaction mixtures were carried out essentially as described by Dolan et al. (2014) with modifications: Tris (2-Carboxyethyl) phosphine (TCEP)-reduced gliotoxin (1 mg/ml; 2 µl), SAM (25 mg/ml in PBS, 3 µl), *A. niger* lysate (20 µl; 3 mg/ml protein) and PBS (75 µl). Negative controls used 20 µl lysis buffer instead of lysate. Reactions were incubated at 37 ^{o}C for 3 h and terminated by adjustment to 15 % (v/v) TCA, vortexed briefly and incubated on ice for 30 min. Samples were centrifuged at 10,000 x *g* for 10 min, 4 ^{o}C.

Supernatants were diluted 1/10 in 0.1 % (v/v) formic acid and spin filtered prior to LC-MS/MS analysis (Agilent Ion Trap 6340) to detect thiomethylated gliotoxin derivatives (Dolan et al., 2014).

2.2.10 Liquid Chromatography Mass Spectrometry (LC-MS)

A 6340 Model Ion Trap LC-Mass Spectrometer (Agilent Technologies, Ireland) with system software V6.2 was used to determine the identity of peptides or metabolites using electrospray ionisation. Bovine serum albumin (BSA) standard (10 fmol) was analysed, identified and used to verify accuracy of identification and optimum machine functionality before samples were analysed.

2.2.10.1 LC-MS/MS Analysis of Peptide Mixtures

Peptide mixtures generated from in-gel digestion of protein spots or bands from SDS-PAGE (Section 2.2.4) were spin filtered (Agilent Technologies 0.22 µm Cellulose Acetate) prior to LC-MS/MS analysis. Samples (Section 2.2.4) (5 µl) were loaded onto a Zorbax 300 SB C-18 Nano-HPLC Chip (75 µm x 150 mm separation column; 40 nL enrichment column) with 0.1 % (v/v) formic acid (Section 2.1.22.1.5) at a flow rate of 4 µl/min. Peptides were eluted over a 15 min gradient of 5 – 100 % (v/v) Acetonitrile/formic acid (Section 2.1.22.1.6) with a post run of 5 min, using a flow rate of 0.6 µl/min. The eluted peptides were ionised and analysed by the mass spectrometer. MS^n analysis was carried out on the 3 most abundant peptide precursor ions in each sample, as selected automatically by the mass spectrometer. The peptides from the MS^n spectra were compared to the NCBI nr database using MASCOT (www.matrixscience.com) for identification of the proteins. For the database search, the criteria were set as a peptide tolerance ± 2 Da and peptide charge 1+, 2+, 3+, with a MS/MS tolerance ± 1 Da and 2 missed cleavages. A fixed modification

Carboxymethyl (C) and a variable modification of oxidation of methionine were also set.

2.2.10.2 LC-MS/MS Analysis of *A. niger* Metabolites

Metabolites isolated by (i) organic extraction from culture supernatants of *A. niger* and *A. nidulans* (Section 2.2.7) and (ii) metabolites obtained from the gliotoxin thiomethylation assay (Section 2.2.9), were analysed by LC-MS/MS. Samples were diluted in 0.1 % (v/v) formic acid (Section 2.1.22.1.5) prior to mass spectrometry and were loaded (1 µl) onto a Zorbax 300 SB C-18 Nano-HPLC Chip (75 µm x 150 mm separation column; 40 nL enrichment column) with 0.1 % (v/v) formic acid (Section 2.1.22.1.5) at a flow rate of 4 µl/min. Metabolites were eluted using the appropriate gradient with a post run of 5 min.

Metabolites isolated from *A. niger* HCl lysates (Section 2.2.3.2) were analysed by LC-MS/MS. Samples were diluted in 0.1 % (v/v) formic acid (Section 2.1.22.1.5) prior to mass spectrometry and were loaded (1 µl) onto a Porous Graphitized Carbon (PGC) Chip (75 µm x 43 mm separation column; 40 nL enrichment column) with 0.1 % (v/v) formic acid (Section 2.1.22.1.5) at a flow rate of 4 µl/min. Metabolites were eluted using the appropriate gradient with a post run of 5 min.

MS^n was carried out on the 3 most abundant precursor ions at each timepoint, with *n* ranging from 2 to 5, depending on the analysis. Singly charged ions were not excluded from the analysis with the precursor range adjusted to include ions with *m/z* between 15 and 2200.

2.2.11 Q-Exactive Analysis

Peptide samples were run on a Thermo Scientific Q Exactive mass spectrometer connected to a Dionex Ultimate 3000 (RSLCnano) chromatography system. Each sample was loaded onto an EASY-Spray PepMap RSLC C18 Column (50 cm x 75 μm), and was separated by an increasing acetonitrile gradient over 120 min at a flow rate of 250 nL/min. The mass spectrometer was operated in positive ion mode with a capillary temperature of 220 ºC, and with a potential of 2500 V applied to the frit. All data was acquired with the mass spectrometer operating in automatic data dependent switching mode. A high resolution (140,000) MS scan (300-2000 Dalton) was performed using the Q Exactive to select the 15 most intense ions prior to MS/MS analysis using HCD (higher-energy collisional dissociation).

Protein identification and label free quantitative (LFQ) analysis was conducted using MaxQuant (version 1.2.2.5: http://maxquant.org/) supported by the Andromeda database search engine to correlate MS/MS data against the *A. niger* Uniprot database and Perseus to organise the data (Version 1.4.1.3). For protein identification the following search parameters were used: precursor-ion mass tolerance of 1.5 Da, fragment ion mass tolerance of 6 ppm with cysteine carbamidomethylation as a fixed modification and a maximum of 2 missed cleavage sites allowed. False Discovery Rates (FDR) were set to 0.01 for both peptides and proteins and only peptides with minimum length of six amino acid length were considered for identification. Proteins were considered identified when a minimum of two peptides for each parent protein was observed.

LFQ intensities measured for individual runs were grouped based on their experimental treatment. The data was the log2 transformed and an ANOVA ($p < 0.05$)

was performed between the control and individual treatment samples to identify differentially abundant proteins. Proteins with statistically significant differential expression were extracted and these were used to generate maps of expression. To improve visual representation of differentially abundant proteins mean values were generated for each treatment and used to build the maps.

A qualitative assessment was also conducted. This involved the identification of proteins that were completely absent in a specific treatment. Those proteins that were completely missing from all replicates of a particular group but present in other groups were determined manually from the data matrix. These proteins are not considered statistically significant as the values for absences are given as NaN (not a number) which is not a valid value for an ANOVA analysis. However the complete absence of a protein from a group may be biologically significant and these proteins were reported as qualitatively differentially expressed.

2.2.12 Intracellular Glutathione Measurement

Intracellular glutathione was measured using a method adapted from the literature (Carberry et al., 2012; Rahman et al., 2006)). Total glutathione (glutathione (GSH) and glutathione disulfide (GSSG)) and GSSG only were measured independently, allowing for the calculation of GSH only. Care was taken throughout all steps in this procedure to avoid exposing the samples to light. All tubes were covered in tinfoil and a lid was kept on the ice box.

2.2.12.1 Sample Preparation

Mycelia from 48 h cultures in PDB were harvested through miracloth and dried on tissue paper, removing as much excess liquid as possible. Mycelia (300 mg) were

weighted into a 2 ml Eppendorf tube and 5 % (w/v) SSA (Section 2.1.20.4) (300 µl) was added along with a tungsten bead. The samples were bead-beaten at 30 Hz for 5 min followed by centrifugation at 12,000 x g for 10 min t 4 ^{o}C. The supernatants were removed to clean microcentrifuge tubes covered in tinfoil and neutralised using triethanolamine (Section 2.1.20.5). The samples were diluted (1/10 – 1/30) in GSH/GSSG Assay Buffer (Section 2.1.20.3) before centrifugation at 12,000 x g for 10 min at 4 ^{o}C. The supernatants were removed to clean microcentrifuge tubes. Samples were stored at – 70 ^{o}C if not assayed immediately.

2.2.12.2 GSH Standard Preparation

GSH (1 mg/ml) (Section 2.1.20.11) was diluted 1/100 in GSH/GSSG Assay Buffer (Section 2.1.20.3) to give a stock concentration of 10 µg/ml. A 26.4 nmol/ml stock was prepared by adding 800 µl of the 10 µg/ml preparation to 200 µl of GSH/GSSG Assay Buffer (Section 2.1.20.3). A series of dilutions was carried out on the 26.4 nmol/ml preparation in order to generate a standard curve.

2.2.12.3 GSSG Standard Preparation

GSSG (2 mg/ml) (Section 2.1.20.2) was diluted 1/100 in GSH/GSSG Assay Buffer (Section 2.1.20.3) to give a stock of concentration 20 µg/ml. A 26.4 nmol/ml stock was prepared by adding 800 µl of the 10 µg/ml preparation to 200 µl of GSH/GSSG Assay Buffer (Section 2.1.20.3). A series of dilutions were carried out on the 26.4 nmol/ml preparation in order to generate a standard curve.

2.2.12.4 Pre-treatment of GSSG Samples

GSSG standards and samples to be assayed for GSSG were pre-treated with 2-vinylpyridine, which covalently reacts with GSH, preventing its oxidation to GSSG,

thereby allowing for the measurement of GSSG only. 2-vinylpyridine (Section 2.1.20.6) (2 µl) was added to 100 µl of a Blank sample, the GSSG standards (Section 2.2.12.3) and samples to be assayed for GSSG (Section 2.2.12.4). This was carried out in a fume hood. The samples were incubated at room temperature for 1 h before triethanolamine (Section 2.1.20.5) (6 µl) was added to each sample to neutralise the 2-vinylpyridine. The samples were incubated for 10 min at room temperature before being assayed.

2.2.12.5 Glutathione Assay

All samples to be assayed for GSH or GSSG were assayed in the same manner. The blank/standard/sample (20 µl) was added to a clear 96-well microtiter plate. To this, 10 mM DTNB + GR (Section 2.1.20.8) (44.2 µl) was added and left for 30 sec. 5 mM NADPH (Section 2.1.20.10) (42 µl) was added to each well and the plate was gently shaken to mix. The absorbance at 412 nm was measured after 1 min 30 sec.

2.2.13 Molecular Biological Methods

2.2.13.1 Isolation of Genomic DNA from *A. niger* CBS513.88

A. niger harvested conidia was used to inoculate 50 ml cultures of Potato Dextrose Broth (Section 2.1.2.1). The cultures were incubated for 24 h, at 30 ºC, with constant shaking at 200 rpm. The cultures were then filtered through sterile Miracloth, washed with sterile water and the mycelia was collected. The mycelial mass was wrapped in tinfoil, snap-frozen in liquid nitrogen and ground to a fine powder using a pestle and mortar. DNA extractions were carried out using the ZR Fungal/Bacterial DNA Kit (Zymo Research, California, USA), following the manufacturer's recommendations. All buffers and reagents were supplied with the kit. Eluted DNA

was quantified by reading the absorbance of the sample at 260 and 280 nm using a Nanodrop 2000 spectrophotometer (Thermo Fisher Scientific).

2.2.13.2 Isolation of RNA from *A. niger* CBS513.88

A. niger liquid cultures, which were inoculated at 30 ºC at the required time, were filtered thought double autoclaved Miracloth, washed with sterile water and the mycelia was collected. The mycelial mass was snap-frozen in liquid nitrogen and ground to a fine powder in a cold mortar and pestle. The RNA was isolated using the RNeasy Kit supplied by Qiagen, according to the manufacturer's instructions. RNA was eluted in RNase-free water (30 µl), quantified using a Nanodrop 2000 spectrophotometer (Thermo Fisher Scientific) and stored at -70 ºC.

2.2.13.3 DNase Treatment

A DNase Kit (Sigma) was used to DNase treat RNA samples. RNA samples (Section 2.2.13.2) were diluted to 125 ng/µl with Molecular Grade Water. 10 X Reaction Buffer (1 µl) and DNase I (1 µl) were added to the RNA samples (8 µl) (125 ng/µl) and the mixture was left to incubate at room temperature for 15 min. Stop solution (1 µl) was added to the reaction and they were then incubated at 70 ºC for 10 min. The samples were chilled on ice and stored at -70 ºC if not for immediate use.

2.2.13.4 cDNA Synthesis

cDNA synthesis was performed using the qScript^{TM} cDNA SuperMix (Quanta Biosciences) using the supplied reagents in the kit and following the manufacturer's instructions. qScript cDNA SuperMix (5X) (4 µl) and RNase-free water (5 µl) were added to the DNase treated RNA (11 µl) (Section 2.2.13.3). Samples were heated for

5 min at 25 ºC, increased to 42 ºC for 30 min, and further increased to 85 º C for 5 min before cooling to 4 º C. After completion, cDNA samples were stored at -20 ºC.

2.2.13.5 Polymerase Chain Reaction (PCR)

Polymerase chain reaction (PCR) was used to amplify fragments of cDNA for cloning and to test for recombinant plasmid presence in *E. coli*. PCR was generally carried out using AccuTaq^{TM} LA DNA Polymerase (Sigma). The PCR reaction conditions can be seen in Table 2.10 and the different cycling parameters required are shown in Table 2.11. Annealing temperatures were estimated as *ca.* 4 ºC below the melting temperature (T_m) of the primers used. Extension times used were *ca.* 1 min/kb of DNA to be synthesised. Denaturing, annealing and extension steps were repeated for 35 cycles. All PCR reactions were carried out in 20 µl volumes using a G-Storm PCR (Roche) System. Primers used are shown on Table 2.12.

Table 2.10: Reaction constituents required for PCR.

Reagent	**Volume per reaction**
10 X Reaction Buffer	2 µl
dNTP Mix (10 mM)	2 µl
Primer F (10 µM)	0.4 µl
Primer R (10 µM)	0.4 µl
DMSO	0.8 µl
DNA Template	10 – 100 ng
Sterile Water	To a final volume of 20.4 µl
AccuTaq^{TM} LA DNA Polymerase	0.2 µl

Table 2.11: PCR cycling conditions.

	Time
Denaturation/ Activation (95 ºC)	3 min
Denaturation (95 ºC)	45 s
Annealing (57 ºC)	40 s
Extension (68 ºC)	1 min 30 s
Final Extension (68 ºC)	10 min

Table 2.12: Primers used to amplify *MT-II* cDNA.

Primer	**Restriction site**	**Sequence (5'- 3')**
MT-II-F	*Hind*III	GCAAGCTTATGACCCCCAAAATCTCTC
MT-II-R	*Xho*I	GCCTCGAGCTAGGGCTTTCTCCCCA

2.2.13.6 PCR Purification

PCR purification was carried out using all the reagents and columns supplied in the QIAquick PCR Purification Kit (Qiagen, UK) following the manufacturer's instructions. For 1 volume of PCR product of interest, 5 volumes of Buffer PB was added and mixed. The solution was transferred to a QIAquick column that was placed in a 2 ml collection tube and centrifuged at 13,000 x g for 1 min. The flow through was discarded. Buffer PE (750 µl) was added to the column and was then centrifuged at 13,000 x g for 1 min. The flow through was discarded and the column centrifuged again at 13,000 x g for 1 min to remove any residual wash buffer. The column was placed in a sterile microcentrifuge tube and sterile water (30 µl) was added to the

column to elute the DNA. The column was allowed to stand for 2 min before being centrifuged at 13,000 x g for 30 s. The DNA was stored at -20 ºC until required for use.

2.2.13.7 Quantitative PCR (qPCR)

qPCR reactions were performed using a LightCycler® 480 Real-Time PCR System (Roche) and Sybr Green Master Mix (Roche). Each reaction had a total volume of 10 µl and was comprised of: 5 µl SYBR Green Master Mix (Roche), 2 µl PCR grade water, 1 µl Primer F (10 pmol/µl), 1 µl Primer R (10 pmol/µl) and 1 µl cDNA (500 ng/µl). The PCR program used consisted of 40 ºC for 10 min, 95 ºC for 10 min followed by 45 cycles of 95 ºC for 10 s, 58 ºC for 20 s, 72 ºC for 10 s. Melting curve analysis was carried out for each experiment. The *A. niger* CBS513.88 Actin primer was used as a reference primer (Bohle et al., 2007). The primers used in the qRT-PCR experiments are shown in Table 2.13. Negative controls containing no cDNA were also performed. Each reaction was replicated a minimum of 4 times on each plate. By comparison of the cycle threshold values of the control (housekeeping gene; *actin*) to the sample, the relative concentration of the template was determined using the second derivative maximum method for relative quantification as described in the Roche Lightcycler manual. Statistically significant differences between the control and treatments were confirmed by comparing the normalised mean crossing points using ANOVA ($p < 0.001$) using Graphpad (PRISM) statistical software.

Table 2.13: Primer sequences used in qRT-PCR experiments.

Primer Name	Sequence 5' – 3'
Actin-qpcr-F	GGTCTGGAGAGCGGTGGTAT
Actin-qpcr-R	GAAGAAGGAGCAAGAGCAGTG
MT-II-qpcr-F	GGTGTACTTGCGACTTCGAC
MT-II-qpcr-R	CAAGGCCAGGAACTCTTTCA

2.2.13.8 Agarose Gel Electrophoresis

Agarose gel electrophoresis was used to separate differently sized DNA fragments, to visualize restriction digest reactions and for estimation of DNA yield. Agarose gels were cast and run using Bio-Rad electrophoresis equipment. Agarose gels between 0.8-1.5 % (w/v) in 1X TAE Buffer (Section 2.1.15.2) were used, although for most applications a 1 % (w/v) strength was suitable. Powdered agarose was added to the appropriate volume of 1X TAE Buffer (Section 2.1.15.2) in a 200 ml flask. This was then gently heated in a microwave, with frequent mixing, until the agarose had dissolved. While allowing the gel to cool, a mould was prepared by inserting the casting unit into the casting holder and sealed. After the gel had cooled to ~50 ºC, the molten gel was poured into the prepared mould. Ethidium bromide (3 µl/100 ml) (Section 2.1.15.3) was added to the casting unit and mixed. A gel comb was inserted and the gel was allowed to set on a level surface. Once set, the gel comb was removed gently, and the set gel in the gel casting unit was placed into the gel electrophoresis tank, with the wells nearer the negative (black) electrode. 1X TAE Buffer (Section 2.1.15.2) was then poured into the tank to fully submerge the gel.

2.2.13.9 Loading and Running Samples

DNA samples were prepared by adding 5 volumes of DNA samples to 1 volume of 6X Loading Dye (Section 2.1.15.4). DNA fragment size was estimated by running molecular weight markers alongside the unknown samples. Two different molecular weight markers were used in this study; 1 kb DNA Ladder (BioLabs, #N3232S) and DirectLoad^{TM} 50 bp DNA Step Ladder (Sigma). Gels were electrophoresed at 80-120 V for 30-60 min and were visualised using a Syngene G:Box.

2.2.14 Cloning

2.2.14.1 Restriction Enzyme Digests

Restriction enzymes and 10 X reaction buffers were obtained from Promega (Southampton, UK). Reactions were carried out according to the manufacturer's instructions, but a typical reaction was performed as follows:

DNA	1 µg
Enzyme 1	0.7 µl
Enzyme 2	0.7 µl
10 X Buffer	2 µl
10 X BSA	0.2 µl
Sterile Water	Bring up to 20 µl

The total reaction volume was always > 10 X the volume of enzyme used in order to prevent high glycerol concentrations, which would cause non-specific digestion (star activity). Reactions were typically carried out at 37 ºC for > 2 h, as per

the manufacturer's instructions. Digestion reactions were visualised by agarose gel electrophoresis (Section 2.2.13.8).

2.2.14.2 Ligation of DNA fragments

Ligation of DNA fragments was required for the cloning of *A. niger* genes into the pEX-N-GST vector (Figure 2.1) for expression in *E. coli*. DNA was digested (Section 2.2.14.1) to give compatible fragments. These fragments were separated by agarose gel electrophoresis (Section 2.2.13.8). Ligation of restricted DNA fragments was carried out using T4 DNA ligase (Promega) according to the manufacturer's instructions. Restriction digests either produce a DNA fragment with an overhang of single-stranded DNA at either end of the double-stranded section, known as sticky ends, or blunt ended molecules, which have no such overhangs. Creation of recombinant molecules usually entailed ligation of small fragments (inserts) to large fragments (backbones). For sticky ended ligation, the preferred ratio of molecules was 3 insert to 1 backbone molecule. This was estimated from the size of the fragments according to the following formula:

$$\frac{\text{Vector (ng)} \times \text{Insert Size (Kb)}}{\text{Vector Size (Kb)}} \times \text{Molar Ratio } \frac{\text{Insert}}{\text{Vector}} = \text{ng Insert}$$

A typical reaction consisted of the following:

Vector DNA	100 ng
Insert DNA	as per equation calculation
2X Rapid Ligation Buffer	5 µl
Fast Ligase	1 µl
Sterile Water	Brought to 10 µl

The reaction was incubated at room temperature for 10 min.

A

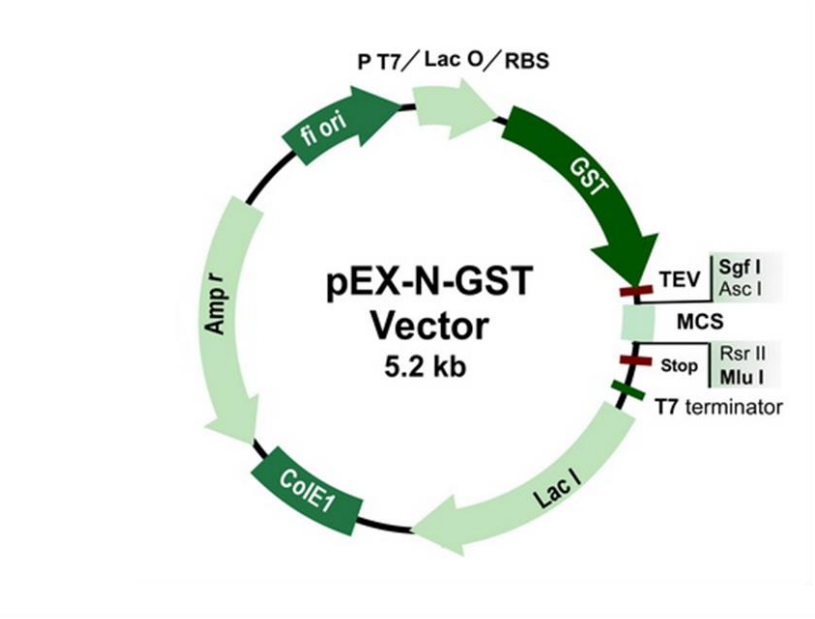

B

Figure 2.1: pEX-N-GST Vector (OriGene). **(A)** Vector map. **(B)** Schematic of the multiple cloning sites.

2.2.14.3 Transformation of Competent Cells

Transformation was carried out using the BL21 Star™ (DE3) Kit from Invitrogen, according to the manufacturer's instructions. Prior to transformation, one vial of chemically competent *E. coli* cells was removed from -70 ºC and allowed to thaw on ice for 30 min. Using ice cold tips, vector (5-10 ng) was added to the cells and

mixed by tapping gently. Vial was incubated on ice for 30 min. Following this, the sample was heated to 42 ºC for 30 s and placed on ice for 2 min. Pre-warmed SOC media (250 µl) (provided in the Kit) was added to the vial and was incubated at 37 ºC for 1 h at 200 rpm. Two different volumes of the transformation reaction (50 µl and 100 µl) were spread onto pre-warmed LB Agar plates (Section 2.1.4.2) containing 100 µg/ml ampicillin. The plates were incubated at 37 ºC overnight. Colony PCR (Section 2.2.14.4) was carried out to verify the presence of the desired insert in the vector of the sample clones.

2.2.14.4 Colony PCR

Bacterial colonies yielded by transformation were directly screened for the presence of the desired plasmid by PCR. Using aseptic techniques, an isolated colony was removed using a sterile tip and placed in a sterile 0.2 ml microcentrifuge tube containing a PCR master mix, having all the components necessary for PCR (Section 2.2.13.5) and also streaked onto a reference plate. cDNA and cDNA negative controls were included and PCR was carried out as described in Section 2.2.13.5, with the exception that the initial denaturing step was increased to 95 ºC for 5 min to allow the bacterial cells to rupture and release DNA for the PCR reaction.

2.2.14.5 Small Scale Plasmid Purification

Plasmid purification was carried out using the Qiagen QIA prep Mini-prep kit according to the Qiagen Plasmid Purification manual. All buffers (P1, P2, N3 and PE) and columns were supplied with the kit and details of buffer constituents are outlined in the Qiagen Plasmid Purification Handbook. An isolated colony was picked aseptically and used to inoculate LB broth (10 ml) (Section 2.1.4.1) containing 100 µg/ml ampicillin (Section 2.1.6). The culture was grown overnight at 37 ºC with

shaking at 200 rpm and the cells were harvested by centrifugation at 2,500 x g for 10 min at 4 ºC. The supernatant was removed and the pellet was resuspended in ice cold Buffer P1 (250 µl) and transferred to a sterile 1.5 microcentrifuge tube. Buffer P2 (250 µl) and Buffer N3 (350 µl) were then added and the tubes were inverted 5 times before centrifugation at 13,000 g for 10 min. The supernatant was transferred to the Qiaprep Spin Column and centrifuged at 13,000 x g for 1 min. The flow through was discarded and the column was washed with Buffer PE (750 µl) and centrifuged at 13,000 x g for 1 min. The flow through was again discarded and the column was centrifuged at 13,000 x g for 1 min to remove residual buffer. The Qiaprep Spin column was placed in a sterile 1.5 ml microcentrifuge tube. The DNA was eluted from the column by addition of sterile water (30 µl) followed by centrifugation at 13,000 x g for 1 min. The purified plasmid was subsequently analysed by DNA Gel Electrophoresis (Section 2.2.13.8) and was stored at -20 ºC until required for use.

2.2.14.6 DNA Sequencing

DNA sequencing of recombinant clones was performed by Source Bioscience (Tramore, Ireland) on a commercial basis.

2.2.15 *E. coli* Expression using the pEX-N-GST expression vector

2.2.15.1 Small Scale Induction of recombinant pEX-N-GST:MT-II clones

After confirmation that the pEX-N-GST:MT-II vectors were correctly transformed into *E. coli*, small scale inductions were carried out to obtain the desired recombinant protein. A 10 ml aliquot of LB broth (Section 2.1.4.1) containing ampicillin (100 µg/ml) (Section 2.1.6) was inoculated with an isolated *E.coli* colony containing pEX-N-GST:MT-II plasmid and was incubated overnight at 37 ºC while

shaking at 200 rpm. This starter culture (500 µl) was used to inoculate a 250 ml conical flask containing LB broth (50 ml) (Section 2.1.4.1) and ampicillin (100 µg/ml) (Section 2.1.6) and the culture was grown at 37 ºC (200 rpm) until an OD600 between 0.6-0.8 was reached. Upon reaching the desired growth level, a 1 ml aliquot of the culture was removed and kept as an un-induced cell reference for subsequent analysis. IPTG (Section 2.1.7) was added to the culture at a final concentration of 0.5 mM. 1 ml aliquots were removed every hour for 3 h and after overnight incubation. The one ml aliquots obtained (un-induced, 1, 2, 3 and overnight post induction) were centrifuged for 5 min at 13,000 x g. The supernatants were removed and the samples with the remaining pellet were stored at -20 ºC until ready for analysis. The samples were analysed by SDS-PAGE (Section 2.2.2.2) and Western Blot analysis (Section 2.2.2.5) to determine whether recombinant protein was expressed and at which time-point optimal protein expression occurred.

2.2.15.2 Large Scale Induction of recombinant pEX-N-GST:MT-II clones

A 100 ml Terrific Broth (Section 2.1.4.3) culture containing 100 µg/ml ampicillin (Section 2.1.6) was inoculated with an isolated *E. coli* colony containing recombinant pEX-N-GST:MT-II plasmid and was incubated overnight at 37 ºC while shacking at 200 rpm. Terrific Broth (Section 2.1.4.3) (2 L) containing 100 µg/ml ampicillin (Section 2.1.6) was inoculated with all the overnight starter culture (100 ml) and the culture was grown at 37 ºC (200 rpm) until an OD600 between 0.6-0.8 was obtained. Upon reaching the desired growth level, a 1 ml aliquot of the un-induced culture was removed and kept for subsequent analysis. IPTG (Section 2.1.7) was added to the culture at a final concentration of 0.5 mM and the culture proceeded to grow overnight. After overnight incubation, the cells were centrifuged (Sorvall Lynx 4000,

Thermo) at 5000 rpm at 4 ºC for 20 min. The supernatant was removed and the cell pellets were stored at -20 ºC.

2.2.16 Determination of Recombinant Protein Solubility

Upon induction of recombinant MT-II protein in *E. coli*, it was necessary to determine its solubility. A pellet harvested from the induction was re-suspended in Lysis Buffer (200 µl) (Section 2.1.5.3) and sonicated for 2 min prior to a 5 min centrifugation step at 13,000 x g at 4 ºC. The supernatant (representing the soluble fraction) was removed carefully to a new 1.5 ml microfuge tube and placed on ice while the pellet (insoluble fraction) was re-suspended in 200 µl of Lysis Buffer (Section 2.1.5.2) and stored on ice. A 20 µl aliquot was removed from each sample and analysed by SDS-PAGE (Section 2.2.2.2) and Western Blot analysis (Section 2.2.2.5).

2.2.17 Extraction and Purification of recombinant protein from *E. coli*

2.2.17.1 Preparation of Cleared *E. coli* Lysates

Cell pellets obtained from Section 2.2.15.2 were thawed on ice for 30 min and re-suspended in Lysis Buffer (Section 2.1.5.3) at 9 ml/ g cells wet weight. A smooth consistency was ensured by pipetting and stirring the mixture for 15 min at room temperature. The mixture was then incubated for 1 h 45 min on ice with shaking. Sodium deoxycholate (5 % (w/v)) (Section 2.1.5.4) was then added at 80 µl/ 9 ml Lysis Buffer, followed by DNase (5 KU/ml) (Section 2.1.5.6) at 40 µl/ 9 ml Lysis Buffer and 2 M magnesium chloride (Section 2.1.5.7) to a final concentration of 10 mM. Sample was further mixed and incubated for 30 min on ice with shaking. Once a smooth consistency was obtained, samples were centrifuged (Sorvall Lynx 4000,

Thermo) at 10,000 rpm for 15 min at 4 ºC. Lysates were collected and passed through 0.45 µm filters. Lysates were retained for further purification and processed on the same day.

2.2.17.2 Purification of GST-Tagged Protein from *E. coli* lysates by Affinity Chromatography

Purification of GST-tagged protein was carried out using an ÄKTA purifier coupled with a XK Column (Amersham Biosciences) packed with GSH agarose (10 ml bed volume) (Section 2.1.16.1). All the buffers used were filter sterilised before passing through the column. Lines were purged prior to use and the column was equilibrated with PBS (Section 2.1.8). Clear lysates (Section 2.2.17.1) were loaded onto the column at a flow rate of 1.5 ml/ min, with absorbance monitored at 254 and 280 nm. The flow through was collected and retained for multiple passes through the column as not all the protein may bind. The column was washed with PBS until no absorbance was detected. Protein was eluted with Elution Buffer (Section 2.1.16.4) and collected in 1 ml fractions. All fractions were analysed by Bradford Protein Assay and the fractions with the highest concentration were pooled together and checked by SDS-PAGE. Free glutathione was removed by dialysis against PBS (Section 2.2.8).

2.2.17.3 TEV Protease Cleavage of GST-MT-II

Further purification of GST tagged protein required cleavage from the GST tag. TEV protease (2 mg/ml; 80 µl) (Promega) was added to the GST tagged protein (1.5 mg/ml, 3 ml) and incubated for 90 min with gentle shaking. After incubation, HisLink^{TM} protein resin (80 µl) (Promega) was added to the mixture and incubated for further 15 min. After centrifugation at 1000 x g for 2 min and supernatant was transferred to a clean tube. The removal of the free GST tag was carried out by gravity

flow. An empty column was packed with GSH agarose beads. Subsequently, sample (containing free protein and GST) was applied to the column. The cleaved GST bound to the GSH beads and the free protein was collected in the flow-through. Sample was analysed by SDS-PAGE to confirm the cleavage.

2.2.18 Dialysis of Recombinant Protein

Dialysis tubing was pre-soaked in PBS (Section 2.1.8) for 10 min prior to use. Sample known volume to be dialysed was added to the dialysis tubing with an additional 25 % free space included to allow for sample volume expansion. The sealed tubing containing the sample was dialysed against 50 volumes. Dialysis was carried out at 4 ºC with stirring. Three buffer changes were carried out at 3 h intervals. Upon completion of dialysis, the sample was removed with a pipette and the volume of sample was then measured, and the concentration was determined.

2.2.19 Generation of MT-II disruption constructs and fungal transformation

The *A. niger MT-II* gene (An02g03100) was deleted by replacing the coding region with the hygromycin selection marker. The deletion cassette was produced by amplification of the fragments corresponding to 5' (2.5 kb) and 3' *MT-II* (2.5 kb) flanking regions using primers OFM24/25 and OFM26/27, respectively (Table 14). The gene coding for hygromycin resistance (*hph*) was amplified from pAN7.1 using primers OFM28/29 indicated in Table 14. A fusion PCR (Clontech HD cloning kit) was performed to ligate the three fragments into SmaI site of pUC19 to generate a *hph*::*MT-II*Δ cassette. Amplification of the disruption cassette (6.945 kb) was carried out by primers OFM34/35 (Table 14). Subsequently, the amplicon was used for transformation and gene replacement in *A. niger* N593.

A. niger N593 (10^6 spores/ml) was inoculated into 100 ml liquid transformation medium (TM) (Section 2.1.2.5.4) and grown for 20 h at 30 ºC. Transformation of fungal spores were performed according to common *Aspergillus* transformation protocols (Punt and van den Hondel, 1992). 2-4 µg linear deletion cassette was used for transformation of generated protoplasts. Protoplasts were plated on TM plates without yeast extract and casamino acids, containing 1.2 M sorbitol as osmotic stabilizer and hygromycin (200 µg/ml; InvivoGen) as selective antibiotic supplemented with uracil and uridine. The plates were incubated at 30 ºC for 4-6 days. Primary transformants were streaked out on the same TM plates without sorbitol.

Table 2.14: Primer sequences used in *MT-II* deletion experiments.

Primer Name	Sequence 5' – 3'
OFM24	TTCGAGCTCGGTACCCGTTTAAACACATCTCGCTTGCAGGCGGTAG
OFM25	TTGATGGTCGTTGTAGTTTGATGGATAGATGTGGACGTTC
OFM26	GAGGGCAAAGGAATAGTCGATAATGGTACCGGATGAATTG
OFM27	ACTCTAGAGGATCCCCGTTTAAACGCCCATCCTCTTTTAGCTTCATG
OFM28	CTACAACGACCATCAAAGTCGTATAG
OFM29	CTATTCCTTTGCCCTCGGACG
OFM34	GTTAGTAAAAGCCTAGCTTTACATC
OFM35	CTATCCATCGGGCTTCAATTGC
OFM46	GGCTTAAAGTTTATCCAGGAGATG
OFM65	CGCCATATCCACCACAACATAG
OFM70	ATGACCCCCAAAATCTCTCCC
OFM71	CTAGGGCTTTCTCCCCACCG

2.2.20 Statistical Analysis

Data analysis was carried out using built-in GraphPad prism version 5.01 functions, as specified.

Chapter 3

Gliotoxin perturbs methionine metabolism in *A. niger*

3 Chapter 3: Gliotoxin perturbs methionine metabolism in *A. niger*

3.1 Introduction

Gliotoxin (GT) is a non-ribosomal peptide secreted by several fungi that can redox cycle and consequently generate reactive oxygen species (Gardiner et al., 2005). This toxin has been extensively studied because of its cytotoxic and immunosuppressive affects on mammalian cells (Müllbacher et al., 1985; Niide et al., 2006). A high-throughput screening study in a single gene deletion library of *Saccharomyces cerevisiae* has been carried out by Chamilos et al. (2008) to identify genes associated with GT resistance or sensitivity. *S. cerevisiae* was used as a fungal eukaryotic model system to investigate the impact of GT on animal cells. Strains lacking *CYS3* and *MEF2* genes were found to be sensitive to GT. These genes are involved in the transsulfuration pathway and mitochondrial translational elongation, respectively, and their absence might have a key role in the survival of the fungi upon GT exposure (Chamilos et al., 2008). Little is known, however, about the affect this toxin has on other fungi.

The production of GT has proven discontinuous amongst fungal species. For example, pathogenic fungi *A. fumigatus* and plant disease biocontrol agent *Trichoderma virens* can produce GT while *A. niger* and *A. nidulans* lack the *gli* cluster responsible for the biosynthesis of the toxin (Patron et al., 2007).

Genome sequencing projects of several *Aspergillus* species have facilitated the transcriptomic and proteomic characterization of these fungi. Comparative proteomic studies using 2D-PAGE coupled to MALDI-ToF mass spectrometry have been carried out in *A. fumigatus* in the presence and absence of GT (Carberry et al., 2012; Schrettl et al., 2010b). Due to the ability of *A. fumigatus* to biosynthesise GT, these studies

illuminated, at least in part, the mechanisms of protection this organism has against its own toxin. Increase abundance of GliT oxidoreductase was found after GT addition and was confirmed to be an essential player in the self-protection process (Carberry et al., 2012; Scharf et al., 2010; Schrettl et al., 2010b). Another participant of this self-protection mechanism is GliA, which is a membrane-localized MFS transporter. Both genes, *gliA* and *gliT* are encoded within the *gli* cluster and appear to have evolved in GT-producing fungi but not GT naïve fungi (Owens et al., 2015; Wang et al., 2014). This system is responsible for the oxidation of dithiol GT and its secretion from the producing species, thereby attenuating the intracellular toxicity of the dithiol form (Section 1.4). Furthermore, transformation of *S. cerevisiae* with either *gliT* or *gliA* has been shown to confer increased resistance to GT (Schrettl et al., 2010b; Wang et al., 2014). Increased abundance of a Cu, Zn superoxide dismutase (SOD) was also observed which lead to speculate that GT may produce superoxide radicals and that SOD aids in the defence against these radicals in *A. fumigatus* (Carberry et al., 2012; Lessing et al., 2007). Moreover, RNA-seq analysis on the impact of GT on *A. fumigatus* wild-type and Δ*gliT* revealed a dysregulation of secondary metabolite clusters (including gliotoxin), ribosome biogenesis and an up-regulation in methionine metabolism among other cellular processes (O'Keeffe et al., 2014).

The affect GT has on other fungi has primarily been studied phenotypically, whereby GT has been shown to inhibit the growth of *Candida albicans* and *Cryptococcus neoformans* (Coleman et al., 2011). The anti-fungal properties of GT have also been observed in *A. niger* (Carberry et al., 2012), although the mechanism of this growth inhibition remains unclear.

As described on Section 1.2, *A. niger* is widely used as a host for the production of native and heterologous proteins, and multiple enzymes with biotechnological uses have been identified in, and purified from *A. niger* (Broekhuijsen et al., 1993; Withers et al., 1998). Indeed, the availability of *A. niger* CBS 513.88 genomic sequence in 2007 (Pel et al., 2007), and the more recent sequencing of a second *A. niger* strain ATCC 1015 (US Department of Joint Genome Institute, 2009) has facilitated its further development as a tractable system for recombinant protein expression. Comparative proteomic and transcriptomic analysis have been undertaken in *A. niger* to investigate changes due to the addition of stress (e.g., carbon starvation (Braaksma et al., 2010; van Munster et al., 2014, 2015; Nitsche et al., 2012) and DTT (Guillemette et al., 2007; MacKenzie and Guillemette, 2005) and antifungals (e.g. caspofungin and fenpropimorph (Meyer et al., 2007), and also changes induced by growth on different media compositions (xylose (Ferreira de Oliveira et al., 2010), and maltose (Lu et al., 2010)). These studies aimed to find ways to overcome the limitations *A. niger* might have during growth under industrial conditions. One of these limitations can be redox stress and the unfolded protein response (UPR) which affects protein over-expression (Al-Sheikh et al., 2004). Thus, it was speculated within my group if understanding the mechanism of GT sensitivity in *A. niger* could provide new insights into factors which negatively affect (Meyer et al., 2015) protein expression. As a result, my focus was to investigate *A. niger* as a model to explore GT cytotoxicity and to reveal its interference with different cellular systems. The work presented in this Chapter is focused on a proteomic/metabolomic investigation of the methionine (Met) pathway and complements observations carried out on *A. fumigatus* and *S. cerevisiae* were GT was shown to dysregulate this pathway (Chamilos et al., 2008; O'Keeffe et al., 2014).

Nonetheless, Chapter 4 provides a full analysis of the different cellular systems dysregulated after GT addition in *A. niger*.

The aims of the work carried out in this Chapter were; (i) to carry out phenotypic analysis of *A. niger* CBS 513.88 in response to gliotoxin (ii) to investigate changes to the proteome of *A. niger* in response to GT with special attention to the methionine and cysteine metabolism, along with sulfur metabolism (iii) to determine changes in the methionine-related metabolite levels in response to GT. These will include measurement of Met, *S*-Adenosylmethionine (SAM), *S*-Adenosylhomocysteine (SAH), Adenosine (Ado) and GSH/GSSG redox balance.

3.2 Results

3.2.1 Phenotypic analysis of *A. niger* CBS 513.88 in response to gliotoxin

Gliotoxin mediated growth inhibition has been observed in an *A. niger* environmental isolate strain (Carberry et al., 2012). In order to characterise the response of *A. niger* to GT using comparative proteomics we selected one of the two *A. niger* sequenced strains (CBS 513.88). Thus, phenotypic assays on *A. niger* CBS 513.88 were carried out in the presence of different concentrations of GT (0 – 10 μg/ml). Figure 3.1 shows that GT causes growth inhibition in *A. niger* CBS 513.88 in a concentration dependent fashion.

A

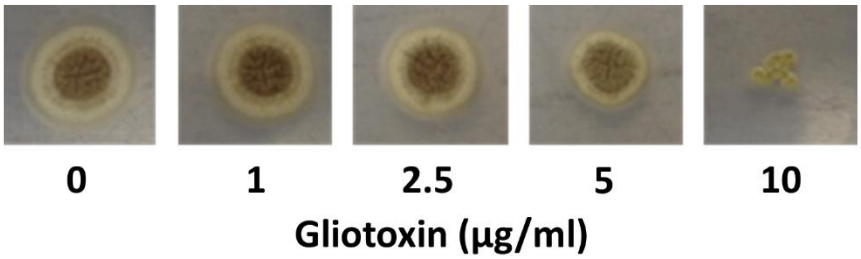

B

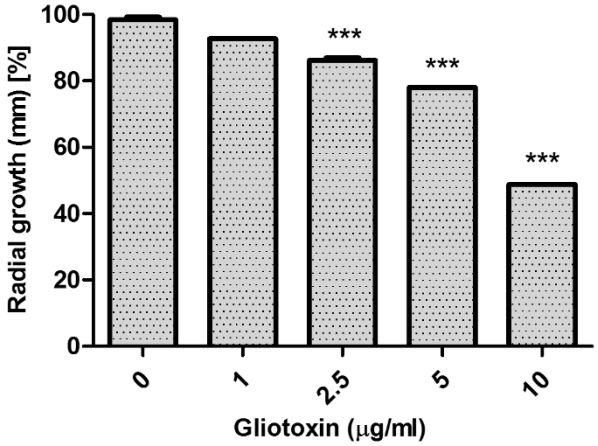

Figure 3.1: GT inhibits *A. niger* CBS 513.88 in a concentration-dependent fashion **(A)** Phenotypic analysis demonstrating GT-mediated growth inhibition after 72 h incubation. **(B)** Graphical representation of the phenotypic analysis shown on (A). Data analysed by one-way ANOVA. (*** $p < 0.0001$).

3.2.2 Label free quantitative (LFQ) proteomics reveals that exogenous gliotoxin alters the abundance of hundreds of proteins in *A. niger* CBS 513.88

A. niger CBS 513.88 was grown for 45 h in PDB prior exposure to MeOH (control) and GT (2.5 μg/ml) for 3 h and 6 h (n = 4, respectively). Mycelia were harvested and protein was extracted as per Section 2.2.3.4. Protein lysates were trypsin digested and ProteaseMax was added as described in Section 2.2.5. Subsequent peptide mixtures were separated on extended LC gradients and subjected to tandem MS using a Thermo Fisher Q-Exactive system. Data analysis was done using the MaxQuant software (Section 2.2.11).

The times of exposure were selected based on preliminary analyses (data not shown) which revealed that 3 h generated a greater proteomic response compared to earlier time points. 6 h was chosen with the aim to observe signs of recovery or enhanced sensitivity by gliotoxin in the fungus. A total of 1364 proteins groups were identified in *A. niger* exposed to 3 h exogenous GT, of which 378 exhibited significantly altered abundance ($p < 0.05$) compared to MeOH-treated controls (Figure 3.2). Of these 378 proteins, 158 proteins showed increased abundance when *A. niger* was exposed to gliotoxin, while 220 proteins were less abundant (Appendix: Tables 1 and 2). On the other hand, when *A. niger* was exposed to exogenous GT for 6 h, a total of 1185 proteins were identified of which 343 were significantly altered in abundance ($p < 0.05$) (Figure 3.2). 187 proteins were increased and 156 showed decreased in abundance upon GT addition (Appendix: Tables 3 and 4).

A

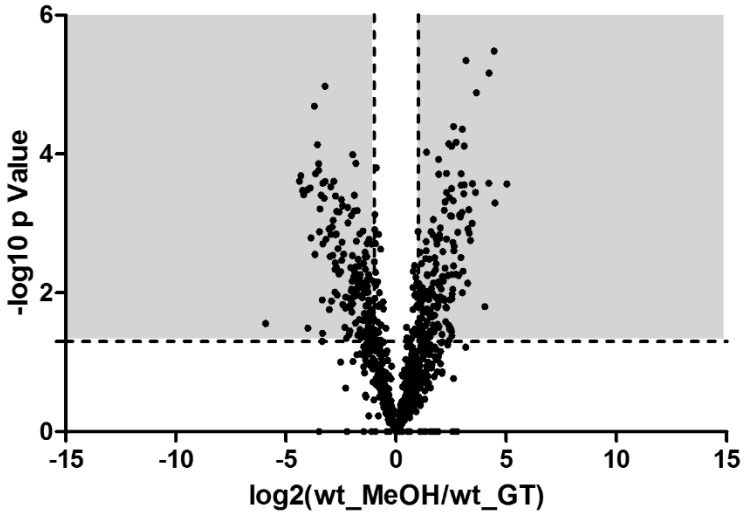

B

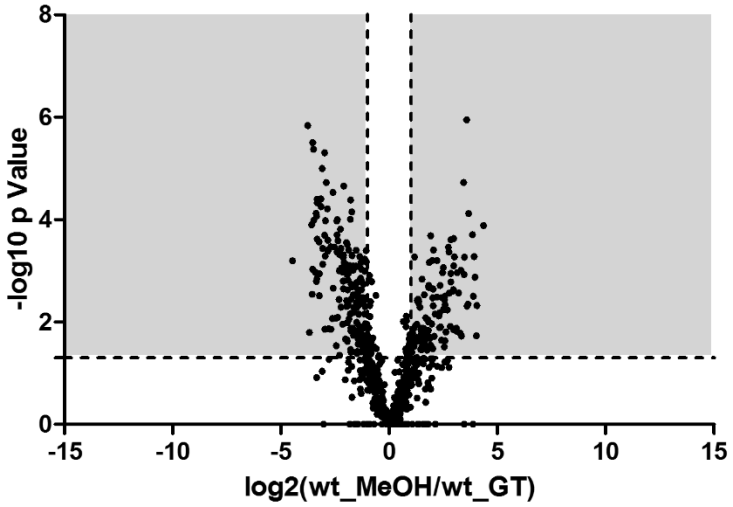

Figure 3.3: Overall impact of GT on *A. niger* CBS 513.88 protein abundance. **(A)** Differentially abundant proteins between *A. niger* exposed to 3 h GT compared to MeOH control. **(B)** Differentially abundant proteins between *A. niger* exposed to 6 h GT compared to MeOH control. Grey shaded areas highlight the significantly ($p < 0.05$) increase ($\log_2$ fold ≥ 1) and decrease ($\log_2$ fold ≤ 1) in protein abundance in each set.

Functional analysis of the differentially abundant proteins was achieved using the Functional Catalogue (FunCat) annotation tool (Ruepp et al., 2004). Following *A. niger* exposure to exogenous GT for 3 h and 6 h, FunCat analysis showed 4 categories over-represented in the increased abundant protein sets at both time points. These included metabolism (3 h; $n = 74$, $p < 0.035$ and 6 h; $n = 99$, $p < 0.0003$), cell rescue, defence and virulence (3 h; $n = 25$, $p < 0.014$ and 6 h; $n = 34$, $p < 0.022$), interaction with the environment (3 h; $n = 16$, $p < 0.001$ and 6 h; $n = 23$, $p < 0.002$) and cell cycle and DNA processing (3 h; $n = 16$, $p < 0.034$ and 6 h; $n = 22$, $p < 0.046$). Categories enriched at 3 h included protein synthesis ($n = 17$, $p < 0.015$) and cellular transport, transport facilitation and transport routes ($n = 31$, $p < 0.016$), while categories enriched only at 6 h include transcription ($n = 18$, $p < 0.0003$) and regulation of metabolism and protein function ($n = 12$, $p < 0.047$) (Figure 3.3). On the other hand, functional classification of proteins with reduced abundance after GT exposure (3 h) were metabolism ($n = 104$, $p < 0.041$), energy ($n = 51$, $p < 8.72e^{-06}$) and cell type differentiation ($n = 17$, $p < 0.047$). Protein with binding function or cofactor requirement (structural or catalytic) was enriched in both time points (3 h; $n = 112$, $p < 1.16e^{-05}$ and 6 h; $n = 76$, $p < 0.001$) and categories over-represented in the decreased abundance set after 6 h included protein fate ($n = 38$, $p < 0.016$) and protein synthesis ($n = 20$, $p < 0.001$) (Figure 3.3).

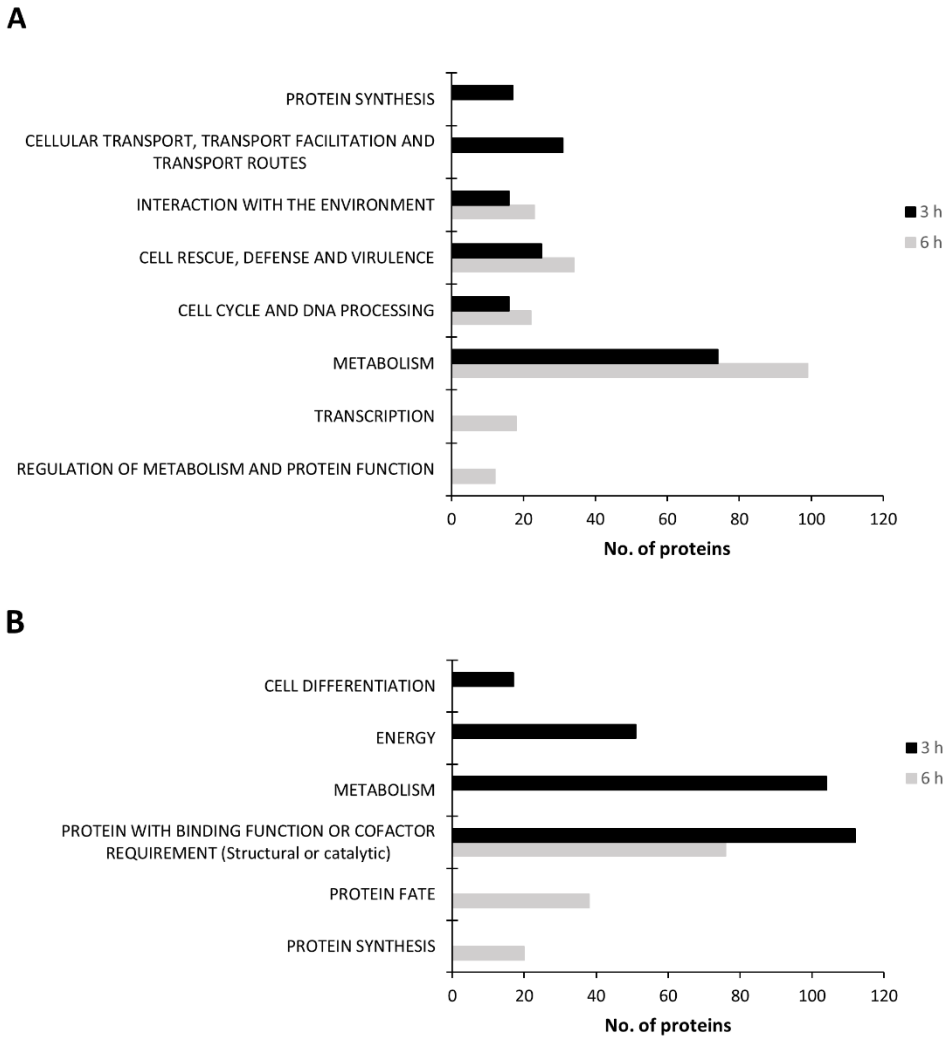

Figure 3.3: GT exposure induces significant changes in protein abundance in *A. niger*. Functional classification into FunCat 1st level categories of **(A)** Protein families with increased abundance in *A. niger* CBS 513.88 exposed to GT compared to the MeOH control and **(B)** Protein families with decreased abundance in *A. niger* CBS 513.88 exposed to GT compared to the MeOH control.

3.2.3 Gliotoxin exposure increases the abundance of proteins involved in the methionine cycle

Dysregulation of enzymes involved in methionine and cysteine metabolism was observed in *A. niger* following exposure to exogenous gliotoxin for 3 h whereby five proteins exhibited reduced and three increased abundance (Figure 3.4). In contrast, 2 proteins decreased in abundance in *A. niger* in response to exogenous GT for 6 h and 2 proteins were evident with increased abundance (Table 3.1).

S-Adenosylhomocysteinase (SAHase), which catalyses the degradation of SAH to homocysteine (Hcy) and Ado, was increased in abundance by $\log_2$ 2.46-fold and 1.45-fold at 3 h and 6 h, respectively, whilst homoserine dehydrogenase was similarly abundant at both time points ($\log_2$1.96-fold at 3 h and $\log_2$1.89-fold at 6 h). Spermidine synthase, involved in methionine recycling and polyamine biosynthesis (Yang cycle) (Sauter et al., 2013) was increased in abundance $\log_2$ 2.00-fold (at 3 h). Of the 5 proteins exhibiting decreased abundance in *A. niger* after 3 h GT exposure, 2 homologous aspartate aminotransferases (An16g05570 and An04g06380) and 2 homologous malate dehydrogenases (An07g02160 and An15g00070), which are part of the TCA cycle and the malate-aspartate shuttle (Lu et al., 2010) also appear to be involved in the generation of pyruvate from cysteine according to KEGG classification. Cysteine synthase, which catalyses the formation of cysteine from *O*-acetylserine, was not detectable after GT exposure (at 3 h). Two additional proteins showing reduced abundance after 6 h GT exposure were An04g06380 ($\log_2$1.90-fold) and An11g09510 ($\log_2$1.03-fold) which are involved in aspartate biosynthesis.

Table 3.1: Abundance changes of proteins involved in the cysteine and methionine metabolism in *A. niger* CBS 513.88 after exposure to gliotoxin (2.5 µg/ml) for 3 h and 6 h, respectively.

Protein Description	Log_2 Fold-change 3h	Log_2 Fold-change 6 h	EC Number	Accession
Cysteine and methionine metabolism				
Adenosylhomocysteinase	↑ 2.463	↑ 1.454	3.3.1.1	An08g01960
Ortholog(s) have spermidine synthase activity, role in pantothenate biosynthetic process, spermidine biosynthetic process and cytosol, extracellular region, nucleus localization	↑ 2.004	-	2.5.1.16	An08g06560
Homoserine dehydrogenase	↑ 1.969	↑ 1.899	1.1.1.3	An02g07430
Cysteine synthase	Absent	-	2.5.1.47	An02g10750
Aspartate transaminase; phenylalanine:alphaketoglutarate aminotransferase	↓ 2.707	-	2.6.1.1	An16g05570
Mitochondrial aspartate aminotransferase	↓ 2.506	↓ 1.906	2.6.1.1	An04g06380
Mitochondrial malate dehydrogenase	↓ 1.418	-	1.1.1.37	An07g02160
Malate dehydrogenase precursor; Malate dehydrogenase	↓ 1.321	-	1.1.1.37	An15g00070
Aspartic beta semi-aldehyde dehydrogenase, aspartate semialdehyde dehydrogenase	-	↓ 1.036	1.2.1.11	An11g09510
Sulfur metabolism				
Has domain(s) with predicted electron carrier activity, molybdenum ion binding, oxidoreductase activity and role in oxidation-reduction process	↑ 1.214		1.8.3.1	An08g08910
ATP sulfurylase	↓ 2.278	-	2.7.7.4	An11g09790

Protein Description	Log_2 Fold-change 3h	Log_2 Fold-change 6 h	EC Number	Accession
Ortholog(s) have electron transporter, transferring electrons from CoQH2-cytochrome c reductase complex and cytochrome c oxidase complex activity	-	↓ 1.515	-	An02g01830

Furthermore, in addition to the dysregulation of the cysteine and methionine metabolism, two SAM-dependent methyltransferases (MTases), which utilize SAM as a methyl donor in trans-methylation reactions, showed *de novo* abundance in response to GT exposure (MT-I and MT-II at 3 h; MT-I and methyltransferase An18g03220 at 6 h) (Table 3.2). Abundance of an *N*-methyltransferase (An02g08430) was also increased ($log_2$1.44-fold at 3 h) after GT addition (Table 3.2). Given the unexpected detection of these MTases and their potential interaction with the methionine cycle, we analysed whether the levels of Met-related metabolites were affected. All together, these data demonstrate the impact GT has in the methionine cycle and cysteine metabolism is greater at 3 h exposure compared to 6 h which suggests that over time, *A. niger* may be able to recover after GT exposure.

Table 3.2: Abundance changes in SAM-dependent methyltransferases in *A. niger* CBS 513.88 after exposure to gliotoxin (2.5 µg/ml) for 3 h and 6 h, respectively.

Protein Description	Log_2 Fold-change 3 h	Log_2 Fold-change 6 h	EC Number	Accession
Putative methyltransferase (MT-II)	Unique	-	-	An02g03100
Putative SAM-dependent methyltransferase (MT-I)	Unique	Unique	-	An08g10700
Ortholog(s) have double-stranded DNA 5'-3' exodeoxyribonuclease activity, single-stranded DNA endodeoxyribonuclease activity, tRNA (m5U54) methyltransferase activity and role in double-strand break repair, tRNA modification	-	Unique	2.1.1.35	An18g03220
Ortholog(s) have histone-arginine N-methyltransferase activity, ribosome binding activity and role in peptidyl-arginine methylation, to asymmetrical-dimethyl arginine, ribosome biogenesis	↑ 1.448	-	2.1.1.-	An02g08430
Aminomethyltransferase	↓ 1.028	-		An08g03070

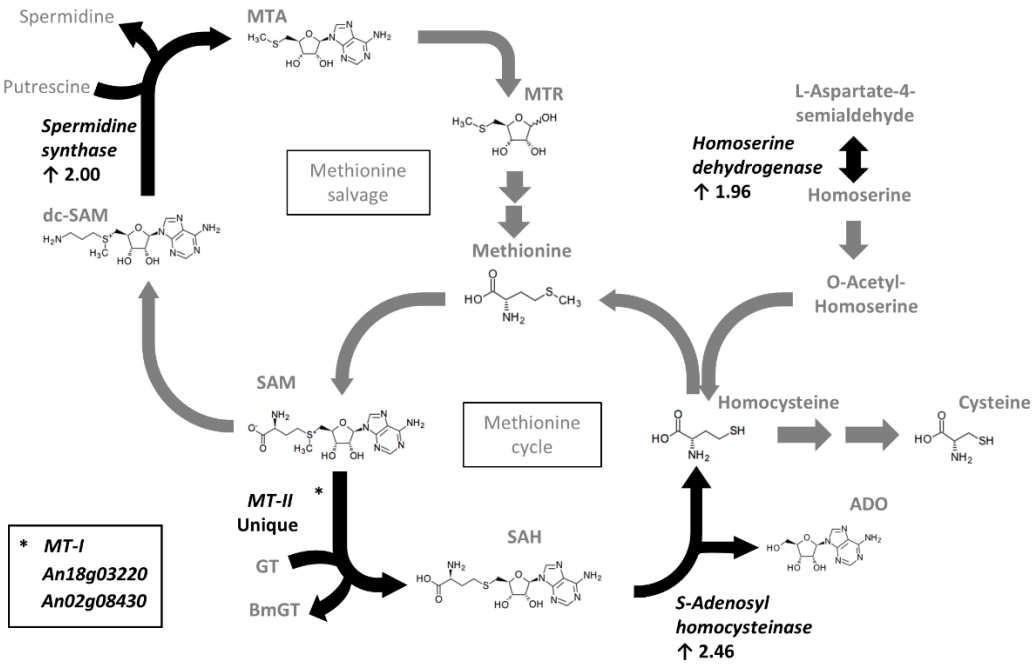

Figure 3.4: GT exposure increases abundance of proteins involved in the methionine cycle. Enzymes in black are increased in abundance after GT addition (3 h) in *A. niger* CBS 513.88. Activity of MT-II, an ortholog of *A. fumigatus* GtmA, utilizes SAM to effect bis-thiomethylation of rGT to BmGT (see Chapter 1 and 5) (Dolan et al., 2014).

3.2.4 Methionine-related metabolite profiling

Characterization of methionine-related metabolites was carried out in order to correlate this data with the proteomic analysis and to assess fundamental changes in the biochemistry of the fungus. For this purpose, several methods of metabolite quantification were used and developed, these included; (i) quantification of intracellular methionine levels using *o*-phthalaldehyde (OPA) derivatization (Section 2.2.8.2), (ii) detection of mycelial SAM, SAH and Ado using a LC-MS/MS-based assay (Section 2.2.10.2) (Owens et al., 2015), and (iii) quantification of GSH/GSSG levels using a spectrophotometric based assay (O'Keeffe et al., 2013) (Section 2.2.12).

Determination of these metabolites was carried out through the preparation of samples grown under identical conditions to those employed for proteomic analyses (*A. niger* CBS 513.88 was grown for 45 h prior addition of GT (2.5 μg/ml) for further 3 h and 6 h).

3.2.4.1 Intracellular methionine measurement

Intracellular methionine levels were measured using a modified HPLC method developed by Sun et al. (2005) (Section 2.2.8.2). Met elution time was identified as 12.307 min (Figure 3.6) and a standard curve was generated at a concentration range of 0.125 – 4 mM. This curve was linear and reproducible (Figure 3.5) and was used in subsequent assays to calculate the amount of intracellular Met in *A. niger* extracts, following previous exposure to either GT or MeOH only.

Met levels were determined in *A. niger* MeOH control extracts and compared to those in GT exposed extracts. The concentration of Met was determined from the standard curves and represented as % concentration (shown as % normalised data).

Results indicated that there was a significant increase in the levels of methionine under gliotoxin exposure for 3 h (p = 0.0132) and 6 h (p = 0.0106) (Figure 3.6). More specifically, the increment of Met appeared to be higher at 6 h compared to 3 h gliotoxin addition.

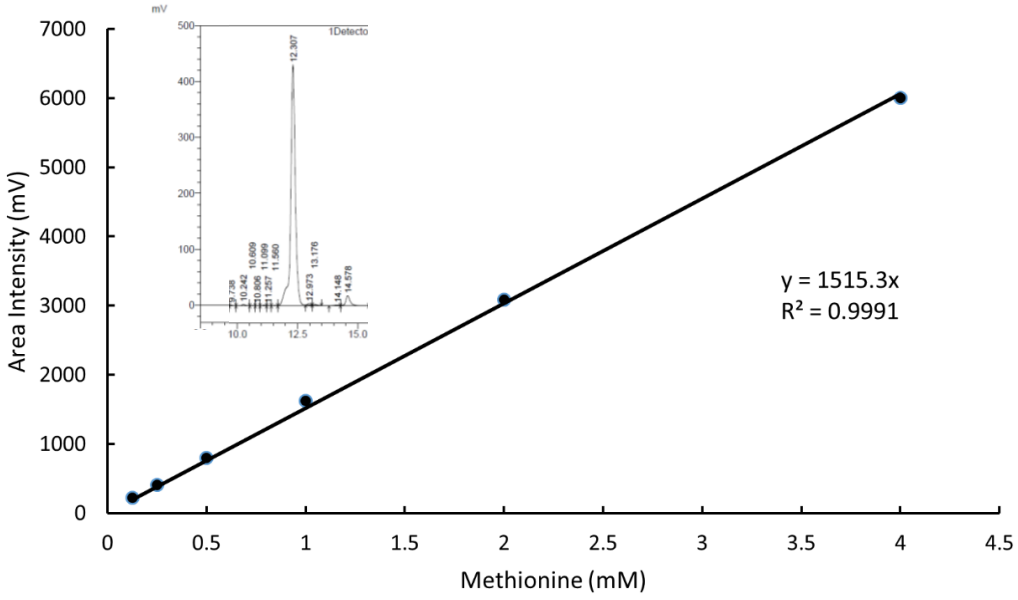

Figure 3.5: Methionine standard curve. Methionine standard elutes at a R_T of 12.307 min

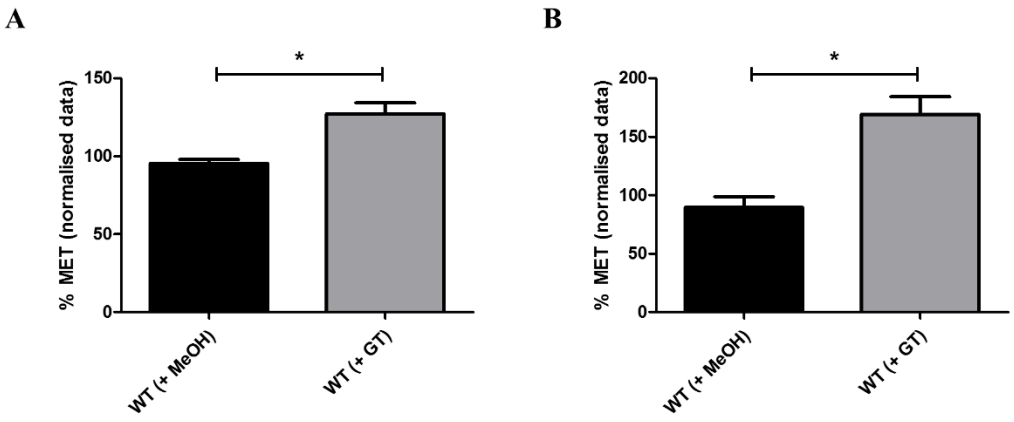

Figure 3.6: Methionine levels were significantly increased in *A. niger* CBS 513.88 exposed to GT (2.5 µg/ml) for **(A)** 3 h (**p* = 0.0132) and **(B)** 6 h (**p* = 0.0106).

3.2.4.2 Intracellular SAM levels

LC-MS detection of SAM was carried out as previously described by Owens et al. (2015) (Section 2.2.10.2). *A. niger* CBS 513.88 was grown for 45 h and exposed to exogenous GT (2.5 µg/ml) for 3 h and 6 h followed by mycelial harvesting. SAM was extracted according to Section 2.2.3.2 (Roeder et al., 2009) and samples were analysed by LC-tandem MS (MS/MS) using electrospray ionization. LC-MS analysis of commercially available SAM standards confirmed the presence of SAM at a retention time (R_T) of 8.5 min. SAM was identified by its intact mass of *m/z* 399 ($C_{15}H_{22}N_6O_5S$) that corresponds to the singly charged ion [$(M + H)^+ = 399$] and its fragmentation pattern (250, 136, 102 and 97 m/z) (Figure 3.7). Analysis of SAM in *A. niger* revealed a significant decrease ($p = 0.0366$) in intensity in GT extracts compared to MeOH control. On the other hand, SAM was significantly increased ($p = 0.0230$) in *A. niger* GT extracts compared to MeOH control (Figure 3.8). This might indicate that

SAM consumption is higher at 3 h GT exposure compared to 6 h and will be further discussed in Section 3.3.

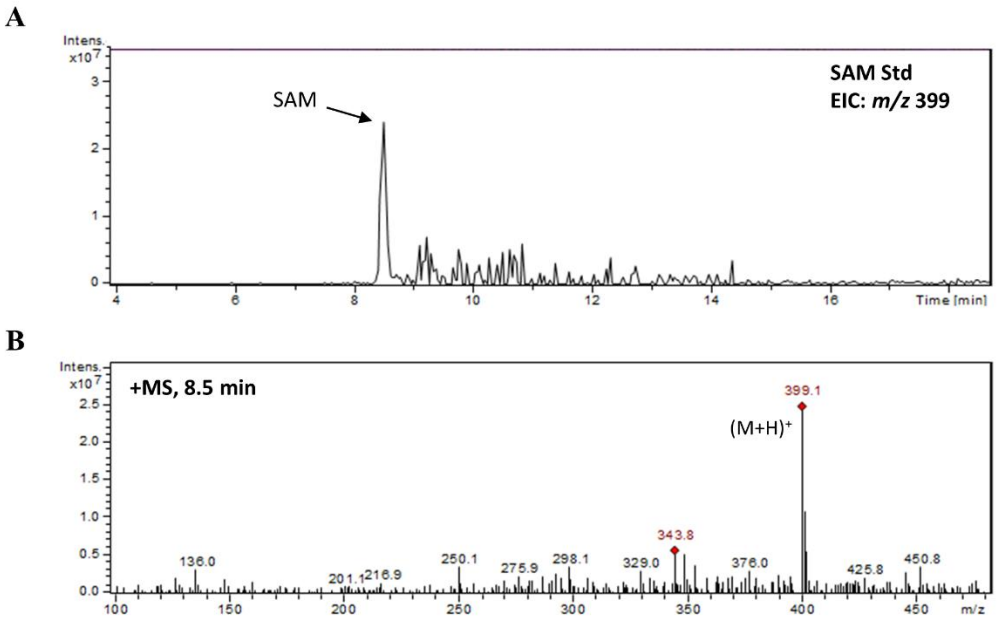

Figure 3.7: (A) Extracted ion chromatograms (EIC) of SAM commercial standard. **(B)** SAM (*m/z* = 399) was used as a reference for identification in *A. niger* lysates.

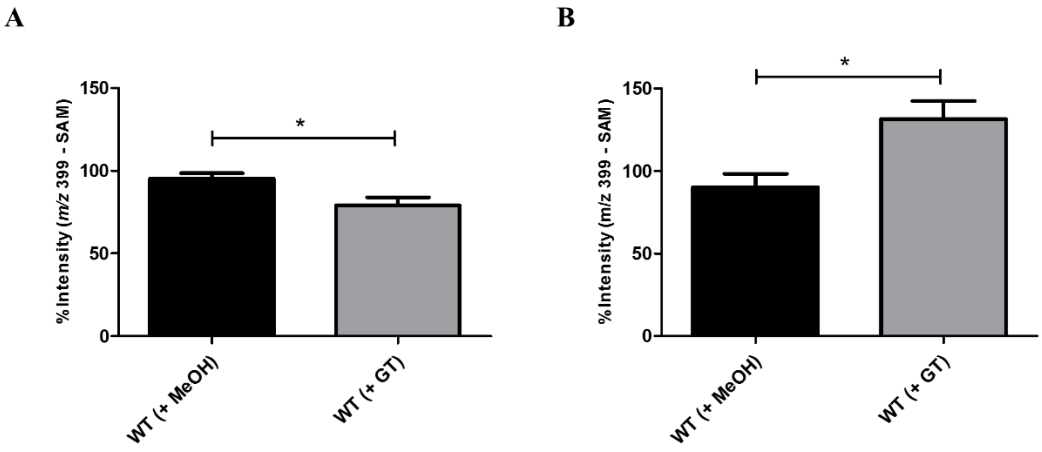

Figure 3.8: (A) Significant reduction in the level of SAM in *A. niger* CBS 513.88 after 3 h GT exposure (2.5 μg/ml) (**p* = 0.0366). **(B)** SAM level was significantly increased in *A. niger* exposed to GT for 6 h (**p* = 0.0230).

3.2.4.3 Intracellular SAH levels

The strategy for the determination of SAH was the same as per Section 3.2.4.2 utilized for SAM identification. In this case, LC-MS analysis of commercially available SAH standards confirmed the presence of SAH at a R_T of 10.5 min. SAH was identified by its whole mass of *m/z* 385 ($C_{14}H_{20}N_6O_5S$) that corresponds to the singly charged ion [$(M + H)^+ = 385$] and its fragmentation pattern (250, 136, 134, 88). When the analysis was carried out on *A. niger* samples (MeOH vs GT), no SAH was detected in any of the chromatograms. Due to the constant absence of SAH, it was speculated if SAH had been degraded or enzymatically broken down into its metabolic products.

To analyse potential SAH breakdown, *A. niger* CBS 513.88 was grown for 48 h in PDB (Section 2.1.2.1) and mycelia extracted as per Section 2.2.3.1. In order to quantify SAH, a standard curve was generated at a concentration range of 6.25 – 400

μg/ml SAH and a linear relationship was obtained between the concentration of SAH and the mAU (Figure 3.9). SAH (50 μg/ml final concentration) was spiked into *A. niger* lysates and samples were analysed using RP-HPLC (Section 2.2.8.1) after 0, 35, 70 and 105 min post-spiking. Spiked SAH eluted at a R_T of 5.66 min, which is comparable to the standard SAH peak at 5.60 min (Figure 3.10). The standard curve was used to quantify the amount of SAH presence or absence after spiking in the sample.

The disappearance of SAH over time was evident in *A. niger* acid lysates containing spiked SAH (Figure 3.10). Interestingly Figure 3.10 indicated that (i) SAH standard is stable in 0.1 M HCl (ii) SAH spiked (50 μg/ml) in *A. niger* lysates (48 μl/rxn lysate) is decreased to approximately 35 μg/ml after 105 min, and (iii) SAH spiked (50 μg/ml) in *A. niger* lysates (96 μl/rxn lysate) is decreased to approximately 10 μg/ml after 105 min. All together these data indicates that SAH disappearance is an enzyme-dependent process.

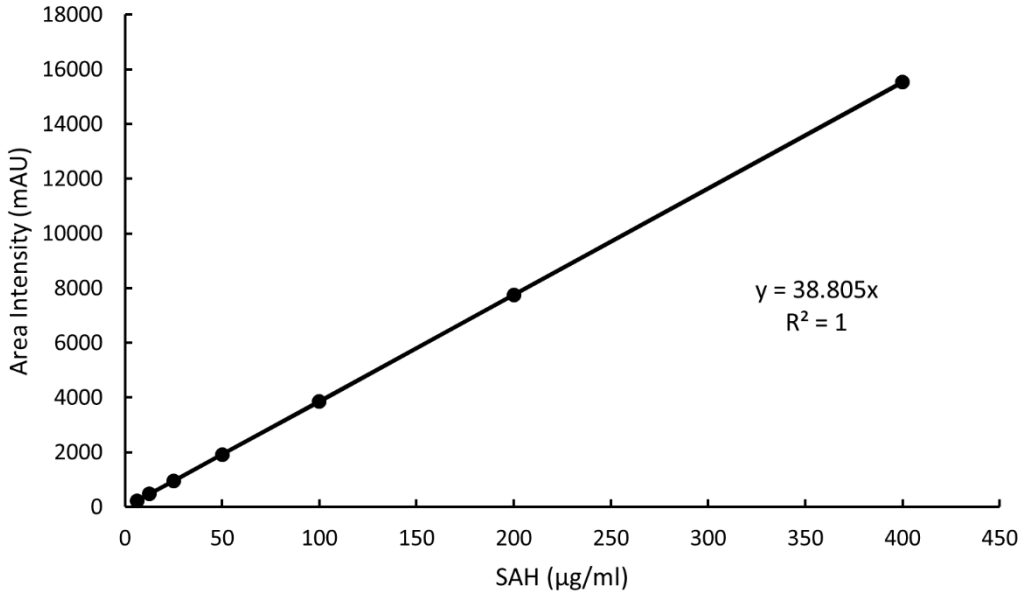

Figure 3.9: SAH Standard curve, generated by RP-HPLC quantification.

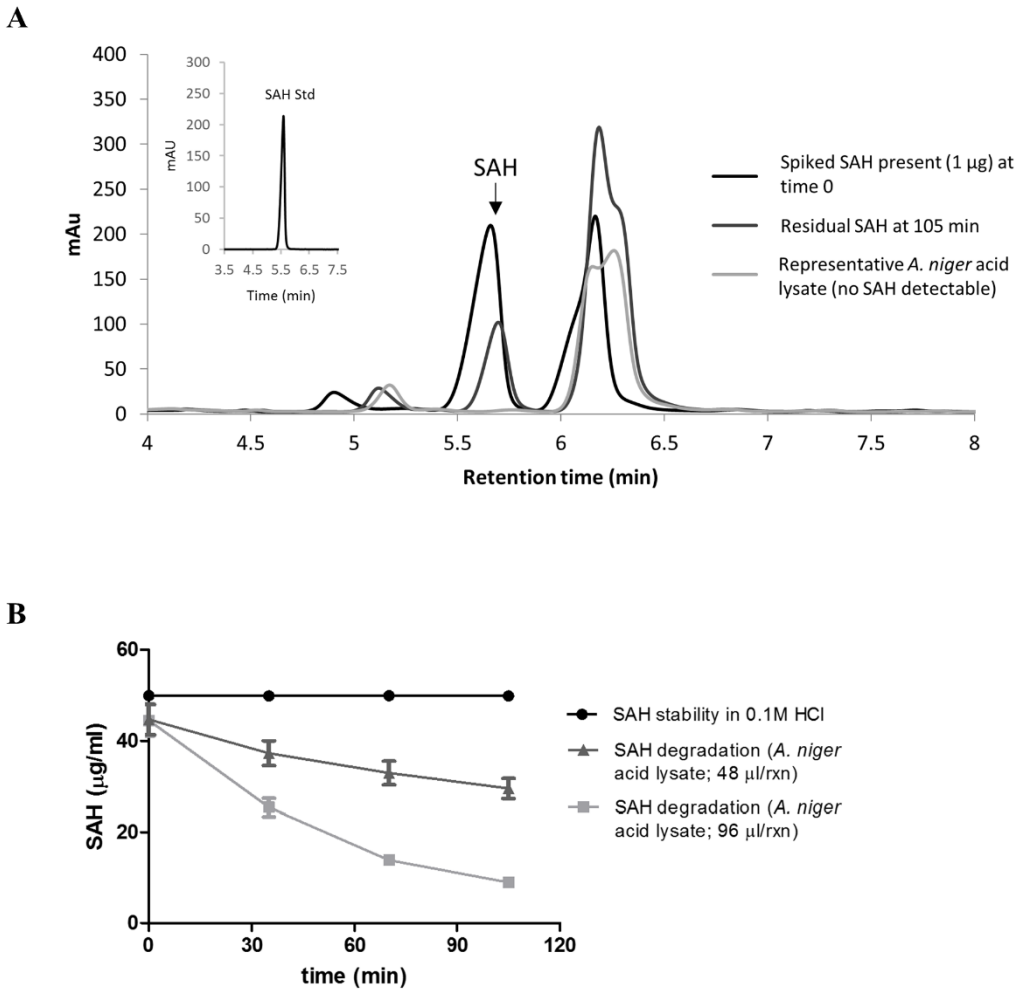

Figure 3.10: A) Overlaid HPLC chromatograms of *A. niger* HCl lysates analysed at time 0 min (black) and 105 min (dark grey) after SAH spiking and *A. niger* HCl lysate with no SAH addition (clear grey). Spiked SAH eluted at R_T = 5.66 min (black arrow). There was no SAH detection in *A. niger* lysates. **B)** SAH degradation activity was found in *A. niger* HCl lysates whereby spiked SAH disappeared in a time- and concentration-dependent fashion.

Based on these observations, subsequent LC-MS/MS identification of constituent proteins, using a Thermo Scientific Q Exactive mass spectrometer, was carried out in *A. niger* acid lysates (Section 2.2.11). The resulting spectra were searched with Sequest HT engine within Proteome Discoverer 1.4. Filters were: (i) peptide filters; set to high peptide confidence and (ii) protein filters; set to two peptides per protein. Overall, 129 proteins were identified using these filters. Table 3.3 represents those proteins with the highest score number (n = 50). The remaining proteins with lower scores (n = 79) are shown on Table 5 of the Appendix (Chapter 9).

Results on Table 3.3 reveal the presence of SAHase (marked in bold), thus potentially explaining the progressive reduction of added SAH and its absence in native, non-spiked samples.

Table 3.3: *A. niger* CBS 513.88 mycelial proteins (*n* = 50) identified in 0.1 M HCl lysates by mass spectrometry. The resulting spectra were searched with Sequest HT engine within Proteome Discoverer 1.4. Data arranged in order of decreasing score.

Protein Description	Score	Coverage (%)	Unique Peptides	AAs	MW (kDa)	Calc. pI	Accession
1,4-alpha-D-glucan glucohydrolase	388.25	31.41	9	640	68.3	4.45	An03g06550
Glyceraldehyde-3-phosphate dehydrogenase	250.80	44.94	8	336	36.2	7.11	An16g01830
Hsp70 protein	143.55	20.72	6	637	69.5	5.17	An07g09990
DnaK-type molecular chaperone	100.80	21.66	6	614	66.8	5.34	An16g09260
F1F0-ATPase complex subunit	94.56	46.70	3	182	20.0	4.89	An14g04180
Protein similar to elongation factor 1 alpha	89.35	20.87	4	460	49.9	8.92	An18g04840
Pyruvate decarboxylase	84.44	31.75	8	567	62.5	6.76	An02g06820
Actin structural protein	64.18	31.73	6	375	41.6	5.58	An15g00560
Phytase (myo-inositol-hexakisphosphate phosphohydrolase); narrow pH optimum at around 2.5, very little activity at pH 5.0	63.65	17.75	3	479	52.5	4.75	An08g11030
Cytoplasmic ATP-citrate lyase	62.80	20.62	5	485	52.8	5.96	An11g00530
Putative transketolase	56.75	19.44	5	684	74.7	6.43	An08g06570
F1F0-ATPase complex subunit	55.29	13.85	3	556	60.0	9.07	An16g07410
Glutamine synthetase	52.38	41.60	6	375	41.6	5.71	An01g08800

Protein Description	Score	Coverage (%)	Unique Peptides	AAs	MW (kDa)	Calc. pI	Accession
Pyruvate kinase	51.43	13.69	3	526	58.1	7.25	An07g08990
6-phosphofructo-1-kinase	50.13	15.58	5	783	85.7	7.18	An18g01670
Phosphopyruvate hydratase	50.12	23.29	5	438	47.3	5.40	An18g06250
Putative UTP-glucose-1-phosphate uridylyltransferase; Leloir pathway enzyme	49.97	22.07	6	521	57.9	7.24	An12g00820
Putative acid aspartic protease, constitutively expressed	49.48	23.62	4	398	43.4	5.01	An02g07210
Translation elongation factor 2	49.12	12.56	6	844	93.6	6.90	An02g05700
Cu,Zn superoxide dismutase	48.59	37.01	2	154	15.9	6.40	An07g03770
Elongation factor 1 beta	48.27	19.54	2	302	33.4	4.69	An08g03490
Has domain(s) with predicted catalytic activity, enoyl-[acyl-carrier-protein] reductase (NADH) activity, fatty acid synthase activity, transferase activity	45.88	14.74	8	1214	134.0	5.66	An01g00050
Glycerol dehydrogenase; D-arabinose 1-dehydrogenase [NAD(P)+]	45.74	19.08	3	325	36.7	6.37	An01g06970
Putative acid alpha-amylase	45.25	31.88	6	505	55.2	4.46	An11g03340
Ortholog(s) have role in intracellular sterol transport and extracellular region, fungal-type vacuole lumen localization	45.12	22.99	2	174	19.3	5.34	An02g03310
Spi1-GTPase binding protein	45.06	23.90	4	251	28.2	4.92	An18g02140
NADP-dependent glutamate dehydrogenase	44.87	17.39	3	460	49.3	6.10	An04g00990

Protein Description	Score	Coverage (%)	Unique Peptides	AAs	MW (kDa)	Calc. pI	Accession
Carboxypeptidase Y family secreted protease	44.52	17.49	5	566	62.6	4.73	An03g05200
ATP:citrate oxaloacetatelyase	44.39	17.53	6	656	71.5	8.19	An11g00510
Sorbitol dehydrogenase	39.84	27.94	5	340	36.9	6.25	An01g03480
Extracellular alpha-glucosidase pro-protein	39.27	7.61	4	985	108.8	5.35	An04g06920
Ortholog of *A. nidulans FGSC A4* : AN3975, AN9193/llmJ, AN2891 and *A. fumigatus Af293* : Afu1g10150, Afu2g04380, Afu3g15150, Afu3g15280, Afu6g03300	38.93	21.67	3	300	33.0	5.97	An16g05930
Putative protease	38.33	18.55	5	663	72.4	5.88	An04g02850
Adenosylhomocysteinase	38.29	12.47	3	449	49.0	6.29	An08g01960
Methionine synthase; 5-methyltetrahydropteroyltriglutamate-homocysteine S-methyltransferase	37.83	16.80	6	774	87.0	6.68	An04g01750
Putative mitochondrial heat shock protein	36.29	17.87	6	666	72.1	5.83	An16g05090
Sedolisin family secreted protease; lysosomal pepstatin-insensitive protease	33.00	10.76	2	595	64.4	5.00	An06g00190
Fatty acid synthase subunit alpha	32.43	4.14	4	1862	204.5	6.23	An01g00060
E2 dihydrolipoamide acetyltransferase	31.57	9.93	3	675	72.6	8.24	An07g02180
Acid phosphatase	31.27	18.47	4	498	54.6	4.64	An12g10630
Alpha-amylase (1, 4-alpha-D-glucan 4-glucanohydrolase)	31.24	13.65	3	498	54.6	4.74	An05g02100

Protein Description	Score	Coverage (%)	Unique Peptides	AAs	MW (kDa)	Calc. pI	Accession
Ortholog(s) have DNA binding activity and cytosol, nucleus localization	30.92	16.26	3	406	43.9	7.99	An04g08860
Mitochondrial malate dehydrogenase	30.47	26.47	3	340	35.7	8.94	An07g02160
Glutamate decarboxylase	30.35	16.89	4	515	58.5	6.20	An08g08840
Putative vacuolar serine proteinase; putative signal sequence for transport into the endoplasmic reticulum; secreted protein	29.78	23.14	4	497	52.8	5.44	An07g03880
F1F0-ATPase complex subunit	29.65	16.50	2	297	32.4	7.85	An01g04630
Cytoplasmic pyruvate carboxylase	28.80	5.29	3	1192	130.8	6.51	An04g02090
Aspergillopepsin A, a pepsin family secreted acid protease	28.51	18.27	3	394	41.3	4.67	An14g04710
Protein similar to dipeptidyl peptidase II	28.18	8.61	2	569	62.9	5.07	An12g05960
Ortholog of *A. oryzae RIB40* : AO090023000241, *Neosartorya fischeri NRRL 181* : NFIA_056230, *Aspergillus wentii* : Aspwe1_0039389 and *Aspergillus clavatus NRRL 1* : ACLA_084080	27.75	23.44	2	192	20.0	7.71	An11g00890

3.2.4.4 Intracellular Ado levels

Due to the absence of SAH in *A. niger* protein lysates, possibly as a result of SAHase activity, levels of Ado were measured. Ado is a by-product of SAHase catalysed reaction (Figure 1. 11), thus quantification of Ado can give an indication of SAH breakdown.

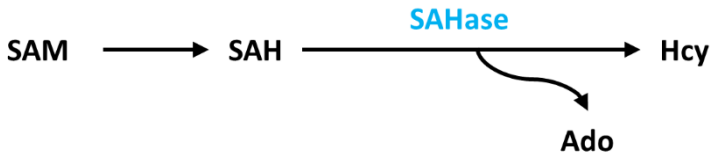

Figure 1.11: SAHase catalysed reaction whereby SAH substrate is hydrolysed into Ado and Hcy.

The same method employed for SAM identification was used to detect Ado in *A. niger* CBS 513.88 samples. Initially, a commercially available Ado standard was analysed by LC-MS to identify its retention time and mass spectrum. Ado eluted at a RT of 10.5 min and was identified by its whole mass of *m/z* 268. This mass corresponds to the singly charged ion [$(M + H)^+ = 268$] and its fragmentation pattern (136) (Figure 3.12). Analysis of Ado in *A. niger* revealed a significant increase ($p = 0.0138$) in intensity in GT extracts compared to MeOH control. Similarly, Ado appeared to be increased after 6 h GT exposure compared to MeOH control, however this increase was not significant (Figure 3.13).

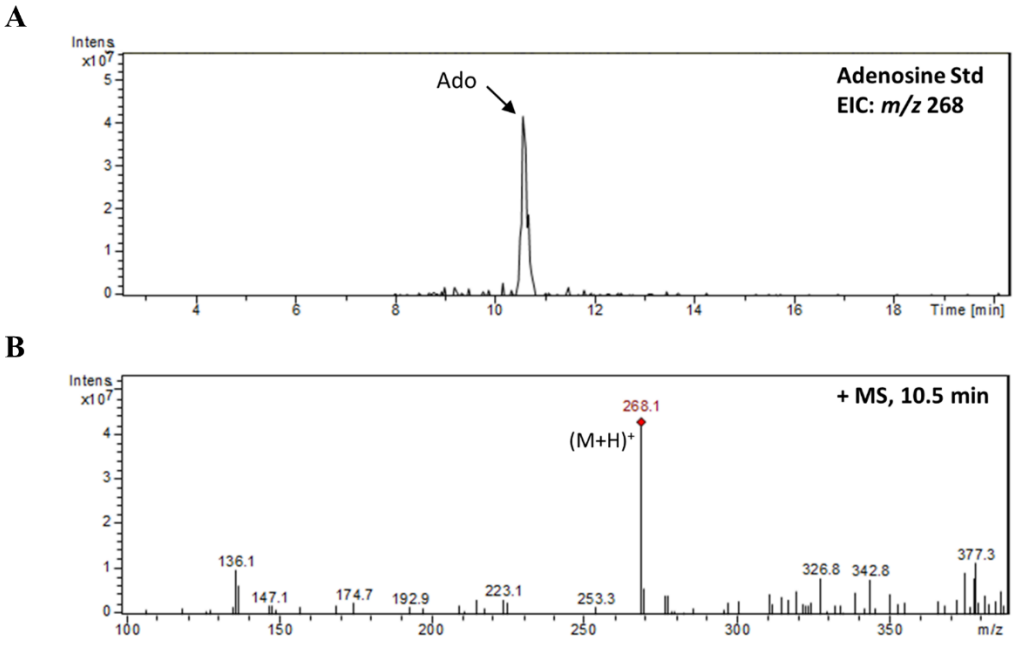

Figure 3.12: EIC of Ado Std. Ado (*m/z* = 268) was used as a reference for identification in *A. niger* lysates.

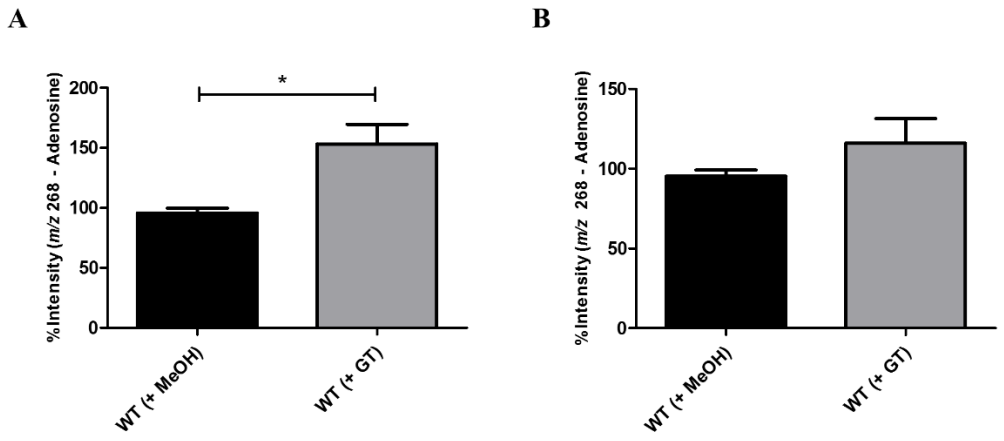

Figure 3.13: (A) Ado levels were significantly increased in *A. niger* lysates after GT exposure (3 h) (**p* = 0.0138) and **(B)** also increased after 6 h but not significant.

3.2.4.5 Intracellular glutathione metabolism

In addition to quantifying metabolites within the Met cycle, one sulphur-derivative from this pathway (GSH) is particularly interesting due to its antioxidant properties. As mentioned in Chapter 1, dysregulation in the level of GSH was observed in *A. fumigatus* Δ*gliT* compared to wild-type after exposure to GT (Carberry et al., 2012). Thus, in order to establish the importance of this molecule in *A. niger* in response to GT, measurement of GSH level was carried out as per Carberry et al. (2012).

Determination of GSH and glutathione disulphide (GSSG) levels in *A. niger* CBS 513.88 under specific conditions was carried out using a spectrophotometric assay (Section 2.2.12). This method requires the construction of a GSH and a GSSG standard curves as described in Section 2.2.12 (26.4 – 0.4125 nmol/ml). A linear relationship occurs between the concentration of GSH and the absorbance at 412 nm

(Figure 3.14). The amount of total GSH and GSSG of the fungal extracts was calculated from the linear equation.

A. niger was grown for 45 h before addition of MeOH (control) and GT (2.5 μg/ml) for further 3 h and 6 h. Mycelia were harvested and lysates were generated for protein quantification (Section 2.2.12) and for glutathione measurement (Section 2.2.12). Lysates destined for glutathione measurement were prepared using sulfosalicyclic acid to provide an acidic medium (Rahman et al., 2006). Additionally samples for the measurement of GSSG levels were treated with 2-vinylpyridine, which reacts with GSH (but not GSSG) (Section 2.2.12). The concentration of was obtained from subtracting GSSG from total GSH (Rahman et al., 2006)

The level of GSH determined in *A. niger* exposed to GT (3 h) was very similar to that measured on the MeOH control, while the amount of GSSG in *A. niger* exposed to GT was higher compared to control (Figure 3.15). Consequently the GSH/GSSG ratio of gliotoxin exposed cultures was lower than that exposed to MeOH (Table 3.4). When the GSH and GSSG levels were measured in *A. niger* samples exposed to 6 h gliotoxin only the GSH concentration appeared to drop slightly compared to that measured on the MeOH control (Figure 3.15). This lead to a decrease GSH/GSSG ratio of GT exposed cultures to that observed in MeOH samples (Table 3.4). The lack of significance observed in these changes may be caused by the low GT concentration.

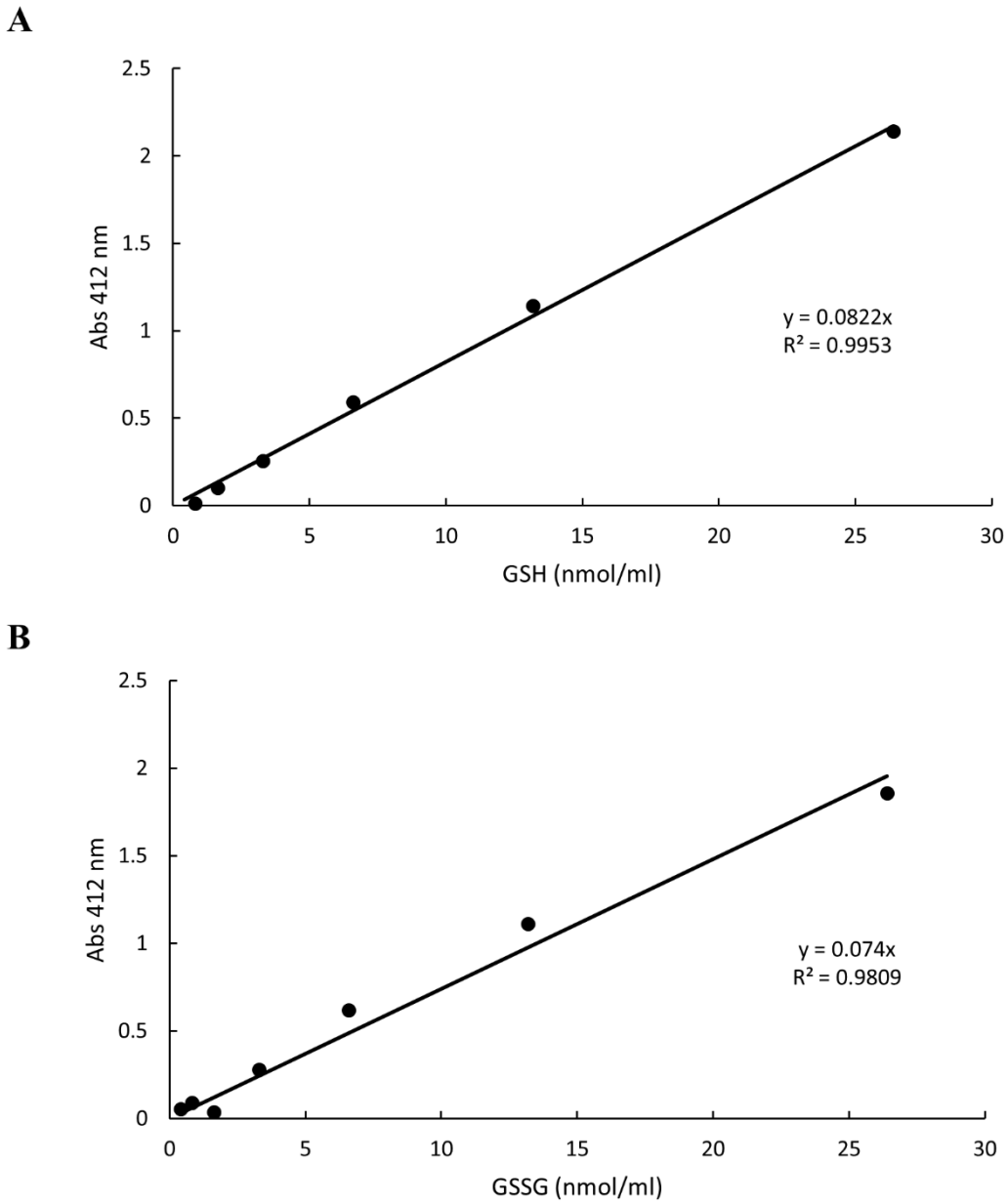

Figure 3.14: GSH and GSSG standard curves. **(A)** Standard curve prepared for the measurement of GSH. **(B)** Standard curve prepared for the measurement of GSSG.

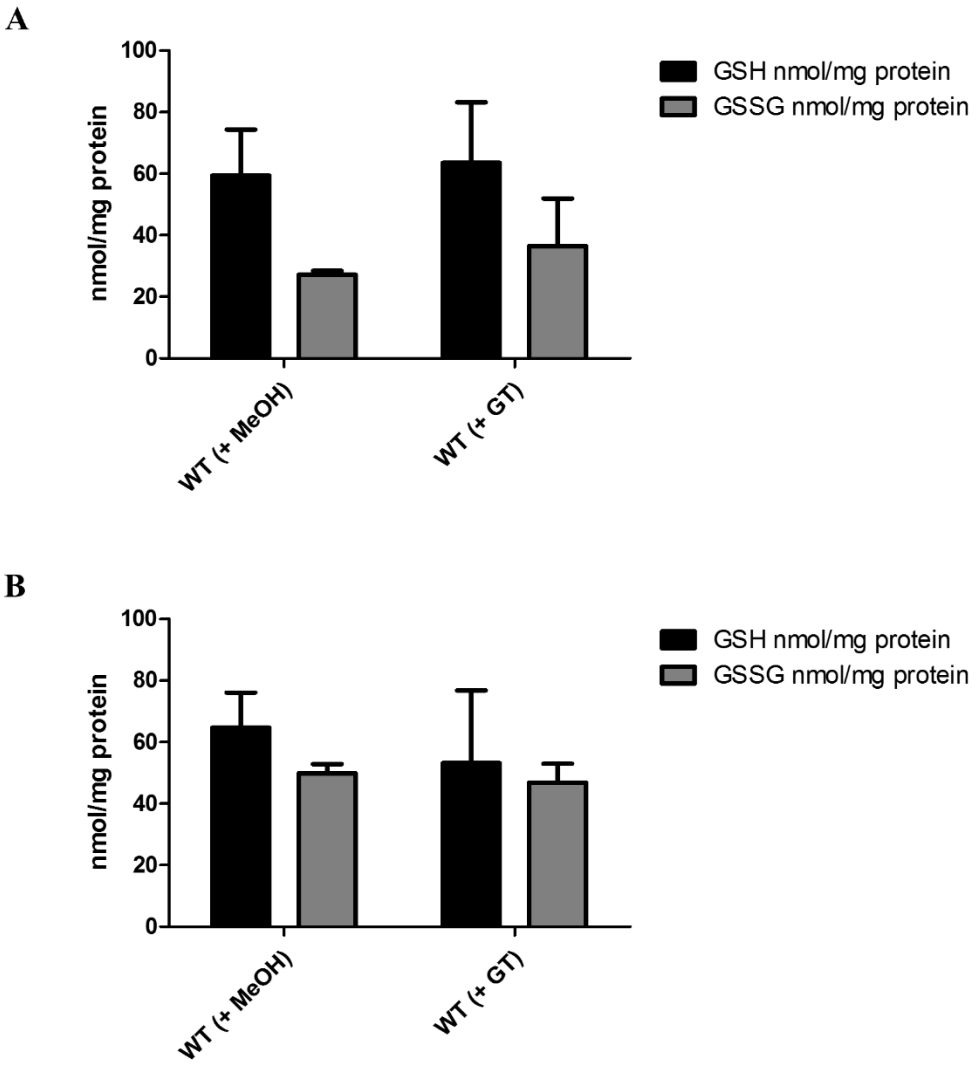

Figure 3.15 The amount of GSH and GSSG in *A. niger* CBS 513.88 in the absence and presence of 2.5 µg/ml GT for **(A)** 3 h and **(B)** 6 h.

Table 3.4: GSH/GSSH ratios for *A. niger* CBS 513.88 after 3 h and 6 h exposure to GT (2.5 µg/ml).

GT exposure time	MeOH Control	2.5 µg/ml GT
	GSH/GSSG	
3 h	2.19	1.74
6 h	1.30	1.13

3.3 Discussion

The work described in this Chapter shows the inhibitory affect that GT has on the growth of *A. niger* CBS 513.88. Comparative proteomic analysis of *A. niger* CBS 513.88 exposed to sub-lethal concentrations of GT (2.5 μg/ml) and MeOH control caused the dysregulation of hundreds of proteins within the proteome of the fungus. An increase abundance of proteins involved in the methionine cycle was observed after GT addition. Furthermore, dysregulation in the levels of metabolites comprising this cycle was also observed under these conditions. Met and Ado levels were significantly higher after GT exposure (3 h) compared to MeOH control while SAM level was decreased. Interestingly, samples extracted from 6 h GT exposed cultures showed an increase in Met, SAM and Ado. The GSH/GSSG ratio in *A. niger* decreased at both time points (3 h and 6 h) after addition of GT, but not significantly.

The affect gliotoxin has in an *A. niger* environmental isolate was phenotypically first observed by Carberry et al. (2012) were a concentration of 5 μg/ml was capable of fully inhibiting *A. niger* growth. Though our results also indicate a gliotoxin-mediated inhibition, the sequenced strain (CBS 513.88) was not as sensitive as the environmental isolate. Differences between strains of *A. niger* (CBS 513.88 vs ATCC 1015) have been observed in terms of genome size and morphology when grown on solid media whereby CBS 513.88 produces brown spores and ATCC 1015 generates black spores (Rokas et al., 2007). Thus is it no surprise that the phenotype of both strains in response to GT is also slightly different. GT-mediated inhibition was also observed in *A. nidulans* (Carberry et al., 2012), which, like *A. niger*, does not contain the *gli* cluster (Patron et al., 2007; Pel et al., 2007b). *A. fumigatus* wild-type exposed

to GT showed no growth inhibition, however Δ*gliT* mutant growth was impaired (Schrettl et al., 2010b).

Proteomic analysis revealed that the response *A. niger* had to exogenous GT was higher at 3 h compared to that at 6 h. 10 proteins involved in methionine metabolism were differentially expressed after 3 h GT exposure relative to 5 proteins after 6 h. Similarly, 4 SAM-dependent methyltransferases (SAM-MTases) underwent differential abundance change at 3 h compared to 2 at 6 h.

S-adenosylhomocysteinase (SAHase) exhibited a $\log_2$ 2.46-fold increase in *A. niger* exposed to 3 h GT while it had a $\log_2$ 1.45-fold increase at 6 h. SAHase catalyzes the hydrolysis of SAH to Hcy and Ado (De La Haba and Cantoni, 1959). SAH is produced as a result of the action of SAM-dependent methyltransferases (SAM-MTases) on cellular substrates like proteins, nucleic acids, lipids and small molecules. SAHase inhibition can lead to the accumulation of SAH in the cytoplasm of the cell which in turn can block methylation reactions (by competitive inhibition of SAM-binding) (Hendricks et al., 2004). Thus the role SAHase has on lowering the concentration of SAH is critical for regulating the methylation ability of the cell (Hendricks et al., 2004). In yeast, downregulation of *Sah1* expression lead to an accumulation of SAH and to a decrease in phosphatidylcholine biosynthesis, which is dependent on three SAM-MTases (Malanovic et al., 2008). In *Arabidopsis*, a missense mutation of the *Sah1* gene (*sah1L459F*) was shown to affect the activity of a CMT3 DNA MTase involved in the methylation of a cytosine base in non-CG sequences. Though no developmental abnormalities were observed the methylation of cytosine was lost (Mull et al., 2006).

Comparative 2D-PAGE proteomics was carried out on *C. albicans* exposed to different antifungal agents including amphotericin B and caspofungin. Analysis revealed the up-regulation of several proteins involved in the biosynthesis of sulphur containing amino acids including SAH1, CYS3, SAM2 and MET6. These authors speculated towards an increase of energy demand produced during the adaptive response to these stresses (Hoehamer et al., 2010). *Sah1* up-regulation was also observed when *C. albicans* was challenged to fluconazole (Copping et al., 2005).

At the metabolite level, LC-MS/MS analysis revealed that SAH was absent in *A. niger* lysates. In addition SAHase activity was observed after spiking SAH in acid lysates. Ado was identified in *A. niger* lysates and appeared to be increased after GT exposure at both time points compared to MeOH, which is in agreement with the SAHase activity observed. Due to the elevated abundance of SAM-MTases after GT exposure (3 h and 6 h) in *A. niger* I hypothesize that the high SAHase activity has a role in decreasing SAH levels that otherwise would inhibit SAM-MTases.

Hcy is a product of SAHase catalysed reactions and at high levels it can be deleterious in fungi (Lo et al., 2002) and humans (Jakubowski, 2006). To lower Hcy levels in the cell, Hcy can be methylated by MET6 to form methionine or it can be re-converted to cysteine by the reverse transsulfuration pathway which involves CBS and CGL (Sieńko et al., 2009). One way or another, both pathways are orientated towards the biosynthesis of amino acids in the cell.

Interestingly, homoserine dehydrogenase (HSDH) was increased in abundance in *A. niger* exposed to GT at 3 h and 6 h ($\log_2$1.96-fold and $\log_2$1.89-fold, respectively) compared to MeOH. HSDH catalyses the reduction of β-aspartate semialdehyde into homoserine, which is involved in the biosynthesis of threonine (Thr), Ile and Met

(Andersen et al., 2011). Biosynthesis of threonine involves the conversion of homoserine to *O*-phospho-L-homoserine which by the elimination of orthophosphate yields Thr in a reaction catalysed by threonine synthase (Ramos and Calderón, 1994). The synthesis of Met from homoserine requires the formation of *O*-acetylhomoserine. In *A. nidulans* homocysteine synthase (Hcs1) generates homocysteine from *O*-acetylhomoserine and sulphide (Grynberg et al., 2001). Thus, the increase abundance of HSDH can translate into the synthesis of Thr or Met.

Interestingly, spermidine synthase (EC: 2.5.1.16) showed a $\log_2$ 2.00-fold abundance increase at 3 h GT addition compared to control. This enzyme is part of the methionine salvage pathway and acts crossroads with polyamine biosynthesis, whereby it donates an aminopropyl group from decarboxylated SAM (dcSAM) to putrescine for the generation of spermidine (Figure 3.4) (Sauter et al., 2013). In *A. nidulans*, up-regulation of the spermidine synthase gene (*spdA*) was observed in response to DNA-damaging agent camptothecin (Malavazi et al., 2006). Additionally, the *spdA* encoded protein was increased in response to farnesol, another stress agent that can cause DNA fragmentation and lead to the generation of reactive oxygen species (ROS) (Wartenberg et al., 2012).

These observations appeared to lead towards the production of Met from different pathways (Yang cycle and methionine cycle) (Figure 3.4), and thus the levels of this metabolite were measured in *A. niger* exposed to GT (3 h and 6 h) compared to MeOH. Indeed Met levels were elevated after GT exposure (at 3 h and 6 h) compared to MeOH control.

Several MTases were increased in *A. niger* after exposure to GT at both timepoints (3 h and 6 h). Two putative MTases (MT-I and MT-II) were de novo present

and a PRMT (protein arginine MTase) was increased in abundance after 3 h GT presence. After 6 h GT exposure, MT-I and tRNA (m5U54)-MTase were uniquely present. PRMT6-catalyzed methylation is proposed to affect gene regulation by modifying protein-nucleic acid interactions (Lakowski and Frankel, 2008) while the methylation of a 5-methyluridine (m5U) residue at position 54 by tRNA (m5U54)-MTases, is a conserved feature in eukaryotic tRNA which, in vitro, influences the fidelity and rate of protein synthesis as well as the stability of tRNA tertiary structure (Johansson and Byström, 2002). The altered expression of these MTases possibly highlight the affect GT has on transcription and translation, as noted by O'Keeffe et al. (2014) for *A. fumigatus* Δ*gliT*. The two putative MTases have been up-regulated in an *A. niger* library in response to reductive stress agent, DTT (MacKenzie and Guillemette, 2005). MT-I contains a domain with identity to the ubiquinone-MT (UbiE/COQ5) domain which includes a predicted SAM-binding motif. It was suggested by these authors that DTT affects the electron transport chain as coenzyme Q is part of it. MT-II, on the other hand is the ortholog of an *A. fumigatus* SAM dependent MTase termed GtmA (Dolan et al., 2014). This MTase has been demonstrated to methylate GT and to play a role in attenuating GT biosynthesis (Dolan et al., 2014). Due to this homology, Chapter 5 characterizes MT-II and describes its role in *A. niger* in the presence of GT.

As mentioned earlier, SAM is the methyl donor for SAM-dependent methylation reactions. In *A. nidulans*, SAM synthetase (*SasA*) catalyses the synthesis of SAM from methionine (Gerke et al., 2012). In terms of metabolite analysis, there was a significant decrease in the level of SAM after 3 h GT exposure compared to control but a significant increase after 6 h GT addition. The decrease of SAM at 3 h, can be a consequence of the increased abundance of a number of SAM-MTases. However, the

higher levels of SAM at 6 h might suggest that the impact GT has on methionine metabolism is lower compared to 3 h. Indeed this correlates with the small number of proteins whose abundance dysregulated at 6 h and the potential use of SAHase and HSDH towards the biosynthesis of amino acids required for fungal growth.

Cysteine synthase (CS) (EC: 2.5.1.47) was not detectable in *A. niger* after exposure to GT for 3 h. *A. nidulans* CS, encoded by the *cysB* gene, utilizes the sulphate assimilation pathway to incorporate sulphide into *O*-acetylserine to form cysteine (Brzywczy et al., 2007). Interestingly, an ATP sulfurylase (ATPS) (EC: 2.7.7.4) was also observed to be decreased only at 3 h GT addition. Encoded by the *sC* gene, ATPS is the second enzyme in a cascade of proteins involved in the assimilation of inorganic sulfate (SO_4^{2-}) (Figure 3.16). This enzyme uses ATP and SO_4^{2-} to form adenosine-5-phosphosulfate (APS) and pyrophosphate (PPi) (Mendoza-Cózatl et al., 2005). APS is then transformed to sulphite and this into sulphide that is incorporated into amino acids like Cys and Met through the action of cysteine synthase (CS) and homocysteine synthase (Hcs1), respectively (Natorff et al., 2003). It thus appears that the decrease observed in CS and ATPS favours the synthesis of Met rather than Cys.

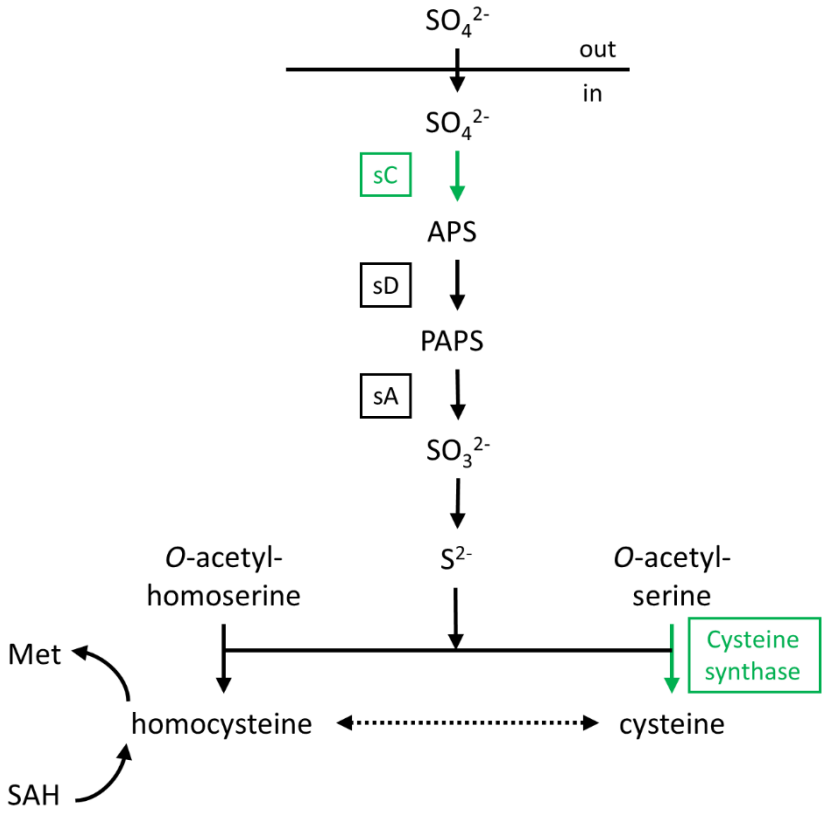

Figure 3.16: Overview on the impact of GT on sulfur assimilation. Squared boxed indicate the enzyme catalysing each reaction in the pathway. In green are those proteins with decreased abundance after GT exposure for 3 h.

Glutathione (GSH) is an essential sulphur-containing peptide that plays an important role in the response fungi have to stress. It behaves as an antioxidant molecule that can react with a number of reactive oxygen species (Figure 3.17) (Pócsi et al., 2004). The effect of GT (2.5 µg/ml) on the GSH/GSSG ratio in *A. niger* was investigated. When *A. niger* was exposed to GT for 3 h, the GSH/GSSG ratio decreased compared to the MeOH control. This was a consequence of an increase in the amount of GSSG and the lack of change in the levels of GSH, which could be indicative of an increase in glutathione peroxidase activity that is a common response

towards oxidative stress. The GSH level could remain the same due to an increase in GSH biosynthesis. Decrease in the GSH/GSSG ratio has been shown in *A. fumigatus* exposed to GT (5 μg/ml) (Carberry et al., 2012; Schrettl et al., 2010b). The decrease in the ratio was due to a reduction in the levels of GSH with no concomitant increase in GSSG, which lead to the hypothesis that GSH was directly reacting with gliotoxin and generating mixed gliotoxin-GSH disulphides thus protecting the fungus by attenuating intracellular reduced GT (Carberry et al., 2012). When *A. niger* was exposed to GT for 6 h there was no clear difference compared to the control. The GSSG levels appeared the same and the GSH levels were slightly decreased after GT exposure compared to control, which could suggest GSH peroxidase activity. The GSH/GSSG ratio has been measured in *A. nidulans* in response to H_2O_2 and diamide over a 10 h time course (Pócsi et al., 2005). Though the ratios were significantly decreased early in the time course, indicating an active response to oxidative stress, over time, the ratio was gradually recovered (Pócsi et al., 2005). Overall, the response *A. niger* had towards GT was not significant which could be explained by the low concentration of GT used (2.5 μg/ml) or by protection against GT through a different mechanism.

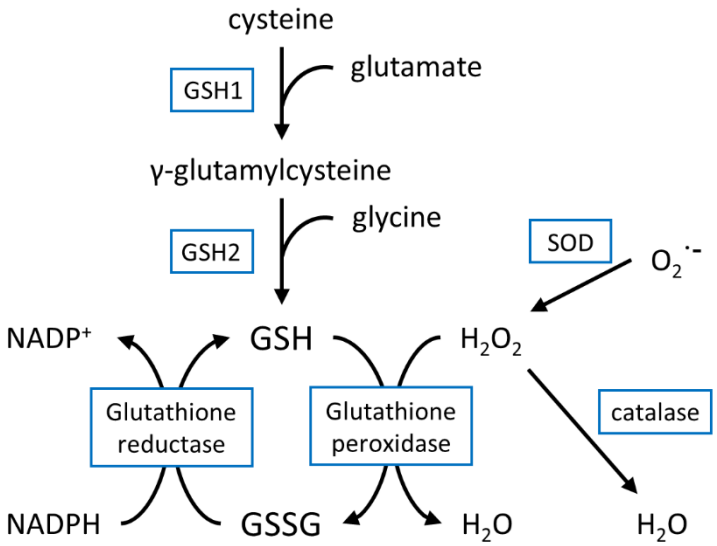

Figure 3.17: Schematic of the glutathione redox cycle and biosynthesis from cysteine.

Dysregulation of Met metabolism has been observed in wheat cultivar exposed to necrotic factor, SnTox3, from the fungus *Stagnospora nodorum* (Winterberg et al., 2014). Upon SnTox3 infiltration up-regulation of genes encoding for SAHase, SAM synthetase, Hcy *S*-methyltransferase and cystathionine β-lyase was observed. These authors hypothesize that a consequence of this up-regulation will be an increase in the levels of SAM and pointed the importance this metabolite has in a series of processes whereby its methyl group is incorporated through the biosynthesis of ethylene, phenylpropanoids and polyamines (Winterberg et al., 2014). Interestingly, phenylpropanoids and their derivatives are sometimes referred to as secondary metabolites and are involved in the plants defence response (Fraser and Chapple, 2011). In *A. nidulans* the VELVET complex coordinates secondary metabolism and sexual development (Bayram et al., 2008). This is a trimeric complex composed by

VeA, VelB and a SAM-dependent methyltransferase LaeA (Bayram et al., 2008). Intriguingly, Gerke et al. (2012) performed protein interaction studies on *SasA* in order to investigate its role in *A. nidulans*. These authors found that SasA has several interaction partners including proteins involved in methionine metabolism, citrate cycle, gluconeogenesis, fungal morphogenesis, stress response and histone-2B (Gerke et al., 2012).

Overall, the work presented in this chapter describes the effect of GT on the metabolism of sulphur containing amino acids in *A. niger* and the importance this pathway has in the overall state of the cell. We propose that, at least in part, the decrease of SAM to exert methylation reactions (e.g. BmGT formation by MT-II, Chapter 5), results in a dysregulation of the Met cycle in *A. niger*. Due to the interconnectivity of this cycle with other cellular processes in the cell and the general response organisms have to stress agents (GT in this study) Chapter 4 will examine how the metabolic network of *A. niger* deals with GT.

Chapter 4

The metabolic network of *A. niger* is dysregulated by gliotoxin exposure

4 Chapter 4: The metabolic network of *A. niger* is dysregulated by gliotoxin exposure

4.1 Introduction

Work described in Chapter 3 described a joint proteomics and metabolomics approach to advance the investigation of SAM metabolism in *A. niger* in response to GT. However, the response this fungus has to GT was observed to extend to several other cellular processes. The metabolic network connects with other cellular processes through regulatory metabolites that bind to transcription factors, riboswitches and other regulatory macromolecules (Grüning et al., 2010). These interactions are required for controlling a cells behaviour depending on its requirements and is attained by mechanisms at the level of transcription, translation and by signal transduction (Gonçalves et al., 2013).

When a perturbation occurs in the cell, a response is triggered were the reconfiguration of the metabolic network is required and can range from; adaptations in production of a few enzymes and behaviour, up to adjustment of the overall growth rate (Grüning et al., 2010). For example, in *A. nidulans*, down-regulation of genes involved in glycolysis and oxidative phosphorylation was observed under carbon starvation (Szilágyi et al., 2013). Intermediates of these pathways are involved in a variety of processes including chromatin modifications, transcriptional repression or signalling (Grüning et al., 2010). One of these intermediates is acetyl-CoA, which is involved in the biosynthesis of secondary metabolites and fatty acids and is a substrate for the acetylation of histones (Hynes and Murray, 2010). Wellen et al. (2009) investigated the affect of ATP-citrate lyase (ACL), which converts citrate into acetyl-CoA, in the maintenance of histone acetylation in mammalian cells and observed that

silencing of ACL resulted in a decreased amount of histone acetylation (Wellen et al., 2009).

A. niger is a well-known secretory workhorse that under industrial production processes, such as submerged batch cultivations, is subjected to prolonged periods of carbon starvation. Under these conditions, *A. niger* activates an autophagic response that has been associated with the recycling of cytoplasmic nutrients, along with cell death (Nitsche et al., 2012). These are speculated to have protective roles related to the degradation of damaged mitochondria or unfolded proteins (Lockshin et al., 2004). Additionally, *A. niger* decreases protein biosynthesis, which is one of the most energy-consuming processes of the cell (Grüning et al., 2010) and increases the secretion of hydrolases that might aid in the scouting or acquisition of carbohydrates (van Munster et al., 2014, 2015). Also, it has been observed that the production of hydrolases depends on functional regulators LAE1 and VEL1 in *Trichoderma reesei* (Seiboth et al., 2012) and VeA in *A. fumigatus* (Dhingra et al., 2012).

Under temperature changes, the fungi *Blastomyces dermatitidis* is able to morphologically change between a yeast (37 ºC) and mould (20 ºC) form. This switch in morphology is known as phase transition (Marty et al., 2015). Marty et al. (2015) deleted *SREB* (siderophore biosynthesis repressor in *Blastomyces*) from *B. dermatitidis* which is a transcription factor (TF) involved in the phase transition and observed that it not only affected iron processes but had an impact in the regulation of lipid biosynthesis and transcription. Overall, fungi challenged by external stimuli generate a response that shows a high degree of cross-talk between metabolic and regulatory processes.

Thus the aim of the work presented in this Chapter was (i) to explore perturbations in the metabolic network of *A. niger* CB513.88 in response to GT exposure (ii) to dissect data groups of selected proteins involved in amino acid metabolism, specifically branched chain amino acids (BCAAs) and perform metabolite quantification on them, (iii) to analyse the secretome under the same conditions to establish relationships with the mycelial proteome and (iv) to carry out complementary 2D-PAGE coupled to LC-MS/MS analysis on an *A. niger* environmental strain exposed to the same amount of GT.

4.2 Results

4.2.1 Label free quantification

Functional classification of proteins identified by label free quantification (LFQ) (Section 3.2.2) (Figure 3.3) revealed that categories describing (i) metabolism, (ii) protein binding function or cofactor requirement and (iii) energy showed the highest levels of dysregulation when *A. niger* CBS 513.88 was exposed to exogenous GT (2.5 μg/ml) for 3 h and 6 h. Identification of a large number of hydrolytic enzymes (n = 65) and proteins involved in amino acid metabolism (n = 37) accounts for the high representation of the metabolism category in the increased and decreased protein set, respectively. The functional category energy is mainly comprised of proteins involved in the TCA cycle, glycolysis and pentose phosphate pathway (PPP).

4.2.1.1 Hydrolytic enzyme abundance is increased in response to GT

In *A. niger* exposed to exogenous GT, the abundance of 22 glycoside hydrolases (GHs) was increased, while that of three (An14g04190, An05g02410, An08g05790) was attenuated at 3 h (Table 4.1). Similarly at 6 h GT exposure, 26 GHs showed increased abundance compared to one that was detectable at lower levels (Table 4.1). Other than GHs, peptidase abundance showed high levels of dysregulation, whereby 16 showed increased and 4 decreased abundance (at 3 h) and 18 increased with 8 showing reduced abundance at 6 h post-GT exposure (Table 4.2). The majority of these degradative enzymes were observed at both time-points (58 % GHs and 44 % peptidases). For the GHs showing increased abundance after GT exposure at both time points, 83 % (n = 25) contained signal peptide (SP), suggesting they could be destined for secretion. Interestingly, the three GHs exhibiting reduced abundance at both time points after GT exposure did not contain SP. Based on the

Carbohydrate-Active Enzymes (CAZy) database (http://www.cazy.org) (Cantarel et al., 2009), there are three GH families that are characteristic for starch degradation; GH13, GH15 and GH31, which mainly consist of α-amylases, α-glucosidases and glucoamylases. The data herein shows the increased abundance of 7 proteins from the GH13 family (AgtC, AamA, AmyC, AgsA, AgtA, GdbA and AgsE), one from the GH15 family (GlaA) and two from the GH31 family (AgdA, AgdB), which could have a role in scavenging starch (glucose) from the media. Some of the GHs identified, other than their typical catalytic module, also contained carbohydrate binding modules (CBMs) that intimately bind to the polysaccharide and prolong their association to facilitate catalysis (Shoseyov et al., 2006).

Table 4.1. Carbohydrate-Active Enzymes (CAZy) undergoing a significant ($p < 0.05$) change in abundance in *A. niger* CBS 513.88 following exposure to gliotoxin (2.5 µg/ml), relative to methanol solvent control. Data sorted by fold change, in descending order.

Protein description	Fold change (Log2) 3 h	Fold change (Log2) 6 h	CAZy Family	Name	SP	Protein IDs
Putative endomannanase; induced by caspofungin	Unique	-	GH76	*dfgC*	-	An14g03520
Glucan beta-1,3 exoglucanase	↑ 4.007	↑ 3.686	GH55	*exsG*	SP	An01g12450
1,4-alpha-D-glucan glucohydrolase; secreted glucoamylase; most highly expressed at the periphery of colonies; repressed by xylose and induced by maltose	↑ 3.667	↑ 3.381	CBM20 GH15	*glaA*	SP	An03g06550
Beta-mannosidase; glycosyl hydrolase family 2; contains several putative N-glycosylation sites	↑ 3.578	↑ 3.239	GH2	*mndA*	SP	An11g06540
Alpha-galactosidase; alpha-N-acetylgalactosaminidase variant A; CreA regulated; protein levels influenced by presence of starch	↑ 3.335	↑ 3.344	CBM13 GH27	*aglA*	SP	An06g00170
Glucan 1,3-beta-glucosidase; putative glucanotransferase; induced by caspofungin	↑ 3.191	↑ 3.352	GH17	*bgtB*	SP	An03g05290
Putative 1,3-beta-glucanosyltransferase; predicted signal peptide secretion sequence	↑ 3.045	↑ 2.305	CBM43 GH72	*geld*	SP	An09g00670
Putative GPI-anchored glucanosyltransferase; cell wall protein; induced by fenpropimorph	↑ 3.035	↑ 2.454	GH16	*crhD*	SP	An01g11010
Putative alpha-galactosidase variant B; expression is induced on xylan; XlnR regulated	↑ 2.994	↑ 3.489	GH27	*aglB*	SP	An02g11150

Protein description	Fold change (Log2) 3 h	Fold change (Log2) 6 h	CAZy Family	Name	SP	Protein IDs
Putative alpha-1,6-mannanase	-	↑ 2.807	GH76	-	-	An07g07700
Putative alpha-glucanotransferase	↑ 2.783	↑ 3.534	GH13	*agtC*	SP	An15g07800
Extracellular alpha-glucosidase pro-protein; the mature form of the enzyme is a heterosubunit protein; AmyR dependant induction on maltose	↑ 2.775	↑ 3.077	GH31	*agdA*	SP	An04g06920
Putative endoglucanase	↑ 2.773	↑ 2.301	CBM1 GH5	*eglB*	SP	An16g06800
Putative acid alpha-amylase; abundantly expressed on d-maltose; most highly expressed at the periphery of colonies; repressed by xylose and induced by maltose	↑ 2.739	↑ 2.986	GH13	*aamA*	SP	An11g03340
Alpha-amylase	↑ 2.530	-	GH13	*amyC*	SP	An04g06930
Ortholog(s) have glucan endo-1,6-beta-glucosidase activity	↑ 2.335	↑ 2.829	GH30	-	SP	An03g00500
Glycosylphosphatidylinositol-anchored chitinase, similar to ChiA of A. nidulans; expression induced by tunicamycin and DTT	-	↑ 2.321	GH18	*ctcA*	SP	An09g06400
Secreted, thermostable beta-galactosidase	↑ 2.290	↑ 3.095	GH35	*lacA*	SP	An01g12150
Has domain(s) with predicted carbohydrate binding, catalytic activity and role in carbohydrate metabolic process	-	↑ 2.236	GH92	-	-	An14g04240
Putative 1,3-beta-glucanosyltransferase; predicted signal peptide secretion sequence	↑ 2.105	↑ 2.832	GH72	-	SP	An08g07350
N-Acetyl-beta-glucosaminidase	↑ 2.089	↑ 2.538	GH20	*nag1*	SP	An09g02240

Protein description	**Fold change (Log2) 3 h**	**Fold change (Log2) 6 h**	**CAZy Family**	**Name**	**SP**	**Protein IDs**
Putative 1,3-alpha-glucan synthase; induced in the presence of cell wall stress-inducing compounds such as Calcofluor White, SDS, and caspofungin	-	↑ 1.942	GH13 GT5	*agsA*	SP	An04g09890
Mannosyl-oligosaccharide 1,2-alpha-mannosidase	-	↑ 1.925	GH47	*msdS*	SP	An01g12550
GPI-anchored alpha-glucanosyltransferase; alpha-glucan transferase; induced by caspofungin/ Alpha-glucanotransferase; alpha-amylase	-	↑ 1.771	GH13	*agtA*	SP	An09g03100
Putative alpha-glucosidase; AmyR dependant induction on maltose	↑ 1.736	↑ 1.362	GH31	*agdB*	SP	An01g10930
Putative beta-glucosidase	-	↑ 1.640	GH3	-	-	An15g01890
Putative 1,3-beta-glucanosyltransferase; predicted signal peptide secretion sequence; induced by caspofungin; expressed during germination	↑ 1.370	-	GH72	*gelA*	SP	An10g00400
Glycogen debranching enzyme; 1,3-alpha-glucan synthase	↑ 1.170	↑ 1.843	GH13	*gdbA*	-	An01g06120
Alpha glucosidase I; expression enhanced by maltose; expression induced by tunicamycin and DTT	↑ 1.166	-	GH63	-	SP	An15g01420
Putative 1,3-alpha-glucan synthase; moderately induced in the presence of cell wall stress-inducing compounds such as Calcofluor White, SDS, and caspofungin	-	↑ 1.011	GH13 GT5	*agsE*	SP	An09g03070
1,4-alpha-glucan branching enzyme	↓ 3.458	↓ 2.198	CBM48 GH13	*gbeA*	-	An14g04190

Protein description	Fold change (Log2) 3 h	Fold change (Log2) 6 h	CAZy Family	Name	SP	Protein IDs
Has domain(s) with predicted cation binding, hydrolase activity, hydrolyzing O-glycosyl compounds activity and role in carbohydrate metabolic process	↓ 1.937	-	GH2	-	-	An05g02410
Ortholog(s) have glycogen phosphorylase activity, role in glycogen catabolic process, response to heat and cell surface, cytoplasm, hyphal cell wall localization	↓ 1.162	-	GT35	-	-	An08g05790

Similar to the GHs, most of the peptidases that were increased in abundance after GT exposure (at 3 h and 6 h) contained SP (68 %). On the contrary, those peptidases that showed decreased abundance after GT exposure lacked SP (9 out of 10). This observation further confirms the potential role of these hydrolases in secretory pathways. The proteases with the highest levels of abundance after GT exposure where classified as members of the A1 pepsin family proteases and S53 sedolisin family proteases, based on MEROPS database (merops.sanger.ac.uk) (Table 4.2). Interestingly, these two families have been observed to be the most abundant under carbon starvation conditions, in *A. niger* (Braaksma et al., 2010), (Nitsche et al., 2012). Generally, extracellular proteases are associated with the hydrolysis of polypeptides into smaller molecules for absorption by the cell while intracellular protease can play important roles in metabolism regulation (Rao et al, 1998). Thus, the increased abundance of peptidases containing SP could indicate a role in scavenging amino acids for diverse metabolic roles within the cell.

Table 4.2 Peptidases undergoing a significant ($p < 0.05$) change in abundance in *A. niger* CBS 513.88 following exposure to gliotoxin (2.5 µg/ml), relative to methanol solvent control. Data sorted by fold change, in descending order.

Protein description	**Fold change (Log2) 3 h**	**Fold change (Log2) 6 h**	**Peptidase Family**	**Name**	**SP**	**Protein IDs**
Pepsin family secreted protease	Unique	-	A01	-	SP	An18g01320
Sedolisin family secreted protease	↑ 4.034	↑ 4.464	S53.007	-	SP	An01g01750
Putative serine carboxypeptidase; acid protease	↑ 3.529	↑ 3.496	S10	*pepF*	SP	An07g08030
Pepsin family secreted protease; only detected under starvation conditions	↑ 3.523	↑ 3.334	A01.080	*pepAb*	-	An01g00370
Carboxypeptidase Y family secreted protease; expression repressed by tunicamycin and DTT	↑ 3.484	↑ 3.152	S10.016	*protF*	SP	An03g05200
Sedolisin family secreted protease; lysosomal pepstatin-insensitive protease	↑ 3.410	↑ 2.600	S53.007	-	SP	An03g01010
Sedolisin family secreted protease; lysosomal pepstatin-insensitive protease	↑ 3.325	↑ 3.155	-	-	SP	An06g00190
Secreted lysosomal Pro-Xaa carboxypeptidase	↑ 3.233	↑ 2.415	S28.004	*protA*	SP	An08g04490
Aspergillopepsin A, a pepsin family secreted acid protease; expression increases by growth without ammonia; under carbon control and pH regulation	↑ 2.645	↑ 2.423	A01.016	*pepA*	SP	An14g04710
Serine-type carboxypeptidase Y family secreted neutral protease	↑ 2.382	↑ 1.657	S10.014	-	SP	An02g04690

Protein description	Fold change (Log2) 3 h	Fold change (Log2) 6 h	Peptidase Family	Name	SP	Protein IDs
Sedolisin family secreted protease; putative lysosomal pepstatin-insensitive protease	↑ 1.981	↑ 3.330	S53.010	*protB*	SP	An08g04640
Putative estherase/lipase/thioesterase; acylaminoacyl-peptidase; repressed by growth on starch and lactate	-	↑ 1.970	S09.012	-	-	An09g02830
Ortholog(s) have extracellular region localization	-	↑ 1.868	S10.016	-	SP	An06g00310
Protein similar to dipeptidyl peptidase II; expression repressed by tunicamycin and DTT	↑ 1.741	-	S28	-	SP	An12g05960
Ortholog(s) have endoplasmic reticulum localization	↑ 1.625	↑ 1.523	M28.010	-	-	An02g06300
Putative protease	-	↑ 1.378	S09.057	*protC*	SP	An04g02850
Vacuolar aminopeptidase Y family secreted protease; expression repressed by tunicamycin and DTT	↑ 1.261	↑ 1.898	M28.001	*ape3*	SP	An03g01660
Prolyl amino peptidase involved in protein degradation; removes N-terminal proline and hydroxyproline residues from peptides	↑ 1.234	↑ 2.160	S33.008	*papA*	-	An11g04730
Ortholog(s) have dipeptidase activity and cytoplasm localization	-	↑ 1.119	M24.A09	-	-	An05g00050
Protein with similarity to D-stereospecific aminopeptidase; acid protease; expression induced by tunicamycin and DTT	-	↑ 1.079	-	-	-	An16g06750
Putative vacuolar serine proteinase; putative signal sequence for transport into the endoplasmic reticulum; secreted protein	↑ 1.076	-	S8	*pepC*	SP	An07g03880

Protein description	Fold change (Log2) 3 h	Fold change (Log2) 6 h	Peptidase Family	Name	SP	Protein IDs
Putative zinc aminopeptidase	-	↑ 1.068	M01.007	*apsA*	-	An04g03930
Ortholog(s) have ubiquitin thiolesterase activity, ubiquitin-specific protease activity, role in protein deubiquitination and cytosol, nucleus localization	Absent	-	C12.003	-	-	An02g13920
Ortholog(s) have endopeptidase activator activity and role in proteasomal ubiquitin-independent protein catabolic process	Absent	-	T01.984	-	-	An04g01870
Putative metallopeptidase	-	Absent	M24.A11	-	-	An01g14920
Ortholog(s) have endopeptidase activator activity and role in proteasomal ubiquitin-independent protein catabolic process	-	Absent	T01.P02	-	-	An04g01800
Ortholog(s) have RNA polymerase II core promoter proximal region sequence-specific DNA binding, cysteine-type peptidase activity	↓ 2.626	-	C01.084	-	-	An01g01720
Has domain(s) with predicted serine-type carboxypeptidase activity and role in proteolysis	↓ 2.121	-	S10	-	SP	An05g01870
Putative dipeptidyl-peptidase V; serine-type peptidase	↓ 1.926	-	S09.012	-	-	An16g08150
Putative glutamate carboxypeptidase-like protein; repressed by growth on starch and lactate	↓ 1.154	↓ 1.775	M20.017	-	-	An11g11180
Ortholog(s) have ubiquitin-specific protease activity, role in endocytosis, protein deubiquitination and cell division site, cytosol, nucleus, transport vesicle localization	↓ 1.013	-	C19.A59	-	-	An09g05480

Protein description	Fold change (Log2) 3 h	Fold change (Log2) 6 h	Peptidase Family	Name	SP	Protein IDs
Ortholog(s) have aminopeptidase activity, role in cellular response to drug, chaperone-mediated protein folding, proteolysis and cytosol, extracellular region, fungal-type vacuole lumen, ribosome localization	↓ 1.006	-	M18.A01	-	-	An02g11940

4.2.1.2 Gliotoxin alters the abundance of proteins involved in the central carbohydrate metabolism

The functional category describing decreased abundance proteins involved in energy metabolism was significantly represented from the sample set of proteins identified by LC-MS/MS (n = 51; p = 8.72e^{-6}) (Section 3.2.2). Fluctuations in the abundance of proteins involved in glycolysis/gluconeogenesis and fermentative pathways was observed after GT exposure in *A. niger* (Table 4.3). Additionally, the majority of enzymes constituting the citric acid cycle were detected and appeared decreased in abundance (Table 4.3) (Figure 4.1).

Glycolytic enzymes altered after GT exposure included the increased abundance of glucokinase (GlkA) and decreased abundance of TpiA, FbaA, Pgi1, PgmB and PgmA. In the fermentative pathway, proteins involved in the degradation of ethanol appeared increased (PdcA and Ach1) and decreased (PdcB, AcuA, AldA and putative alcohol dehydrogenase) after GT addition to *A. niger*. Subunit E1 (α and β) and E2 of the pyruvate dehydrogenase complex were decreased in the presence of gliotoxin at both time points (An07g09530, An01g00100 and An07g02180, respectively). This enzyme represents the link between glycolysis and the TCA cycle whereby pyruvate, the product of glycolysis is decarboxylated and oxidised into acetyl-CoA (Minic, 2015). The next two steps in the citric acid cycle involve the condensation of acetyl-CoA with oxaloacetate to form citrate catalysed by CitA (decreased) and subsequent conversion into isocitrate by Aco1 (decreased). Two subunits form the oxoglutarate dehydrogenase complex in *A. niger* (An04g04750 and An11g11280) that catalyses the conversion of α-ketoglutarate to succinyl-CoA. An04g04750 showed a $\log_2$ 2.25-fold decrease at 3 h while An11g11280 was decreased $\log_2$ 1.85-fold at 3 h, which could

result in a reduction in the levels of succinyl-CoA. Those enzymes responsible for the conversion of oxaloglutarate to oxaloacetate (OAA) showed decreased abundance after GT addition to *A. niger*. These enzymes include; succinate CoA-ligase (An17g01670), succinate dehydrogenase (An02g12770), fumarate hydratase (FumR) and malate dehydrogenase (Mdh1 and MdhA). The decrease of most enzymes involved in the citric acid cycle would suggest a reduction in the levels of ATP and citrate that are essential for energy production in the mitochondria.

Table 4.3: Abundance changes of proteins involved in the central carbon metabolism in *A. niger* CBS 513.88 after exposure to gliotoxin (2.5 μg/ml) for 3 h and 6 h, respectively.

Protein description	Fold change (Log2) 3 h	Fold change (Log2) 6 h	EC number	Alias	Accession
Glycolysis/Gluconeogenesis					
Pyruvate decarboxylase	↑ 2.829	↑ 2.908	4.1.1.1	*PdcA*	An02g06820
Acetyl-CoA hydrolase	↑ 1.509	↑ 1.519	3.1.2.1	*Ach1*	An16g07110
Putative glucokinase	↑ 1.474	↑ 1.286	2.7.1.2	*GlkA*	An12g08610
Triosephosphate isomerase	↓ 2.988	↓ 3.474	5.3.1.1	*TpiA*	An14g04920
Fructose bisphosphate aldolase	↓ 2.947	↓ 1.585	4.1.2.13	*Fba1*	An02g07470
Aldehyde dehydrogenase	↓ 2.586	↓ 1.029	1.2.1.3	*AldA*	An08g07290
Putative glucose-6-phosphate isomerase	↓ 1.680	-	5.3.1.9	*Pgi1*	An16g05420
Pyruvate decarbolylase	↓ 1.670	-	4.1.1.1	*PdcB*	An09g01030
Putative phosphoglucomutase	↓ 1.644	-	5.4.2.2	*PgmB*	An02g07650
Phosphoglycerate mutase	↓ 1.412	↓ 1.469	5.4.2.1	-	An16g02990
Putative acetyl-CoA synthase	↓ 1.338	Absent	6.2.1.1	*AcuA*	An04g05620

Protein description	Fold change (Log2) 3 h	Fold change (Log2) 6 h	EC number	Alias	Accession
TCA cycle					
Putative phosphoenolpyruvate carboxykinase	1.31494	1.79362	4.1.1.49	-	An11g02550
Fumarate hydratase	↓ 3.603	↓ 2.842	4.2.1.2	*fumR*	An12g07850
Mitochondrial aconitate hydratase	↓ 3.366	↓ 2.764	4.2.1.3	*aco1*	An08g10530
ATP:citrate oxaloacetatelyase	↓ 3.092	↓ 2.208	2.3.3.8	-	An11g00510
Putative citrate synthase; predicted N-terminal mitochondrial import signal and a C-terminal peroxisomal target sequence (AKL)	↓ 2.999	↓ 3.639	2.3.3.1	*citA*	An09g06680
Succinate dehydrogenase (ubiquinone)	↓ 2.877	↓ 1.820	1.3.5.1	-	An02g12770
E2 dihydrolipoamide acetyltransferase	↓ 2.831	↓ 2.609	2.3.1.12	-	An07g02180
Cytoplasmic ATP-citrate lyase	↓ 2.712	↓ 2.342	2.3.3.8	-	An11g00530
Cytoplasmic pyruvate carboxylase	↓ 2.573	↓ 2.027	6.4.1.1	*pyc*	An04g02090
Putative oxoglutarate dehydrogenase; induced by growth on starch and lactate	↓ 2.257	-	1.2.4.2	-	An04g04750
Ortholog(s) have succinate-CoA ligase (ADP-forming) activity, role in succinyl-CoA metabolic process and mitochondrial nucleoid localization	↓ 2.159	↓ 1.854	6.2.1.4/ 6.2.1.5	-	An17g01670

Protein description	**Fold change (Log2) 3 h**	**Fold change (Log2) 6 h**	**EC number**	**Alias**	**Accession**
Pyruvate dehydrogenase (lipoamide)	↓ 2.092	-	1.2.4.1	-	An01g00100
Dihydrolipoamide S-succinyl transferase	↓ 1.852	-	2.3.1.61	-	An11g11280
Alpha subunit E1 of the pyruvate dehydrogenase complex	↓ 1.481	↓ 1.623	1.2.4.1	*pda1*	An07g09530
Mitochondrial malate dehydrogenase	↓ 1.418	-	1.1.1.37	*mdh1*	An07g02160
Malate dehydrogenase precursor; Malate dehydrogenase	↓ 1.321	-	1.1.1.37	*mdhA*	An15g00070

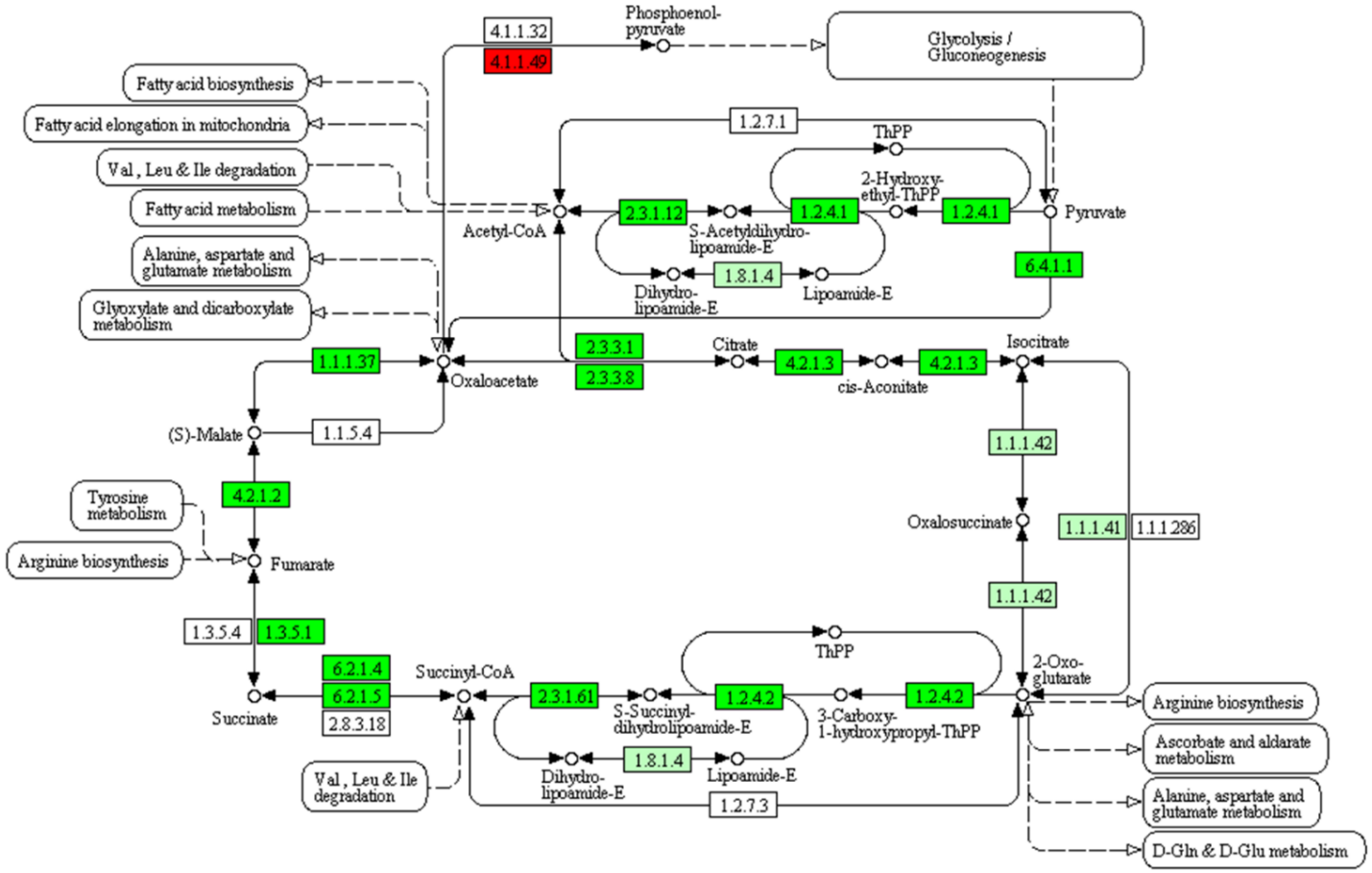
4.1.1.32
4.1.1.49
Phosphoenol-pyruvate
Glycolysis / Gluconeogenesis
Fatty acid biosynthesis
Fatty acid elongation in mitochondria
Val, Leu & Ile degradation
Fatty acid metabolism
Alanine, aspartate and glutamate metabolism
Glyoxylate and dicarboxylate metabolism
1.2.7.1
ThPP
2-Hydroxy-ethyl-ThPP
2.3.1.12
1.2.4.1
1.2.4.1
Pyruvate
Acetyl-CoA
S-Acetyldihydro-lipoamide-E
1.8.1.4
Dihydro-lipoamide-E
Lipoamide-E
6.4.1.1
1.1.1.37
Oxaloacetate
2.3.3.1
2.3.3.8
Citrate
4.2.1.3
cis-Aconitate
4.2.1.3
Isocitrate
(S)-Malate
1.1.5.4
1.1.1.42
Tyrosine metabolism
4.2.1.2
Arginine biosynthesis
Fumarate
Oxalosuccinate
1.1.1.41
1.1.1.286
1.1.1.42
1.3.5.4
1.3.5.1
ThPP
6.2.1.4
6.2.1.5
2.8.3.18
Succinyl-CoA
2.3.1.61
1.2.4.2
1.2.4.2
2-Oxo-glutarate
Succinate
S-Succinyl-dihydrolipoamide-E
3-Carboxy-1-hydroxypropyl-ThPP
Arginine biosynthesis
Ascorbate and aldarate metabolism
1.8.1.4
Dihydro-lipoamide-E
Lipoamide-E
Val, Leu & Ile degradation
1.2.7.3
Alanine, aspartate and glutamate metabolism
D-Gln & D-Glu metabolism

Figure 4.1: *A. niger* CBS 513.88 citric acid cycle obtained from KEGG database (http://www.genome.jp/kegg/kegg1.html). KEGG enzyme entries are represented as rectangular boxes with 4 number digits. Green boxes represent proteins that were decreased in abundance after GT exposure and include oxoglutarate dehydrogenase (1.2.4.2), dihydrolipoamide S-succinyl transferase (2.3.1.61), succinate CoA-ligase activity (6.2.1.4, 6.2.1.5), succinate dehydrogenase (1.3.5.1), fumarate hydratase (4.2.1.2), malate dehydrogenase (1.1.1.37), citrate synthase (2.3.3.1), ATP:citrate oxaloacetatelyase (2.3.3.8), aconitate hydratase (4.2.1.3), pyruvate carboxylase (6.4.1.1), pyruvate dehydrogenase (1.2.4.1) and E2 dihydrolipoamide acetyltransferase (2.3.1.12). Red box represents a protein with increased abundance after GT exposure, phosphoenlpyruvate carboxykinase (4.1.1.49).

4.2.1.3 Exogenous gliotoxin affects the abundance of proteins involved in amino acid metabolism in *A. niger*

FunCat classification of the altered protein abundance in *A. niger* CBS 513.88 revealed an enrichment of proteins involved in amino acid metabolism upon exogenous GT exposure (at 3 h and 6 h). The abundance of 9 proteins was increased while that of 22 was attenuated at 3 h (Table 4.4). Similarly at 6 h GT exposure, 9 proteins showed increased abundance compared to 17 that were attenuated. Most of these enzymes were observed at both time points (n = 20, 54 %). From the proteins showing increased abundance after GT exposure at both time points, 67 % (n = 6) were involved in amino acid biosynthesis. Proteins involved in the biosynthesis of branched chain amino acids (BCAAs) included An14g00780 and An01g14130, those for the biosynthesis of aromatic amino acids were two homologous proteins An01g06150 (known as ARO3 in *S. cerevisiae*) and An04g03620 that are 3-deoxy-7-phosphoheptulonate synthases. An13g01080 (*S. cerevisiae* HIS1) and An17g02330 (*S. cerevisiae* SER3) are involved in histidine and serine biosynthesis, respectively. Two homologous glutaminases (An02g13750 and An11g07960) and a glutamate decarboxylase (An08g08840) were increased in abundance and are involved in nitrogen metabolism. Butyryl-CoA dehydrogenase (An01g12960) and D-amino acid oxidase (An01g02430) play different roles in the metabolism of BCAAs.

Of the 26 proteins decreased in *A. niger* in response to exogenous GT, 13 are involved in amino acid catabolism, specifically BCAA catabolism were 6 proteins were identified (An14g04420, An13g03150, An17g01150, An04g05720, An08g05400 and An07g04280). Proteins involved in glutamate (An02g14590 homolog of *S.cerevisiae* GDH2 and An17g00910 homolog of UGA1), phenylalanine

(An11g02170) and threonine (An08g07290 and An04g03400) catabolism were also identified. The other 13 proteins unrelated to catabolism were involved in a wide range of processes including (i) biosynthesis (An01g11930 known as HIS5 in *S. cerevisiae*, An02g03250 known as LEU1, An02g07500 as LYS1 and An15g02340 as ARG1, (ii) oxidative deglycation of glycated amino acids (An11g05340 and An02g08980), (iii) nitrogen metabolism (An11g02980 homolog of AMD2 *S. cerevisiae*, An01g08800 known as GLN1) and (iv) components of the malate-aspartate shuttle (An16g05570, An04g06380 and An03g01120 which all resemble *S. cerevisiae* AAT2) which exchange NADH formed in the cytosol for mitochondrial NAD^+ (Lu et al., 2010).

Table 4.4: Abundance changes of proteins involved in amino acid metabolism in *A. niger* CBS 513.88 after exposure to gliotoxin (2.5 µg/ml) for 3 h and 6 h (n = 37).

Protein description	Fold change (Log2) 3 h	Fold change (Log2) 6 h	EC number	Alias	Accession
Ortholog(s) have extracellular region localization	↑ 2.852	↑ 2.688	N/A		An02g13750
ATP phosphoribosyltransferase	↑ 2.107	↑ 1.126	2.4.2.17		An13g01080[B]
Ortholog(s) have role in isoleucine biosynthetic process, mitochondrial translation and cytosol, mitochondrial intermembrane space, mitochondrial matrix, nucleus localization	↑ 1.808	-	N/A		An14g00780[B]
Glutamate decarboxylase	↑ 1.742	↑ 1.313	4.1.1.15		An08g08840[C]
Ortholog(s) have butyryl-CoA dehydrogenase activity and role in fatty acid beta-oxidation using acyl-CoA dehydrogenase	↑ 1.575	↑ 1.327	1.3.99.-		An01g12960
Putative glutaminase	-	↑ 1.630	3.5.1.2		An11g07960
Ortholog(s) have D-amino-acid oxidase activity and role in D-alanine metabolic process, D-valine metabolic process	-	↑ 1.486	1.4.3.3		An01g02430
3-deoxy-7-phosphoheptulonate synthase	↑ 1.409	↑ 1.119	2.5.1.54		An01g06150[B]
Phosphoglycerate dehydrogenase	↑ 1.366	↑ 1.315	1.1.1.95		An17g02330[B]
Ortholog(s) have 3-deoxy-7-phosphoheptulonate synthase activity	↑ 1.092	↑ 1.119	2.5.1.54		An04g03620[B]

Protein description	Fold change (Log2) 3 h	Fold change (Log2) 6 h	EC number	Alias	Accession
Putative beta-isopropylmalate dehydrogenase	↑ 1.058	-	1.1.1.85	*leu2A*	An01g14130[B]
Has domain(s) with predicted 3-hydroxyisobutyrate dehydrogenase activity, coenzyme binding, nucleotide binding, phosphogluconate dehydrogenase (decarboxylating) activity and role in pentose-phosphate shunt, valine metabolic process	Absent	-	1.1.1.31		An14g04420[C]
Histidinol-phosphate aminotransferase	Absent	-	2.6.1.9		An01g11930[B]
NAD+-dependent glutamate dehydrogenase	Absent	-	1.4.1.2		An02g14590[C]
Ortholog(s) have 3-isopropylmalate dehydratase activity, role in leucine biosynthetic process and cytosol localization	Absent	-	4.2.1.33		An02g03250[B]
Putative fumarylacetoacetate hydrolase	Absent	↓ 4.025	3.7.1.2		An11g02170[C]
Has domain(s) with predicted catalytic activity and role in metabolic process	-	Absent	1.2.4.4		An13g03150[C]
Putative acyl-CoA dehydrogenase; induced by fenpropimorph	↓ 4.438	↓ 3.883	1.3.99.3; 1.3.8.7		An17g01150[C]
Putative ketothiolase; 3-ketoacyl-CoA thiolase	↓ 4.020	↓ 3.464	2.3.1.16	*pot1*	An04g05720[C]
Saccharopine dehydrogenase	↓ 3.294	↓ 2.434	1.5.1.7	*lys1*	An02g07500[B]
Putative acetyl-CoA acetyltransferase; 3-ketoacyl-CoA thiolase; induced by fenpropimorph	↓ 3.245	↓ 3.103	2.3.1.16		An08g05400[C]
Alanine transaminase	↓ 3.058	↓ 2.499	2.6.1.2		An11g02620

Protein description	Fold change (Log2) 3 h	Fold change (Log2) 6 h	EC number	Alias	Accession
Ortholog(s) have fructosyl-amino acid oxidase activity		↓ 2.908	1.5.3.-		An11g05340
Aspartate transaminase; phenylalanine:alphaketoglutarate aminotransferase	↓ 2.708	-	2.6.1.1		An16g05570
Aldehyde dehydrogenase involved in ethanol utilization; repressed by growth on starch and lactate	↓ 2.586	↓ 1.029	1.2.1.3	*aldA*	An08g07290[C]
Argininosuccinate synthase	↓ 2.520	-	6.3.4.5		An15g02340[B]
Putative aldehyde dehydrogenase	↓ 2.510	↓ 3.849	1.2.1.5;1.2.1.3		An04g03400[C]
Mitochondrial aspartate aminotransferase	↓ 2.507	↓ 1.906	2.6.1.1	*mAspAT*	An04g06380
Putative amidase/acetamidase	↓ 2.278	↓ 2.726	3.5.1.4		An11g02980
Has domain(s) with predicted oxidoreductase activity and role in oxidation-reduction process	↓ 2.278	↓ 2.960	1.5.3.-		An02g08980
Glutamine synthetase; induced by growth on starch and lactate	↓ 1.976	↓ 3.008	6.3.1.2		An01g08800
Aspartate transaminase; phenylalanine:alphaketoglutarate aminotransferase	-	↓ 1.861	2.6.1.1		An03g01120
Gamma-aminobutyrate transaminase	↓ 1.683	↓ 1.790	2.6.1.19; 2.6.1.22		An17g00910[C]
Aspartate carbamoyltransferase	↓ 1.526	-	2.1.3.2; 6.3.5.5		An08g07420[C]

Protein description	Fold change (Log2) 3 h	Fold change (Log2) 6 h	EC number	Alias	Accession
Has domain(s) with predicted acyl-CoA dehydrogenase activity, flavin adenine dinucleotide binding activity and role in oxidation-reduction process	↓ 1.363	-	1.3.99.10; 1.3.8.4		An07g04280[C]
Pentafunctional arom polypeptide; contains:3-dehydroquinate synthase,3-dehydroquinate dehydratase (3-dehydroquinase), shikimate 5-dehydrogenase, shikimate kinase, and EPSP synthase domains	-	↓ 1.241	1.1.1.25; 2.7.1.71; 2.5.1.19; 4.2.1.10		An08g06810
Aminomethyltransferase	↓ 1.029	-	2.1.2.10		An08g03070[C]

[B]Protein was involved in amino acid biosynthesis. [C]Protein was involved in amino acid catabolism.

Alterations in proteins of BCAA metabolism showed the highest levels of dysregulation. Valine (Val), leucine (Leu) and isoleucine (Ile) are jointly denoted as BCAAs as they contain a branched carbon skeleton. Intracellular BCAAs and phenylalanine (Phe) levels were measured in order to correlate the proteomic data with the metabolite analysis. Determination of these amino acids was carried out using the same HPLC-based *o*-phthalaldehyde (OPA) derivatization method used for methionine quantification (Section 2.2.8.2).

Sample preparation was carried out following Section 2.2.3.1 under identical growth conditions to those employed for proteomic analyses. The standard curve generated for methionine (Section 3.2.4.1) was used in the assay to calculate the amount of intracellular BCAAs and phenylalanine in *A. niger* extracts with and without GT. RP-HPLC analysis of Val, Phe, Leu and Ile standards showed a peak at a retention time of 13.045 min for Val, 13.547 min for Phe and 14.560 min for Leu and Ile which co-eluted in the same peak (Figure 4.2).

Met levels were determined in *A. niger* MeOH control extracts and compared to those in GT exposed extracts. The concentration of amino acids was determined from the standard curve (Section 3.2.4.1) and represented as % concentration (shown as % normalised data). Results indicated that there was a significant increase in the levels of all amino acids measured under GT exposure for 3 h and 6 h (Figure 4.2). The increase of these amino acids appeared to be higher at 6 h compared to 3 h GT addition.

A

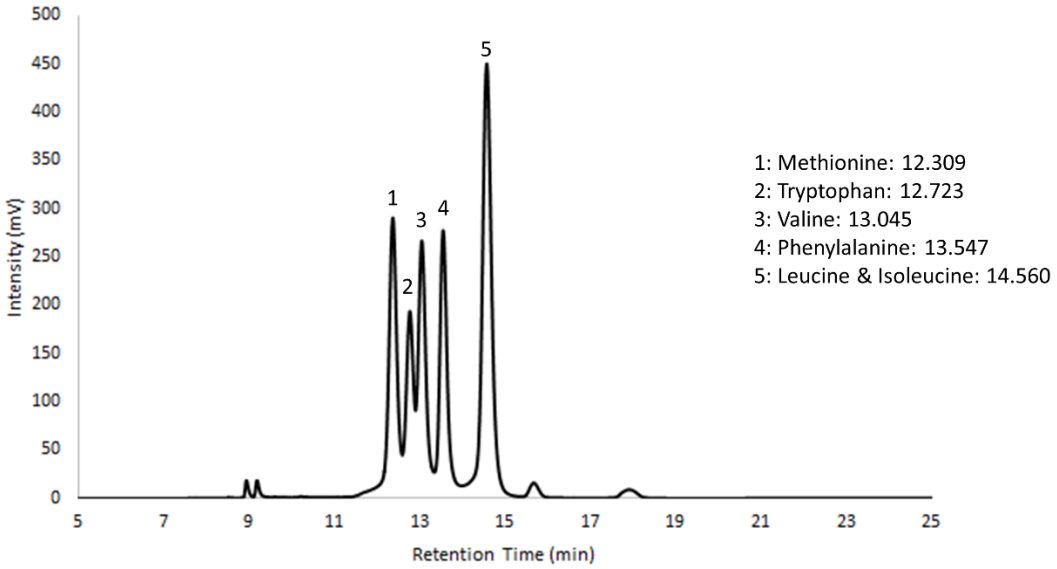

B

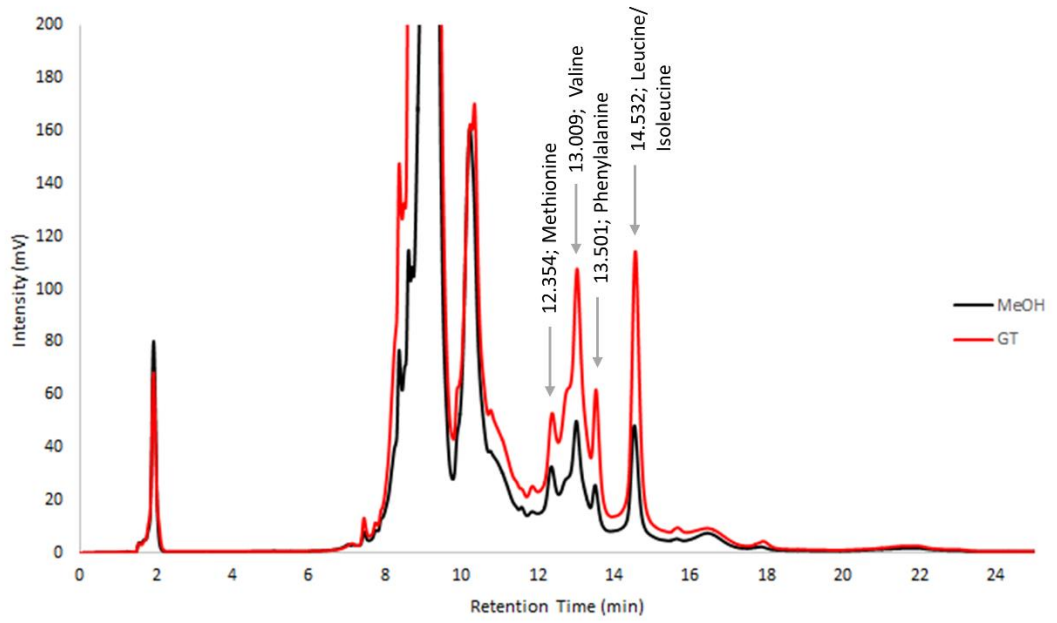

Figure 4.2: RP-HPLC combined with FLD detection of selected amino acids in *A. niger* mycelial lysates. **(A)** BCAAs and Phe standards eluting at a retention time of 13.045 min (val), 13.547 min (phe) and 14.560 min (leu/ile) **(B)** Overlaid HPLC analysis of *A. niger* control (black) compared to GT exposed (red).

A

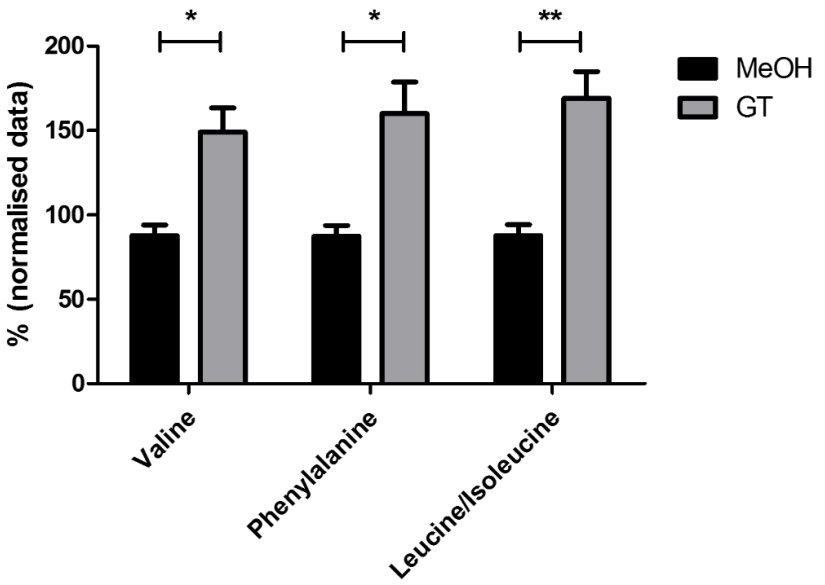

B

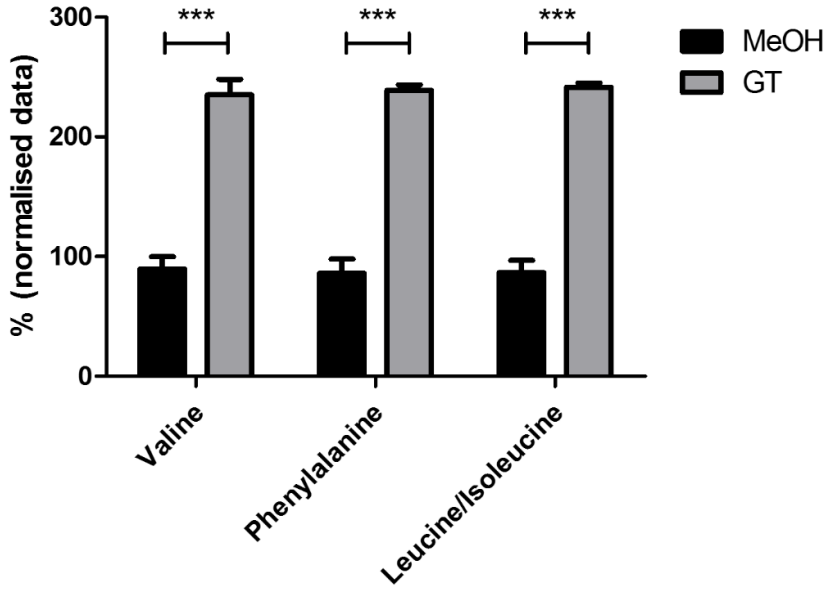

Figure 4.3: BCAAs and Phe levels were significantly increased in *A. niger* CBS 513.88 exposed to GT (2.5 μg/ml) for **(A)** 3 h (*$p < 0.05$) (**$p < 0.01$) and **(B)** 6 h (***$p < 0.001$). Amino acids levels under GT exposure were normalised to the levels obtained under MeOH control and plotted as % (normalised data).

4.2.2 GT alters the extracellular proteome (secretome) of *A. niger* CBS 513.88

A. niger CBS 513.88 was grown for 45 h in potato dextrose broth (PDB) prior exposure to methanol (control) and GT (2.5 μg/ml) for 3 h and 6 h (n = 4, respectively). Supernatants were harvested and protein was extracted as per Section 2.2.3.4.1. Protein lysates were trypsin-digested and ProteaseMax was added as described in Section 2.2.11. Subsequent peptide mixtures were separated on LC gradients and subjected to tandem MS using a Thermo Fisher Q-Exactive system. Data analysis was done using the MaxQuant software (Section 2.2.11). A total of 161 extracellular proteins were identified in *A. niger* exposed to 3 h exogenous GT, of which 11 exhibited significantly altered abundance ($p < 0.05$) compared to MeOH-treated controls. Of these proteins, 8 exhibited increased abundance when *A. niger* was exposed to GT, while 3 proteins were less abundant (Table 4.5). When *A. niger* was exposed to exogenous GT for 6 h, a total of 146 proteins were identified of which 20 were significantly altered in abundance ($p < 0.05$). 10 proteins were increased and 10 showed decreased abundance upon GT addition (Table 4.5).

Of the total (n = 22) extracellular proteins dysregulated after GT addition, 11 were glycoside hydrolases (GHs), 2 were secreted peptidases (An02g01550 and An12g03300) and 2 were cell wall components (An14g02100 and An03g04190). The GHs increased in abundance included AgdA, AglA, LacA An01g01540 and AgtC. Interestingly, all of them, with the exception of An01g01540, were also increased in abundance in the mycelial proteome in response to GT. Those GHs shown to have decreased abundance were DfgC, GlaA, XynB, CrhB, An03g05530 and AbfB. Surprisingly, two GHs (DfgC and GlaA) found to be increased in the mycelial proteome appeared at decreased levels in the secretome. DfgC was uniquely present

in the mycelia at 3 h GT addition while it was decreased in abundance in the secretome only after 6 h GT addition. GlaA, on the other hand, showed increased abundance after GT exposure at both 3 h and 6 h GT exposure in the mycelial proteome while it appeared slightly decreased in the secretome after 6 h. This observation could be explained by a detrimental affect GT has in the secretory pathway of these two enzymes.

Table 4.5: *A. niger* CBS 513.88 supernatant proteins (n = 22) undergoing significant differential expression ($p < 0.05$) following exposure to gliotoxin (2.5 μg/ml) relative to the control.

Protein description	Fold change (log2) 3 h	Fold change (Log2) 6 h	Name	GH	SP	Accession
Extracellular alpha-glucosidase pro-protein; the mature form of the enzyme is a heterosubunit protein; AmyR dependant induction on maltose	↑ 2.689	↑ 4.009	*agdA; algU*	GH31	SP	An04g06920[A,B]
Alpha-galactosidase; alpha-N-acetylgalactosaminidase variant A; CreA regulated; protein levels influenced by presence of starch; N-glycosylation verified at 6 of 8 potential N-glycosylation sites	↑ 1.950	↑ 3.297	*aglA*	CBM13; GH27	SP	An06g00170[A,B]
Ortholog(s) have extracellular region localization	↑ 1.937	↑ 3.144	-	-	SP	An11g00100
Ortholog(s) have endoribonuclease activity, role in RNA catabolic process, apoptotic process, cell morphogenesis and cytosol, extracellular region, fungal-type vacuole localization	↑ 1.844	-	-	-	-	An02g06980[A,B]
Glycosylphosphatidylinositol (GPI)-anchored cell wall mannoprotein	↑ 1.773	↑ 1.764	*cwpA*	-	SP	An14g02100
Secreted, thermostable beta-galactosidase; XlnR regulated	-	↑ 1.618	*lacA*	GH35	SP	An01g12150[A,B]
Putative alpha,alpha-trehalase; expression repressed by tunicamycin and DTT	↑ 1.424	↑ 1.794	-	GH65	SP	An01g01540
Secreted serine protease	↑ 1.415	↑ 1.832	-	-	SP	An02g01550

Protein description	**Fold change (log2) 3 h**	**Fold change (Log2) 6 h**	**Name**	**GH**	**SP**	**Accession**
Putative alpha-glucanotransferase	↑ 1.343	↑ 2.711	*agtC*	GH13	SP	An15g07800[A,B]
6-hydroxy-D-nicotine oxidase 6-HDNO	-	↑ 1.276	-	-	SP	An03g00460
Phytase; expression repressed by tunicamycin and DTT	-	↑ 1.228	*phyA3*	-	SP	An12g01910[A,B]
Ortholog(s) have spore wall localization	↓ 1.621	↓ 2.637		-	SP	An03g04190
Ortholog of *A. fumigatus Af293* : Afu1g06590, Afu7g06750, *A. oryzae RIB40* : AO090011000051, *Aspergillus wentii* : Aspwe1_0046559, Aspwe1_0170184 and *Aspergillus sydowii* : Aspsy1_0042124	-	↓ 1.504		-	SP	An15g07520
Putative endomannanase; induced by caspofungin	-	↓ 1.496	*dfgC; manB*	GH76	-	An14g03520[A]
Ortholog(s) have role in hyphal growth, response to cold, response to heat, response to oxidative stress, response to salt stress, sporocarp development involved in sexual reproduction	-	↓ 1.249		-	SP	An01g06280
Putative GPI-anchored glucanosyltransferase; induced by caspofungin	↓ 1.184	-	*crhB*	CBM18; GH16	SP	An07g07530
Pepsin family secreted acid protease; predicted signal sequence for secretion	↓ 1.169	↓ 3.197	*protG; pepAc*	-	SP	An12g03300
Secreted endo-1,4-xylanase; glycoside hydrolase family 11; highly expressed on xylose; expression repressed by tunicamycin and DTT; XlnR regulated	-	↓ 1.154	*xynB; xlnB*	GH11	SP	An01g00780

Protein description	Fold change (log2) 3 h	Fold change (Log2) 6 h	Name	GH	SP	Accession
Endo-beta-1,4-glucanase	-	↓ 1.119	-	GH12	SP	An03g05530
1,4-alpha-D-glucan glucohydrolase; secreted glucoamylase; most highly expressed at the periphery of colonies; repressed by xylose and induced by maltose; AmyR dependant induction on maltose	-	↓ 1.077	*glaA*	CBM20; GH15	SP	An03g06550[B]
Alpha-arabinofuranosidase B, glycosyl hydrolase involved in degradation of plant cell wall polysaccharide L-arabinan; glycosylated; abundantly expressed on D-xylose	-	↓ 1.044	*abfB*	CBM42; GH54	SP	An15g02300
Putative RNase T2	-	↓ 1.042	-	-	SP	An01g10580

SP: Presence of signal peptide; [A]Protein was identified by LFQ proteomic in mycelial lysates at 3 h. [B]Protein was identified at 6 h.

4.2.3 Comparative 2D-PAGE analysis of *A. niger* environmental isolate following exposure to gliotoxin (2.5 µg/ml) for 3 h

Comparative proteomic analysis of *A. niger* environmental isolate (Env. Isol.) exposed to GT under the same experimental conditions as Carberry et al. (2012) was carried out in order to observe similarities or differences compared to the sequenced CBS 513.88 strain. *A. niger* was cultured ($n = 5$, biological replicates) for 45 h in AMM and exposed to 3 h GT (2.5 µg/ml) before the mycelia were harvested and protein was extracted as described in Section 2.2.3.3. The protein lysates were TCA/Acetone precipitated and resuspended in IEF Buffer before separation on pH 4 – 7 strips. Following separation by 12 % SDS-PAGE, staining with Colloidal Coomassie was performed and analysed using Progenesis^{TM} SameSpot Software (Nonlinear Dynamics Ltd. UK) (Figure 4.4).

Thirty five proteins were found to be differentially expressed; 17 proteins had a fold increase ≥ 1.2 ($p < 0.05$) while 18 had a fold decrease ≥ 1.2 ($p < 0.05$) in *A. niger* exposed to GT when compared to MeOH control. These spots were excised from the gels, trypsin digested as described in Section 2.2.4 and analysed by LC-MS/MS (Section 2.2.10.1).

A

pH 4 _____ 7

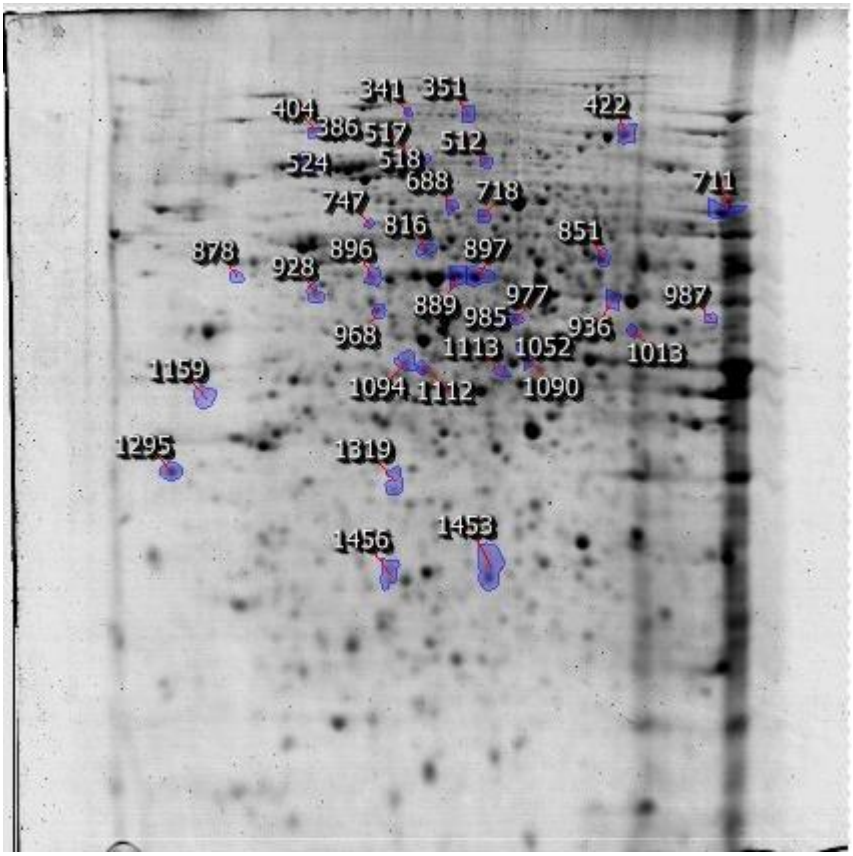

Colloidal Coomassie stained 2D-PAGE gel
of *A. niger* mycelial proteins: MeOH

B

pH 4 _____ 7

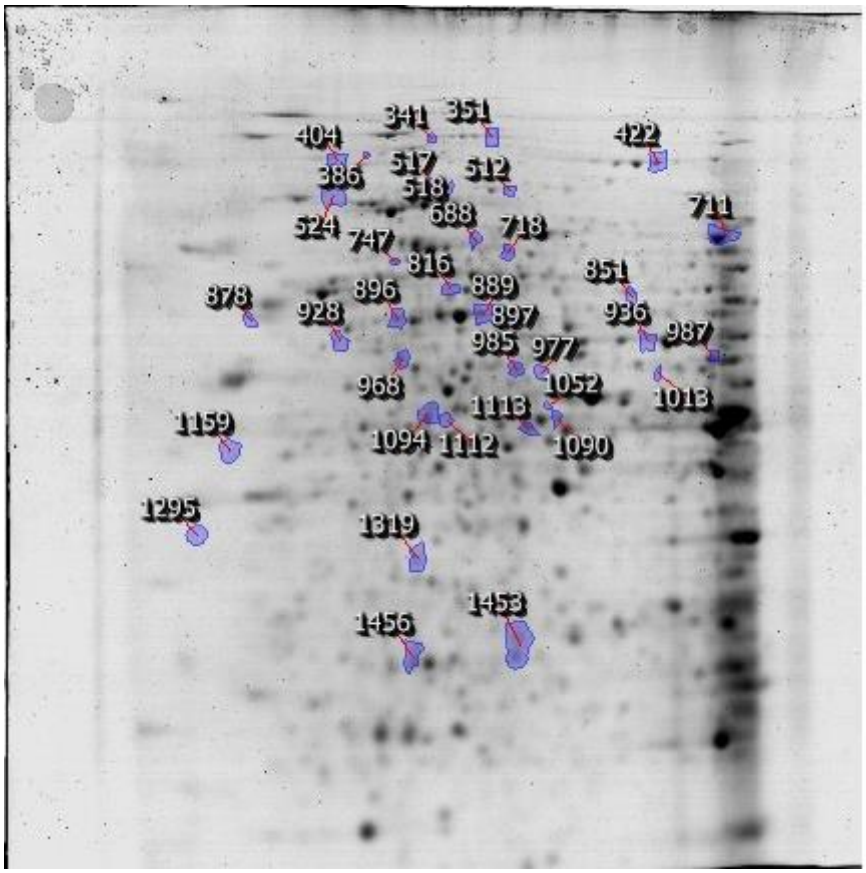

Colloidal Coomassie stained 2D-PAGE gel
of *A. niger* mycelial proteins: GT

Figure 4.4: 2D-PAGE analysis of *A. niger* environmental isolate **(A)** MeOH control and **(B)** following exposure to gliotoxin (2.5 µg/ml) for 3 h. The proteins were first separated on pH 4- 7 strips followed by SDS-PAGE. Proteins found to be significantly differentially expressed ($p < 0.05$), after analysis using Progenesis™ SameSpot software, are numbered.

4.2.4 LC-MS/MS identification of differentially expressed proteins

Thirty five proteins were identified from the excised spots by LC-MS/MS (Table 4.6). The protein identified as having the highest fold increase in *A. niger* in response to GT compared to MeOH was acetyl-CoA hydrolase (An16g07110) which was also excised from two different spots (987 and 711). The protein with the highest fold decrease was Hsp90 chaperone (An09g06590).

The majority of the proteins identified by 2D-PAGE were involved in the central carbon metabolism which includes acetyl-CoA hydrolase, pyruvate decarboxylase, E2 dihydrolipoamide acetyltransferase, triose phosphate isomerase, phosphogucomutase, phosphopyruvate hydratase, fructose bisphosphate aldolase and aconite hydratase. Other proteins identified were associated with the folding and transport of newly synthesised proteins and include An04g09170 (ATPase activity), An02g07190, molecular chaperone Hsp90 (An09g06590) and Hsp70 (An07g09990).

Table 4.6: Proteins undergoing significant differential expression ($p < 0.05$) in *A. niger* environmental isolate following exposure to gliotoxin (2.5 μg/ml) relative to the control. Protein identification was achieved by 2D-PAGE and LC-MS/MS.

Protein description	Fold Change	Coverage (%)	tMr	tpI	Protein IDs	Spot No.
Proteins with increased abundance						
Acetyl-CoA hydrolase; protein levels influenced by the presence of lactate	2.7	4%	58455	6.04	An16g07110[A]	987
Ortholog(s) have ATPase activity, ubiquitin binding activity	1.8	2%	90612	5.04	An04g09170	878
Ortholog(s) have mRNA binding activity, role in negative regulation of MAPK cascade and cytosol localization	1.7	3%	38867	5.55	An07g07150	1113
Pyruvate decarboxylase; protein levels influenced by presence of starch	1.6	9%	62934	5.80	An02g06820[A]	1090
Putative zinc aminopeptidase	1.6	2%	98060	5.21	An04g03930	341
Ortholog(s) have poly(A) RNA binding activity, role in regulation of nuclear-transcribed mRNA poly(A) tail shortening, regulation of translational initiation and cytoplasmic stress granule, nucleus, ribosome localization		2%	82600	5.66	An01g03050	
Acetyl-CoA hydrolase; protein levels influenced by the presence of lactate	1.5	22%	58455	6.04	An16g07110[A]	711
Homoserine dehydrogenase	1.5	18%	38892	5.49	An02g07430[A]	1094
E2 dihydrolipoamide acetyltransferase	1.4	6%	51645	6.02	An07g02180	747

Protein description	Fold Change	Coverage (%)	tMr	tpI	Protein IDs	Spot No.
Triose-phosphate-isomerase	1.3	16%	27008	5.61	An14g04920	1456
Putative phosphoglucomutase; Leloir pathway enzyme; induced by caspofungin	1.3	8%	60555	5.69	An02g07650	718
Pyruvate decarboxylase; protein levels influenced by presence of starch	1.3	7%	62934	5.8	An02g06820[A]	688
Ortholog(s) have role in positive regulation of RNA polymerase II transcriptional preinitiation complex assembly, proteasome regulatory particle assembly, ubiquitin-dependent protein catabolic process	1.3	3%	53804	5.66	An02g07190	896
Ortholog(s) have protein domain specific binding activity	1.3	3%	44282	5.67	An18g06230	985
Phosphopyruvate hydratase	1.2	17%	47358	5.30	An18g06250	968
Actin structural protein	1.2	17%	41818	5.37	An15g00560	1453
Ortholog(s) have 5S rRNA binding, structural constituent of ribosome activity, role in ribosomal large subunit assembly and cytosol localization	1.2	5%	34946	8.69	An08g05730[A]	1319
Proteins with decreased abudance						
Hsp90 chaperone	3.8	4%	79781	4.95	An09g06590	386
Fructose-bisphosphate aldolase; repressed by growth on starch and lactose	3.2	9%	39664	5.52	An02g07470[A]	1052
S-adenosylmethionine synthase	3.1	23%	42127	5.67	An08g02700	977

Protein description	Fold Change	Coverage (%)	tMr	tpI	Protein IDs	Spot No.
Elongation factor 1 beta	2.8	63%	33465	4.42	An08g03490	1295
Phosphopyruvate hydratase	2.7	42%	47358	5.39	An18g06250	897
Aldehyde dehydrogenase involved in ethanol utilization; repressed by growth on starch and lactate	2.2	11%	54124	6.15	An08g07290[A]	851
Has domain(s) with predicted nucleic acid binding, nucleotide binding activity	2.2	3%	35415	8.93	An07g02990	1112
Mitochondrial aspartate aminotransferase	2.1	8%	47036	8.94	An04g06380[A]	1013
Phosphopyruvate hydratase	2.0	32%	47358	5.39	An18g06250	889
Hsp70 protein; induced by growth on starch and lactate	1.5	11%	65401	5.34	An07g09990	518
Ortholog(s) have role in hyperosmotic response, response to antibiotic, response to salt stress and intracellular localization	1.5	10%	52522	5.36	An01g06960	816
Mitochondrial aconitate hydratase	1.4	9%	85819	6.35	An08g10530[A]	422
ATP synthase subunit beta	1.4	9%	55647	5.18	ASPNIDRAFT_211159	928
Hsp70 protein; induced by growth on starch and lactate	1.4	8%	73168	5.09	An07g09990	524
Ortholog(s) have 5S rRNA binding, structural constituent of ribosome activity, role in ribosomal large subunit assembly and cytosol localization	1.4	5%	34946	8.69	An08g05730	1159

Protein description	Fold Change	Coverage (%)	tMr	tpI	Protein IDs	Spot No.
Putative citrate synthase; predicted N-terminal mitochondrial import signal and a C-terminal peroxisomal target sequence (AKL)	1.3	13%	52225	8.57	An09g06680[A]	936
Ortholog(s) have RSC complex, SWI/SNF complex, cytoplasm localization	1.3	5%	73459	5.07	An07g02300	404
Ortholog(s) have poly(A) RNA binding activity, role in regulation of nuclear-transcribed mRNA poly(A) tail shortening, regulation of translational initiation and cytoplasmic stress granule, nucleus, ribosome localization	1.2	9%	78883	5.73	An01g03050	351

tMr: theoretical molecular mass; tpI: theoretical isoelectric point; Spot No. from Figure 4.4; [A]Protein also detected by LFQ analysis (Section 3.2.2) on *A. niger* CBS 513.88.

4.3 Discussion

Alterations in the proteome of *A. niger* CBS 513.88 in response to exogenous GT were investigated and compared to that exposed to MeOH control. A significant dysregulation of the metabolic network in *A. niger* occurred under GT addition and involved the increase in abundance of hydrolytic enzymes (GHs and proteases), the decrease in mitochondrial energy metabolism and dysregulation of amino acid biosynthesis and catabolism. A significant increase in the levels of BCAAs and Phe was observed under GT addition compared to MeOH. The secretome of *A. niger* CBS 513.88 was also investigated under the same conditions and it was observed that GHs and proteases were the main proteins to be secreted. Additionally, using 2D-PAGE/LC-MS/MS analysis, the proteome of an *A. niger* Env. Isol. was also investigated and showed a correlation with that of the CBS 513.88 strain in terms of energy metabolism.

A significantly increased abundance of hydrolytic enzymes was observed after exposure to GT (at 3 h and 6 h) in *A. niger* CBS 513.88. The up-regulation of glycoside hydrolases (GHs) and proteases has been demonstrated in transcriptomic and proteomic analysis of *A. niger* and *A. nidulans* grown under carbon starvation (van Munster et al., 2014, 2015; Nitsche et al., 2012; Szilágyi et al., 2013). Like GT exposure, carbon starvation is a type of stress that triggers a response by filamentous fungi. Munster et al. (2014) proposed that the increased number of genes encoding CAZymes observed under carbon limitation could have a scouting role during starvation, releasing sugars from complex polysaccharides (van Munster et al., 2014). Of the glycoside hydrolases showing increased abundance in response to GT, 22 out of 30 were also identified in the extracellular proteome of *A. niger* grown on carbon

limitation. These include GlaA, AamA, AgdA, CrhD, BgtB, GelD, BxgA, AglA, NagA, An03g00500, MsdS, EglB, AgdB, AglB, An14g04240 (no SP), AmyC, MndA, An07g07700 (no SP), GelA, DfgC (no SP), An08g07350, CtcA (van Munster et al., 2015). Due to the presence of a N-terminal signal peptide (SP) in the majority (83 %) of GHs with increased abundance after GT addition, I hypothesise that this response is a consequence of a carbon limitation or a glucose demand induced by GT, whereby *A. niger* responds by synthesizing these enzymes in order to breakdown complex carbohydrates. In agreement with this hypothesis, some of these GHs; AamA, AmyC, GlaA, AgdA and AgdB, have been predicted to have a role in starch degradation and are under the control of AmyR, which is the transcriptional regulator of starch degrading enzymes (Yuan et al., 2008). Also, AglB and LacA appeared to be regulated by both XlnR and AraR under D-xylose treatment while AglA and AgsA were solely regulated by XlnR and AraR, respectively, under SEB (steam-exploded sugarcane bagasse) (de Souza et al., 2013). The transcriptional activator XlnR controls the regulation of the xylanolytic/cellulolytic system in *A. niger* (van Peij et al., 1998a). AraR is a transcriptional regulator that can interact with XlnR and plays a role in polysaccharide degradation (Battaglia et al., 2011).

Interestingly, some of the proteins with increased abundance in response to GT were possibly involved in autolysis or cell wall remodelling. NagA has a role in the degradation of cell wall component chitin (Pusztahelyi et al., 2006) and along with An07g07700, was identified in *A. niger* under carbon starvation (van Munster et al., 2014; Nitsche et al., 2012). CtcA (endo-chitinase) is an ortholog of the GPI-anchored *A. nidulans* ChiA, which is thought to remodel the structure of chitin to a looser arrangement during growth (Yamazaki et al., 2008).

In addition to the increase in GHs, a number of peptidases also showed increased abundance after GT exposure at both time points. These proteases (68 %) also contained a SP indicating a potential extracellular role. Studies on protease activity in *A. niger* are mainly focused in exploiting its naturally high secretion capacity in biotechnology by manipulating *A. niger* strains that are more efficient in recombinant protein production (Guillemette et al., 2007). Extracellular proteases generally play a role in the breakdown of large polypeptides into smaller molecules for absorption by the cell (Rao et al., 1998). Thus, protease activation has been shown to occur under nutrient limitation i.e. carbon or nitrogen (Nitsche et al., 2012) (McNeil et al., 1998).

In this study, we observed that 13 out of 22 peptidases with increased abundance after GT exposure were also expressed in *A. niger* grown under carbon starvation (Braaksma et al., 2010) (Nitsche et al., 2012). These proteases include An18g01320, An01g01750, PepF (An07g08030), An01g00370, An03g01010, An06g00190, PepA (An14g04710), An02g04690, An08g04640, An09g02830, An12g05960, An03g01660, PepC (An07g03880). Though these authors relate the increase in proteases to an autolytic process observed in aging cultures during batch cultivation, I hypothesize that although autolysis might be occurring at a low extent, this is a general response to meet nutrient requirements. Also, because a number of proteases lacked SP (7 out of 22), it is suggested that intracellular proteolytic activity is activated during GT exposure and could have a role in disposing of intracellular damaged proteins. Overall, this data indicates that the response *A. niger* has to GT is very similar to the response it has under carbon starvation and suggests that GT causes a nutrient requirement that leads to the production of hydrolytic enzymes.

The secretome of *A. niger* under GT exposure was clearly enriched in hydrolases, mainly GHs. Three extracellular GHs (AgdA, AglA, LacA) with increased abundance under GT addition were also observed to be increased in the proteome of *A. niger*. Interestingly these proteins are regulated by AmyR, XlnR and AraR, respectively, and reinforce the idea of nutrient scavenging from the media. An01g01540 is an α,α trehalase with similarity to TreA of *A. nidulans* which plays a role in the hydrolysis of trehalose into glucose. TreA localizes in the conidiospore wall and is necessary for development on trehalose as a carbon source (d'Enfert and Fontaine, 1997). Enzymes containing a glycosylphosphatidylinositol (GPI) anchoring signal at the protein C-terminus were increased (AgtC) and decreased (CrhB and CwpA) after GT exposure. In fungi, GPI-anchored proteins can be found attached to the β-1,3-glucan or the chitin part of the cell wall (Damveld et al., 2005). Plaine et al. (2008) studied the effect of caspofungin on *C. albicans*, using a library of potential GPI-anchored gene mutants, in order to elucidate roles of GPI proteins. These authors hypothesised about functions in cell wall structure and remodelling (Plaine et al., 2008).

It was surprising to observe that DfgC and GlaA decreased in the secretome while they were highly increased in abundance within the mycelial proteome. This could point towards a defect in the secretory pathway of these GHs. The affect of DTT on the secretory system of *A. niger* was investigated by Guillemette et al. (2007) where they observed an up-regulation of genes that encode for vesicle transport proteins and endoplasmic reticulum (ER)-associated degradation (ERAD) proteins (Guillemette et al., 2007). Other GHs found at decreased abundance in the secretome were XynB and AbfB, an endo-1,4-β-xylanase B and arabinofuranosidase B, respectively. XynB is a xylanolytic enzyme controlled by XlnR while AbfB is involved in the hydrolysis of

arabinoxylan and arabinan. Both enzymes appeared increased in abundance when *A. niger* was grown on xylose which indicates their role in the degradation of polymers (Lu et al., 2010).

Glucose can be used as a sole carbon substrate for the growth of filamentous fungi, where it can be catabolized into pyruvate and acetyl-CoA through glycolysis (Lu et al., 2010). There are three irreversible steps in glycolysis that cannot be used in gluconeogenesis in the cell which include (i) conversion of glucose to glucose-6-phosphate by hexokinases, (ii) phosphorylation of fructose 6-phosphate and (iii) conversion of phosphoenolpyruvate to pyruvate. In *A. nidulans*, deletion of two hexokinase genes (*hxkA* and *glkA*) was shown to abolish growth on glucose as the sole carbon source (Flipphi et al., 2003). However no nutritional deficiencies were observed in single mutant Δ*glkA* (Flipphi et al., 2003). Increased abundance of GlkA in *A. niger* in response to GT suggests glucose uptake from the media and potential utilization towards glycolysis. On the other hand, six glycolytic enzymes (An07g06780, TpiA, Fba1, Pgi1, PgmB and An16g02990) were abundance-decreased after GT addition and catalyse reversible reactions within the pathway that can either be indicative of glycolysis or gluconeogenesis depletion (Figure 4.5).

Pyruvate can be transported into the mitochondria where by the action of the pyruvate dehydrogenase complex it is converted to acetyl-CoA. Citrate synthase then condenses oxaloacetate derived from the cytoplasm with acetyl-CoA to form citrate and start the TCA cycle. Both of these enzymes were decreased in abundance in response to GT for 3 h and 6 h along with aconitate hydratase which converts citrate to isocitrate. TCA cycle enzymes succinate CoA-ligase, dihydrolipoamide S-succinyl transferase, succinate dehydrogenase, FumR and malate dehydrogenase (Mdh1,

MdhA) were also decreased after GT exposure for 3 h. Pusztahelyi et al. (2011) mapped the intracellular proteome of *A. nidulans* in response to menadione stress agent and found fluctuating protein expression patterns for the glycolytic enzymes PgmB (repression) and FbaA (induction) and for TCA cycle enzymes AcoA, MdhA and MdhC (repressed) (Pusztahelyi et al., 2011). They proposed that the dysregulation observed is due to *A. nidulans* having to cope with glucose shortages (Pusztahelyi et al., 2011). Though FbaA was induced in Pusztahelyi et al. (2011) study, Pocsi et al. (2005) found it highly repressed in response to GSH/GSSG redox imbalance. They speculated that this repression might result in intracellular accumulation of fructose-1,6-bisphosphate, which can protect mitochondria functionality (Pócsi et al., 2005).

In the cytoplasm, pyruvate can either be converted to oxaloacetate (OAA) by pyruvate carboxylase or to acetaldehyde by pyruvate decarboxylase. If OAA is formed, it can be transported to the mitochondria where it will be incorporated into the TCA cycle. Acetaldehyde is the first intermediate of ethanol catabolism (alcohol fermentation), which is another pathway fungi can use to produce energy (Hynes and Murray, 2010). In *A. nidulans*, deletion of cytochrome C which is an essential component of the oxidative respiratory pathway led to production of ethanol and persistent viability through its ability to ferment (Bradshaw et al., 2001). Two pyruvate decarboxylases were differentially dysregulated in *A. niger* exposed to GT, whereby PdcA was increased at 3 h and 6 h and PdcB was decreased only after 3 h, indicating acetaldehyde production at both time points. In *A. nidulans, aldA* gene encodes for aldehyde dehydrogenase which converts acetaldehyde to acetate (Flipphi et al., 2009; Mathieu et al., 2005). Acetyl-CoA is then formed from acetate via acetyl-CoA synthase (AcuA) or acetyl-CoA hydrolase (Ach1) (Carman et al., 2008) and also it can be produced from cytoplasmic citrate through the action of ATP-citrate lyase (encoded

by *aclA* in *A. nidulans*) (Reiser et al., 2010). In *A. niger* exposed to GT, AcuA and ATP-citrate lyase were decreased in abundance and Ach1 was increased at 3 h and 6 h GT exposure. Decrease in abundance of ATP-citrate lyase, aldehyde dehydrogenase and alcohol dehydrogenase was observed by Carberry et al. (2012) when *A. fumigatus* was exposed to exogenous GT (Carberry et al., 2012).

The dysregulation of the TCA cycle and fermentative pathways upon GT addition can be a consequence of a glucose limitation and would entail an overall reduction of the energy metabolism. This could explain why there is such an increase in the abundance of hydrolytic enzymes containing signal peptide.

The central carbon metabolism is a very well interconnected metabolic network where carbohydrates are converted into metabolic precursors (Minic, 2015). Figure 4.5 indicates the interconnectivity of the TCA cycle where intermediates like acetyl-CoA are involved in the biosynthesis of fatty acids and some secondary metabolites, and in the acetylation of proteins including histones as previously mentioned (Hynes and Murray, 2010). 2-oxoglutarate is a precursor of glutamate and glutamine which are involved in nitrogen assimilation while pyruvate is a precursor for Leu biosynthesis (Minic, 2015).

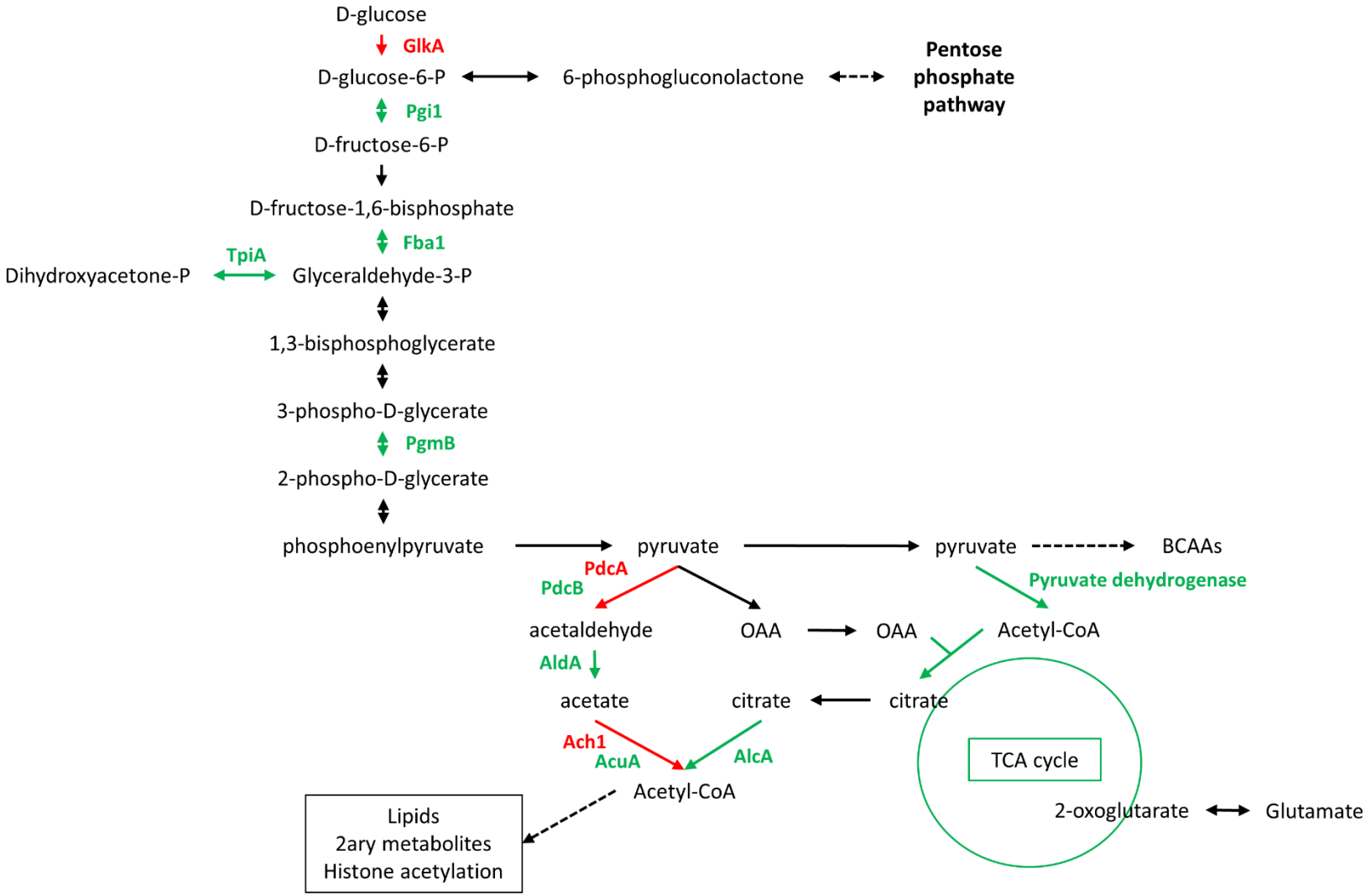
D-glucose
GlkA
D-glucose-6-P
6-phosphogluconolactone
Pentose phosphate pathway
Pgi1
D-fructose-6-P
D-fructose-1,6-bisphosphate
Fba1
TpiA
Dihydroxyacetone-P
Glyceraldehyde-3-P
1,3-bisphosphoglycerate
3-phospho-D-glycerate
PgmB
2-phospho-D-glycerate
phosphoenylpyruvate
pyruvate
pyruvate
BCAAs
PdcA
PdcB
Pyruvate dehydrogenase
acetaldehyde
OAA
OAA
Acetyl-CoA
AldA
acetate
citrate
citrate
Ach1
AcuA
AlcA
TCA cycle
Acetyl-CoA
2-oxoglutarate
Glutamate
Lipids
2ary metabolites
Histone acetylation

Figure 4.5: Reactions of the central carbon metabolism dysregulated in *A. niger* in response to GT for 3 h. Enzymes in red appeared as increased after GT addition (glucokinase, GlkA; pyruvate decarboxylase, PdcA and acetyl-CoA hydrolase, Ach1) while those in green were decreased in abundance (glucose-6-phosphate isomerase, Pgi1; fructose bisphosphate aldolase, Fba1; triosephosphate isomerase, TpiA; phosphoglucomutase, PgmB; pyruvate decarboxylase PdcB; aldehyde dehydrogenase, AldA; acetyl CoA-synthase, AcuA; ATP-citrate liase, AclA; pyruvate dehydrogenase and enzymes involved in the citric acid cycle).

Analysis of the proteins included in the amino acid metabolism category revealed a dysregulation of proteins involved in BCAAs, Phe and His metabolism and nitrogen assimilation among others. Genes encoding for enzymes involved in amino acid biosynthesis are induced in response to amino acid starvation (Ljungdahl and Daignan-Fornier, 2012). In filamentous fungi this genetic system is called cross-pathway control while in yeast it is termed general amino acid control (GAAC) (Hinnebusch, 2005). The transcriptional activator for GAAC is named Gcn4 and CpcA for the cross-pathway control. Several *A. niger* enzymes homologous to proteins encoded by genes under the control of Gcn4 in *S. cerevisiae* where observed to be dysregulated in response to GT at 3 h and 6 h, which included; *HIS1*, *HIS5*, *ARG1*, *LYS1*, *ARO3*, *SER3*, *AAT2*, *LEU1* and *GDH2* (Brisco and Kohlhaw, 1990; Ljungdahl and Daignan-Fornier, 2012).

Two enzymes An02g03250 (with 3-isopropylmalate dehydratase activity) and β-isopropylmalate dehydrogenase appeared decreased and increased, respectively when *A. niger* was exposed to GT for 3 h. Their homologs in yeast, LEU1 and LEU2 catalyse the conversion of α-isopropylmalate into α-ketoisocaproate which is part of the leucine biosynthetic pathway (Kohlhaw, 2003). These enzymes are cytoplasmic and appear to be regulated differently. *LEU1* is slightly up-regulated by transcription factor Gcn4 while *LEU2* maintains basal levels of expression (Kohlhaw, 2003). Though both enzymes are involved in the biosynthesis of leucine, the difference in abundance between them could be due to GT having different affects on their regulation. Two homologous 3-deoxy-7-phosphoheptulonate synthases (An01g06150 and An04g03620) were increased at both 3 h and 6 h exposure to GT. In *A. nidulans*, the An01g06150 ortholog (encoded by *aroG*), catalyses the first step in the shikimate pathway, which ultimately leads to the biosynthesis of folates, ubiquinone and

aromatic amino acids (Hartmann et al., 2001). Interestingly, my data revealed that Phe levels were increased after GT addition at both time points in *A. niger*. D-amino acid oxidase (DAO) is a FAD-containing flavoenzyme that plays a catabolic role whereby D-amino acids are used as carbon and energy sources (Pollegioni et al., 2008). Takahashi et al. (2014) recombinantly expressed a DAO from the thermophilic bacteria *Rubrobacter xylanophilus* and found it had high affinity for branched-chain D-amino acids (Takahashi et al., 2014). In *A. niger*, DAO (An01g02430) was increased only after 6 h exposure to GT which could imply a role in carbon metabolism. Overall, the increase in proteins involved in amino acid biosynthesis might suggest their use in the biosynthesis of GHs and peptidases.

Of the proteins with decreased abundance in response to GT in *A. niger*, approximately 50 % were involved in BCAA catabolism. An13g03150 is an ortholog of *A. nidulans* putative branched-chain keto acid (BCKAs) dehydrogenase (E1β subunit), which catalyses the oxidative decarboxylation of BCKAs to their respective acyl-CoA derivatives being (i) isovaleryl-CoA for leucine, (ii) isobutyryl-CoA for valine and (iii) 2-methylbutanoyl-CoA in the case of isoleucine (Rodríguez et al., 2004). After decarboxylation, each acyl-CoA derivative is catabolised through three independent pathways that will lead to the citric acid cycle (Figure 4.6).

Acyl-CoA dehydrogenase (An17g01150) from *A. niger* showed strong similarity to AcdA from *A. nidulans*. AcdA was investigated by Reiser et al. (2010) as a potential fatty acid (FA)-CoA dehydrogenase involved in peroxisomal β-oxidation. Though they observed that AcdA was induced by FA, the Δ*acdA* mutant resulted in no detectable phenotype on FAs as sole carbon sources, thus concluding that this enzyme had no function in the β-oxidation pathway (Reiser et al., 2010). It was argued

by Maggio-Hall et al. (2008) that acyl-CoA dehydrogenases were not specific to β-oxidation, as they can also be involved in the degradation of Val, Leu and Ile, as recently confirmed in *A. nidulans* (Maggio-Hall et al., 2008). Indeed, acyl-CoA dehydrogenase (An07g04280) from *A. niger* showed strong homology to IvdA from *A. oryzae* and *A. thaliana*. In *A. oyzae*, *ivdA* gene encodes for an isovaleryl-CoA dehydrogenase (IVD) that catalyses the conversion of isovaleryl-CoA to 3-methylcrotonyl-CoA in the leucine catabolism (Figure 4.6) (Yamashita et al., 2007). In *Arabidopsis thaliana*, isovaleryl-CoA dehydrogenase (AtIVD) was found to have substrate specificity towards isovaleryl-CoA and also to isobutyryl-CoA which is an intermediate of the valine degradation pathway (Däschner et al., 2001).

Interestingly, An01g12960 is the *A. niger* ortholog of *A. nidulans scdA*, which encodes an acyl-CoA dehydrogenase involved in mitochondrial β-oxidation of fatty acids and catabolism of BCAAs (Maggio-Hall et al., 2008). It was the only acyl-CoA dehydrogenase found increased in abundance after GT addition in *A. niger*. Maggio et al (2008) provided evidence that mitochondrial β-oxidation of fatty acids and catabolism of BCAAs utilize the same acyl-CoA dehydrogenase encoded by *scdA*. In fungi, FA β-oxidation can serve for ATP and energy production.

Putative 3-hydroxyisobutyrate dehydrogenase (An14g04420) is involved in valine metabolism whereby it catalyses the oxidation of 3-hydroxyisobutyrate to methylmalonate semialdehyde (Figure 4.6) (Kazakov et al., 2009). Its homolog in *C. albicans* (Hpd1) was additionally observed to have substrate specificity towards 3-hydroxypropionate, which is an intermediate of the β-oxidation pathway (Otzen et al., 2014). Two homologous 3-ketoacyl-CoA thiolases (An04g05720 and An08g05400) were abundance-decreased in *A. niger* after GT addition. Based on KEGG

classification, these thiolases are involved in the generation of acetyl-CoA and propionyl-CoA from 2-methyl-acetoacetyl-CoA (Figure 4.6). In bacteria, these enzymes are also known as KATC and catalyse the last step in isoleucine degradation (Kazakov et al., 2009). The increase in BCAAs biosynthesis and decrease in catabolism might reflect the use of pyruvate for BCAAs production. At the metabolite level, both valine and leucine/isoleucine were increased in *A. niger* in response to GT for 3 h and 6 h. These amino acids can subsequently be used as the building blocks for protein synthesis. Surprisingly, GT has been shown to affect the biosynthesis of BCAAs by interfering with acetolactate synthase (ALS) in tobacco plants, which catalyses the first step in the biosynthesis of these amino acids (Haraguchi et al., 1996). These authors observed that GT-mediated growth inhibition was reduced when growth medium was supplemented with valine, leucine and isoleucine and hypothesised towards the protective effects of amino acids in tobacco plants (Haraguchi et al., 1996).

Additionally, alteration of proteins involved in nitrogen metabolism was observed in response to GT. NAD^+-linked glutamate dehydrogenase (An02g14590, GDH2) was not detected after 3 h GT exposure while glutamine synthetase (An01g08800, GLN1) was decreased after 3 h and 6 h exposure to GT in *A. niger*. GDH2 provides ammonium for the synthesis of glutamine by GLN1 (Ljungdahl and Daignan-Fornier, 2012). A decrease of these enzymes could lead to the accumulation of glutamate which is a precursor for the biosynthesis of multiple amino acids.

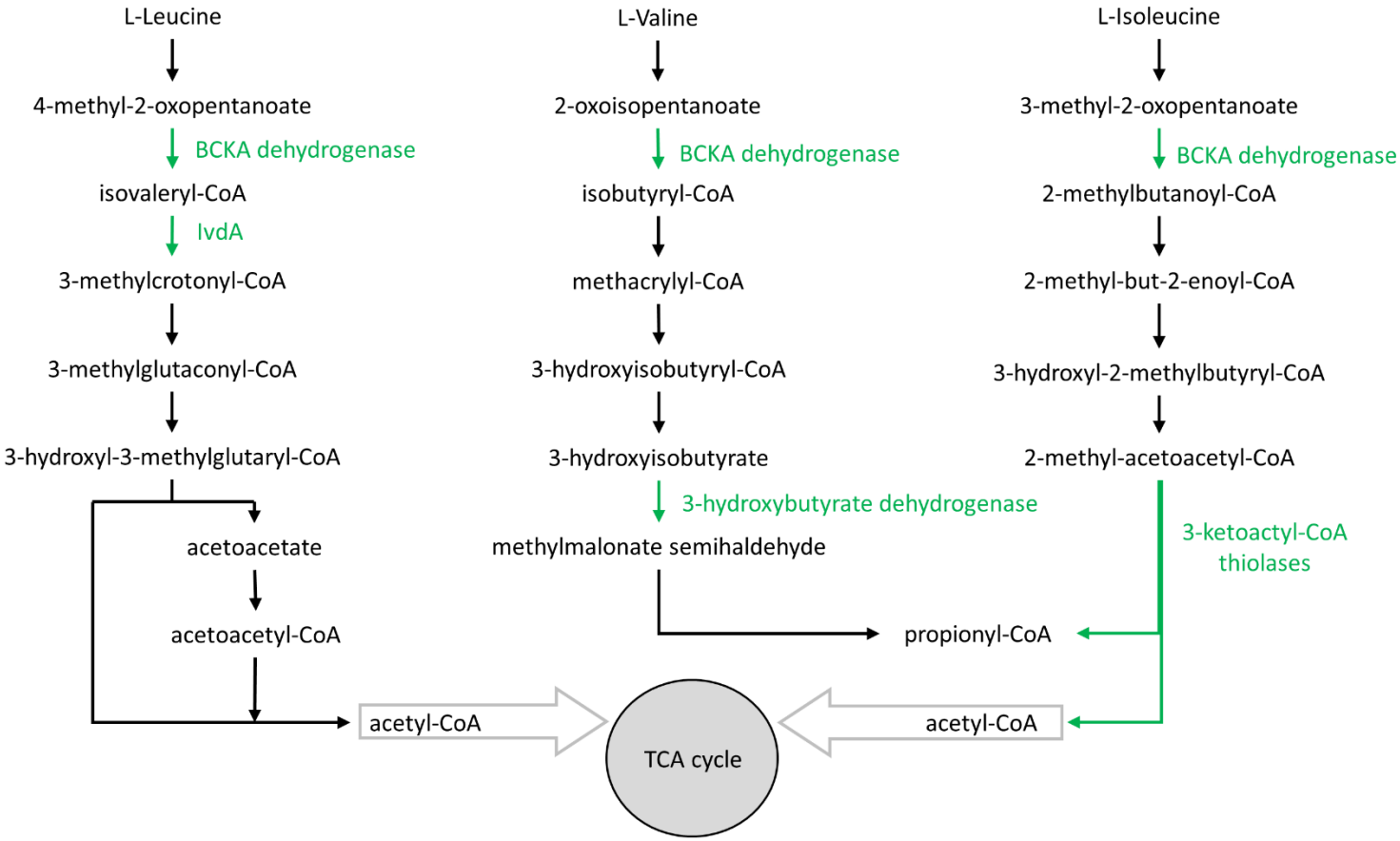

Figure 4.6: Overview of the BCAAs catabolism. Proteins decreased in abundance after GT addition in *A. niger* are denoted in green font.

The proteome of *A. niger* environmental isolate was also investigated when exposed to GT for 3 h (2.5 μg/ml). When exposed to GT, 17 protein spots were found differentially increased, which corresponded to 15 proteins while, 18 proteins showed decreased levels. Three proteins were identified from multiple spots, acetyl-CoA hydrolase was identified from 2 individual spots, pyruvate decarboxylase was also identified from two individual spots, and so was phosphopyruvate hydratase which indicates the presence of isoforms of these proteins, possibly as a result of posttranslational modifications. Some of the proteins identified in this investigation, overlap with those identified for *A. niger* CBS 513.88 exposed to GT for 3 h (LFQ proteomic analysis). The proteins showing increased abundance for both investigations were involved in the central carbon metabolism (Acetyl-CoA hydrolase and pyruvate decarboxylase), methionine metabolism (homoserine dehydrogenase) and ribosome assembly (An08g05730 with 5S rRNA binding activity). Those proteins with decreased abundance in both studies were involved in glycolysis and the TCA cycle, and included: fructose bisphosphate aldolase, aldehyde dehydrogenase, aspartate aminotransferase, triose phosphate isomerase, aconitate hydratase and citrate synthase. The effect GT has on the depletion of the TCA cycle on both *A. niger* strains is thus confirmed. *S*-adenosylmethionine synthase, involved in SAM biosynthesis as described in Chapter 3, was decreased in abundance in the Env. Iso. This observation is surprising considering SAM is needed for multiple methylation reactions including the methylation of GT (as described in Chapter 5) but could be the reason as to why the level of GT sensitivity is higher in the Env. Isol. strain compared to the CBS 513.88. Also different from the CBS 513.88 strain was the increase in abundance of the E2 subunit of the pyruvate dehydrogenase complex.

Proteins dysregulated only in the *A. niger* Env. Isol. and not in the sequenced strain included a putative zinc aminopeptidase (An04g03930), which was increased in abundance after GT addition. In the genus *Aspergillus*, this peptidase is known as AspA and was described to be cytosolic, thus it does not contain signal peptide. It is a M1 family member which acts preferentially on the N-terminal lysine of substrates (Basten et al., 2001). *A. niger* An02g07190 (TbpA) is an ortholog of *S. cerevisiae* Rpt3 and was increased after GT addition. Rpt3 is a component of the 19 S ATPase subunit of the proteasome, where ubiquitinated proteins are degraded (Peth et al., 2013).

Increased abundance of An04g09170 (Cdc48 in *A. fumigatus*) was also observed in the Env. Iso. after GT exposure. Cdc48 is an ATPase that mediates the release of ubiquitinated tRNA linked nascent peptides from ribosomes to destruction by the proteasome (Verma et al., 2013). Cdc48 was observed increased in *A. fumigatus* in response to heat shock stress (Albrecht et al., 2010) and in *A. nidulans* in response to farnesol (Wartenberg et al., 2012). These authors pointed towards the increase of Cdc48 as part of the UPR-mediated stress response to farnesol (Wartenberg et al., 2012). Overall the increase of Rpt3 and Cdc48 in response to GT is indicative of damaged and improperly folded proteins.

On the contrary, two heat shock proteins Hsp90 and Hsp70 were decreased in abundance after GT exposure in *A. niger* Env. Iso. Heat shock proteins are molecular chaperones generally linked to the folding of newly synthesised proteins, thus, its decrease suggests that GT effects the appropriate folding and nuclear transport of proteins (Pusztahelyi et al., 2011).

Finally, it is clear from the data above that GT majorly affects the metabolic network of *A. niger* and consequently the regulatory processes associated with it. It is

worth noticing that the Velvet complex is involved in the regulation of several pathways of this network like the catabolism of BCAAs, the production of cellulases and proteases (Dhingra et al., 2012; Roze et al., 2010; Seiboth et al., 2012). Apart from the functionality of the Velvet complex in secondary metabolism, it has been observed that the production of CAZymes and proteases depends on functional regulators BcVEL1 and BcLAE1, in *Botrytis cinerea*, which are the *A. nidulans* orthologs of VeA and the SAM-dependent methyltransferase LaeA, respectively (Schumacher et al., 2015). LaeA in *A. nidulans* was shown to control the expression of carbohydrate metabolism enzymes such as Hülle cell-specific α-mutanase, which is involved in establishment of fully mature fruiting bodies (Sarikaya Bayram et al., 2010). In *Trichoderma reesei*, LAE1 (*A. nidulans* LaeA ortholog) has been shown to regulate the expression of genes involved in lignocellulose degradation whereby in a *lae1* deletion mutant, a number of cellulases and xylanases where no longer expressed. Additionally, XYR1, the cellulase and hemicellulase transcriptional regulator, was shown to be dependent on LaeA and vice versa (Seiboth et al., 2012). The deletion of *vel1*, which is the *T. reesei* ortholog of *A. nidulans veA*, also diminished the expression of xylanases, cellulases and XYR1 when grown on lactose (Karimi Aghcheh et al., 2014). The *A. niger* ortholog of XYR1, XlnR, was described as the transcriptional activator of xylanolytic enzymes (van Peij et al., 1998b). Herein, *A. niger* exposed to GT led to an increased abundance of AglB, LacA and AglA, which are under the control of XlnR. In *A. fumigatus*, deletion of *veA* was shown to cause a reduction of protease activity (Dhingra et al., 2012). It was proposed by Roze et al. (2010) that VeA acts as a negative regulator of BCAA catabolism when they observed that a Δ*veA* mutant in *A. parasiticus* was able to generate high levels of metabolites derived from the catabolism of Val, Leu and Ile (Roze et al., 2010). Thus, it is possible that the

dysregulation of hydrolytic enzymes and BCAA after GT addition, are mediated by alterations to the Velvet complex.

The work presented here, in addition to the work described in Chapter 3, shows the changes occurred in the metabolic network of *A. niger* and its connections with other processes in the cell in response to GT. Through this analysis I was able to identify putative enzymes and assign functionality to one of them (MT-II, Chapter 5) which appear to play an important role in *A. niger* defence mechanism against GT.

Chapter 5

S-Methylation of exogenous gliotoxin by *Aspergillus niger*

5 Chapter 5: *S*-methylation of gliotoxin by *Aspergillus niger*

5.1 Introduction

Thiol methylation takes place in numerous biological transmethylation reactions. These reactions are catalysed by thiomethyltransferases (TMTs) and are usually SAM dependent, whereby the methyl group of SAM is transferred to a substrate. Although not as common as *N*- or *C*- methylations, *S*-methylation has been reported in thiol containing small molecules and biological thiols of proteins containing cysteine and methionine residues (Attieh et al., 2000a; Dolan et al., 2014; Scharf et al., 2014; Sengupta et al., 2014; Zhao et al., 2012).

A cysteine methyltransferase from *S. cerevisiae* was shown to methylate trehalose-6-phosphate synthase (TPS), which is an enzyme involved in the formation of trehalose-6-phosphate and subsequently trehalose (Sengupta et al., 2014). Trehalose has an important role as a stabilizer of cellular structures and protection of biological membranes and enzymes under stress conditions (Voit, 2003). Due to the reduction of trehalose levels as a consequence of the deletion of cysteine methyltransferase compared to wild type, it was proposed that the cysteine methyltransferase had a role in protecting the yeast from various stress conditions (Sengupta et al., 2014). Protein thiomethylation has also been observed in *Euglena gracilis*, whereby a methionine *S*-methyltransferase was observed to methylate cytochrome c (Farooqui et al., 1985). Although these results indicate a role of TMTs in thiomethylating proteins, a greater amount of research has been done on small molecule methylation.

Several plant TMTs have been described in relation to detoxification mechanisms. PpSABATH1, a TMT identified in *Physcomitrella patens*, displayed high levels of activity towards thiobenzoic acid (Zhao et al., 2012). Interestingly,

exposure of *P. patens* to thiobenzoic acid induced the expression of the *PpSABATH1* gene and overexpression of *PpSABATH1* in transgenic plants increased the tolerance to thiobenzoic acid, thus suggesting the role *PpSABATH1* has in the detoxification of xenobiotic thiols (Zhao et al., 2012). In *Brassica oleraccea*, a TMT was observed to methylate several thiols including bisulfide ion, aromatic thiols and thiocyanate (Attieh et al., 2000a, 2000b). Recombinant expression of the TMT indicated a preference for thiocyanate as the methyl acceptor. These reactive thiols are formed during the hydrolysis of glucosinolates, indicating the potential role of this enzyme as a detoxification mechanism of reactive thiols generated from glucosinolate degradation (Attieh et al., 2000a, 2000b).

In bacteria, Li et al. (2012) identified an *S*-methyl derivative of holomycin in *Streptomyces clavuligerus*. Holomycin is a naturally occurring antibiotic characterised for the presence of a disulphide bridge which is formed by the action of a thioredoxin oxidoreductase (HlmI) on the dithiol precursor (Li and Walsh, 2011). Deletion of *HlmI* sensitized *S. clavuligerus* to exogenous holomycin however no growth impairment was observed when *S,S'*-dimethylhydroholomycin was exogenously added. Based on these observations, Li et al. (2012) proposed the *S*-methylation of holomycin as a back-up mechanism for self-protection against dithiol forms of metabolites when HlmI is absent (Figure 5.1). Other TMTs have been implicated in the biosynthesis of antibiotics. A TMT from *Streptomyces lasaliensis*, Ecm18, catalyses the final step in the biosynthesis of echinomycin from its precursor triostin A (Watanabe et al., 2006). This step involves the conversion of the disulphide bond in triostin A into a thioacetal bridge and the transfer of a methyl group into a receiving sulphur atom in echinomycin (Hotta et al., 2014; Watanabe et al., 2006). In the same way, TrsK, which is

homologous to Ecm18, catalyses the last step in echinomycin formation in *Streptomyces triostinicus* (Hotta et al., 2014; Praseuth et al., 2008) (Figure 5.1).

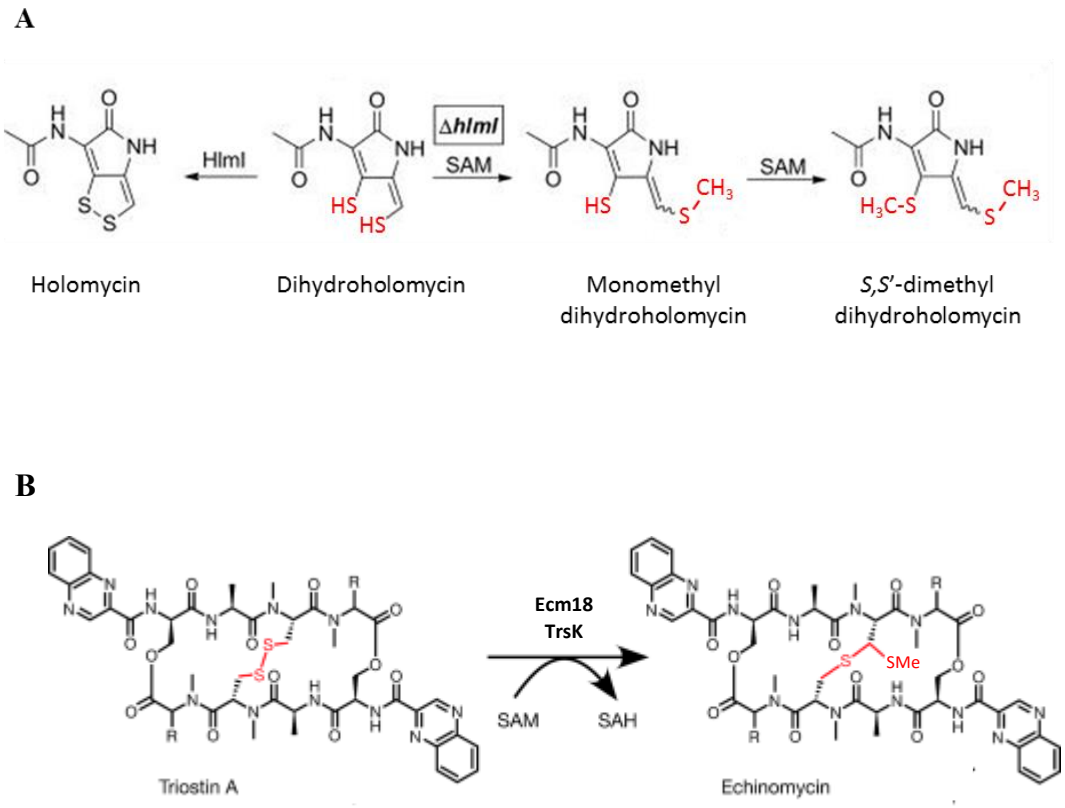

Figure 5.1: Bacterial TMTs involved in secondary metabolism. **(A)** Schematic representation of homolycin thiomethylation in *S. clavuligerus* (Image addapted from Li et al., 2012). **(B)** Ecm18 from *S. lasaliensis* and TrsK from *S. triostinicus* catalyse the last step in the biosynthesis of echinomycin (Image addapted from Hotta et al., 2014).

In fungi, several thiomethylated derivatives of secondary metabolite toxins have been reported. The first thiomethyl derivative of gliotoxin, which is an epipolythiodioxopiperazine (ETP) type of toxin, was extracted and separated by layer chromatography in culture filtrates of *Gliocladium delisquenses* (Kirby and Sefton, 1980). Bisdethiobis(methylthio)gliotoxin (BmGT) has also been observed in other fungal species like *A. fumigatus* (Amitani et al., 1995) and *Penicillium* spp. (Sun et al., 2012), Other bis(methylthio)-derivatives that arise from known ETP-type toxins include; didethiobis(methylthio)hyalodendrin produced by *Hyalodendron* spp (Boente et al., 1991), chetoseminudin B identified in *Chaetomium seminudum* (Fujimoto et al., 2004), bionectin C which was isolated from the fungus *Bionectra byssicola* (Zheng et al., 2006) and chetracin D that was isolated from *Oidiodendron truncatum* (Li et al., 2012b; Welch and Williams, 2014) (Figure 5.2). Although limited of information about the functionality of these derivatives can be found in the literature, it is interesting to note that ETPs contain a characteristic disulphide bridge which accounts for the deleterious affects of the toxin, and methylation of the free thiols renders an inactive toxin. Despite of the presence of these methylated ETPs in fungi, the TMTs responsible of their generation have remained elusive, until very recently.

Compound	Structure
Bisdethiodi(methylthio) gliotoxin	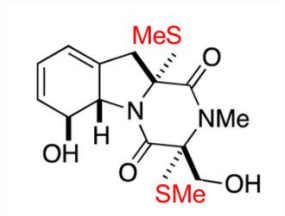
Bisdethiodi(methylthio) hyalodendrin	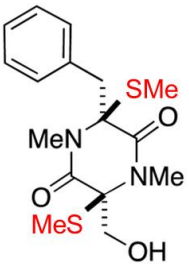
Chetoseminudin B	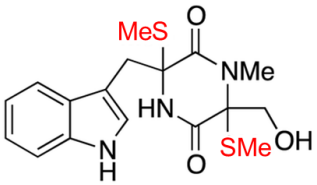
Chetracin D	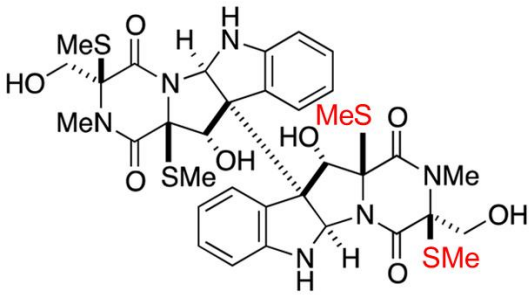
Bionectin C	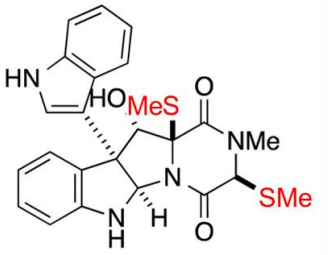

Figure 5.2: *Bis*-thiomethyl derivativesof ETP toxins. Adapted from (Welch and Williams, 2014).

The first fungal gliotoxin *bis*thiomethyltransferase (GtmA) (Dolan et al., 2014), termed thiol thiomethyltranferase (TtmA) in Scharf et al. (2014), was identified in *A. fumigatus*, where it catalyses the methylation of dithiol gliotoxin (rGT) to form *bis*dethiobis(methylthio)gliotoxin (BmGT) (Figure 5.3). Unexpectedly, the deletion of *gtmA* from *A. fumigatus* does not seem to confer increased sensitivity to exogenous gliotoxin, and instead leads to an over-production of exogenous gliotoxin. In effect, BmGT formation primarily seems to serve as a negative regulatory mechanism to effect attenuation of gliotoxin biosynthesis in *A. fumigatus* (Dolan et al., 2014). Puzzlingly, although orthologs of *gtmA* are detected in certain gliotoxin-naïve fungi, including *A. niger* (Dolan et al., 2014), the functionality of the encoded enzyme remains obscure, although BmGT formation has been demonstrated in *A. nidulans* upon exposure to exogenous gliotoxin (Scharf et al., 2014).

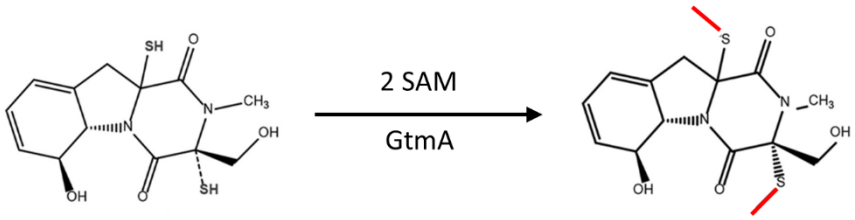

Figure 5.3: *Bis*-thiol methylation of rGT to BmGT by GtmA in A. fumigatus (Dolan et al., 2014).

The objectives of the work presented in this chapter were, (i) to investigate the mechanism of GT thiomethylation in fungi unable to synthesise GT, (ii) to recombinantly express the *A. niger* orthologue of GtmA, termed MT-II, (iii) to characterise recombinant MT-II and (iv) to assess functionality of the *A. niger* Δ*MT-II* mutant.

5.2 Results

5.2.1 *In vivo bis*-thiomethylation of gliotoxin in *Aspergillus* spp.

Proteomic analysis discussed in Chapter 3, revealed that when exogenous GT is added to *A. niger* (3 h and 6 h), it increases the abundance of a number of SAM dependent methyltransferases. Two of these enzymes (MT-I and MT-II) showed unique abundance under GT-exposure conditions (Table 3.2, Chapter 3). Furthermore, the two methyltransferases were also observed to be induced by dithiothreitol (DTT; 20 mM) in an *A. niger* subtraction library (MacKenzie and Guillemette, 2005). Interestingly, we and others have noted that MT-II is an ortholog of GtmA (AFUA_2G11120), which is a SAM-dependent gliotoxin *bis*-thiomethyltransferase, rGT to BmGT (Dolan et al., 2014; Scharf et al., 2014).

Based on this observation, and in order to confirm if *A. niger* CBS513.88 is capable of thiomethylating gliotoxin, gliotoxin (final conc. 2.5 µg/ml) was added to *A. niger* liquid cultures over a 4 h period and 2 ml aliquots of supernatant were organically extracted as described in Section 2.2.7. Uptake of GT by *A. niger* was observed followed by conversion to BmGT, which is secreted to the culture medium over a 4 h time-course (Figure 5.4). An identical *in vivo bis*-thiomethylation process is observed in *A. nidulans* FGSC4 exposed to exogenous gliotoxin (2.5 µg/ml) over a 4 h period (Section 2.2.7) (Figure 5.4). Interestingly, *A. nidulans* is also sensitive to exogenous gliotoxin (Carberry et al., 2012) and is devoid of the *gli* cluster responsible for gliotoxin biosynthesis (Patron et al., 2007). This observation shows that gliotoxin-naïve *Aspergillus spp.* are able to *bis*-thiomethylate exogenous gliotoxin (Scharf et al., 2014).

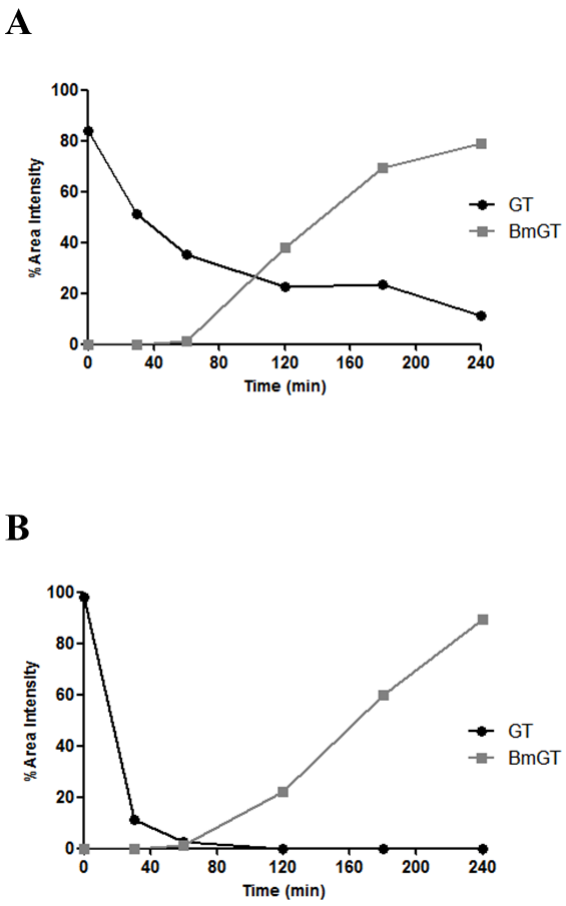

Figure 5.4: *In vivo* <u>*bis*</u>-thiomethylation of gliotoxin by *Aspergillus spp*. **(A)** Gliotoxin (2.5 µg/ml) added to *A. niger* CBS 513.88 cultures is converted to BmGT over 4 h. **(B)** The same process occurs in *A. nidulans* FGSC4.

Y Axis on graphs represents Area Intensity (%) of GT (black) and BmGT (grey) obtained from LC-MS/MS analysis as described in Section 2.2.10.2.

5.2.2 *In vitro bis*-thiomethylation of gliotoxin by *A. niger* CBS 513.88 lysates

5.2.2.1 Development of a SAM-dependent methyltransferase (SAM-MTase) Assay

GT thiomethylation was analysed using a novel LC-MS/MS based assay (Section 2.2.9). This procedure provides an accurate method for the determination of GT thiomethyl derivatives, specifically *mono*- and *bis*-thiomethyl gliotoxin. This protocol presents an advantage compared to spectrophotometric-based MTase assays in that it can differentiate between mono- and bis-thiomehyl derivatives of a dithiol substrate (i.e. rGT). GT, and its thiomethyl-derivatives have known mass and fragmentation patterns that facilitate the detection of these metabolites. The masses of gliotoxin, monodethiomono(methylthio)gliotoxin (MmGT) and BmGT are 327, 343 and 357 respectively (Figure 5.5). The identity of these masses was confirmed by comparison to commercial standards in the case of GT and BmGT and by comparison of mass spectral data with that of MmGT as published by Dolan et al. (2014).

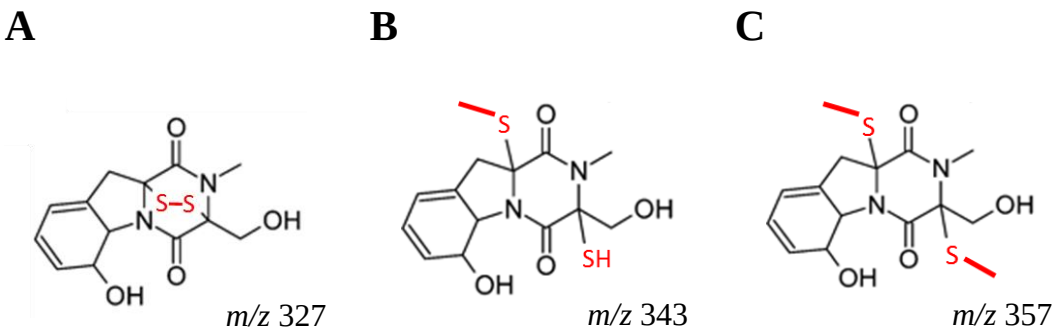

Figure 5.5: Structure and mass (+ H^+) of **(A)** GT (*m/z* 327), **(B)** MmGT (*m/z* 327) and **(C)** BmGT (*m/z* 327).

5.2.2.2 Methylation analysis by *A. niger* CBS 513.88 protein lysates

Using the aforementioned LC-MS/MS assay for the determination of GT thiomethyl derivatives (Figure 5.6) (Section 2.2.9), significant ($p < 0.0006$) MmGT (*m/z* 343) was detectable only in reactions catalysed by protein lysates derived from *A. niger* previously exposed to exogenous gliotoxin (2.5 μg/ml for 3 h) (Figure 5.6). When unexposed control lysates were used (protein lysates derived from *A. niger* liquid cultures exposed to methanol only), no thiomethylation of GT was detectable (Figure 5.6). These data strongly suggest that a specialized thiol methyltransferase, present only after GT exposure, possibly MT-II, mediates the observed bioactivity.

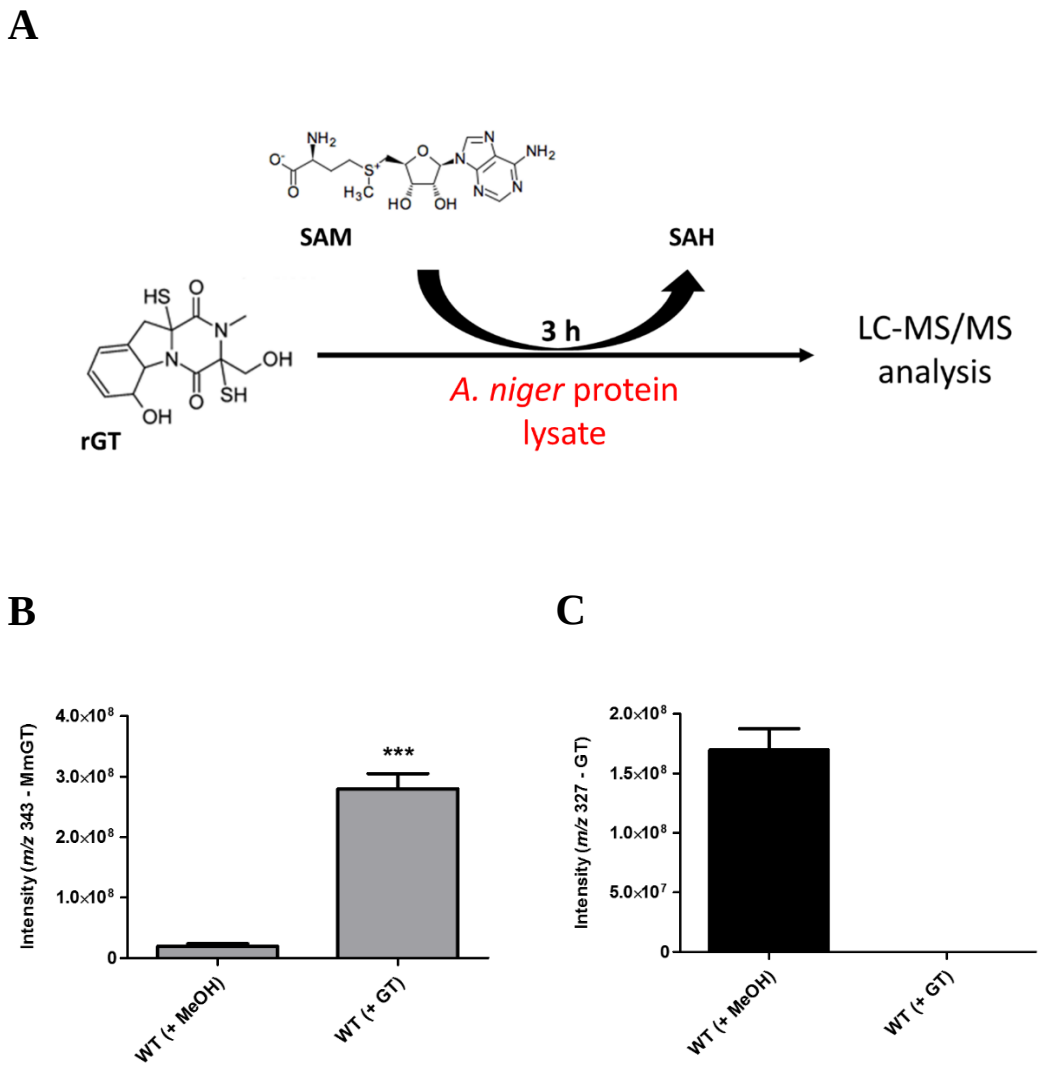

Figure 5.6: (A) Schematic representation of the LC-MS/MS based *in vitro* gliotoxin methylation assay. **(B)** *A. niger* protein lysates obtained from un-induced cultures are unable to methylate gliotoxin. **(C)** *A. niger* protein lysates obtained from GT induced cultures are responsible for methylating gliotoxin.

5.2.3 Recombinant expression of MT-II in E. coli

Based on the homology of MT-II to GtmA, MT-II was chosen as the candidate MTase responsible for the observed methylation. First, quantitative reverse transcriptase PCR (qRT-PCR) was performed on *A. niger* CBS 513.88 in order to examine *MT-II* expression under a range of culture conditions using specific primers (Table 2.13) to yield a *MT-II* amplicon. qRT-PCR analysis (Section 2.2.13.7) confirmed the up-regulation ($p < 0.0001$) of *MT-II* in *A. niger* wild-type exposed to exogenous GT for 3 h compared to MeOH (Figure 5.7). In agreement with the observations in MacKenzie et al. (2005), *MT-II* was also induced by DTT, but by almost 1000 times less on an equivalent molar basis of additive (GT: 7.7 µM versus DTT: 10 mM) (Figure 5.7). Thus, recombinant expression of MT-II as a GST fusion protein (Section 2.2.15) seemed the next step in the quest to confirm this enzyme as the one responsible for BmGT formation.

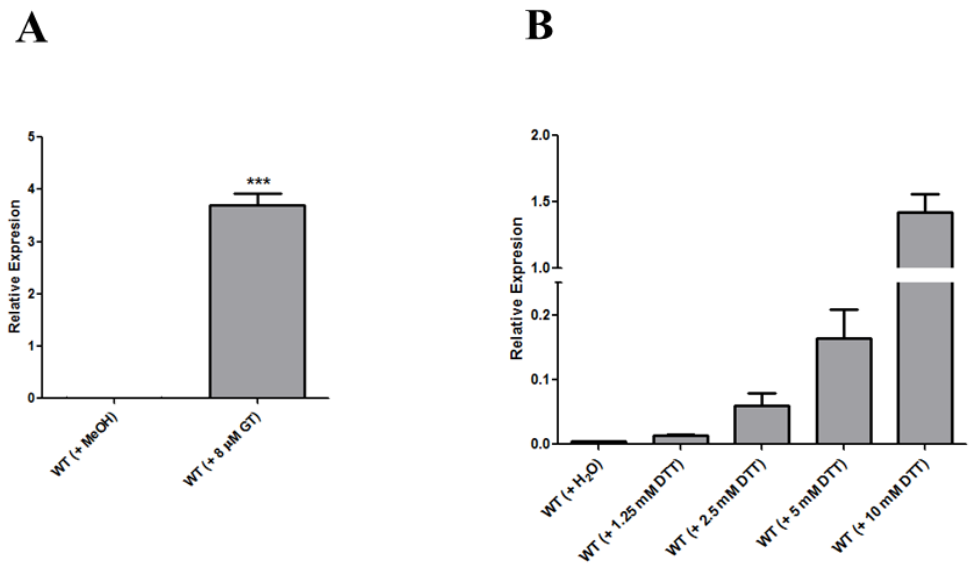

Figure 5.7: qRT-PCR confirms increased levels of *MT-II* expression in response to exogenous **(A)** GT (8 μM, 3.69 fold increase) and **(B)** DTT (10 mM, 1.42 fold increase).

5.2.3.1 Amplification of *MT-II*

Primers were designed to amplify the *MT-II* open reading frame and also to incorporate two restriction sites, *Hind*III and *Xho*I into the forward and reverse primers, respectively, to allow for directional cloning into the pEX-N-GST expression vector (Section 2.2.13.5). cDNA was isolated from *A. niger* CBS 513.88 cultures exposed to MeOH control ($cDNA_{MeOH}$) and gliotoxin (2.5 μg/ml) ($cDNA_{GT}$) for 3 h.

A. niger synthesised cDNA was PCR amplified using *MT-II* and actin (*act*) (Bohle et al., 2007) primers, separately and the *MT-II* cDNA PCR product was verified by gel electrophoresis (Figure 5.8). *MT-II* was expressed when PCR was carried out with $cDNA_{GT}$, compared to $cDNA_{MeOH}$, which indicates that gliotoxin exposure up-regulates *MT-II*. Thus *MT-II* was amplified from *A. niger* $cDNA_{GT}$.

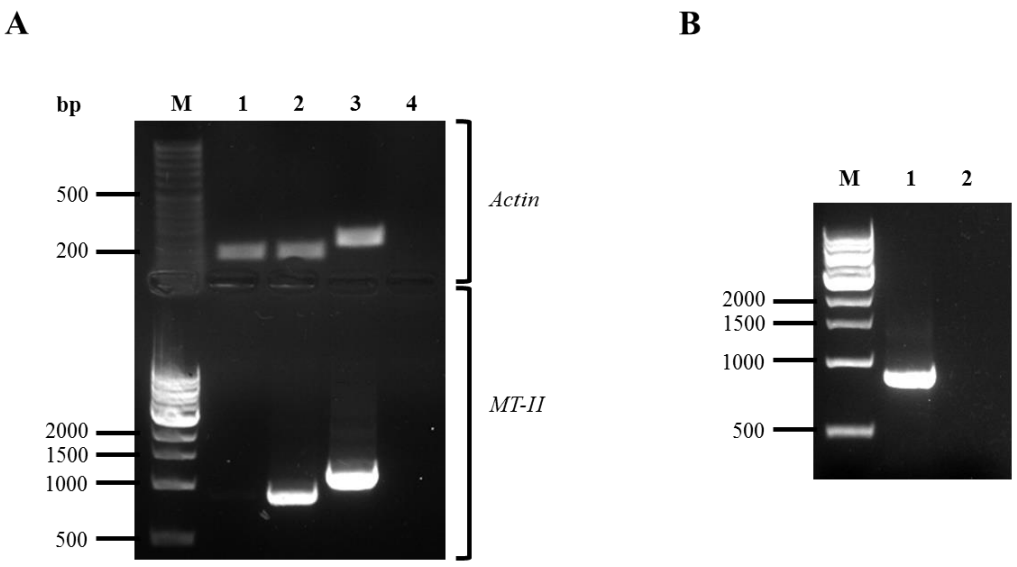

Figure 5. 8: (A) PCR amplification of $cDNA_{MeOH}$ and $cDNA_{GT}$ using *MT-II* and *actin* primers. Lane M: Molecular weight marker ladder. Lane 1: *actin* $cDNA_{MeOH}$ product at 170 bp and absence of *MT-II* $cDNA_{MeOH}$ product. Lane 2: *actin* $cDNA_{GT}$ product at 170 bp and *MT-II* $cDNA_{GT}$ product at 864 bp. Lane 3: DNA amplification PCR product of *actin* (232 bp) and *MT-II* (1127 bp). Lane 4: Negative control with PCR master mix present but no DNA. **(B)** Amplification of *MT-II* from $cDNA_{GT}$ (lane 1). Lane 2: Negative control.

5.2.3.2 Cloning of *MT-II* into the pEX-N-GST vector

After amplification, band purification and restriction digestion was carried out (Section 2.2.14.1). MT-II cDNA was ligated into the pEX-N-GST vector through the restriction sites *Hind*III and *Xho*I (Section 2.2.14.2). Consequent transformation in One Shot BL21 cells was carried out (Section 2.2.14.3). Analysis of transformants was based on selection of colonies grown on LB agar (100 µg/ml ampicillin), overnight at 37 ^{o}C. After overnight incubation, colony PCR was performed using individual colonies as the template DNA (Section 2.2.14.4). PCR products were analysed by gel

electrophoresis (Figure 5.9). A PCR product corresponding to the size of the *MT-II* cDNA product was obtained for two of the colonies.

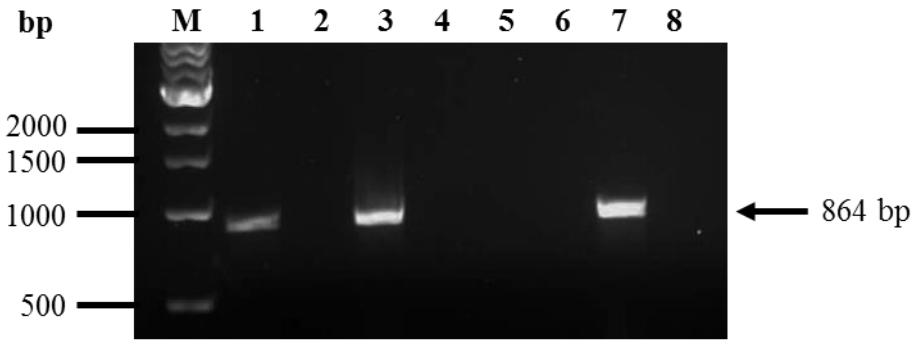

Figure 5.9: Colony PCR of transformed BL21 *E. coli* cells containing *MT-II* cDNA within the pEX-N-GST vector. Lane M: Molecular weight marker ladder. Lanes 1 – 6: Colonies screened by PCR for *MT-II* (864 bp). Of the six colonies analysed, two were PCR positive (lanes 1 and 3), with an expected product at 864 bp. Lane 7: PCR product using $cDNA_{GT}$ as the template (positive control). Lane 8: Negative control, PCR master mix only (no DNA present). This is to check for cross contaminating DNA.

The two positive colonies 1 and 3 were grown overnight and restriction digested with *Hind*III and *Xho*I to confirm the integration of *MT-II* into pEX-N-GST (Figure 5.10).

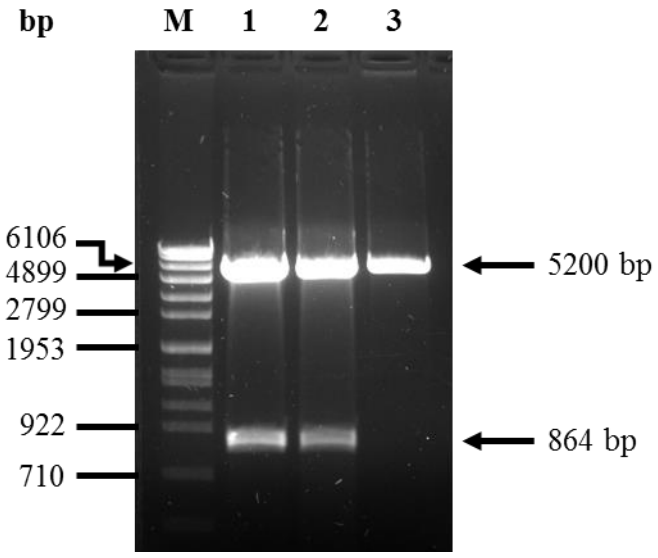

Figure 5.10: Restriction digest to confirm *MT-II* integration into the pEX-N-GST plasmid. Lane M: Molecular weight marker ladder. Lane 1 and 2: Digested pEX-N-GST vector with *MT-II* cDNA inserted produced two DNA bands as expected at approximately 5.2 Kb and 864 bp, respectively. Lane 3: Digested pEX-N-GST vector.

The restriction digestions and colony PCR confirmed the presence of the *MT-II* gene in the pEX-N-GST plasmid.

5.2.3.3 Sequence analysis of the pEX-N-GST/*MT-II* clones

The plasmid was sequenced to confirm that *MT-II* remained in frame to enable protein expression. Sequence analysis was performed on a commercial basis (Source Bioscience, Ireland), and was compared to the predicted sequences according to BLAST, with ID An02g03100 (CBS 513.88 strain). The sequencing of the *MT-II* cDNA in the pEX-N-GST plasmid confirmed the correct sequence of *MT-II* and also a correct ligation and cloning into the plasmid (Figure 5.11). There is one discrete residue change, which results in an alteration of amino acid sequence (Table 5.2). The translated MT-II protein sequence was aligned with the predicted protein sequence in BLAST and this alignment confirmed that the gene remained in-frame for protein expression (Figure 5.12).

```
Sequence_1: MT-II in pEX-N-GST Sequenced
Sequence_2: MT-II (An02g03100) Predicted
Identities: 863/864 (99 %)

Seq_1     CCAACGACCGAAAACCTGTATTTTCAGGGCGCGATCGCCGGCGCGCCAGATCTCAAGCTT    60
          ||||||||||||||||||||||||||||||||||||||||||||||||||||||||||||
Seq_2     ------------------------------------------------------------    0

Seq_1     ATGACCCCCAAAATCTCTCCCTCCTCATACCTCACCCCAGCATTTGTATCCCGCTACCAC    120
          ||||||||||||||||||||||||||||||||||||||||||||||||||||||||||||
Seq_2     ATGACCCCCAAAATCTCTCCCTCCTCATACCTCACCCCAGCATTTGTATCCCGCTACCAC    60

Seq_1     CTTGCCGAGAAACTCACTGGCGTCTTCGTGGCCCCTCTCGTCCAGCACTCTGGTATCCTG    180
          ||||||||||||||||||||||||||||||||||||||||||||||||||||||||||||
Seq_2     CTTGCCGAGAAACTCACTGGCGTCTTCGTGGCCCCTCTCGTCCAGCACTCTGGTATCCTG    120

Seq_1     TCTACCCCGAGTAACAAACCTATGGCTGTCTTCGACAATGCCTGCGGACTGGGAATTGTA    240
          ||||||||||||||||||||||||||||||||||||||||||||||||||||||||||||
Seq_2     TCTACCCCGAGTAACAAACCTATGGCTGTCTTCGACAATGCCTGCGGACTGGGAATTGTA    180

Seq_1     TCCAGCTATTTGAACAGCACGCTGCCTGAGGACGTCAAGAGACATTGGACGCTGACTTGC    300
          ||||||||||||||||||||||||||||||||||||||||||||||||||||||||||||
Seq_2     TCCAGCTATTTGAACAGCACGCTGCCTGAGGACGTCAAGAGACATTGGACGCTGACTTGC    240
```

```
Seq_1    GGGGATATAACGGAGCTGATGGTGGAGTATACCAAGTTGCGAATTGAGAGGGAAGGGTGG    360
         ||||||||||||||||||||||||||||||||||||||||||||||||||||||||||||
Seq_2    GGGGATATAACGGAGCTGATGGTGGAGTATACCAAGTTGCGAATTGAGAGGGAAGGGTGG    300

Seq_1    GTGAACGCTGAGGCGAAGGTCGTGGATGCTCAATGTACGGGGCTGCCGGCGGATAAGTAT    420
         ||||||||||||||||||||||||||||||||||||||||||||||||||||||||||||
Seq_2    GTGAACGCTGAGGCGAAGGTCGTGGATGCTCAATGTACGGGGCTGCCGGCGGATAAGTAT    360

Seq_1    ACGCATGTGTTGACGGCTTTTGCTTTTATGATGATACCTGATGCGAGGGCTGCGATGAGA    480
          ||||||||||||||||||||||||||||||||||||||||||||||||||||||||||||
Seq_2    ACGCATGTGTTGACGGCTTTTGCTTTTATGATGATACCTGATGCGAGGGCTGCGATGAGA    420

Seq_1    GAATGCTTCCGTATCCTCCAGTCCGGGGGTGTACTTGCGACTTCGACGTGGAGGAATTCT    540
         ||||||||||||||||||||||||||||||||||||||||||||||||||||||||||||
Seq_2    GAATGCTTCCGTATCCTCCAGTCCGGGGGTGTACTTGCGACTTCGACGTGGAGGAATTCT    480

Seq_1    TCGTGGCTCGTCATCATGAAAGAAGCCATCGAAACCACGGCCTGGAACGTCAAGTTCCCC    600
         ||||||||||||||||||||||||||||||||||||||||||||||||||||||||||||
Seq_2    TCGTGGCTCGTCATCATGAAAGAAGCCATCGAAACCACGGCCTGGAACGTCAAGTTCCCC    540

Seq_1    ACCATGAAAGAGTTCCTGGCCTTGCATAACGAAGGCTGGGGCGACGAGTCTTTCGTGAAA    660
         ||||||||||||||||||||||||||||||||||||||||||| ||||||||||||||||||
Seq_2    ACCATGAAAGAGTTCCTGGCCTTGCATAACGAAGGCTGGGACGACGAGTCTTTCGTGAAA    600

Seq_1    GCTCGGTTCGAAGAGGAAGGGTTCGAAGATGTGGAAGTCACTGCTGTGCAGAGGGAGACC    720
         ||||||||||||||||||||||||||||||||||||||||||||||||||||||||||||
Seq_2    GCTCGGTTCGAAGAGGAAGGGTTCGAAGATGTGGAAGTCACTGCTGTGCAGAGGGAGACC    660

Seq_1    TCATTGACTATATCCGAATTCATGGAGGTCGGTGGAGGAATGATCCCCATTGTGACCGGT    780
         ||||||||||||||||||||||||||||||||||||||||||||||||||||||||||||
Seq_2    TCATTGACTATATCCGAATTCATGGAGGTCGGTGGAGGAATGATCCCCATTGTGACCGGT    720

Seq_1    GCCTTTTGGACACCCGAGCAGCGGGAGAAGTATGAGGCGAAGGCACCGGTGGTGATCAGG    840
         ||||||||||||||||||||||||||||||||||||||||||||||||||||||||||||
Seq_2    GCCTTTTGGACACCCGAGCAGCGGGAGAAGTATGAGGCGAAGGCACCGGTGGTGATCAGG    780

Seq_1    GAGTATCTGGAGGAGAAGTTTGGAGCTGATGGGGTGATTAGGATGGAGCCGGTGGCTGTT    900
         ||||||||||||||||||||||||||||||||||||||||||||||||||||||||||||
Seq_2    GAGTATCTGGAGGAGAAGTTTGGAGCTGATGGGGTGATTAGGATGGAGCCGGTGGCTGTT    840

Seq_1    CTTGCGGTGGGGAGAAAGCCCTAG    924
         ||||||||||||||||||||||||
Seq_2    CTTGCGGTGGGGAGAAAGCCCTAG    864
```

Figure 5.11: Alignment of the sequence of *MT-II* cDNA within the pEX-N-GST vector with the sequence predicted from BLAST. Alterations of residues are highlighted in yellow.

```
Identities: 286/287 (99 %)

Predicted     ------------------------------MTPKISPSSYLTPAFVSRYHLAEKLTGVFV    30
Sequenced     GDHPPKSDIIPTTENLYFQGAIAGAPDLKLMTPKISPSSYLTPAFVSRYHLAEKLTGVFV    60
                                             ******************************

Predicted     APLVQHSGILSTPSNKPMAVFDNACGLGIVSSYLNSTLPEDVKRHWTLTCGDITELMVEY    90
Sequenced     APLVQHSGILSTPSNKPMAVFDNACGLGIVSSYLNSTLPEDVKRHWTLTCGDITELMVEY    120
              ************************************************************

Predicted     TKLRIEREGWVNAEAKVVDAQCTGLPADKYTHVLTAFAFMMIPDARAAMRECFRILQSGG    150
Sequenced     TKLRIEREGWVNAEAKVVDAQCTGLPADKYTHVLTAFAFMMIPDARAAMRECFRILQSGG    180
              ************************************************************

Predicted     VLATSTWRNSSWLVIMKEAIETTAWNVKFPTMKEFLALHNEGWDDESFVKARFEEEGFED    210
Sequenced     VLATSTWRNSSWLVIMKEAIETTAWNVKFPTMKEFLALHNEGWGDESFVKARFEEEGFED    240
              ****************************************** ****************

Predicted     VEVTAVQRETSLTISEFMEVGGGMIPIVTGAFWTPEQREKYEAKAPVVIREYLEEKFGAD    270
Sequenced     VEVTAVQRETSLTISEFMEVGGGMIPIVTGAFWTPEQREKYEAKAPVVIREYLEEKFGAD    300
              ************************************************************

Predicted     GVIRMEPVAVLAVGRKP    287
Sequenced     GVIRMEPVAVLAVGRKP    317
              *****************
```

Figure 5.12: MT-II protein sequence translated from cloned cDNA. Sequencing was performed on a commercial basis from Source Bioscience Sequencing, Ireland. This figure shows that the cloned DNA for *MT-II* (Sequenced, underlined in red) is in frame with the N-terminal GST tag (yellow). The pEX-N-GST vector (underlined in green) shows the location of the TEV cleavage site (blue).

One of the observed amino acids was not as predicted (Table 5. 2). This change may indicate non-conserved aspects of the gene or they may be due to errors introduced during the amplification of the cDNA by PCR.

Table 5.2: Sequence of residue that result in a different protein sequence between the predicted protein sequence from BLAST (CBS 513.88) and the actual sequenced strain (CBS 513.88)

Predicted (BLAST)		**Sequenced (clone MT-II)**	
Residues	Amino Acid	Residues	Amino Acid
GAC	Aspartic Acid (D)	GGC	Glycine (G)

5.2.3.4 Expression and purification of MT-II-GST

Detection of the recombinant MT-II expression in *E. coli* was carried out by induction using IPTG followed by SDS-PAGE and Western Blot analysis. Small scale cultures were induced and grown for 3 h in LB, with samples taken pre-induction and each hour post-induction. Western blot resulted in an approximate molecular mass of 58.9 kDa, which was expected of the recombinant MT-II-GST, only in the insoluble fraction of the lysates (Figure 5.13).

In order to improve MT-II solubility, the cultures were grown on Terrific Broth and induced with IPTG for 12 h (25 ^{o}C). One ml samples were removed before induction with IPTG and after 12 h induction. These extracts were subjected to SDS-PAGE and Western blot analysis (Figure 5.14). Both SDS-PAGE and Western showed the presence of MT-II-GST at the correct molecular mass, 58.9 kDa. Soluble recombinant MT-II was observed on lane 4.

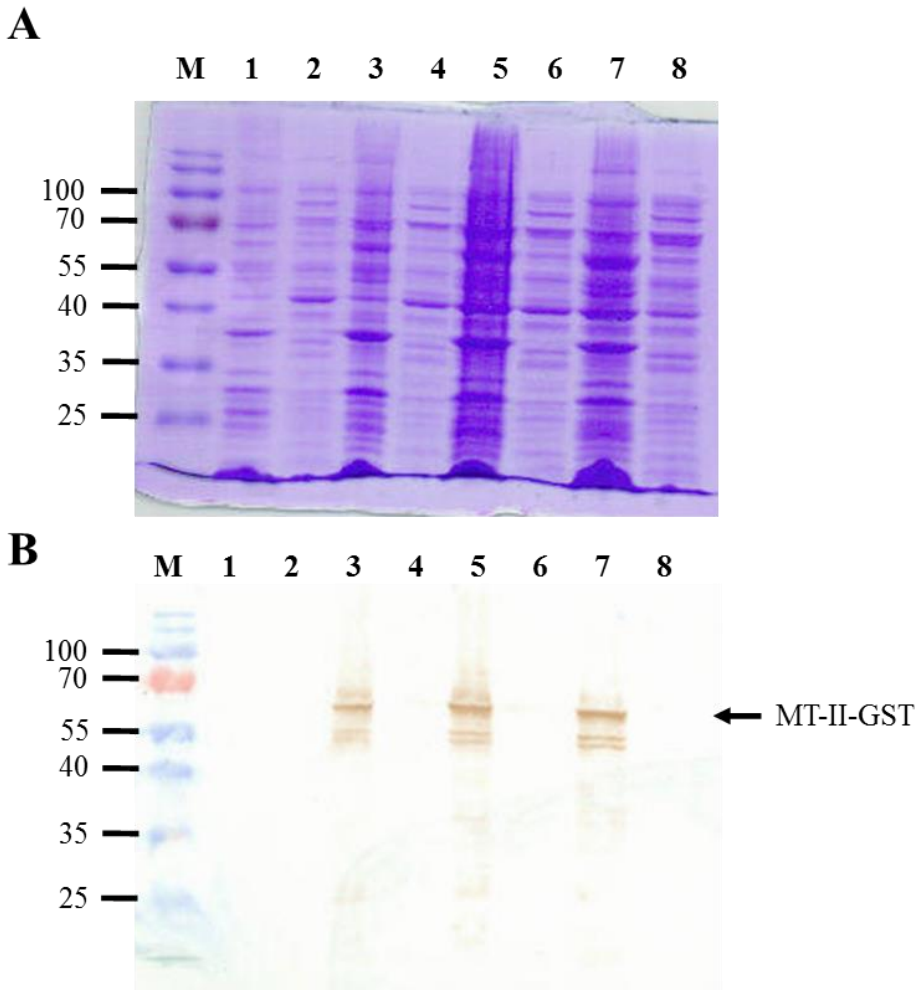

Figure 5.13: Expression and solubility evaluation of recombinant MT-II grown in LB. SDS-PAGE **(A)** and Western Blot **(B)** analysis of MT-II. Lane M: Protein molecular mass marker. Lane 1: Un-induced cells, pellet fraction (insoluble). Lane 2: Un-induced cells, supernatant fraction (soluble). Lane 3: Induced cells (1 h), pellet fraction (insoluble). Lane 4: Induced cells (1 h), supernatant fraction (soluble). Lane 5: Induced cells (2 h), pellet fraction (insoluble). Lane 6: Induced cells (2 h), supernatant fraction (soluble). Lane 7: Induced cells (3 h), pellet fraction (insoluble). Lane 8: Induced cells (3 h), supernatant fraction (soluble).

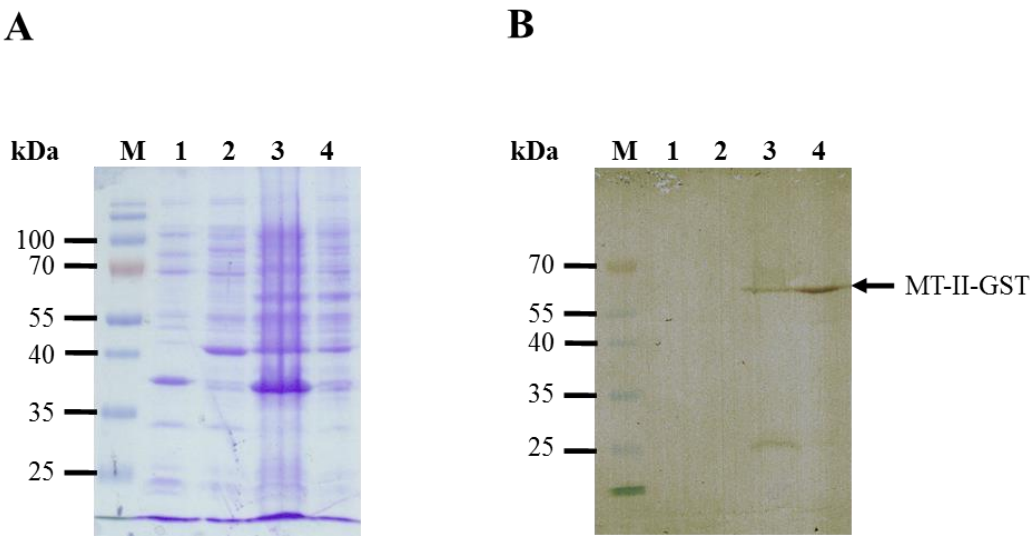

Figure 5.14: (A) SDS-PAGE and **(B)** Western blot analysis of recombinant MT-II (rMT-II) solubility. Lane M: Protein molecular mass marker. Lane 1 and 2 contain the un-induced cells (insoluble and soluble fraction, respectively); Lane 3 and 4 contain the induced cells (12 h) (insoluble and soluble fraction, respectively).

The soluble fraction containing the recombinant MT-II-GST, was subjected to GSH-Agarose affinity chromatography using an AKTA Purifier-100 (Figure 5.15) (Section 2.2.17.2). The optical density was monitored throughout the purification at 280 nm. GST tagged MT-II binds to the GSH ligand and impurities are removed by washing with buffer (until low mAUs observed). Recombinant MT-II was eluted under mild, non-denaturing conditions (elution buffer: 10 mM reduced glutathione in 50 mM Tris-HCl, pH 9).

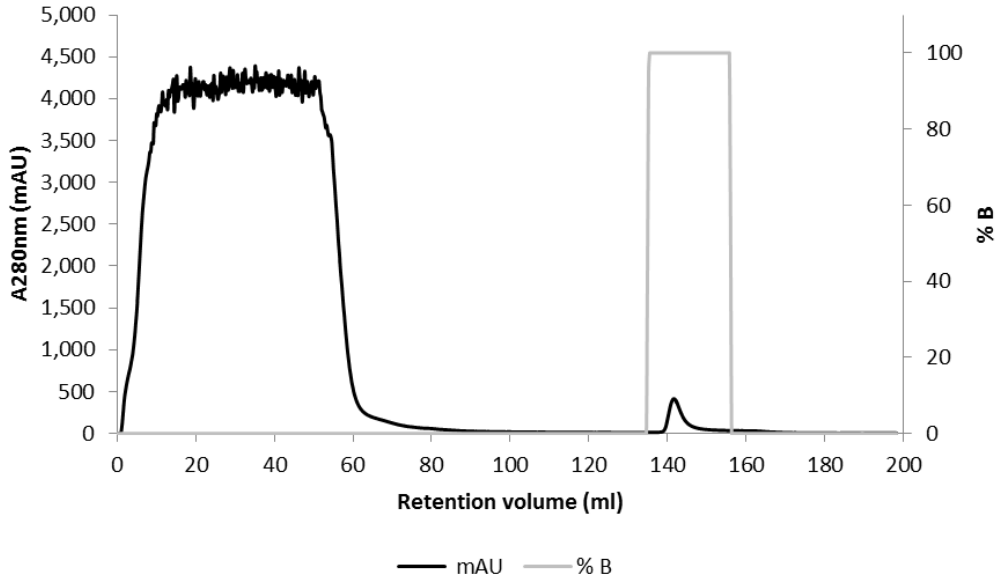

Figure 5.15: AKTA purification of MT-II-GST protein purified by GSH-agarose affinity chromatography. The *E. coli* induced lysates (soluble fraction) (~ 200 ml) were allowed to bind the column at a flow rate of 1 ml/min, and the flow through was collected over 1 h period on ice. The column was washed with PBS until the mAUs dropped to 0 – 10 and the MT-II-GST protein was eluted in one ml fractions with elution buffer (% B). The recombinant MT-II-GST protein eluted as a concentrated peak spanning 4x one ml fractions.

Protein purity was assessed by SDS-PAGE and LC-MS/MS analysis of digested MT-II-GST protein. Peptides (8 % coverage) corresponding to an UbiE/COQ5 family methyltransferase (An02g03100) were identified (Figure 5.16).

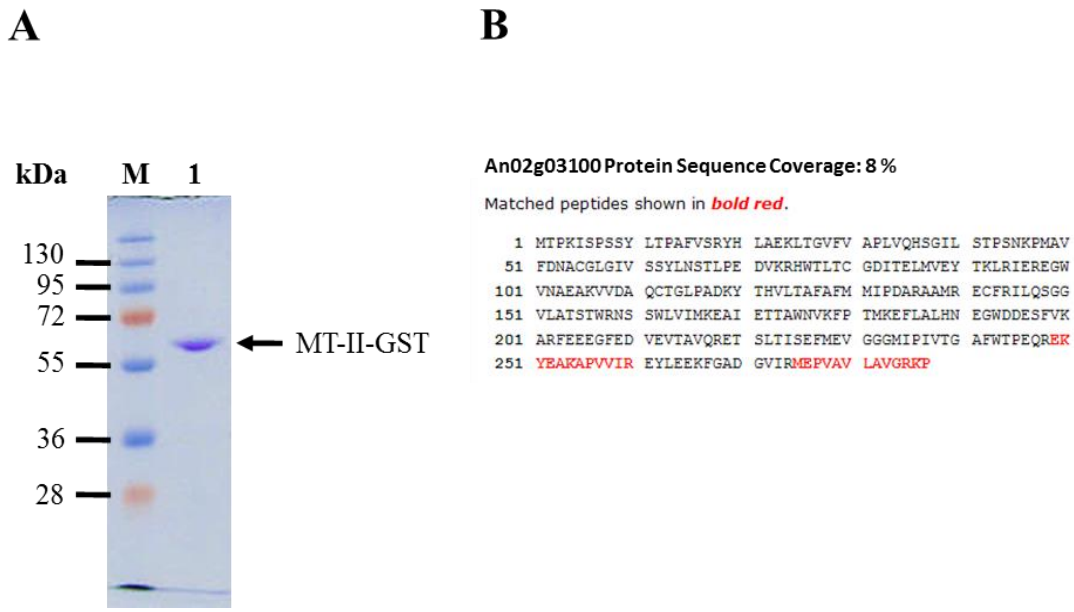

Figure 5.16: (A) SDS-PAGE analysis of MT-II-GST protein. Lane M contains the molecular weight marker. Lane 1 contains the purified MT-II-GST. **(B)** Confirmation of identity by LC-MS/MS analysis (8 % sequence coverage)

5.2.4 Assessment of MT-II activity

5.2.4.1 SAM MTase Assay using recombinant MT-II

GT *bis*-thiomethylation was carried out as per Section XZ with modifications: reduced GT (1 mg/ml; 2 µl) and SAM (5 mg/ml; 3 µl) were used as substrates of the reaction catalysed by MT-II-GST (30 pmol/reaction) (Figure 5.17). After 3 h reaction time (unless stated otherwise), products were analysed by LC-MS/MS (Section 2.2.10.2).

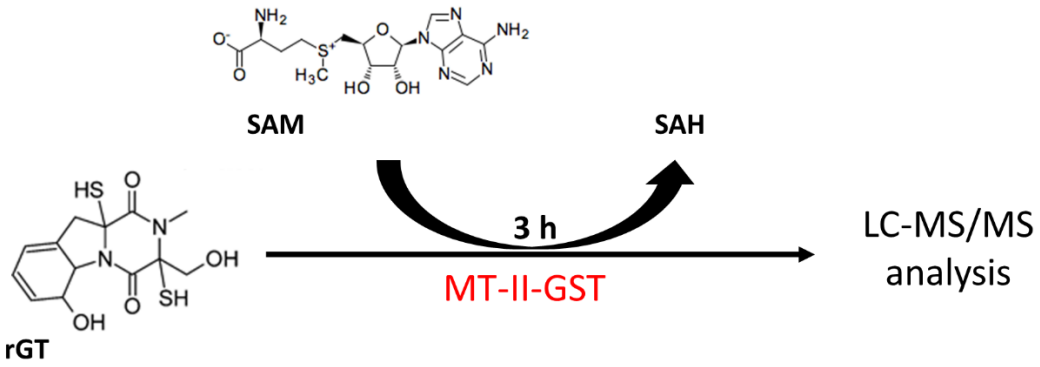

Figure 5.17: Schematic representation of the LC-MS/MS based in vitro rGT methylation assay using MT-II-GST.

In order to measure the generation of gliotoxin methyl derivatives, standard curves for GT and BmGT were constructed as per Section XZ (Figure 5.18). The standards were prepared at a concentration range of 20 – 1.25 µg/ml. A linear relationship occurs between the concentration of GT and BmGT and the area intensity. The standard curves were used in subsequent assays to calculate the amount of GT, MmGT and BmGT in MT-II-GST catalysed reactions. In order to measure MmGT,

known levels of GT and BmGT obtained from the standard curves after 3 h reaction time were subtracted from the initial gliotoxin concentration (20 µg/ml).

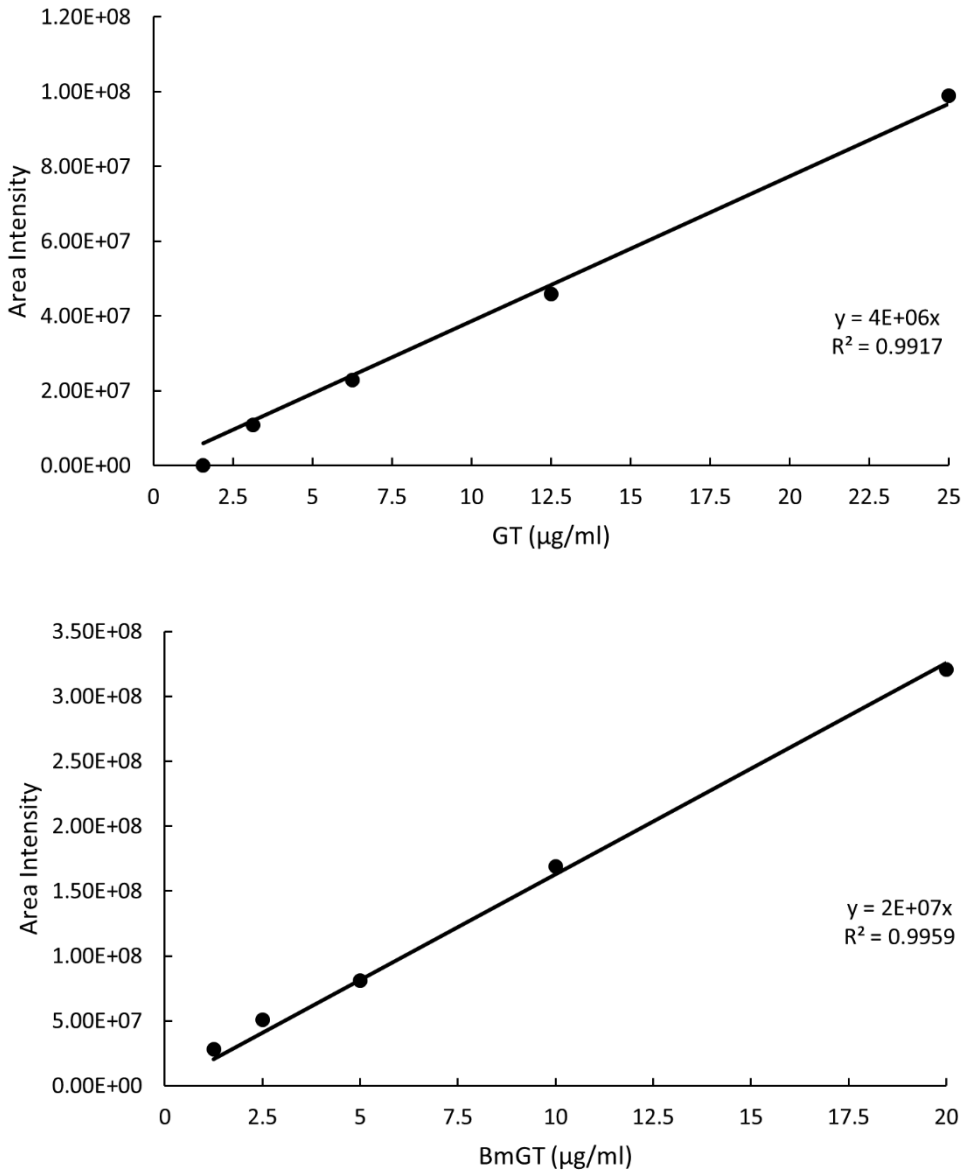

Figure 5.18: GT and BmGT standard curves. **(A)** Standard curve prepared for the measurement of GT. **(B)** Standard curve prepared for the measurement of BmGT.

5.2.4.2 Biochemical characterization of MT-II

Figure 5.19 depicts how, *in vitro*, MT-II-GST progressively thiomethylates dithiol GT, using SAM as the methyl donor, through the sequential formation of MmGT and then BmGT. Indeed BmGT levels were highest after 3 h reaction time, compared to 1 h (43 % final) and 2 h (73 % final) (Figure 5.20).

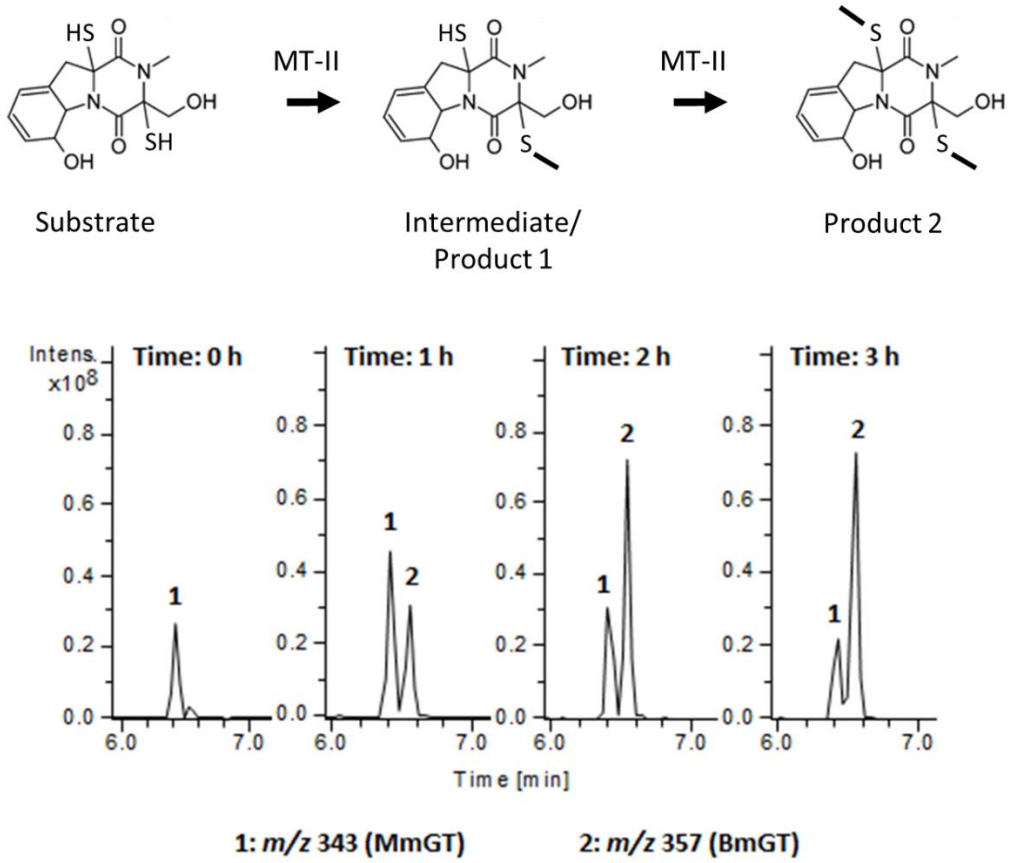

Figure 5.19: MT-II-GST mediates the progressive thiomethylation of rGT through the formation first of MmGT and then BmGT. EIC of *m/z* 343 (MmGT) and *m/z* 357 (BmGT) at different reaction times.

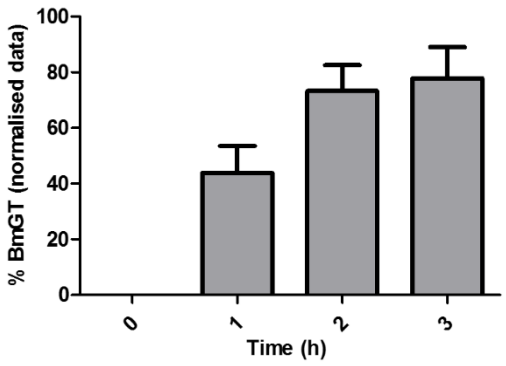

Figure 5.20: The effect of reaction time on MT-II catalysed -thiomethylation of rGT.

In order to further characterise recombinant MT-II, the capacity of this enzyme to methylate GT to MmGT and BmGT was investigated (enzyme concentration, reaction temperature, pH and inhibitors).

5.2.4.2.1 Characterization of BmGT formation by MT-II

To test the effect of temperature on MT-II activity, the SAM-MTase assay was carried out as in Section 2.2.9 with the samples incubated at 4 ºC, 20 ºC, 30 ºC, 37 ºC and 50 ºC. Generation of BmGT was optimal at 37 ºC, followed closely by 30 ºC. Reduced bis-thiomethylation was observed at 4 ºC, 20 ºC and 50 ºC (Figure 5.21). Investigation into the effect of pH on the activity of MT-II was also undertaken. Here, assays were carried out over a range of pH values; 3, 5, 7.5, 9 and 11. Results are shown in Figure 5.21 whereby it is clear that pH has an effect on the activity of MT-II with optimal BmGT formation occurring at pH 7.5.

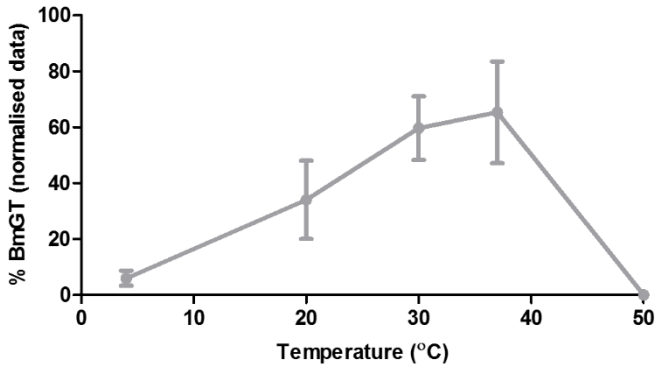

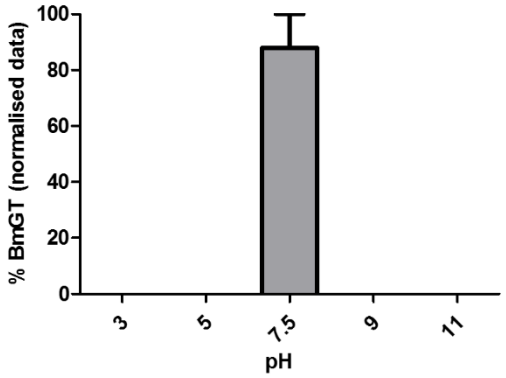

Figure 5.21: The effect of temperature **(A)** and pH **(B)**, on the conversion of GT to BmGT by MT-II.

For further optimization of the *bis*-thiomethylation of rGT by MT-II-GST, an evaluation into the affect of enzyme concentration was carried out. Figure 5.22 shows that BmGT formation is dependent on MT-II concentration, whereby 120 pmol/reaction resulted in approximately 90 % *bis*-thiomethylation. Reduced BmGT levels were observed at 30 pmol/reaction and 60 pmol/reaction compared to 120 pmol/reaction. Additionally, MmGT and BmGT levels were observed to decrease and

increase, respectively, and simultaneously, as the concentration of MT-II increased. This data could suggests that rGT methylation proceeds in a sequential manner, involving MmGT release and re-binding to MT-II. Finally and with the purpose of examining the affect of methyltransferase inhibitors, SAM-MTase assay was carried out as in Section 2.2.9 with the addition of increasing concentrations of SAH. Analysis of this data revealed that SAH inhibited BmGT formation in a concentration-dependent fashion, whereby a 2 fold molar excess of SAH over SAM led to a 74 % decrease in activity compared to SAH absence (Figure 5.23).

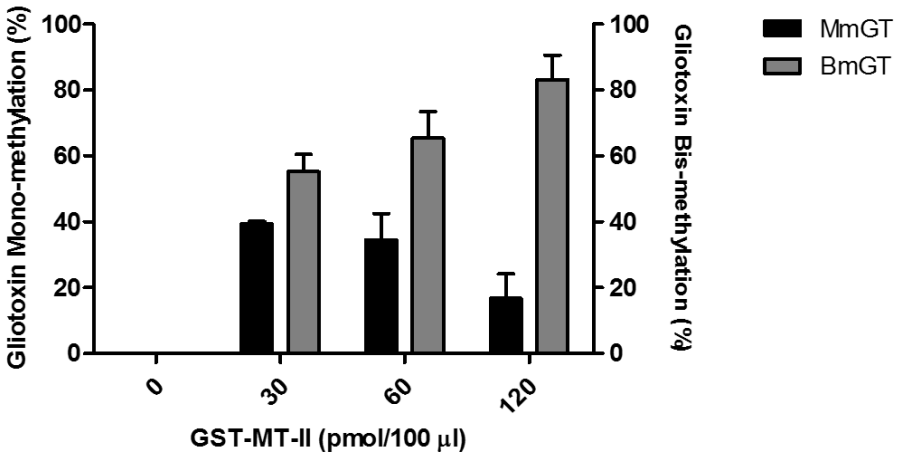

Figure 5.22: The effect of MT-II concentration on the ability to thiomethylate GT.

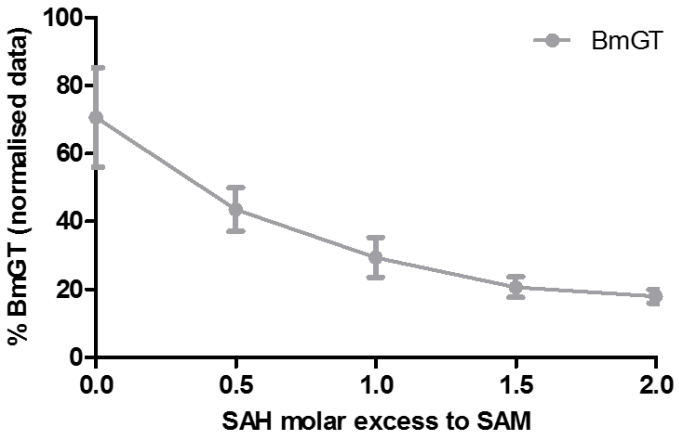

Figure 5.23: SAH inhibits MT-II catalysed BmGT formation in a concentration dependent fashion.

5.2.4.2.2 Characterization of MmGT formation by MT-II

Following the establishment of optimal conditions required for BmGT formation by MT-II, an evaluation of the effect of temperature, pH and enzyme concentration on MmGT formation was carried out. The SAM-MTase assay was carried as per Section XZ with minor modifications. rGT (2 µl; 1 mg/ml) and SAM (3 µl; 50 mg/ml) concentrations remained the same, however (i) MT-II concentration was used at 7.5 pmol/reaction (unless stated differently) and (ii) the reaction time was 15 min. The optimal reaction temperature and pH appeared to be 37 ºC and pH 7.5, respectively (Figure 5.24). The affect of increasing concentrations of enzyme on the rate of MmGT formation is shown in Figure 5.24. A progressive decrease and increase in the levels of GT and MmGT, respectively, indicate that mono-thiomethylation of gliotoxin is dependent on MT-II concentration.

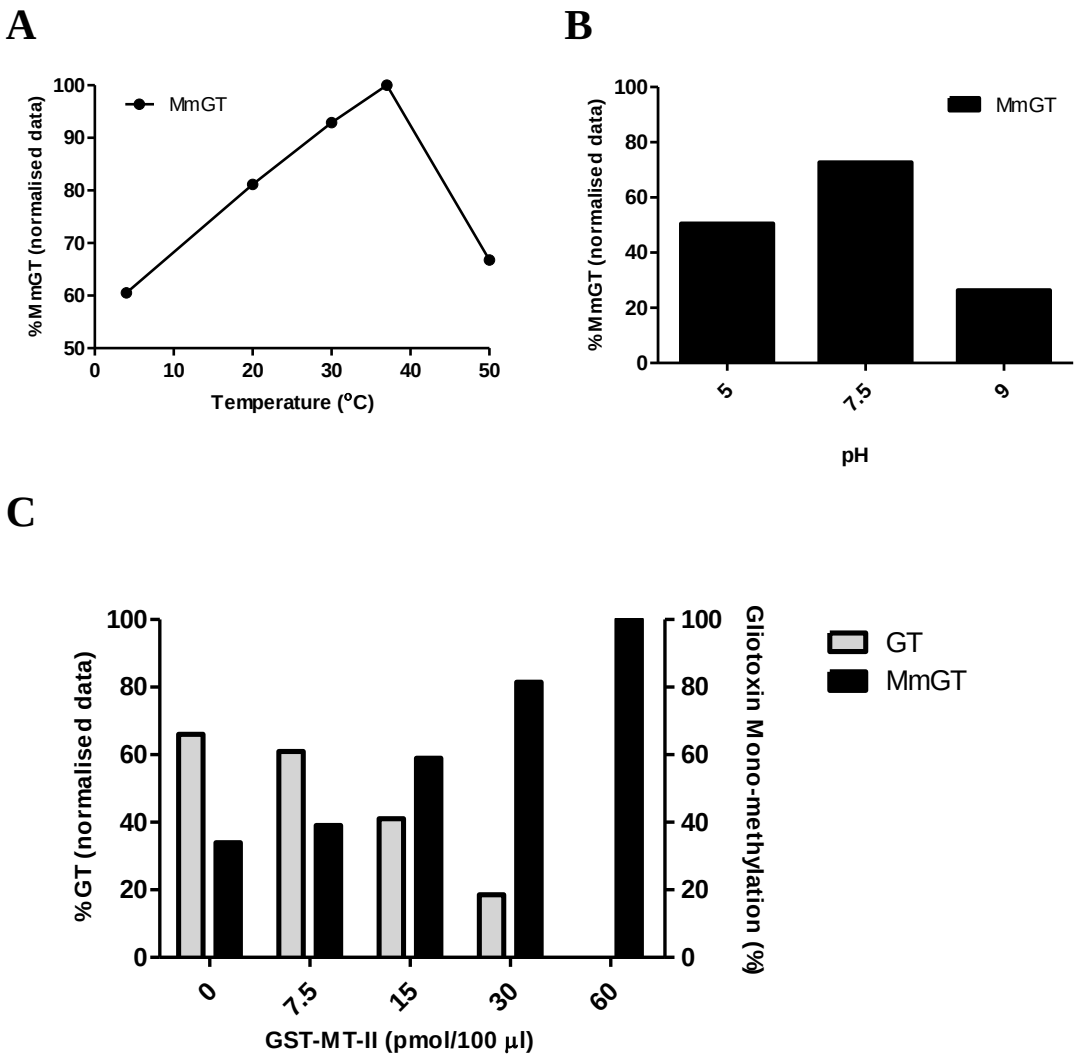

Figure 5.24: Biochemical analysis of recombinant MT-II-GST on the ability to mono-thiomethylate gliotoxin. **(A)** The affect of temperature and **(B)** pH, on the conversion of GT to MmGT by MT-II. **(C)** The affect of concentration on the conversion of GT to MmGT.

5.2.4.2.3 rGT methylation due to MT-II and not GST

The SAM-MTase assay was carried out as per Section XZ using a different GST-tagged protein (lipocalin-GST) as a negative control to confirm that there is no GST

interference. Figure 5.25 indicates that the dithiol GT used as a substrate for the reaction remains un-methylated, and there is no MmGT or BmGT detected in the resultant reaction mixture.

TEV-mediated cleavage of purified MT-II-GST was carried out following Section 2.2.17.3 (Figure 5.25). Pure MT-II was used as a positive control in the SAM-MTase assay. Figure 5.25 shows that pure MT-II *bis*-thiomethylates rGT using SAM as a methyl donor, as observed when used MT-II-GST.

A **B**

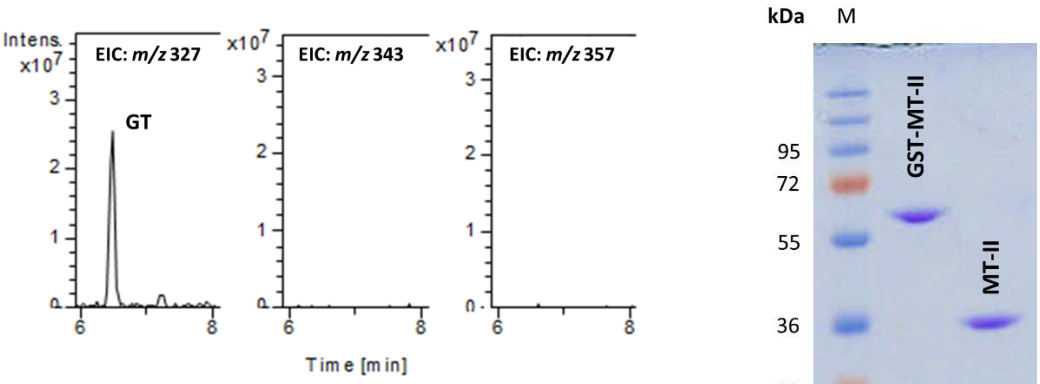

C

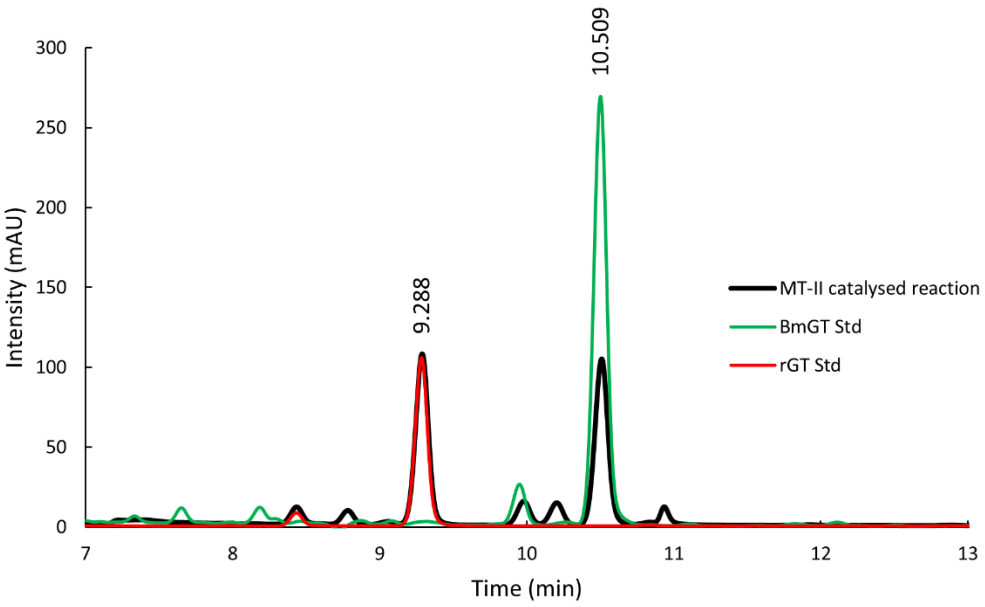

Figure 5.25: (A) GST-tagged lipocalin is unable to methylate rGT. **(B)** SDS-PAGE analysis of GST-MT-II before and after TEV cleavage. **(C)** Pure MT-II *bis*-thiomethylates rGT using SAM as a methyl donor.

5.2.5 Genetic manipulation of *MT-II* gene within *A. niger*

The generation of *A. niger* Δ*MT-II* was performed by Dr. Özlem Sarikaya-Bayram through the course of this work. A summary of this is provided in Section 2.2.19 and Section 5.2.5.1. Screening for the Δ*MT-II* phenotype following transformation was part of this work and is described in Section 5.2.5.2.

5.2.5.1 Generation of *MT-II* disruption constructs and fungal transformation

Deletion of *MT-II* in *A. niger* was undertaken in order to assess functionality of the recombinant MT-II. *A. niger* N593 strain (which is a uridine auxotroph) was used in this study for inactivation of *MT-II*, as *A. niger* CBS 513.88 proved refractory to transformation.

Diagnostic PCRs on MT-II transformants (Section 2.2.19) were performed with OFM65/46 (Table 2.14) for in-locus cassette control, and OFM70/71 (Table 2.14) for *MT-II* ORF amplification (Figure 5.26). Results show amplification of in-locus deletion cassette (2712 bp) in Δ*MT-II* confirming gene deletion and the absence of this band in the WT (Figure 5.26).

A

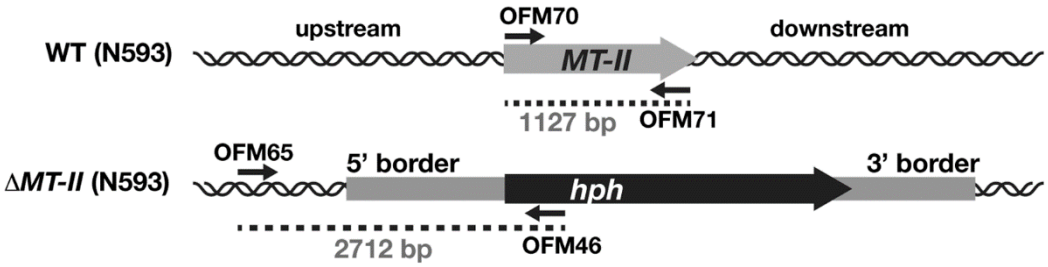

B

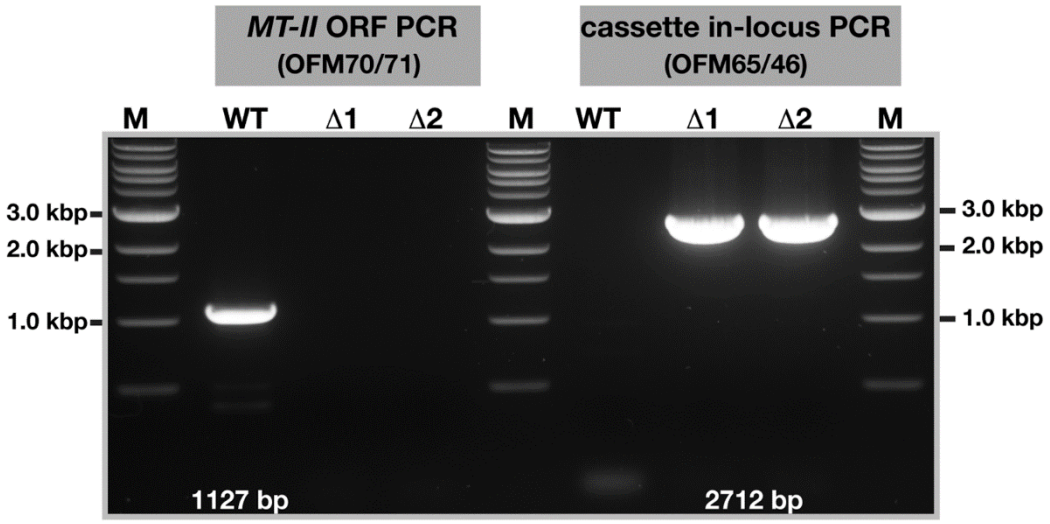

Figure 5.26: (A) A comparative depiction of the *MT-II* WT and *MT-II* deletion loci in *A. niger* N593 strain. OFM70/71 amplifies *MT-II* open reading frame (ORF). OFM65/46 only amplifies in-locus deletion cassette. Grey shades indicate the border of deletion cassette used for gene replacement/transformation. OFM65 binds 310 bp upstream of hygromycin (*hph*) cassette 5' border. **(B)** Gel electrophoresis confirmation of MT-II deletion by diagnostic PCR. Δ1 and Δ2 represent two independent *MT-II* knock-out strains. Only Δ1 was used for further experiments. MT-II ORF (1127 bp) is amplified from WT and missing in Δ1 and Δ2. OFM65/46 amplifies in-locus deletion cassette (2712 bp). 50 ng genomic DNA was used as template for PCR reactions.

5.2.5.2 *A. niger ΔMT-II* acquires a GT hypersensitivity phenotype

Availability of the *A. niger* Δ*MT-II* mutant lead to the comparative metabolite analysis against the *A. niger* WT (N593). Both strains were grown in TM liquid cultures (Section 2.1.2.5.4) for 45 h prior exposure to exogenous gliotoxin (2.5 μg/ml) for 3 h. Supernatants (6 ml) were extracted from the cultures at time 0 and 3 h after gliotoxin addition. Organic extractions of supernatants were generated according to Section 2.2.7. Sample extracts (WT versus Δ*MT-II*) were analysed by RP-HPLC (Section 2.2.8.3). A BmGT commercial standards was also analysed by RP-HPLC in order to obtain their retention times to facilitate the identification of these metabolites in the samples (Figure 5.27). Comparative PR-HPLC analysis revealed that BmGT is not produced in *A. niger* Δ*MT-II* culture supernatants after 3 h gliotoxin addition. However BmGT is observed as a peak with a retention time of 10.490 min in the WT culture supernatants after 3 h exposure to GT (Figure 5.27). Overall, comparison of both strains revealed the presence of GT at time 0 and the presence of BmGT only in WT cultures at time 3 h (Figure 5.28). This data indicates that Δ*MT-II* is unable to thiomethylate exogenously added GT and further confirms that MT-II is responsible for in vivo formation if BmGT in *A. niger*.

A. niger Δ*MT-II* was investigated for an altered phenotype in the presence of gliotoxin. *A. niger* WT (N593) and Δ*MT-II* were grown on TM (Section XZ). Δ*MT-II* growth was significantly ($p < 0.0001$) reduced under GT addition compared to wild-type (Figure 5.29), which strongly infers that MT-II has a protective function against exogenous GT.

A

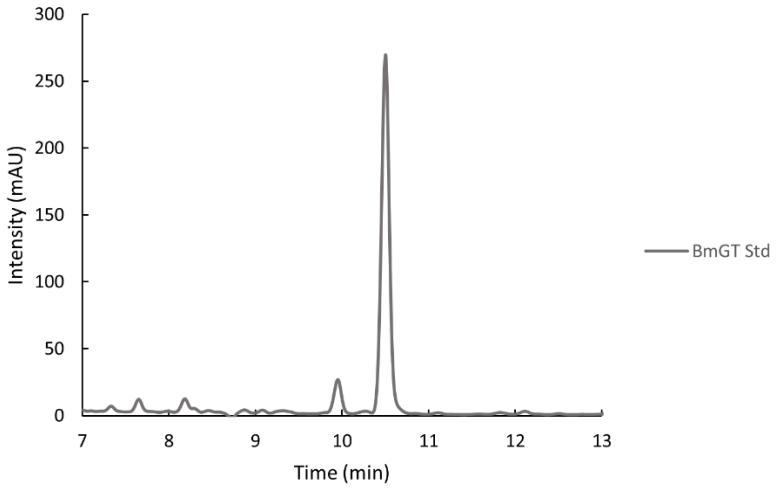

B

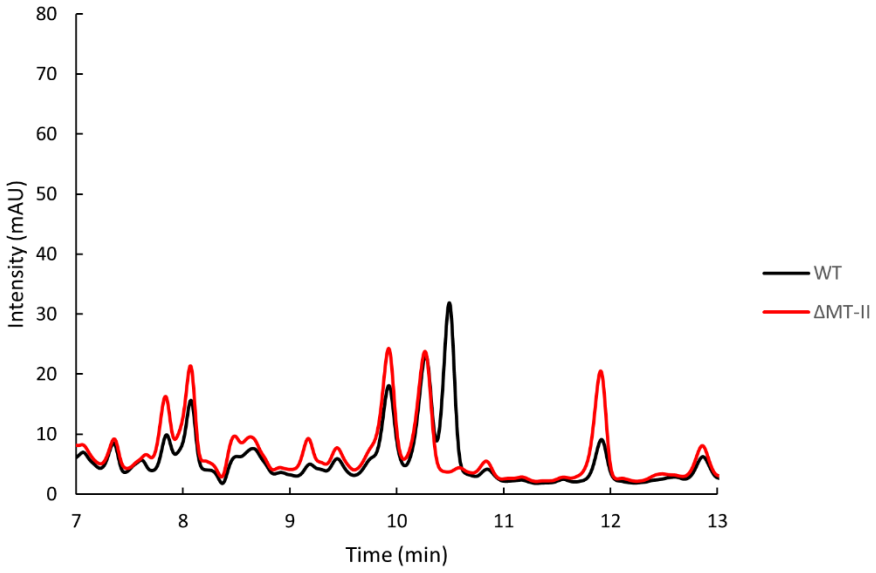

Figure 5.27: (A) HPLC chromatogram of BmGT standard (grey; R_T: 10.501 min) detected at a wavelength of 280 nm. **(B)** HPLC chromatogram of organic extracts from *A. niger* WT (black) and Δ*MT-II* (red) supernatants after 3 h gliotoxin exposure, overlaid. BmGT (R_T: 10.490) was identified in the WT culture supernatant but was not found in Δ*MT-II*.

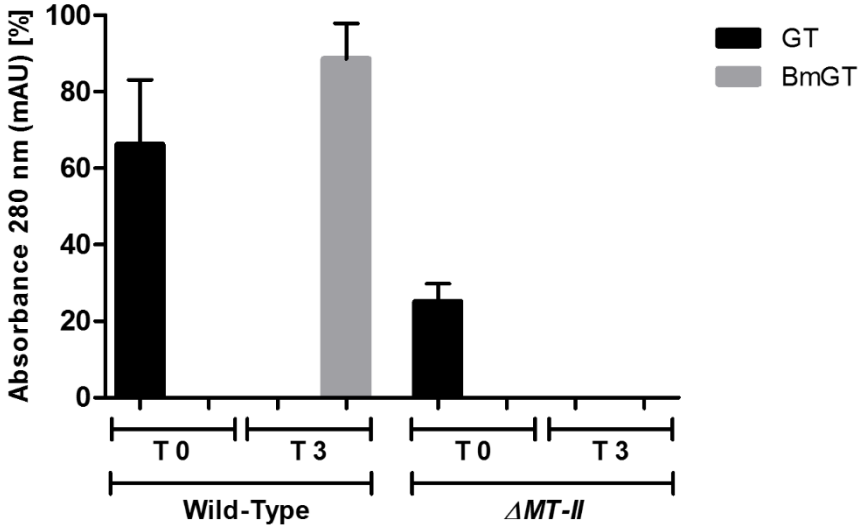

Figure 5.28: In vivo *bis*-thiomethylation does not occur in Δ*MT-II* compared to wild-type. Graphical representation of Figure 5.27 at time 0 h and 3 h.

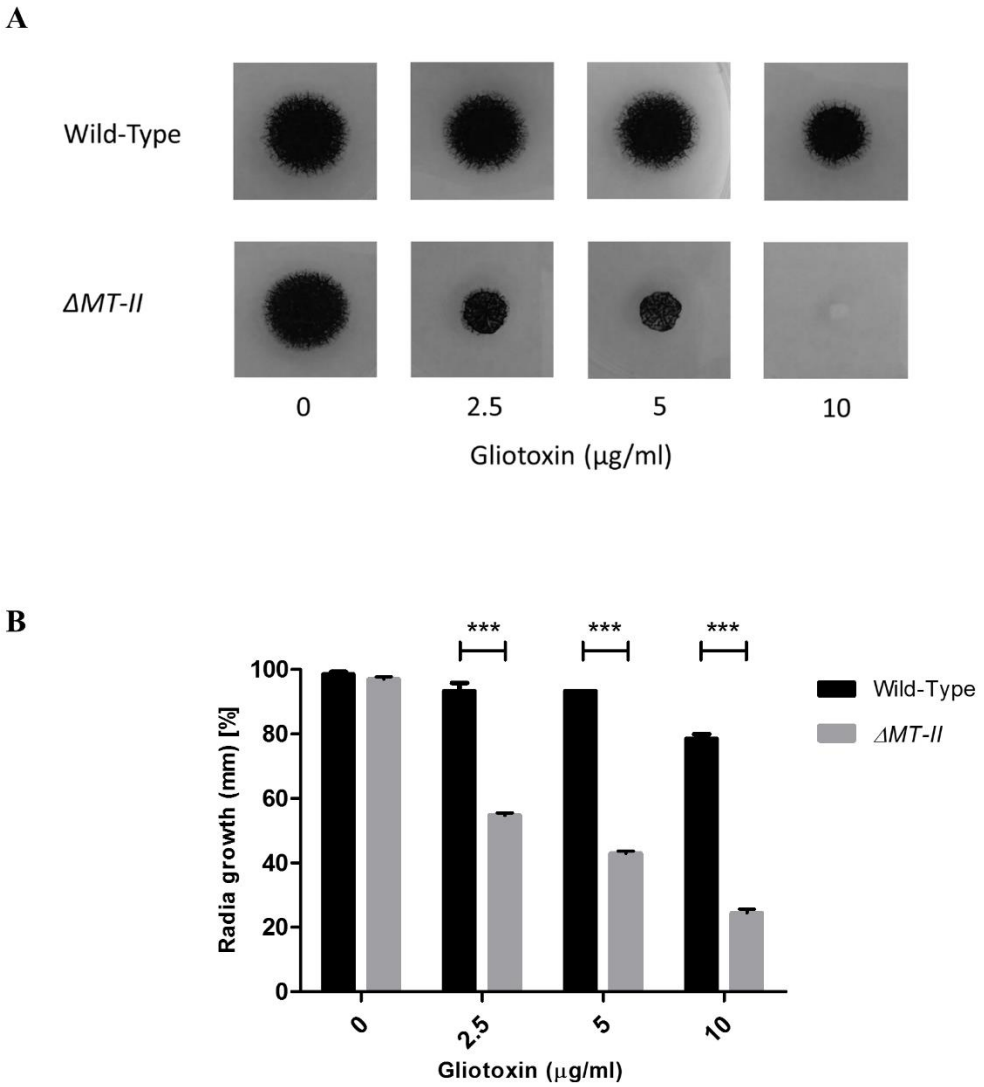

Figure 5.29: (A) Phenotypic assay reveals that Δ*MT-II* is highly sensitive to GT compared to wild-type. **(B)** Graphical representation of phenotypic analysis shown in Figure A.

5.3 Discussion

Overall, work described in this Chapter shows the identification and characterization of a putative SAM-dependent MTase, MT-II, in *A. niger*. Furthermore, MT-II biological function was assessed through the generation of an *A. niger* Δ*MT-II* mutant that was shown to be inhibited in the presence of exogenous GT, thus confirming the role MT-II has in protection against GT reactive thiols. This is the first demonstration of a fungal SAM-MTase involved in the defence against GT and not regulation (as observed in Dolan et al. (2014)), of a GT-naïve fungus (*A. niger*).

The methylation of GT by *Aspergillus* species which are unable to biosynthesise this toxin has been observed once in *A. nidulans*, however, no methyltransferase was ever associated to the process (Scharf et al., 2014). Here, we confirm the *in vivo bis*-thiomethylation of exogenous GT by *A. niger*, which is another fungi unable to biosynthesise GT. Thus, GT fed to *A. niger* in liquid cultures must enter the cells in order to be methylated, and the resulting BmGT product is released into the media. *A. nidulans* was also observed to *bis*-thiomethylate exogenous GT, further emphasizing the ability of GT-naïve fungi to carry out this modification.

Recent mechanisms for analysing methylation of small molecules by SAM-dependent methyltransferases are based on continuous photometric analysis (Figure 5.30). These assays are based on the action of SAH nucleoside, which catalyses the conversion of SAH into adenine and *S*-ribosylhomocysteine (Figure 5.30). The adenine product is then converted to hypoxantine by adenine deaminase, leading to an absorbance decrease at 265 nm that can be detected by UV spectrophotometry (Figure 5.30) (Aktas and Narberhaus, 2009; Dorgan et al., 2006). These assays do not require

the reaction to be stopped thus are referred as continuous assays, however they are unable to distinguish multiple methylations of the same substrate.

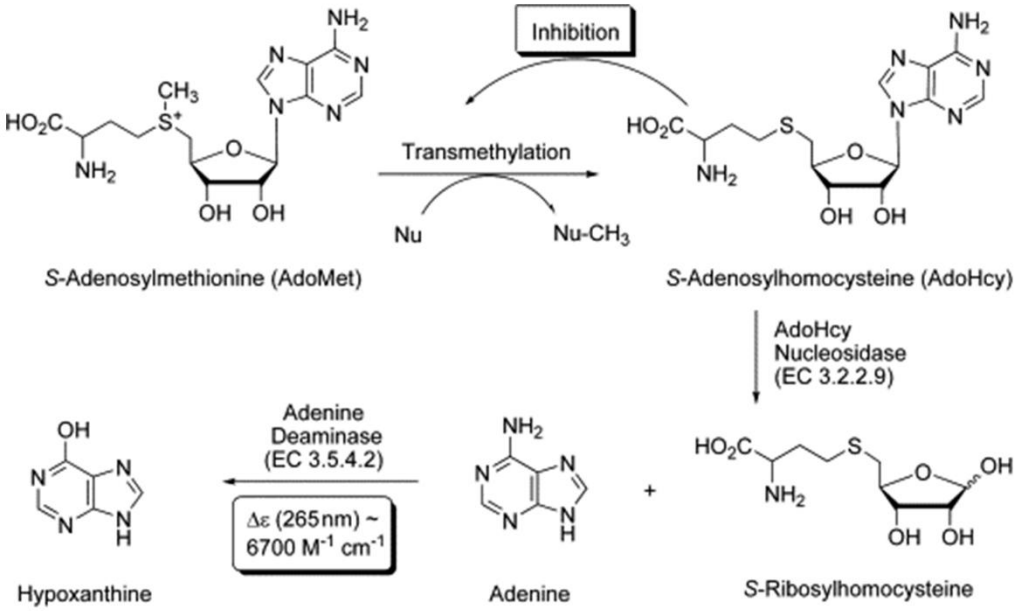

Figure 5.30: Scheme of continuous SAM dependent MTase assays based on spectrophotometric analysis. Image obtained from (Dorgan et al., 2006).

Reduced GT contains two thiol groups that can be potentially methylated by SAM-methyltransferase activity. The development of the SAM-MTase assay allowed the use of several catalysts (*A. niger* protein lysates and MT-II-GST) and a wider product detection (MmGT, BmGT). Using this assay, it was observed that methylation of rGT occurred only when *A. niger* lysates obtained from GT induced cultures were used. On the contrary, no methylation was observed using *A. niger* lysates obtained from MeOH control cultures. These results imply the induction (under GT exposure) of an enzyme able to catalyse the methylation of this toxin.

Since MT-II is the closest homologue to *A. fumigatus* GtmA (Dolan et al., 2014), MT-II was selected as the best candidate protein to carry the thiomethylation of GT. qRT-PCR for *MT-II* in *A. niger* showed increased expression of *MT-II* under GT conditions compared to MeOH control. Interestingly, and in correlation with the proteomic data described in Chapter 3, MT-II was shown to be up-regulated in an *A. niger* library in response to stress agent, DTT (MacKenzie and Guillemette, 2005). In agreement with this observation, qRT-PCR for *MT-II* in *A. niger* showed an increase expression of *MT-II* proportional to the concentration of DTT. DTT is routinely used to stabilize enzymes and proteins that contain free thiol groups as it reduces disulphide bonds and maintains proteins in a reduced state. Coiner et al. (2006) observed that enzyme assays aimed at investigating the methylation activity of an *O*-methyltransferase CrSMT1 using flavonoids and caffeic acid as substrates revealed no transmethylation activity. Interestingly, high background levels of transmethylation activity were observed when no substrate was added in the reaction. These authors showed that CrSMT1 was able to methylate the DTT present in the reaction mixture as the enzyme stabilizer and led to the characterization of the enzyme as a *S*-methyltransferase with high affinity towards benzene and furfuryl thiols (Coiner et al., 2006).

MT-II was recombinantly expressed in order to assess functionality and biochemically characterise the enzyme. Using the SAM-MTase assay, the enzymatic products of MT-II were identified as MmGT and BmGT. Thus, MT-II catalyses the sequential methylation at both thiol groups of dithiol GT, whereby MmGT is the first product and acts as an intermediate for the *bis*-thiomethylation reaction, and BmGT is the final product (Figure 5.31).

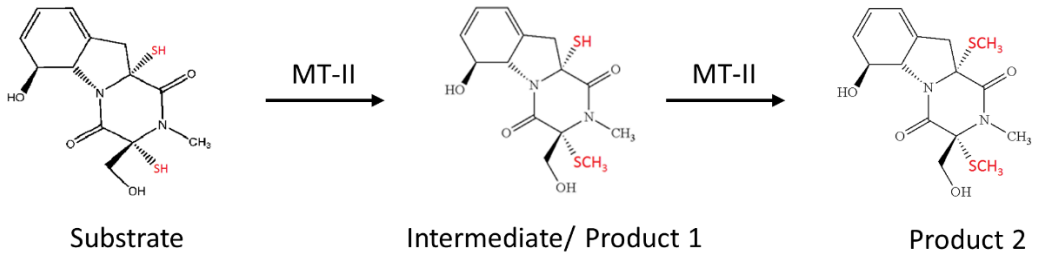

Figure 5.31: Proposed model for the methylation of rGT by MT-II. Progressive methylation at a thiol group of rGT (1st) and MmGT (2nd) by MT-II in *A. niger*.

Initially, the ability of MT-II to *bis*-thiomethylate dithiol GT was investigated. MT-II displayed optimal activity at 37 ºC, followed closely by 30 ºC. Further to this, investigation into the effect of pH was also necessary. Interestingly, BmGT was only observed at pH 7.5. In agreement with the results obtained for *A. niger* MT-II, recombinant cysteine methyltransferase (CMT) from *Saccharomyces cerevisiae* also displayed the same optimum temperature and pH (Sengupta et al., 2014).

A concentration course study of MT-II-GST was also carried out to investigate the extent of BmGT formation. 100 % conversion of rGT to BmGT was observed after 3 h incubation using MT-II-GST at 120 pmol/reaction (Figure 5.32). The increase in BmGT formation correlated with the increase in the amont of MT-II. Furthermore, analysis of MT-II activity was examined in the presence of an MTase inhibitor. It was observed that addition of SAH into the reaction mixture inhibited generation of BmGT, and that this inhibition increased at higher SAH levels. This is in full agreement with the fact that SAH acts as a competitor for SAM utilization, therefore preventing MT-II to bind its methyl donor (Hendricks et al., 2004)

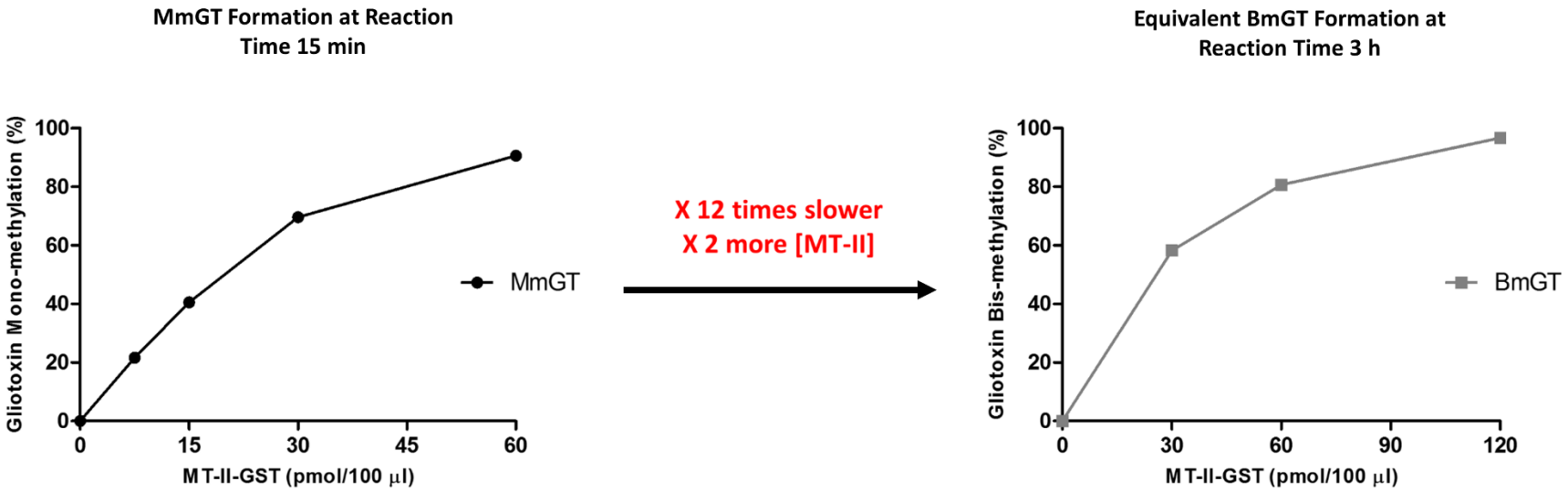

Figure 5.32: Comparative MmGT (left) and BmGT (right) formation at different times, and also amounts of MT-II-GST. Diagrams related to Figure 5.22 (BmGT) and 5. 24 (MmGT).

Studies on GT have described that modifications like methylation of the thiol groups renders this metabolite inactive (Gardiner et al., 2005). Thus, it is feasible to hypothesise that MT-II inactivates dithiol GT by methylating both thiols. Through the characterization of MT-II, generation of a *mono*-thiomethyl derivative (MmGT) was observed at shorter reaction times and lower enzyme concentrations indicating that when there is enzyme limitation, only one methyl group is incorporated into GT. This observation led to the characterization of MT-II on the ability to *mono*-thiomethylate GT. Though the temperature and pH were in correlation with those observed for generating BmGT, the time of reaction (15 min) and concentration of enzyme (7.5 pmol/reaction) was much shorter and lower, respectively (Figure 5.32). It thus appears that *mono*-methylation by MT-II is a much faster reaction compared to *bis*-thiomethylation and that this subsequent activity results in a progressive incorporation of methyl groups (Figure 5.32) (Dolan et al., 2014).

Despite MmGT contains a reactive free thiol that can potentially reduce the bioactivity of proteins, it is a possibility that MT-II naturally behaves as a *mono*-methyltransferase rather than a *bis*-methyltranferase, and that due to the structure of gliotoxin, biologically needs to methylate both thiols. Figure 5.32 shows that ~100 % MmGT formation is reached after 15 min reaction time using MT-II at 60 pmol/reaction while it takes 3 h and double the amount of enzyme to reach full BmGT formation. Overall, *mono*-thiomethylation of GT by MT-II occurs 12 times faster compared to *bis*-thiomethylation.

As described in the Introduction, in plants, the biological function of thiol methyltransferases cTMT1 and PpSABATH1, has been associated with the detoxification of xenobiotics (Attieh et al., 2000a, 2000b; Zhao et al., 2012). In *A.*

fumigatus, however, GtmA has been demonstrated to play a role in the *bis*-thiomethylation of endogenously produced GT which in turn attenuates GT biosynthesis (Dolan et al., 2014). Due to the absence of the GT biosynthetic machinery in *A. niger*, we hypothesise that MT-II is responsible for the detoxification of xenobiotic thiols, and that specifically it represents an ancient defence strategy against ETP-producing fungi occupying identical environmental niches as *A. niger*. To support this hypothesis, an *in vivo bis*-thiomethylation analysis was carried out in *A. niger* WT and Δ*MT-II* and was observed that the mutant was unable to methylate exogenous GT. Furthermore, *A. niger* Δ*MT-II* was more sensitive to exogenous GT compared to wild-type and thus positions this enzyme as a requirement for *A. niger* survival in the presence of thiol containing toxic metabolites.

Chapter 6

Diagnostic strategies for the detection of siderophore secreting microorganisms

6 Chapter 6: Diagnostic strategies for the detection of siderophore secreting microorganisms

6.1 Introduction

6.1.1 Aspergillus fumigatus and Invasive Aspergillosis (IA)

Aspergillus fumigatus is a ubiquitous fungus with a saprophytic lifestyle in soil and decaying organic matter (Latge, 1999). *A. fumigatus* displays characteristic traits that position this fungus as a fundamental part of the nutrient recycling ecosystem and as a human opportunistic pathogen (Rhodes, 2006). One of these traits is the capacity to withstand temperatures over 50 ºC like those encountered in decaying vegetation (Dagenais and Keller, 2009) and to germinate and grow efficiently at 37 ºC which is required to infect mammalian hosts (Rhodes, 2006). Another characteristic is the ability to sense and utilize different carbon and nitrogen sources that contribute to its role as a saprophyte and as a pathogen (Rhodes, 2006). The primary mode of reproduction of *Aspergillus spp*. is asexual, whereby small spores (2 -3 μm diameter) named conidia are released from the conidiophores and dispersed in the environment (Latge, 1999). The size of these spores is ideal for infiltrating deep into the alveoli (Dagenais and Keller, 2009). Due to the ubiquity of *A. fumigatus*, the average person will inhale at least serval hundred conidia per day (Latge, 1999).

An infection caused by an *Aspergillus* species is termed aspergillosis and *A. fumigatus* is the major causative agent (Latge, 1999). Depending on the immune status of the person, any environmental strain of *A. fumigatus* can be pathogenic (Debeaupuis et al., 1997). Immunocompromised individuals including those with tuberculosis, leukemia and transplant patients are the most at risk of infection. There are three main forms of aspergillus-related lung disease which include allergic, saprophytic and

invasive disease (Al-Alawi et al., 2005). Invasive aspergillosis (IA) is the most serious form of the disease, with mortality rates between 40-90 % depending on the site of infection and treatment program applied (Lin et al., 2001). IA is normally observed in the lungs but it can disseminate to other organs like the brain, liver, kidney, gut, sinuses and skin (Barton, 2013).

In healthy individuals, when conidia are inhaled the pulmonary immune system prevents the colonization of the respiratory system (Balloy and Chignard, 2009). This involves (i) the mucociliary system and respiratory epithelial cells which ensure the clearance of conidia and hyphae and (ii) alveolar macrophages and neutrophils that phagocytose conidia (Arnold and Griffin, 2014). Hyphae cannot be phagocytosed as they are too big and instead neutrophils release chemicals that damage hyphae (ROS) and starve the fungi from necessary nutrients (Arnold and Griffin, 2014). Thus, the presence of spores in immunocompetent hosts is innocuous and only when innate immunity is dysfunctional, can the spores develop and invade the body (Balloy and Chignard, 2009; Dagenais and Keller, 2009).

6.1.2 Current Diagnosis of Aspergillosis

The high mortality rate associated to IA makes early diagnosis a critical factor to improve patient survival (von Eiff et al., 1995). Early diagnosis appears complex with current methods where a lack of specificity and sensitivity is persistent.

The main approaches to laboratory diagnosis include direct microscopy, histopathological examination of biopsy material, cell culture, antigen or antibody detection and DNA detection (Barton, 2013). Direct microscopy is a simple method involving the examination of specimens under the microscope that inherently lacks specificity as hyphae seen may be from different filamentous fungi (Barton, 2013;

Johnson et al., 2014). Additionally, hyphal structures can only be observed if present in abundance and consequently at a late stage of infection (Johnson et al., 2014). Histological examination of biopsy material involves demonstrating tissue invasion by a filamentous fungus, which has two major drawbacks. First, obtaining tissue samples is often contraindicated due to the medical risks associated with the disease (e.g. low platelet count) and second, identifying fungi from mycelium of tissue sections requires culturing the fungus from the same specimen to confirm a positive diagnosis (Barton, 2013; Johnson et al., 2014). An advantage of culturing *Aspergillus* spp. is that other than giving a diagnosis it can be further used to test for antifungal resistance or susceptibility. However this diagnostic strategy is very slow (5 – 7 days), requires a biopsy of a sterile site and specialised expertise for species determination (Johnson et al., 2014).

Less invasive methods of diagnosing IA commercially available include the Platelia® *Aspergillus* (Bio-Rad, France) ELISA test and the β-D-glucan EIA (Fungitell). Both are based on the detection of fungal cell wall antigens using different strategies. The Platelia® test detects galactomannan (GM), a polysaccharide present in most *Aspergillus* and *Penicillium* species (Latgé et al., 1994). This test is a sandwich ELISA where monoclonal antibody (EB-A2) detects the β-(1, 5)-linked galactofuranoside side-chain residues of the galactomannan molecule (Stynen et al., 1995). EB-A2 needs to bind four or more galactofuranoside epitopes for detection to occur, thus secreted antigens with fewer epitopes will not be detected and might compromise the sensitivity of the assay (Mennink-Kersten et al., 2004). Additionally, cross-reactivity with other filamentous fungi, bacteria or drugs has been observed while antifungal therapy causes a decrease in the sensitivity of GM (Marr et al., 2005).

1,3 β-D-glucan (BDG) has a wider distribution in the fungal kingdom (*Aspergillus* spp, *Candida* spp, *Fusarium* spp and *Acremonium* spp) than GM which can obstruct the specificity of diagnosis (Hope et al., 2005). Like GM, BDG appears as a circulating antigen in patients with IA, however was found to be non-antigenic (Johnson et al., 2014; Lehmann and Reiss, 1978). Alternatively, BDG detection is based on its ability to activate a coagulation cascade of serine proteases in the lysates of horseshoe crabs (*Limulus polyphemus*) amoebocytes. Serine protease (factor G) of the cascade can then cleave a synthetic chromogenic substrate that generates a product detectable by spectrophotometry (Barton, 2013). Though this assay might constitute a potential diagnostic method the lack of specificity and formal guidelines translates in a low implementation in the clinical practice.

Similarly, PCR detection as a diagnostic strategy is limited by the lack of standardization and validation procedures which restricts its widespread application as a diagnostic tool (Hope et al., 2005; Steinbach, 2013).

These drawbacks have led in an effort to develop more reliable, robust and rapid methods to diagnose IA.

6.1.3 The potential of metabolites as biomarkers of infection

The ability of *Aspergillus spp*. to produce a wide range of extracellular metabolites and enzymes has been the base for recent research, at least in part due to a potential increase in specificity through the absence of cross-reactive epitopes in patient samples (Johnson et al., 2014).

One of these secretory enzymes is gliotoxin oxidoreductase (GliT) which has immunoreactivity with non-neutropenic patient sera and shows no homology with

human or other fungal proteins (Shi et al., 2012b). The potential of GliT as a diagnostic marker was used by Shi et al. (2012a) where they developed an ELISA using recombinant GliT as the coating antigen and anti-GliT antibodies for detection. Despite GliT was detected in serum samples from infected animals and patients with IA and showed more sensitivity than the GM test it was unable to detect GliT early in the infection (Shi et al., 2012a).

Since gliotoxin is present in the sera of IA infected patients the potential as a biomarker of infection has been proposed (Fox et al., 2004; Puri et al., 2009). Further research has considered GT derivative, BmGT, as a more reliable marker of IA since it was found more frequently than GT in samples from patients at risk of IA but not in serum from healthy donors or neutropenic patients with no signs of infection (Domingo et al., 2012).

Research has considered the role iron has as a nutrient during infection. Under these conditions, the mammalian immune system limits iron availability in infected areas of the hosts or areas exposed to environmental microbes (Ganz, 2009). Pathogens like *A. fumigatus* have developed strategies to acquire iron from the host under iron-limiting conditions. One strategy involves the biosynthesis of siderophores, which are low molecular mass iron chelators that balance the acquisition and storage of iron. *A. fumigatus* has two intracellular siderophores named hyphal ferricrocin and conidial hydroxyferricrocin that distribute and store iron and two extracellular siderophores known as Fusarinine C (FusC) and Triacetylfusarinine C (TAFC) that mobilize extracellular iron (Schrettl and Haas, 2011) (Figure 6.1).

A **B**

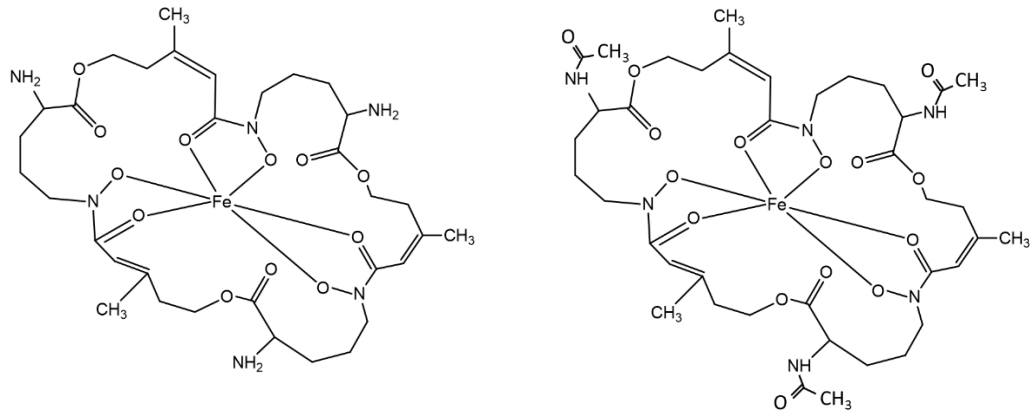

Figure 6.1: Structure of ferrated **(A)** Fusarinine C (FusC) and **(B)** TAFC.

Genes that are required for the biosynthesis of intracellular and extracellular siderophores were identified by Schrettl et al. (2007). Starting from the same precursor, L-ornithine, SidA catalyses the first step on the biosynthesis of both intracellular and extracellular siderophores (Schrettl et al., 2004). After this first step, the pathway splits in two where SidF, SidD and SidG lead to the synthesis of FusC and TAFC and SidC catalyses the formation of ferricrocin (Figure 6.2) (Schrettl et al., 2007). It was observed that deletion of genes encoding the biosynthesis of extracellular siderophores (Δ*sidF* and Δ*sidD*) decreased growth, conidiation and resistance to oxidative stress under iron limitation (Schrettl et al., 2007). Δ*sidA*, eliminates the entire siderophore system and results in the avirulence of *A. fumigatus* as shown in a murine model of IA (Hissen et al., 2005). Additionally, a decrease in growth and survival of *A. fumigatus* was observed after phagocytosis by murine alveolar macrophages when defects in the siderophore system occur (Schrettl et al., 2010c). HapX is a bZIP-type

regulator that positively affects siderophore production in *A. fumigatus*. *A. fumigatus* Δ*hapX* was used to infect mouse models of IA and appeared to attenuate virulence compared to wild type (Schrettl et al., 2010a).

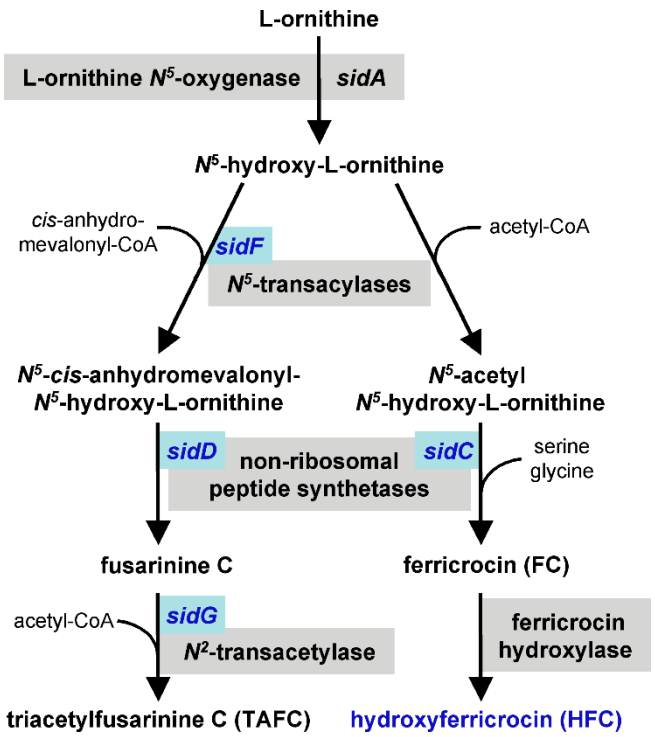

Figure 6.2: *A. fumigatus* siderophore biosynthetic pathway. Obtained from Schrettl et al. (2007).

The utility of siderophores as diagnostic markers was tested by Petrik et al. (2010) using ^{68}Gallium (Ga) to label TAFC as a potential radiopharmaceutical for IA detection. Due to the similar characteristics of ^{68}Ga to those of Fe^{3+}, TAFC was able to chelate ^{68}Ga (68Ga-TAFC) and when injected into mice models, appeared to be excreted in urine in non-infected mice while on the IA rat model, ^{68}Ga-TAFC appeared to accumulate in the infected lung tissue (Petrik et al., 2010). This research shows the utility of siderophores as biomarkers of IA and has led to the development of other diagnostic tests to detect this analytes (Doyle et al., 2011).

The aims of this Chapter were to (i) develop an ELISA based diagnostic method for the detection of FusC and to (ii) validate this assay with biological samples.

6.2 Materials and Methods

6.2.1 Materials

6.2.1.1 Minimal Media without Iron

6.2.1.1.1 Trace Elements without Iron

$Na_2B_4O_7 \cdot 10H_2O$ (40 mg), $CuSO_4 \cdot 5H_2O$ (400 mg), $MnSO_4 \cdot 10H_2O$ (800 mg), $Na_2MoO \cdot 2H_2O$ (800 mg) and $ZnSO_4 \cdot 7H_2O$ (8 g) were dissolved in order in 800 ml of distilled water. A few drops of concentrated HCl were added to maintain the solution. Solution was then then brought to 1 L with distilled water.

6.2.1.1.2 L-Glutamine (0.3 M)

L-Glutamine (43.8 g) was dissolved in 800 ml distilled water. The pH was adjusted to 6.5 and the final volume was brought up to 1 L. The solution was filter sterilised and stored at room temperature.

6.2.1.1.3 Minimal Media

Salt solution (50X, 20 ml) (Section 2.1.2.4.2), glucose (10 g) and trace elements without iron (1 ml) (Section 6.2.1.1.1) were added to 800 ml distilled water and dissolved. The pH was adjusted to 6.5 and made up to 1 L with distilled water. The solution was autoclaved at 105 ºC for 30 min. Filter sterilised L-glutamine (66.3 ml) (Section 6.2.1.1.2) was added to the solution. The solution was stored at room temperature.

6.2.1.1.4 MM Agar

Agar (9 g) (Fisher Chemical) was added to 500 ml of MM Liquid media (Section 6.2.1.1.3), before it was autoclaved at 105 ºC for 30 min. The solution was

allowed to cool to ~ 50 ºC before being poured (25 ml) into 90 mm sterile Petri dishes, under sterile conditions. The plates were allowed to set and stored at 4 ºC.

6.2.1.2 Solvent A: 0.1 % (v/v) Trifluoroacetic Acid (TFA)

TFA (20 µl) was added to 20 ml of distilled water. Solution was prepared fresh on the day.

6.2.1.3 2.24 M $FeSO_4 \cdot 7\ H_2O$

$FeSO_4 \cdot 7\ H_2O$ (1.56 g) was dissolved in deionised water (2.5 ml). The solution was prepared fresh on the day of use.

6.2.1.4 Carbonate coating buffer

6.2.1.4.1 250 mM Sodium Carbonate (Na_2CO_3)

Na_2CO_3 (10.6 g) was dissolved in 350 ml of distilled water. The solution was stirred and brought to 400 ml with distilled water.

6.2.1.4.2 250 mM Sodium Hydrogen Carbonate ($NaHCO_3$)

$NaHCO_3$ (16.8 g) was dissolved in 700 ml of distilled water. The solution was stirred and brought to 800 ml with distilled water.

6.2.1.4.3 5 X Carbonate Coating Buffer

To 250 mM $NaHCO_3$ solution (800 ml) (Section 6.2.1.4.2) add 250 mM Na_2CO_3 solution (Section 6.2.1.4.1) until pH is adjusted to 9.6. The solution was stored at 4 ºC.

6.2.1.4.4 1 X Carbonate Coating Buffer

5 X Carbonate Coating Buffer (20 ml) (Section 6.2.1.4.3) was added to 80 ml distilled water. This solution was prepared immediately prior to use.

6.2.1.5 Blocking solution

Sucrose (10 g) and BSA (1 g) were added to 80 ml 1 X Carbonate Coating Buffer (Section 6.2.1.1.4). This solution was stirred until everything was dissolved and brought to 100 ml with 1 X Carbonate Coating Buffer (Section 6.2.1.4.4). The solution was prepared immediately before use.

6.2.1.6 ELISA Stop Solution

H_2SO_4 (28.4 ml) was added to 972 ml of distilled water and stored at room temperature.

6.2.1.7 Clinical samples

Normal human serum samples were obtained from the Irish Blood Transfusion Service (IBTS). Infected human serum samples were supplied by Prof. Anna-Maria Eis-Hübinger (Bonn, Germany). Dr Thomas F. Patterson (University of Texas) supplied normal, uninfected and infected samples of guinea pig as part of an NIH-funded initiative to combat IA.

6.2.2 Methods

6.2.2.1 Iron-free glassware

Glassware used for culturing in iron-deplete conditions was treated with 1 mM EDTA overnight. After treatment with EDTA, flasks were rinsed with concentrated

HCl (20 ml) for a few minutes to remove iron. Finally flasks were washed several times with deionised water to remove traces of HCl.

6.2.2.2 *A. fumigatus* growth, maintenance and storage

A. fumigatus ATCC 46645 was maintained on MM agar plates (Section 6.2.1.1.4). A sterile inoculation loop was used to seed conidia onto agar plates from conidial stocks. Plates were incubated at 37 ºC for 5-7 days with periodic checking until fully grown. Conidia were harvested from agar plates by adding sterile PBST (Section 2.1.9) onto the plate and rubbing the surface with an inoculation loop to dislodge the conidia. Harvested conidia were centrifuged at 3000 rpm for 15 min and washed again with sterile PBS (10 ml) (Section 2.1.8). Harvested conidia were stored at 4 ºC until required.

6.2.2.3 *A. fumigatus* growth for siderophore production

A. fumigatus ATCC 46645 harvested conidia was used to inoculate 100 ml of iron free MM (Section 6.2.1.1.3). The cultures were incubated for 72 h, at 37 ºC, with constant shaking at 200 rpm. The cultures were then filtered through Miracloth and the supernatant was collected into 50 ml falcons. The mycelial mass was discarded and the collected supernatants were snap-frozen in liquid nitrogen until needed. Prior to use for siderophore purification, supernatant was filtered using 0.22 µm filter units.

6.2.2.4 FusC purification

A C_{18} Sep-Pak column (Waters Corp.) was removed from the packaging and placed into a holder over a 50 ml beaker. The column was first wetted with 100 % methanol (6 ml), followed by equilibration with solvent A (6 ml) (Section 6.2.1.2). *A. fumigatus* filtered supernatants (50 ml) (Section 6.2.2.3) were added to the Sep-Pak

and allowed to flow. Once all the supernatant has been loaded (50 ml), the column is washed with Solvent A (6 ml) (Section 6.2.1.2) and eluted with 100 % Acetonitrile (2 ml). Elution was collected in four 1.5 ml Eppendorf tubes (500 µl/tube). Finally, the tubes were placed in a Speedivac (Thermo Scientific) and dried under vacuum and centrifugation. Samples were checked regularly until most of the acetonitrile was evaporated and they were pooled together until complete dryness. Once the samples were dry, they were resuspended in MilliQ water and stored at -20 ºC until required.

6.2.2.5 RP-HPLC detection of FusC

Purified FusC (Section 6.2.2.4) was diluted 1/10 in H_2O and loaded (20 µl) on a C_{18} RP-HPLC column (Agilent Zorbax Eclipse XBD-C18, 4.6 x 150 mm). Gradient elution was performed by Solvent A consisting of 0.1 % (v/v) TFA in 99.9 % HPLC grade water (Sigma-Aldrich) and Solvent B consisting of 0.1 % (v/v) TFA in 99.9% acetonitrile (Sigma-Aldrich).

Table 6.1: RP-HPLC Gradient for FusC detection.

Time	% B
0	5
5	5
16	55
19	100
21	5

6.2.2.6 FusC quantification

FusC concentration was measured using the method of Schrettl et al. (2010b) with modifications. Overall, FusC was saturated with $FeSO_4 \cdot 7\ H_2O$ (Section 6.2.1.3)

and measured photometrically using a molar extinction factor of 2996/440 nm ($M^{-1}cm^{-1}$) (Schrettl et al., 2010a). Purified FusC (20 µl) (Section 6.2.2.4) was added to deionised water (980 µl) and this dilution was named S1. A control (C1) was prepared by transferring 1 ml of deionised water to a plastic cuvette and this was used to blank at 440 nm. The A_{435nm} of the iron-free sample (S1) was measured. Subsequently S1 was saturated by the addition of 2.24 M $FeSO_4 \cdot 7\ H_2O$ (Section 6.2.1.3) to give S2. The solution was inverted and left for 5 min and room temperature for the FusC to bind to the iron. At this stage a characteristic colour change can be clearly observed. S2 was diluted to ensure absorbance is in the range of 0.2 – 1.8. A negative control/blank was prepared by the addition of 10 µl of 2.24 M $FeSO_4 \cdot 7\ H_2O$ (Section 6.2.1.3) to deionised water (1 ml) (C2). C2 was transferred to a 1 ml plastic cuvette and this control solution was used to blank at 435 nm. The A_{435nm} of the saturated sample (S2) was measured. The concentration of FusC (µg/ml) was determined using the following equations:

$$[\text{FusC}]\text{M} = \frac{\text{A435nm S2}}{2996} \times \text{Dilution Factor}$$

$$\frac{[\text{FusC}]\mu\text{g}}{\text{ml}} = [\text{FusC}]\text{M} \times 1000 \times 789\text{g/mol}$$

Where 789g/mol is the molecular mass of ferrated FusC. The ratio between $FusC^{+Fe}/FusC^{-Fe}$ was used as a way to standardize inter-batch FusC quantification.

6.2.2.7 Immunoblotting

FusC dilutions and control samples were spotted (2 µl) onto a nitrocellulose membrane and allowed to dry. 5 % (w/v) Marvel in PBST was used to block the samples on the membrane and was left for 30 min at room temperature (RT). Blocker was then removed and anti-FusC antibody (Dr Natasha Gordon and Prof. Sean Doyle, unpublished) diluted 1/500 in 1 % (w/v) Marvel in PBST was added to the membrane and left for 30 min, shaking at RT. After incubation the membrane was washed twice with PBST and the anti-rabbit IgG-HRP conjugate (1/1000) diluted in 1 % (w/v) Marvel in PBST was added and left incubating for 30 min. Ultimately the membrane was washed twice with PBST and was resolved using DAB substrate buffer (Section 2.1.13.4).

6.2.2.8 FusC ELISA Plate Coating

Purified FusC (Section 6.2.2.4) was diluted to 0.7 µg/ml (unless stated otherwise) using the appropriate volume of 1 X Carbonate Coating Buffer (Section 6.2.1.4.4). Microtitre plates were coated with purified FusC (0.7 µg/ml) (100 µl) at 4 ºC overnight. Subsequently, the plates were washed 4 times with PBST (200 µl) (Section 2.1.8). Blocking solution (200 µl) (Section 6.2.1.5) was added to each well and incubated at 37 ºC for 2 h. The blocking solution was then removed from the wells and plates were left to dry overnight at 37 ºC. Once the plates were dry, they were sealed and stored in foil bags with desiccant at 4 ºC.

6.2.2.9 FusC-ELISA assay

6.2.2.9.1 FusC Standard Curve

Purified FusC was quantified (Section 6.2.2.6) and diluted in PBST (Section 2.1.9) to a concentration of 500 µg/ml which will be referred as 10 X calibrator, unless otherwise stated. FusC calibrator was diluted (10X; 500 µg/ml) 1/10 in PBST (Section 2.1.9) to obtain the top calibrator (50 µg/ml) (Table 6.2). Remaining FusC calibrators (150 µl each; 0 – 25 µg/ml) were prepared by serial dilutions of FusC top calibrator in PBST (Table 6.1).

Table 6.2: Recommended dilution and serial dilution procedures for preparation of calibrators.

FusC Calibrator (µl)	Diluent (µl)	Concentration (µg/ml)	Tube
30 of 10X Stock	270	50	T1
150 T1	150	25	T2
150 T2	150	12.5	T3
150 T3	150	6.25	T4
150 T4	150	3.125	T5
150 T5	150	1.56	T6
150 T6	150	0.78	T7
0	150	0	T8

6.2.2.9.2 Preparation of clinical samples obtained from Guinea Pigs

Urine, bronchoalveolar lavage (BAL) and serum samples were diluted 1/5 in sample diluent to a final volume of 100 µl.

6.2.2.9.3 Preparation of serum samples obtained from individuals

Serum samples were centrifuged to pellet cell debris and spiked with 50 µg/ml Proteinase K (final concentration of 2.5 µg/ml). Samples were incubated for 1 h at 56 ºC and then 10 min at 100 ºC to inactivate Proteinase K. Finally samples were centrifuged for 15 min at 13,000 x g and diluted 1/20 in sample diluent.

6.2.2.9.4 FusC-ELISA procedure

All samples (calibrators or diluted specimens (Section 6.2.2.9.1, Section 6.2.2.9.2 and Section 6.2.2.9.3)) to be assayed for FusC were assayed in the same manner. FusC coated ELISA plates (Section 6.2.2.8) were removed from the 4 ºC and brought to room temperature prior to use. ELISA was started by adding 50 µl of calibrators (0 – 50 µg/ml) or diluted specimens (i) to microtiter plates, followed by equivalent volumes (50 µl) of anti-FusC antibody, or (ii) co-incubated with equivalent volumes (50 µl) of anti-FusC antibody for 1 h, prior to addition to microplates. Following addition, incubate plates at room temperature for 1 h. After incubation for 1 h, plates were washed using PBST (4 times: 250 µl/well), followed by addition of anti-rabbit horseradish peroxidase conjugate (100 µl/well) for 1 h at room temperature. After conjugate removal and washing (4 times with PBST), excess wash buffer was removed by banging plates upside-down on tissue paper and using Tetramethylbenzidine (TMB) (MOSS, Inc.) substrate (100 µl/well) for 15 min, and then terminating the reaction by addition of Stop solution (100 µl/well) (Section 6.2.1.6). The absorbance was measured at 450/620 nm using a microtite plate reader and standard curves of A450/620nm versus log FusC concentration (0 – 50 µg/ml) constructed, from which the concentration of FusC in culture supernatants, normal or clinical specimens, of animal and human origin, was computed.

6.3 Results

The investigation of diagnostic strategies using siderophores as biomarkers of fungal infection was started by Dr. Natasha Gordon and Prof. Sean Doyle (Maynooth University), who generated several FusC conjugates and antisera to be used for the development of a FusC-ELISA (Enzyme-linked immunosorbent assay) (Doyle et al., 2011). A summary of this work is provided in Section 6.3.1 and Section 6.3.2. This Chapter will describe the generation of a competitive ELISA specific for FusC in an effort to bring this technology close to a commercial stage.

6.3.1 Development of a FusC immunogen

FusC was conjugated to Keyhole Limpet Hemocyanin (KLH) via N-hydroxysulfosuccinimidyl-4-azidobenzoate (sHSAB). KLH (3 mg) was reacted through the amine reactive NHS of sHSAB (3 mg) (approx. 2700 molar excess of sHSAB over KLH) for 1 h at room temperature in the dark and unbound cross-linker was removed using a G-25 PD10 column. Subsequently, sHSAB-KLH was photoactivatably crosslinked with FusC (1 mg) under UV light (302 nm) for 10 min at a distance of 5 cm. Putative conjugate (KLH-sHSAB-FusC) were dialysed overnight in PBS (Doyle et al., 2011). Analysis of FusC-KLH conjugate was assessed by the Siderotec Assay^{TM} (www.emergenbio.com), colorimetrically after iron addition and by SDS-PAGE (Doyle et al., 2011). After confirming conjugation, rabbits were immunized with FusC-KLH and anti-sera was obtained (referred in this chapter as SC1; Table 6.3) and used for the development of the ELISA.

Table 6.3: Anti-sera generated after immunization.

Immunized Conjugate	Conjugate ID
KLH-sHSAB-FusC	SC1

6.3.2 Developemtn of FusC conjugate

FusC was conjugated to SATA (N-succinimidyl-S-acetylthioacetate) modified cationised BSA (cBSA) via SMCC crosslinker. SATA was used to introduce thiol groups onto cBSA to form an activated protein SATA-cBSA. SMCC (succinimidyl 4-[N-maleimidomethyl] cyclohexane-1-carboxylate) was reacted through the NHS ester group to the amine groups of FusC for 2 h, at RT to from a SMCC-FusC complex. Both SATA-cBSA and SMCC-FusC were combined and incubated for 30 min at room temperature where the maleimide group of SMCC reacted with the thiol groups introduced by SATA (Doyle et al., 2011). Final conjugate (cBSA-SATA-SMCC-FusC) was dialysed 3 times with stirring at 4 ºC.

6.3.3 FusC purification and quantification

A. fumigatus ATCC46645 was grown for 72 h in MM under iron-free conditions to induce FusC production (Section 6.2.2.3). FusC was purified from culture supernatants by passage through Sep-Pak C_{18} silica columns (yield: approximately 20 mg/100 ml culture supernatant) (Section 6.2.2.4). Once purified, FusC was analysed by RP-HPLC and compared to a FusC standard (R_T = 11.089 min) (Figure 6.3). FusC quantification was carried out based on Schrettl et al. (2010) (Section 6.2.2.6) method which is based on the ability of ferrated FusC to absorb at 440 nm. RP-HPLC analysis of FusC-Fe^{3+} and FusC+Fe^{3+} was carried out at two wavelengths (254 nm and 440 nm) (Figure 6.4). It was observed that at 254 nm, FusC-Fe^{3+} elutes at a R_T of 11.097 min which correlates with the standard while FusC+Fe^{3+} elutes at a R_T of 10.260 min. When the same samples were seen at 440 nm, only FusC+Fe^{3+} was detected (R_T = 10.260 min) (Figure 6.4). While detection of the ferric and iron-free form of FusC was possible at 220 nm, several other metabolites are absorbed at this wavelength and can interfere in the detection process, which could account for the high absorbance values observed. On the other hand, at 440 nm, only ferrated FusC was evident, thus decreasing the interference of other absorbing metabolites and increasing the sensitivity and specificity of detection. This will be in agreement with the lower absorbance values observed at 440 nm compared to those at 220 nm. Thus quantification was carried out with the ferrated form of FusC at 440 nm.

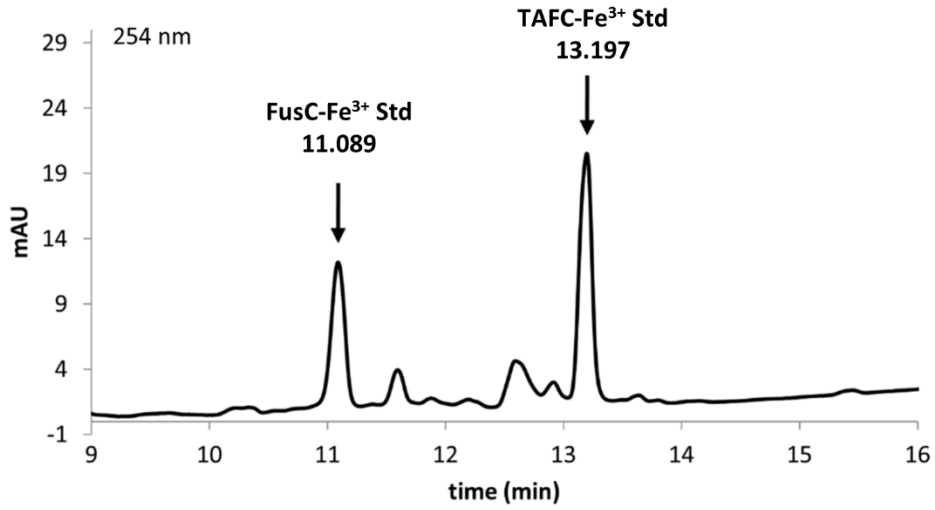

Figure 6.3: RP-HPLC chromatogram of non-ferrated FusC and TAFC standards at 254 nm. FusC standard was used as a reference for the purification process.

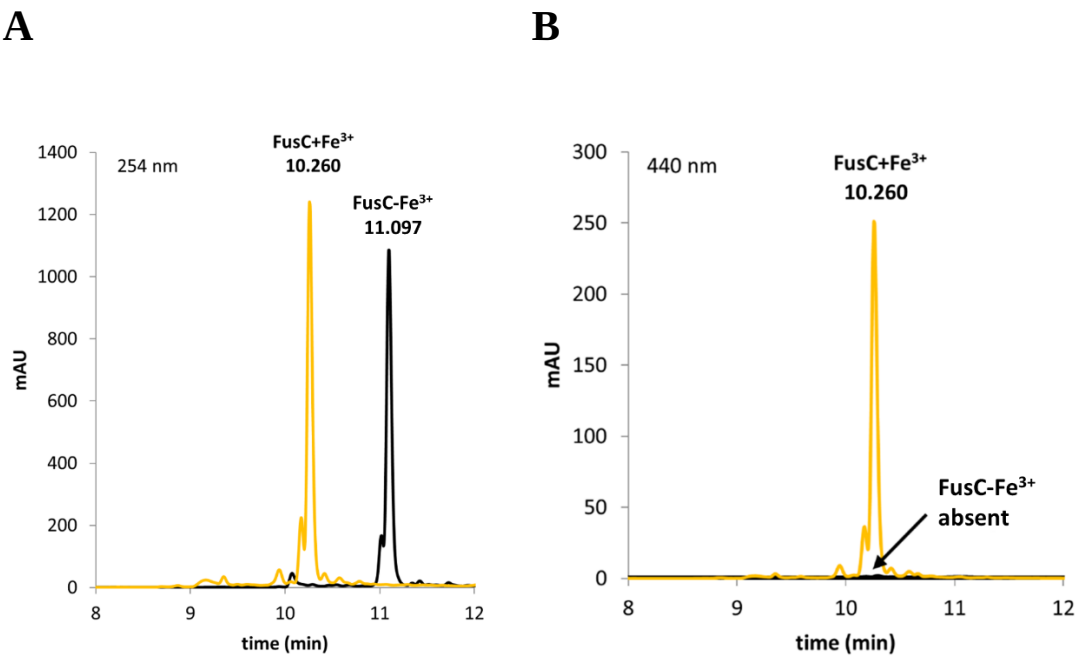

Figure 6.4: RP-HPLC analysis of FusC+Fe^{3+} and FusC-Fe^{3+} at 254 nm **(A)** and 440 nm **(B)**.

(A) Ferrated (yellow) and non-ferrated (black) FusC are present at a R_T of 10.620 min and 11.097 min, respectively, at a wavelength of 254 nm. Both peaks show equal absorbance values.

(B) RP-HPLC chromatogram of ferrated (yellow) and non-ferrated (black) FusC at 440 nm. Only ferrated FusC (R_T = 10.620 min) was detected at this wavelength.

6.3.4 FusC ELISA strategy

This assay was designed for the quantitative determination of FusC in biological fluids by competitive ELISA. The assay principle is based on the competition between immobilised and free FusC (known as calibrator) for monospecific IgG (anti-FusC, SC1) (Figure 6.5). Thus, the higher the amount of free FusC in a specimen, the lower the antibody binding to the immobilised FusC and ultimately the lower colour development in the microwell plate (Figure 6.5).

In order to confirm if SC1 (anti-sera) was suitable for the development of the FusC ELISA immunoblots were performed against free FusC (Section 6.2.2.7). Figure 6.6 indicates that SC1 specifically reacts with FusC in a concentration dependent manner while it shows no reactivity towards BSA control.

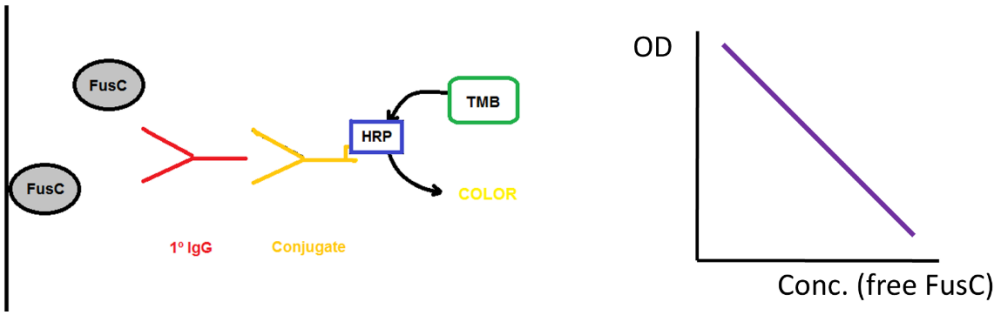

Figure 6.5: Schematic description of the detection of FusC by competitive ELISA. 1º IgG: Anti-FusC antibody (SC1); Conjugate: anti-species; HRP: horseradish peroxidase; TMB; tetramethylbenzidine.

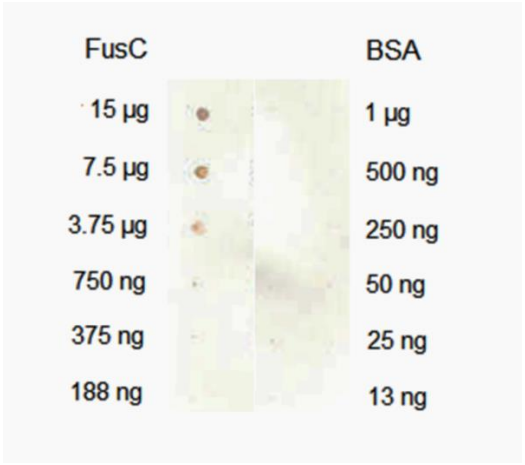

Figure 6.6: Immunoblot analysis of FusC using rabbit anti-sera (SC1). Anti-FusC reactivity was observed.

6.3.5 Optimization of FusC-ELISA

6.3.5.1 Antigen coating

ELISA plates were coated with either FusC (Section 6.2.2.4) or conjugated-FusC (cBSA-SMCC-SATA-FusC) (Section 6.3.2). Both antigens showed reactivity towards SC1 and were coated following Section 6.2.2.8 at an equivalent FusC concentration. A range of calibrators (free FusC) were generated (0 – 76 μg/ml) to check for competition. Figure 6.7 indicates that both coated antigens compete against the calibrator for SC1 binding. However FusC alone appears to give higher absorbance values compared to cBSA-SMCC-SATA-FusC. This observation could be a result of a high amount of FusC coated in the well due to the small size of the peptide. In contrast, FusC conjugated to a carrier protein (cBSA) will occupy a bigger surface area and less FusC will be coated in the well.

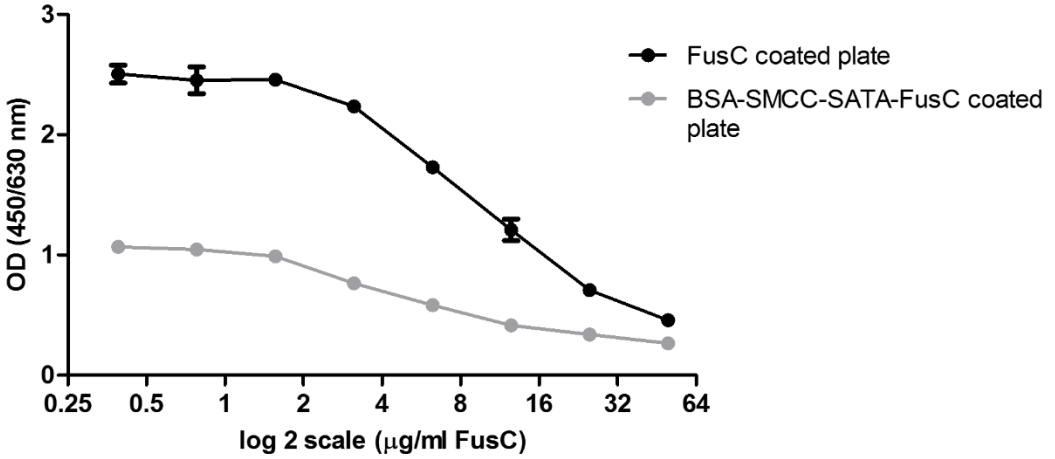

Figure 6.7: ELISA testing antigen coating. Signal obtained from a FusC coated plate (black) and BSA-SMCC-SATA-FusC coated plate (grey).

6.3.5.2 Establishing antigen coating concentration

As FusC appeared to be a better coating antigen for the ELISA (Section 6.3.5.1), it was coated at different concentrations on the microtiter well plate, ranging from 4.4 to 0.034 μg/ml. The FusC-competitive ELISA was carried out using three concentrations of calibrator (Free-FusC) been; (i) 0 μg/ml Free-FusC, where no competition should occur, (ii) 0.56 μg/ml Free-FusC, where very low levels of competition should be observed and (iii) 76 μg/ml Free-FusC, that should result in high competition and low absorbance values. In order to select a working antigen coating concentration the signal to noise ratio (or greatest absorbance difference between the high and low calibrator) was determined (Figure 6.8). The signals observed when the plate was coated with 1.1 and 0.55 μg/ml FusC appeared to give a good ratio and absorbance values. The higher the absorbance ratio, the better the resolution of the assay. For this reason, 0.7 μg/ml was selected as the optimum FusC coating concentration.

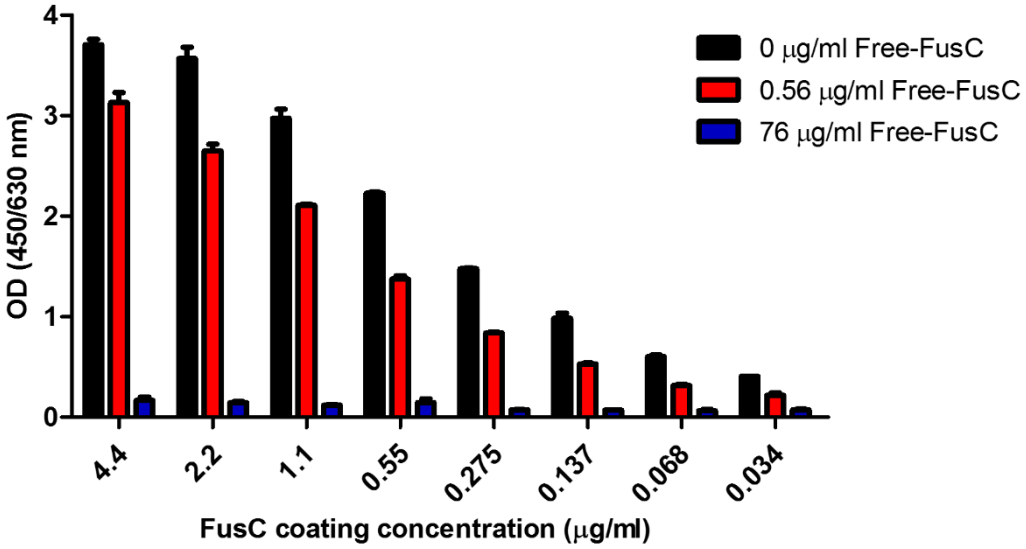

Figure 6.8: Titration of FusC coating concentration. ELISA was carried out using three calibrators (Free-FusC); 0 μg/ml (black), 0.56 μg/ml (red) and 76 μg/ml (blue).

6.3.5.3 Calibrator optimization

Calibrators generate standard curves that are used for the quantification of antigens in samples. In the FusC-ELISA, free-FusC is the calibrator whereby increasing its concentration leads to lower absorbance values. Thus a ready to use stock of calibrator (free-FusC) was generated in order to facilitate samples and curve generation (Section 6.2.2.9.1).

As FusC could be present in biological samples in the ferrated and non-ferrated form, reactivity towards both forms of FusC was tested. Thus, ELISA was performed on a FusC coated plate (0.7 μg/ml) using a ferrated and non-ferrated calibrator at different concentrations (0 – 50 μg/ml). ELISA showed that both calibrators compete equally for SC1 as both curves appear to overlap (Figure 6.9). Thus it was confirmed that FusC may not need to be ferrated in the ELISA in terms of detection.

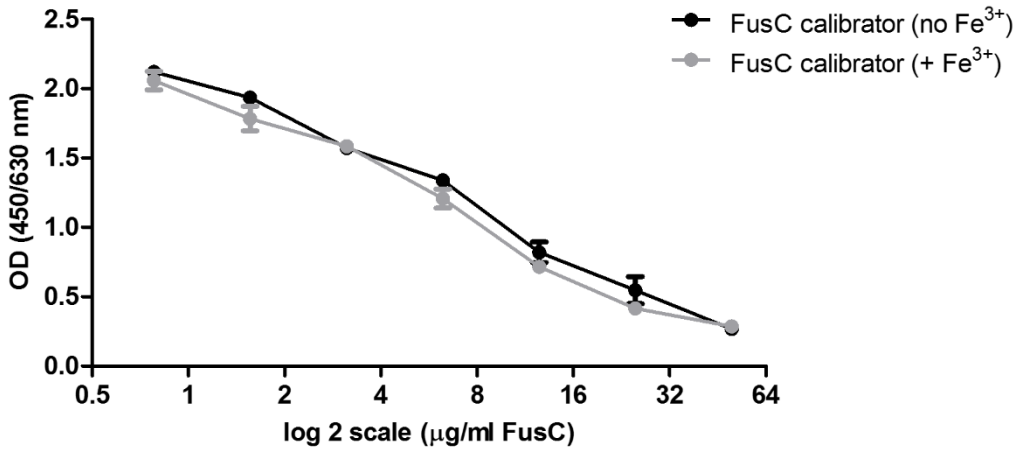

Figure 6.9: ELISA test with ferrated (grey) and non-ferrated (black) calibrator

6.3.5.4 Anti-sera (SC1) stability test

Obtaining a reactive anti-sera towards an antigen of interest is an essential part of an ELISA test. In this ELISA, SC1 was a valuable part of the assay and it was used at the highest dilution possible (1/2000 final dilution in well) (Section 6.3.1). Accelerated temperature tests on SC1 were performed to determine the stability of the anti-sera, thus preparations of SC1 were stored at 4 ºC and 37 ºC for several days. Reagents stored at 37 ºC represent an accelerated way of checking for degradation. ELISAs were carried out as per Section 6.2.2.9.4 using a low FusC calibrator (0.78 μg/ml) and the anti-sera stored at both temperatures. The stability of SC1 was evaluated by generating a time line (Figure 6.10) with the days of storage at 4 ºC and 37 ºC. Figure 6.10 indicated that after 19 days of storage at both temperatures, SC1 showed similar OD values throughout the time-course demonstrating no signs of instability.

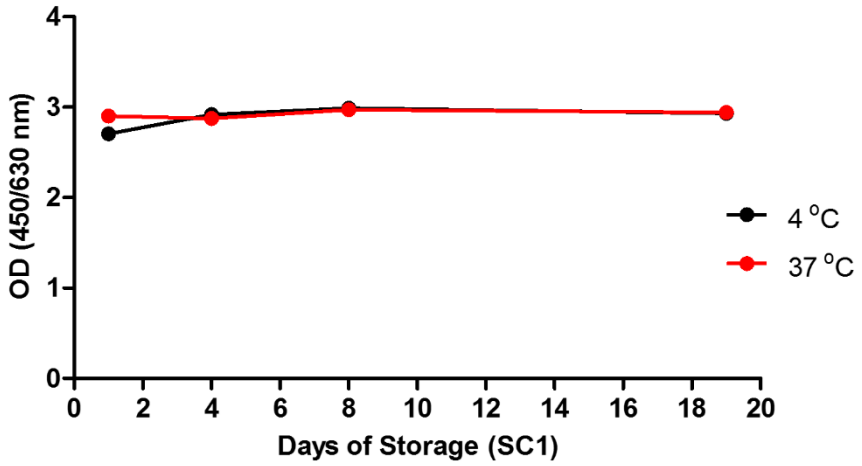

Figure 6.10: Temperature stress test at 4 ºC and 37 ºC for 20 days of anti-sera (SC1) after preparation of ready to use stocks.

6.3.5.5 Optimizing conjugate concentration

Different dilutions of the HRP anti-species conjugate were prepared to test for optimum signal. Standard curves were generated with the calibrators (0 – 76 µg/ml). Dilutions 1/250 and 1/500 gave the best signals in the assay (Figure 6.11). For subsequent assays a 1/350 dilution was selected as optimum for FusC detection.

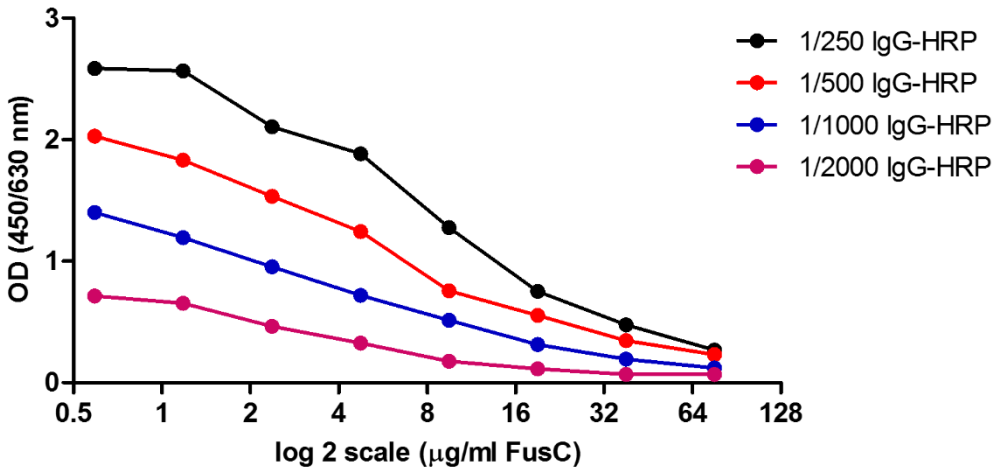

Figure 6.11: FusC standard curves using different dilutions of secondary antibody (anti-species IgG-HRP).

6.3.5.6 Optimizing washing diluent

A commercial wash diluent and PBST (Section 2.1.8) were used to optimize the ELISA plate washing step. Figure 6.12 indicates that the commercial diluent works slightly better compared to PBST and was selected as the washing diluent.

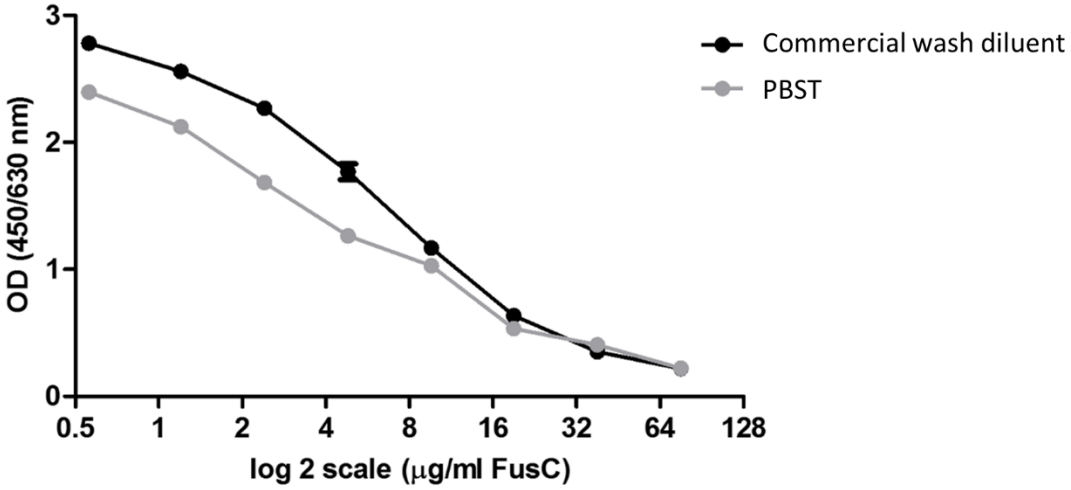

Figure 6.12: FusC-ELISA using different washing diluents. Commercial wash dilutent (black) and PBST (grey)

6.3.5.7 Stability testing of ELISA kit

After testing all the individual components of the ELISA (Table 6.4), stability tests were performed on the full kit.

Table 6.4: FusC ELISA kit components

ELISA Components	Description
Microtiter plates	Coated with FusC (0.7 μg/ml)
Calibrator	FusC (10X; 500 μg/ml)
Anti-FusC antibody	SC1 (1/2000 final)
HRP-conjugate	Anti-rabbit IgG diluted 1/350
Wash buffer concentrate	Biotrin (20X)
Tetramethylbenzidine (TMB)	Ready to use from Moss Inc.
Stop solution	Ready to use (Section 6.2.1.6)

ELISA kits were placed at a 37 ºC incubator on day 1 and were tested for stability periodically over weeks (Figure 6.13). After 77 days, the calibrators seemed to compete at the same level as day 1 and the standard curves appeared to overlap or shown minor OD shifts. Overall, this test indicates the robustness of the FusC-ELISA.

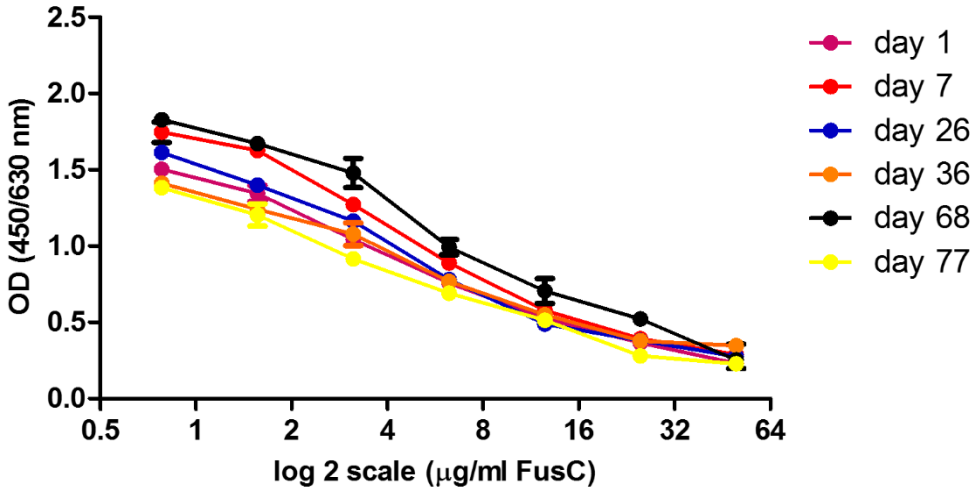

Figure 6.13: Stability test of FusC-ELISA carried out at 37 ºC.

6.3.6 FusC ELISA validation

Once the ELISA was completed we proceeded to the evaluation of FusC presence in clinical samples.

6.3.6.1 Guinea Pig Panel

Clinical specimens were obtained from a Guinea Pig animal model of invasive pulmonary aspergillosis and control specimens (urine, BAL and serum; normal or uninfected guinea pigs and disease-state). All specimens were assayed at a dilution of 1/5 in the FusC-ELISA. FusC was detectable in the BAL, urine and sera of immunocompromised guinea pigs experimentally inoculated with *A. fumigatus* but not in normal or uninfected animals (Figure 6.14). Interestingly low levels of FusC were detected in the serum of normal guinea pigs and in some of the infected ones. This result could be due to several reasons like; normal sera may contain endogenous low levels of FusC or unspecific binding could be occurring. In terms of some of the infected samples showing low levels of FusC, this could be a result of sample interference or an incorrect assessment of the state of the sample by GM testing.

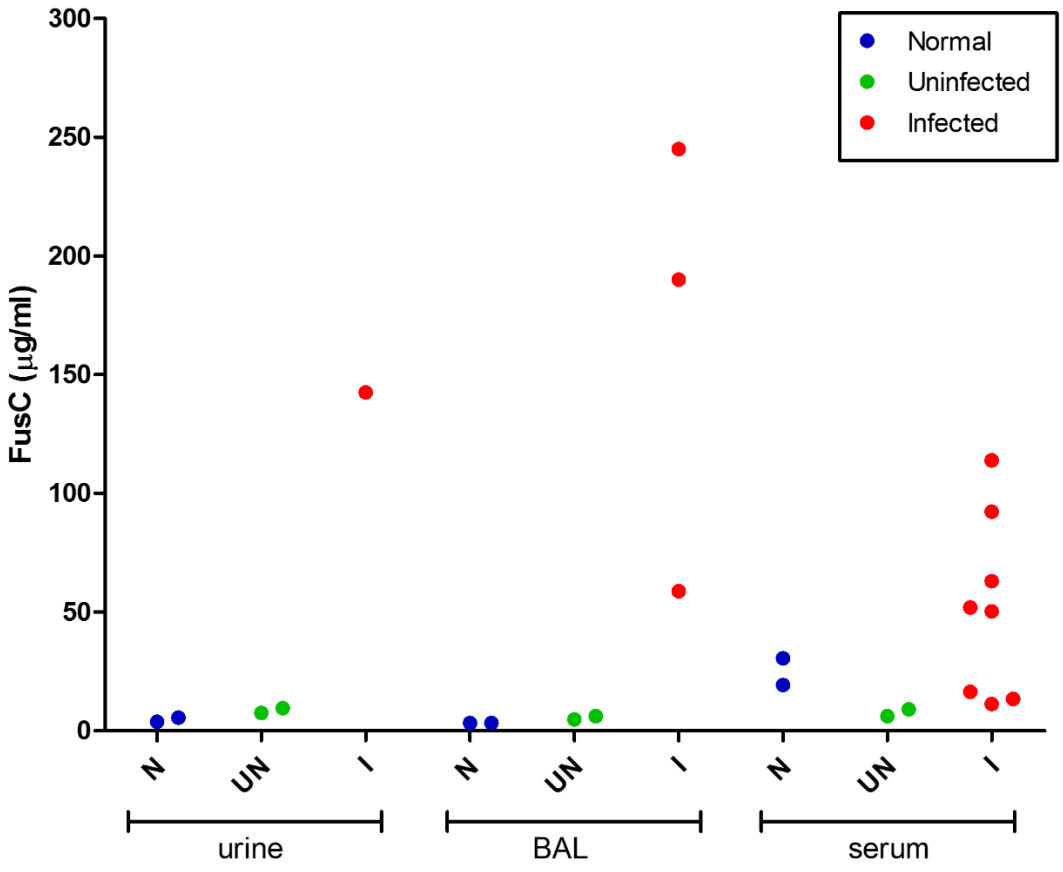

Figure 6.14: ELISA detection of FusC concentrations in urine, BAL and sera of animal model (Guinea Pig) of invasive pulmonary aspergillosis.

6.3.6.2 Human serum panel: Establishing the cut-off value

A set of human serum samples were obtained from the Irish Blood Transfusion Service known to be negative for aspergillus infection. 20 samples were utilized on the FusC-ELISA and results were expressed as index values (I.V.) representing the concentration of FusC in the sample divided by the cut-off concentration.

The cut-off value for the FusC ELISA was established by determining the concentration of 10 randomly selected negative serum samples. The cut-off value of

the assay was calculated by adding twice the standard deviation to the mean absorbance of the ten samples (Table 6.5). The established cut-off value was determined to be 19.691 µg/ml.

Table 6.5: Establishing the cut-off value of the FusC ELISA

Mean of 10 negative samples	Standard deviation (STDEV)	2 X STDEV	Cut-off value
13.254	3.2189	6.4378	19.691

The FusC levels obtained from serum samples were calculated as Index Values (I.V.) as follows: the mean concentration for each serum sample was divided by the cut-off value (19.691 µg/ml). An I.V. greater than 1 was considered positive where values between 1 – 2 were slightly positive, between 2 – 4 were medium positive and greater thatn 4 were considered highly positive. From the 20 samples screened all appeared negative (Figure 6.15).

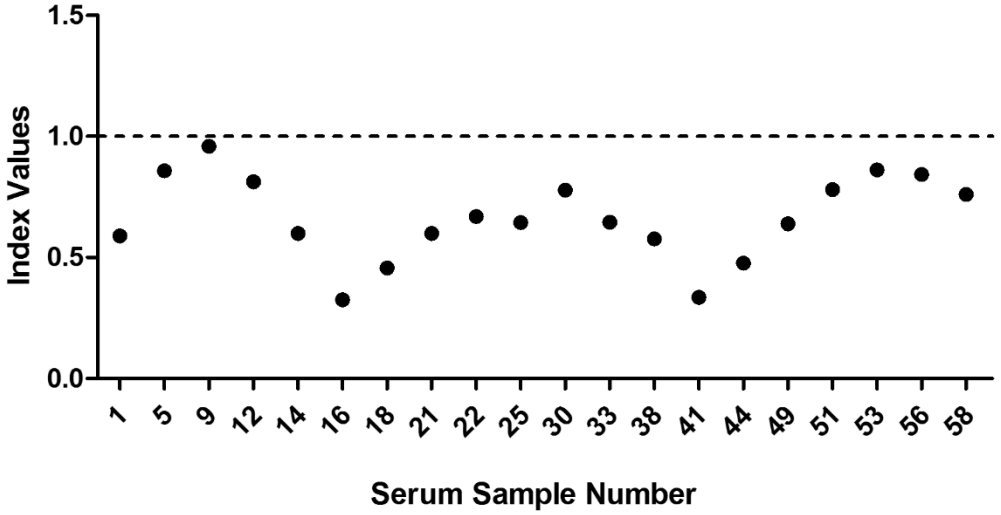

Figure 6.15: Normal human sera samples (n = 20) screened for false positives.

6.3.6.3 Human serum panel: comparison with GM assay

Disease-state sera (n = 10) from individual patients with IA (Section 6.2.1.7) was screened in the FusC-ELISA and compared to the results obtained in the GM test. Samples were represented as I.V. and values greater than 1 were considered seropositive. Of the 10 samples tested, 6 appeared positive by the FusC-ELISA (Figure 6.16). All the sera samples were positive by the GM assay thus the results showed might indicate either the remaining 4 samples are false negatives or the FusC-ELISA is more specific than the GM test (Table 6.6).

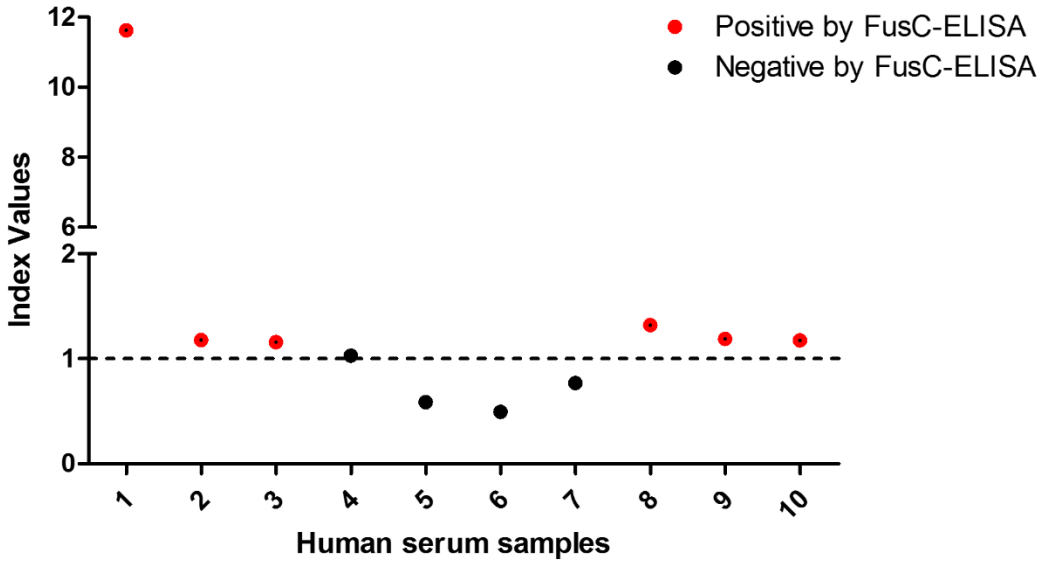

Figure 6.16: FusC-ELISA result for 10 human sera samples determined to have an aspergillus infection by GM. Those samples in red represent positive samples by FusC-ELISA.

Table 6.6: Comparison of ELISA results between the GM and FusC assay.

Sample No.	Sample ID	GM Assay	FusC-ELISA
1	9-7075	P	P
2	9-BS5039	P	P
3	9-BS5394	P	P
4	9-BS7581	P	N
5	9-BS7822	P	N
6	10-BS3768	P	N
7	10-BS3943	P	N
8	10-6563	P	P
9	10-BS671	P	P
10	10-BS87	P	P

6.4 Discussion

This Chapter describes the development of an ELISA assay for the detection of FusC and the validation of this test on clinical samples. The FusC-ELISA shows the detection of FusC in guinea pig and clinical samples but not in controls. Thus it potentially provides a method for detecting infections caused or associated with *A. fumigatus* that is simple and accurate.

Within all the possible ELISA formats, a competitive ELISA appeared to be the best option as it is highly sensitive to complex or impure samples and is the method of choice for low molecular mass analytes (Gan and Patel, 2013). The key principle in this type of ELISA is the competition between the antigen bound to the plate and the sample antigen for the binding to the primary antibody. Coating small molecules, like FusC, on a microtiter plate can be problematic due to the small size of the analyte as it might not bind well to the solid phase of the plate and could be masked by the blocking solution. Due to these problems, small antigens can be attached to a larger protein that facilitates absorption to the solid phase of the plate. For this reason, a FusC conjugate (cBSA-SATA-SMCC-FusC) was used to coat a microtiter plate and was compared against a plate coated with FusC alone. Surprisingly, FusC appeared to be a better coating antigen compared to the BSA conjugate.

After coating, either calibrators or specimens, followed by the primary antibody (SC1) were added to the wells that are coated with FusC. An incubation period occurs where FusC in the plate and in the sample will compete for the binding to SC1. Following a washing step, only SC1 bound to the FusC on the plate will remain. Competition was observed with the SC1 antisera as signals observed using a high calibrator appeared low indicating that SC1 doesn't bind the FusC on the plate. On the

contrary, when a low calibrator is added ODs appeared high as most of the SC1 will bind to the FusC on the well. The reactivity of SC1 and FusC lead to the generation of a standard curve (0 – 50 μg/ml) that was used for the quantification of specimens. Iron is one of the most abundant elements in all living organisms where it is a key component of many proteins including haemoglobin. It is also majorly used in the construction and automobile industry and in combination with other elements makes up for daily used products. Thus iron can be found everywhere. Due to the high possibility that specimens might contain traces of iron, the ELISA was tested for competition using ferrated and unferrated calibrators. Results indicated that competition was unaffected and reinforced the practicality of the assay. It should also be considered that iron chelation by FusC could have occurred prior to ELISA.

The use of polyclonal serum (SC1) can be of advantage over monoclonal antibodies specially in terms of signal amplification. Polyclonal antibodies (mainly IgG subclass) recognise multiple epitopes in the target antigen thus providing a more robust detection. Due to the small size of FusC, it is possible that the anti-sera generated is already specific for one epitope thus increasing specificity and lowering the chances of cross-reactivity. Polyclonal antibodies, though, are susceptible to batch variability, which is why the ELISA was performed at a very high dilution of SC1 (1/2000). Monoclonal antibodies, on the other hand, do not present this inconsistency between batches as once hydridomas (cells designed to produce an antibody of interest) are made, they are a constant source of antibodies with no batch variation. For these reasons, polyclonal antibodies can limit the commercial applications of an ELISA and monoclonal antibodies are preferred (Kuang et al., 2013).

Once SC1 is bound to the plate via FusC, it reacted with an anti-rabbit IgG HRP secondary antibody that after substrate addition (TMB) will generate a chromogenic signal. Accelerated temperature stability tests were carried out on the ELISA kit during a period of approximately 3 months. Results showed that the standard curved generated at day 1 were equivalent to those obtained at day 77 and indicate that the FusC-ELISA is a very stable assay, which is advantageous for commercial purposes.

Normal human serum samples obtained from the IBTS were used to establish a cut-off value which was determined to be 19.691 μg/ml FusC (equivalent of 1 I.V.). From the 20 samples tested all appeared to be negative however fluctuations in the levels of FusC were observed and could be due to trace amounts of FusC in the sample or cross-reactivity with human analytes. Normally, serum samples require special treatment and buffers prior the use on an ELISA as they contain antibodies that can interfere in the assay (Dufresne et al., 2012). This is why in this assay proteinase K addition was required to pre-treat all human serum (Section 6.2.2.9.3). Of the 10 human samples determined to be positive by GM ELISA, 6 were also seropositive by FusC-ELISA but 4 were addressed as seronegative. This could indicate a higher reactivity to *A. fumigatus* GM polysaccharide.

Additionally, a guinea pig panel assessed by GM test and found to have normal, uninfected and infected specimens was screened with the FusC-ELISA. This panel contained urine, BAL and serum samples. All the urine and BAL samples tested for FusC antigen correlated to the results obtained in the GM assay. The serum specimens on the other hand showed false positives in two of the normal samples (> 19.619 μg/ml) and seronegative values for three of the infected specimens. This result can be

explained by the fact that guinea pig serum samples were not treated with proteinase K and cross-reactivity might have occurred.

Though the GM assay is routinely used as a diagnostic method for IA it has been shown that GM detection might depend on the immune status of the host (Shi et al., 2012a). In patients with prolonged neutropenia the sensitivity of the assay ranges 72 – 82 % compared to non-neutropenic patients with a 40 – 55 % sensitivity (Trof et al., 2007). In non-neutropenic patients were angioinvasion and necrosis is limited, GM levels in serum tend to appear negative (Verweij et al., 2000). Recently, RNAseq analysis of *A. fumigatus* mycelia incubated in blood revealed an up-regulation of genes involved in siderophore homeostasis and was indicative of siderophore production in blood (Irmer et al., 2015). Also, transcriptomic analysis of *A. fumigatus* germlings during the initial stages of murine infection revealed that genes from the siderophore biosynthetic pathway and siderophore transporters were highly represented (McDonagh et al., 2008). *In vitro* studies on *A. fumigatus* have shown how the fungus is capable of removing iron from transferrin with the aid of siderophore secretion (Hissen et al., 2004). Transferrin is an iron-binding protein found in human serum. Hissen et al. (2004) also observed the early secretion of siderophores during *A. fumigatus* growth *in vitro*. It is interesting to note that these authors measured siderophore concentration through a colorimetric test known as the CAS (Chrome Azurol S) assay which, similarly to the Siderotec^{TM} are compatible with culture supernatants but not biological samples (Hissen et al., 2004) (www.emergenbio.com).

Overall, FusC represents a promising biomarker of infection and appears to have potential benefits compared to the GM assay like greater specificity and early detection. Though further research has to be carried out and the use of monoclonal

antibodies should be considered, in combination with other diagnostic strategies it could improve the diagnosis of IA.

Chapter 7

Discussion

7 Chapter 7: Discussion

This discussion will describe how *A. niger* exposure to GT facilitates a systems biology approach to explore the response of fungi to GT and will reveal interesting aspects of the organismal biochemistry. Resultant data have revealed new insights into the fungal metabolic network in response to the stress agent, GT, specifically with respect to primary metabolism, in addition to characterising a thiol MTase-mediated GT resistance system. Moreover, this thesis proposes a functional crosstalk between primary and secondary metabolism and describes the putative involvement of these systems in other cellular processes such as chromatin modification and regulation.

7.1 GT perturbs the metabolic network of *A. niger*

Comparative proteomic analyses of *A. niger* exposed to different stress agents have been carried out in order to investigate the overall stress response of this fungus (Braaksma et al., 2010; Guillemette et al., 2007; MacKenzie and Guillemette, 2005; Meyer et al., 2007; van Munster et al., 2014, 2015; Nitsche et al., 2012). Though proteomic studies take into account all cellular processes implicated in the adaptation to this response, carbon metabolism has attracted most of the attention (van Munster et al., 2014, 2015; Nitsche et al., 2012). Sulphur is another essential nutrient for fungi as it is a component of (i) cysteine and methionine amino acids which are required for protein synthesis, (ii) GSH and EGT which participate in the defence response against oxidative stress (Fahey, 2013; Pócsi et al., 2004), and (iii) cofactors like iron-sulphur clusters that are implicated in enzyme regulation and ribosome and cofactor biosynthesis (Xu and Møller, 2011). Sulphur can be obtained from the assimilation of sulphate or the catabolism of methionine and cysteine (Thomas and Surdin-Kerjan,

1997). Overall it is surprising that the implications of sulphur metabolism in response to stress agents have received, so far, limited attention.

Chapter 3 described the dysregulated abundance of proteins involved in the methionine cycle in *A. niger* in response to exogenous GT, compared to MeOH controls. Several metabolites constituting this cycle also showed altered levels after GT addition. Increase in abundance of several MTases and SAHase correlates with a decrease in SAM levels and an increase in Ado levels. It was concluded that due to the interconnectivity of SAM in the metabolic network, specifically as a methyl donor in methylation reactions (i.e., endogenous or BmGT formation), the level of this metabolite was decreased after GT exposure. I also conclude that, as SAH is a by-product of methylation reactions and an inhibitor of MTases (Hendricks et al., 2004), the increase in abundance of SAHase could be necessary to enable *A. niger* to dissipate SAH and avoid global MTase inhibition. The abundance of spermidine synthase and homoserine dehydrogenase was higher after GT treatment compared to control conditions. As both enzymes are part of pathways (Yang cycle and Hcy biosynthesis) which can lead to the generation of methionine (Sauter et al., 2013), the level of this metabolite was measured and increased in the presence of GT. I propose that the high levels of methionine are a result of the activity of the Yang and methionine cycle in order to sustain, at least in part, methylation reactions (e.g., BmGT formation). The decrease in abundance of ATP sulphurylase (sC) and cysteine synthase might also account for the high activity of the methionine cycle and might indicate that methionine synthesis is favoured over cysteine synthesis. Though dysregulations in the GSH/GSSG ratio have been observed in *A. fumigatus* Δ*gliT* compared to wt and in Δ*gliT* exposed to GT (Carberry et al., 2012), no significant changes appeared to occur in *A. niger*. GSH acts as a major antioxidant in cells under oxidative stress thus the

results observed imply that *A. niger* has a different response compared to *A. fumigatus* Δ*gliT* and that the defence mechanism against GT might involve other players (e.g. SOD, catalase).

In plants, a similar systems biology approach to that deployed here to evaluate *A. niger* exposure to GT was undertaken by Wintenberg et al. (2014), where wheat leaves were exposed to SnTox3 fungal effector protein. SnTox3 is secreted by the wheat pathogen *Stagnospora nodorum* during the early stages of infection. Dysregulation of the methionine metabolism at the genetic and proteomic level was observed upon SnTox3 infiltration. These authors proposed that the increase of methionine metabolism will lead to high levels of Hcy and observed that the ability of the pathogenic fungus to cause disease was impeded in the presence of Hcy. Thus it was hypothesised that Hcy metabolism might play an unknown role in host defence (Winterberg et al., 2014). Interestingly, upregulation of genes involved in other defence responses like secondary metabolism and protein resistance was also observed (Winterberg et al., 2014).

Dysregulation of proteins involved in sulphur metabolism has been shown in *C. albicans* challenged to antifungals. Increased abundance of SAH1 was found in response to caspofungin while MET6, SAM2 and CYS3 were increased in the presence of amphotericin B (Hoehamer et al., 2010). In *Arabidopsis* a missense mutation of *sah1L459F* gene (*sah1* homolog) was shown to reduce DNA methylation at cytosine residues (Mull et al., 2006).

It is clear that sulphur metabolism is involved in the adaptive response of organisms under stress and that due to the modularity and interconnectivity of metabolic networks it is not the only cellular system affected (Grüning et al., 2010).

The methionine cycle is involved in the formation of polyamines, ethylene, organic molecules (GSH, EGT) and amino acids (Met, Cys) (Saint-Macary et al., 2015; Sauter et al., 2013; Sheridan et al., 2015). Crosstalk of sulphur metabolism with secondary metabolism and iron regulation (Amich et al., 2013; Gerke et al., 2012; Yang et al., 2015), chromatin regulation (Gerke et al., 2012; Mull et al., 2006), signal transduction and protein synthesis (Paik et al., 2007; Schubert et al., 2003) takes place and contributes to the response to stress.

Comparative proteomics also highlighted that under GT addition, multiple hydrolases containing signal peptides were significantly increased (Figure 7.1). This observation was very interesting as most of these enzymes are of great relevance for the biotechnology industry. Glycoside hydrolases (GHs) and peptidases have been shown to be increased in expression under nutrient limitation in *A. niger* (van Munster et al., 2014, 2015; Nitsche et al., 2012; Szilágyi et al., 2013), and thus, by analogy I conclude that, possibly, most of these enzymes are destined for secretion to scavenge and degrade polymeric nutrients from the media. I propose that GT induces a nutrient requirement which leads to the production of hydrolytic enzymes.

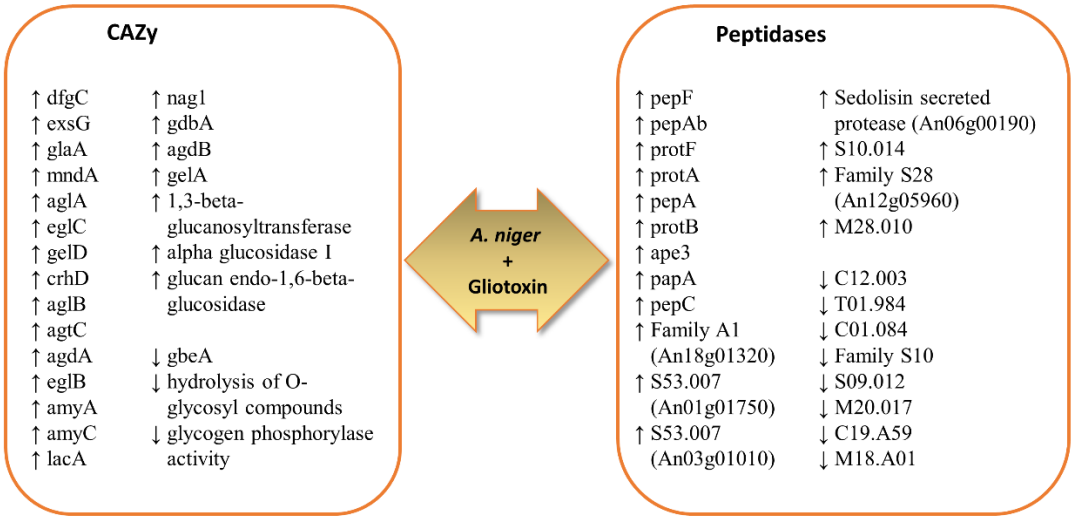

Figure 7.1: Abundance of hydrolytic enzymes is dysregulated in *A. niger* CBS 513.88 in response to GT (2.5 µg/ml).

Several GHs with increased abundance in *A. niger* after GT exposure are under the control of transcriptional regulators (TRs) AmyR (TR of starch degrading enzymes) (Petersen et al., 1999), XlnR (TR of xylanases and cellulases) (van Peij et al., 1998a) and AraR (TR that interacts with XlnR) (de Souza et al., 2013). Observations made by Seiboth et al. (2012) and Kubicek et al (2013) established a co-regulation between XlnR and LAE1 in *T. reesei* and hypothesised about an epigenetic control of cellulase production and SM cluster regulation. Though it is well established that the Velvet complex regulates fungal sexual development and secondary metabolism, recent work has demonstrated the influence of this complex in other cellular functions, like hydrolytic enzyme formation and control of amino acid biosynthesis (Figure 7.2) (Roze et al., 2010; Sarikaya Bayram et al., 2010; Seiboth et al., 2012)

Agents known to trigger the UPR and ERAD response in *A. niger* (DTT and tunicamycin) have been used to investigate bottlenecks occurring in the secretory pathway of the fungus (Guillemette et al., 2007; MacKenzie and Guillemette, 2005). In the dithiol form (rGT), GT is a reducing agent containing thiol groups that could potentially have a similar, or augmented, affect in *A. niger* to that of DTT. Comparison of the *A. niger* response after GT addition (described herein) versus the response obtained after DTT exposure, revealed an overlap in the dysregulated abundance of some proteins including; methyltransferases (MT-I, MT-II), GHs (CtcA, α-glucosidase I) and peptidases (aminopeptidase) (Guillemette et al., 2007; MacKenzie and Guillemette, 2005).

The observed increased abundance of multiple hydrolytic enzymes (with SP) in response to GT could potentially cause ER stress and consequently activate the ER stress response. Analysis of *A. niger* secretome after GT addition revealed that approximately 50 % of the dysregulated proteins where GHs and peptidases, which overlapped with the intracellular mycelial proteome. It was interesting however to see that two of the GHs (DfgC and GlaA) with increased abundance intracellularly were decreased in the secretome and thus it was concluded that a defect in the secretory pathway could be occurring.

Abundance dysregulation of proteins involved in central carbon metabolism (i.e., glycolysis, fermentation and TCA cycle) was observed in *A. niger* exposed to GT compared to MeOH control. The decrease observed in most of these proteins can be a result of a glucose limitation that will consequently reduce energy metabolism (ATP and NADH reduction). A decline in the levels of ATP, for example, is a serious alarm in the cell which signals to regulatory systems in order to prevent the failure of the

energy state (Grüning et al., 2010). One of the compensatory mechanisms is to increase nutrient uptake (Grüning et al., 2010; Wullschleger et al., 2006)) which could be a reason as to why there is such a significant increase in the number of hydrolytic enzymes upon GT exposure.

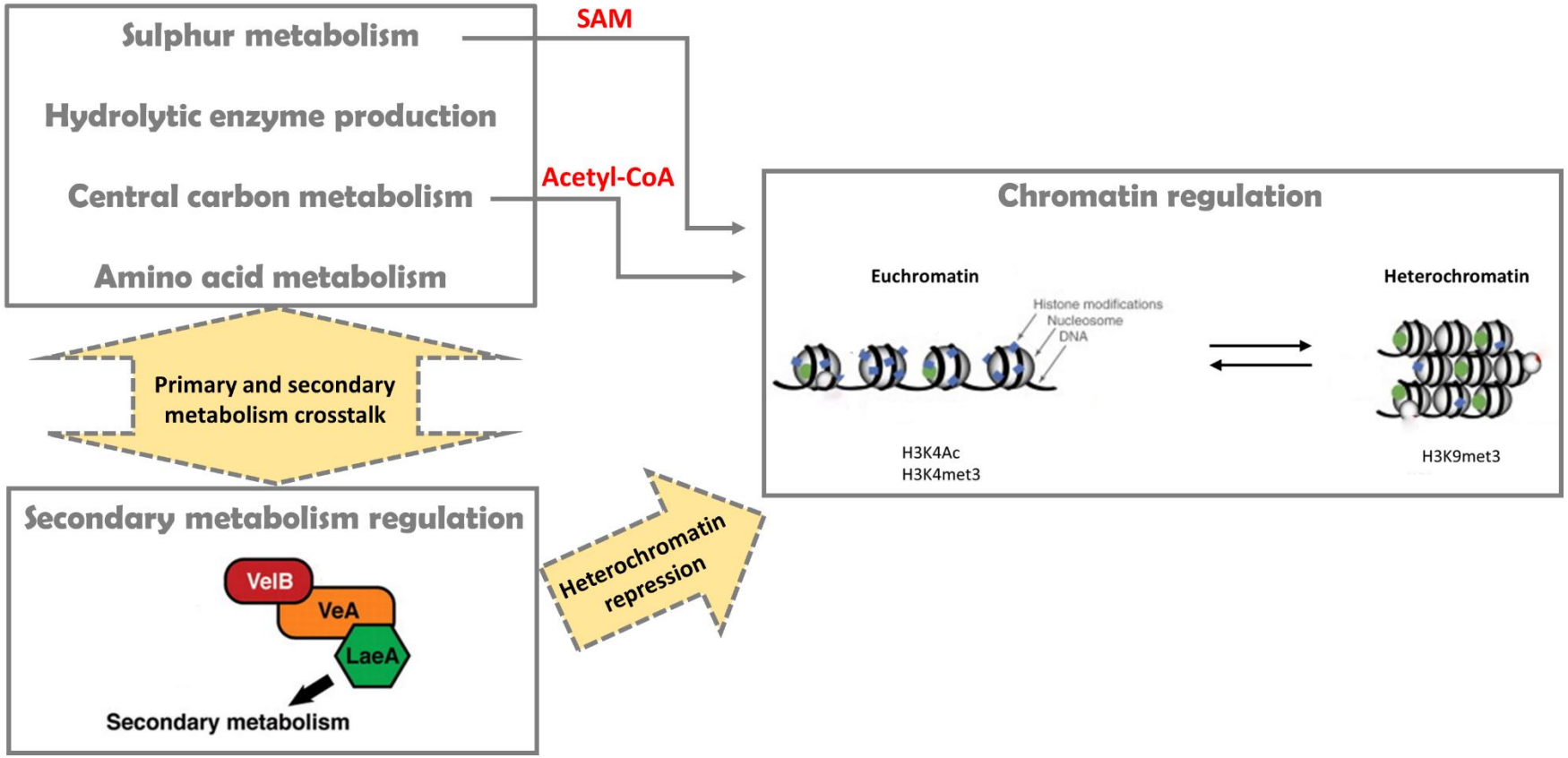
Sulphur metabolism
Hydrolytic enzyme production
Central carbon metabolism
Amino acid metabolism
SAM
Acetyl-CoA
Primary and secondary metabolism crosstalk
Secondary metabolism regulation
VelB
VeA
LaeA
Secondary metabolism
Heterochromatin repression
Chromatin regulation
Euchromatin
Heterochromatin
Histone modifications
Nucleosome
DNA
H3K4Ac
H3K4met3
H3K9met3

Figure 7.2: Overview of how GT affects *A. niger* primary metabolism and the potential implications on secondary metabolism and chromatin regulation. Adapted and redrawn from (Bayram et al., 2008; Grüning et al., 2010).

Acetyl-CoA is an important molecule that can be obtained from citrate and acetate in the cytoplasm and from pyruvate in the mitochondria. As mentioned in Chapter 4, acetyl-CoA plays an important role in chromatin regulation as it is the only acetyl donor of histone acetyltransferases (HATs) (Hynes and Murray, 2010). Thus HATs, like MTases, depend on the concentration of acetyl-CoA and SAM, respectively, which falls under metabolic control (Figure 7.2). Furthermore, acetyl-CoA is also the source of acetyl groups for secondary metabolites (e.g. Non Ribosomal Peptides) (Sheridan et al., 2015).

Amino acid biosynthesis and catabolism was dysregulated in *A. niger* in the presence of GT. It was concluded in Chapter 4 that the increase of proteins involved in amino acid biosynthesis coupled with the high levels of Val, Phe, Leu/Ile observed, possibly indicates the use of these amino acids in the synthesis of hydrolytic enzymes. The high dysregulation observed in BCAAs metabolism compared to the metabolism of other amino acids could imply a different regulatory mechanism triggered by GT. Interestingly, a connection between BCAAs and the Velvet complex was observed in *A. parasiticus* by Roze et al. (2010) that proposed a role for VeA as a negative regulator of BCAA production.

Thus, it appears that within the metabolic network of *A. niger*, there is a significant crosstalk between primary metabolism (sulphur metabolism, central carbon metabolism, hydrolytic enzyme production and amino acid biosynthesis) and secondary metabolism regulation (Velvet complex) (Figure 7.2). This could suggest that the dysregulation of these pathways could be mediated by alterations in the Velvet complex.

Comparative proteomic analysis of *A. niger* Env. Isol. in the presence and absence of GT, showed the dysregulation of several processes. In the same way as the response observed in the *A. niger* sequenced strain (CB 513.88), the major functional category affected was metabolism. Additionally, two proteins involved in the UPR-stress response (Cdc48 and Rpt3) appeared increased, while molecular chaperone (Hsp70 and Hsp90) were decreased. The reduction in chaperone levels involved in the folding of nascent proteins is an indication of ER-stress (Pusztahelyi et al., 2011).

7.2 Activation of a Thiol Methyltransferase-Mediated GT Resistance System

Comparative proteomic analysis of *A. niger* exposed to GT led to the identification and characterization of a putative SAM-MTase (MT-II). It was unequivocally described in Chapter 5 that MT-II acts as to effect protection against exogenous GT in *A. niger* by formation of BmGT.

In 2014, the first fungal SAM-dependent thiol methyltransferase was characterised in *A. fumigatus* (Dolan et al., 2015). Named GtmA, this MTase was shown to act as a negative regulator of GT biosynthesis whereby deletion of the *gtmA* gene resulted in an increase in GT production. Phylogenetic analysis of the distribution of GtmA in the Eurotiales order (Figure 7.3) was inferred by Dolan et al. (2014) and revealed that GtmA homologs were found throughout most of the Ascomycetes. It was suggested that the distribution of GtmA homologs in fungi that also synthesise ETP toxins may reflect the regulatory mechanism observed in *A. fumigatus*, however, no investigations were carried out as to why some GT-naïve fungi (e.g. *A. niger*) also contained homologs of this gene (*MT-II* in *A. niger*) (Dolan et al., 2014).

A

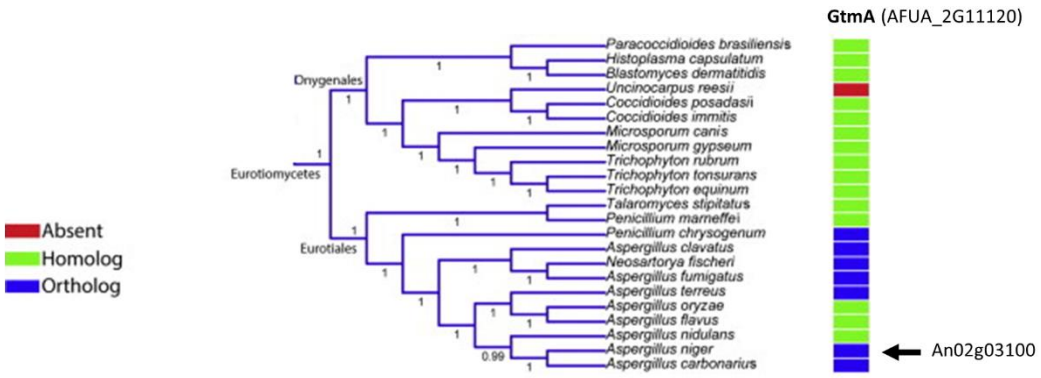

B

```
MT-II  10   YLTPAFVSRYHLAEKLTGVFVAPLVQHSGILSTPSNKPMAVFDNACGLGIVSSYLNSTLP  69
            + T +FV RY   EKLTG++   LV +SG+ +T S KP+ V DNACG+G VSS LN TL
GtmA   11   FQTKSFVDRYKYTEKLTGLYAQTLVDYSGVANT-SQKPLIVLDNACGIGAVSSVLNHTLQ  69

MT-II  70   EDVKRHWTLTCGDITELMVEYTKLRIEREGWVNAEAKVVDAQCTGLPADKYTHVLTAFAF  129
            ++ K+ W LTCGD++E M+E TK R++ EGWVNAE K+V+A  TGLP   YTHV  AF F
GtmA   70   DEAKKTWKLTCGDLSEGMLETTKRRLQDEGWVNAETKIVNALDTGLPDGHYTHVFVAFGF  129

MT-II  130  MMIPDARAAMRECFRILQSGGVLATSTWRNSSWLVIMKEAIETTAWNVKFPTMKEFLALH  189
               PDA AA++ECFRIL SGG+LA+STW+N +W+ IMK AIET   N+ FPT KEF+ALH
GtmA   130  QSFPDANAALKECFRILASGGILASSTWQNFNWIPIMKAAIETIPGNLPFPTQKEFIALH  189

MT-II  190  NEGWGDESFVKARFEEEGFEDVEVTAVQRETSLTISEFMEVGGGMIPIVTGAFWTPEQRE  249
            N GW  ES++++  E+ GF DV+V  V +ETS+ I EF EV   +IP +   FWT EQRE
GtmA   190  NAGWDSESYIQSELEKLGFRDVKVIPVPKETSIPIDEFFEVCMMIIPYLLPKFWTEEQRE  249

MT-II  250  KYEAKAPVVIREYLEEKFGADGVIRMEPVAVLAVGRKP  287
             +E   P+V+R+YL++ +GA+G + +E VA++  G KP
GtmA   250  SHEKDVPMVLRQYLQDTYGANGQVPLEAVALITTGLKP  287
```

Figure 7.3: (A) Phylogenetic tree of GtmA homologs in *Aspergillus spp*. Arrow indicates *A. niger* MT-II ortholog (An02g03100). Figure adapted from Dolan et al. (2014) **(B)** Alignment of the amino acid sequence of *A. niger* MT-II with *A. fumigatus* GtmA (Dolan et al., 2014) using BLASTP. Both sequences shared 53 % identity.

Amino acid sequence comparison of GtmA and MT-II revealed a 53 % shared identity (Figure 7.3) and the presence of a SAM domain characteristic of all SAM dependent methyltransferases. The methylation capacity of MT-II was proven using GT as a substrate for the enzymatic reaction and SAM as a methyl donor source.

Plant and bacterial MTases have shown to methylate reactive thiol metabolites derived from the biosynthesis of antibiotics and glucosinolates as part of their detoxification strategies (Attieh et al., 2000a; Li et al., 2012a; Sengupta et al., 2014). In agreement with these investigations, the increased sensitivity of *A. niger* Δ*MT-II* compared to wild-type established the role MT-II has in protection against GT. Thus, it was concluded that this GT resistance system might represent an ancient mechanism of protection developed by fungi against ETP-producers inhabiting the same environmental niche. Interestingly, Smith et al. (2015) (Elizabeth Smith, Maynooth University, personal communication) have shown that *A. fumigatus* GtmA confers GT resistance on *S. cerevisiae*, and Manzanares-Miralles et al. (2015) revealed that *MT-II* expression in yeast also provided resistance to GT.

Though GT was methylated by MT-II in *A. niger*, a number of questions remain to be answered:

A. Due to the sequential methylation of two different thiol groups in the same GT molecule, and the rapid incorporation of the 1st methyl group, is MT-II primarily a *mono*-methyltransferase?
B. As GT is one of several ETPs found in nature, what is the specificity of MT-II towards other ETPs, compared to GT?

Recently, the potential use of BmGT as a biomarker of Aspergillus infection was investigated (Domingo et al., 2012) which established the utility of fungal natural

products as valuable diagnostic markers. The efficacy of a different fungal natural product (FusC) was evaluated in Chapter 6 through the development of an ELISA test. In this Chapter it was demonstrated that FusC was detected in clinical samples of animal and human origin. Thus the FusC-ELISA represents a promising alternative for the detection fungal infections.

To conclude, the work presented in this thesis provides the first systems biology approach to investigate how a non-GT producer (*A. niger*) responds to the stress agent, GT. This work has revealed that GT dysregulates the *A. niger* methionine cycle (metabolites and proteins) due, partially, to the decrease in SAM levels consequent to MT-II-catalysed BmGT formation. Furthermore, a regulatory crosstalk between several metabolic pathways (sulphur, central carbon, amino acid) and secondary metabolism which can have effects on chromatin regulation, was suggested. Overall, this work has yielded significant insight into the biological impact and practical applications of natural products.

Chapter 8

Bibliography

8 Chapter 8: Bibliography

Aghcheh, R. K., and Kubicek, C. P. (2015). Epigenetics as an emerging tool for improvement of fungal strains used in biotechnology. *Appl. Microbiol. Biotechnol.* doi:10.1007/s00253-015-6763-2.

Aktas, M., and Narberhaus, F. (2009). In vitro characterization of the enzyme properties of the phospholipid N-methyltransferase PmtA from Agrobacterium tumefaciens. *J. Bacteriol.* 191, 2033–41. doi:10.1128/JB.01591-08.

Al-Alawi, A., Ryan, C. F., Flint, J. D., and Müller, N. L. (2005). Aspergillus-related lung disease. *Can. Respir. J.* 12, 377–87. Available at: http://www.ncbi.nlm.nih.gov/pubmed/16307029.

Albrecht, D., Guthke, R., Brakhage, A. a, and Kniemeyer, O. (2010). Integrative analysis of the heat shock response in Aspergillus fumigatus. *BMC Genomics* 11, 32. doi:10.1186/1471-2164-11-32.

Al-Sheikh, H., Watson, A. J., Lacey, G. A., Punt, P. J., MacKenzie, D. A., Jeenes, D. J., et al. (2004). Endoplasmic reticulum stress leads to the selective transcriptional downregulation of the glucoamylase gene in Aspergillus niger. *Mol. Microbiol.* 53, 1731–42. doi:10.1111/j.1365-2958.2004.04236.x.

Amich, J., Schafferer, L., Haas, H., and Krappmann, S. (2013). Regulation of sulphur assimilation is essential for virulence and affects iron homeostasis of the human-pathogenic mould Aspergillus fumigatus. *PLoS Pathog.* 9, e1003573. doi:10.1371/journal.ppat.1003573.

Amitani, R., Taylor, G., Elezis, E. N., Mitchell, J., Cole, P. J., Wilson, R., et al. (1995). Purification and characterization of factors produced by Aspergillus fumigatus which affect human ciliated respiratory epithelium . *Infection and Immunity*. 63 (9): 3266-71.

Andersen, M. R., Nielsen, M. L., and Nielsen, J. (2008). Metabolic model integration of the bibliome, genome, metabolome and reactome of Aspergillus niger. *Mol. Syst. Biol.* 4, 178. doi:10.1038/msb.2008.12.

Andersen, M. R., Salazar, M. P., Schaap, P. J., Van De Vondervoort, P. J. I., Culley, D., Thykaer, J., et al. (2011). Comparative genomics of citric-acid-producing Aspergillus niger ATCC 1015 versus enzyme-producing CBS 513.88. *Genome Res.* 21, 885–897. doi:10.1101/gr.112169.110.

Archer, D. B. (2000). Filamentous fungi as microbial cell factories for food use. *Curr. Opin. Biotechnol.* 11, 478–83.

Asztalos, A., Daniels, M., Sethi, A., Shen, T., Langan, P., Redondo, A., et al. (2012). A coarse-grained model for synergistic action of multiple enzymes on cellulose.

Biotechnol. Biofuels 5, 55. doi:10.1186/1754-6834-5-55.

Attieh, J., Kleppinger-Sparace, K. F., Nunes, C., Sparace, S. a., and Saini, H. S. (2000a). Evidence implicating a novel thiol methyltransferase in the detoxification of glucosinolate hydrolysis products in Brassica oleracea L. *Plant, Cell Environ.* 23, 165–174. doi:10.1046/j.1365-3040.2000.00541.x.

Attieh, J., Sparace, S. A., and Saini, H. S. (2000b). Purification and properties of multiple isoforms of a novel thiol methyltransferase involved in the production of volatile sulfur compounds from Brassica oleracea. *Arch. Biochem. Biophys.* 380, 257–66. doi:10.1006/abbi.2000.1896.

Balibar, C. J., and Walsh, C. T. (2006). GliP, a multimodular nonribosomal peptide synthetase in Aspergillus fumigatus, makes the diketopiperazine scaffold of gliotoxin. *Biochemistry* 45, 15029–38. doi:10.1021/bi061845b.

Balloy, V., and Chignard, M. (2009). The innate immune response to Aspergillus fumigatus. *Microbes Infect.* 11, 919–927. doi:10.1016/j.micinf.2009.07.002.

Barton, R. C. (2013). Laboratory Diagnosis of Invasive Aspergillosis : From Diagnosis to Prediction of Outcome. *Scientifica* 459405. http://dx.doi.org/10.1155/2013/459405.

Basten, D. E., Visser, J., and Schaap, P. J. (2001). Lysine aminopeptidase of Aspergillus niger. *Microbiology* 147, 2045–50. doi:10.1099/00221287-147-8-2045.

Battaglia, E., Benoit, I., van den Brink, J., Wiebenga, A., Coutinho, P. M., Henrissat, B., et al. (2011). Carbohydrate-active enzymes from the zygomycete fungus Rhizopus oryzae: a highly specialized approach to carbohydrate degradation depicted at genome level. *BMC Genomics* 12, 38. doi:10.1186/1471-2164-12-38.

Bauerle, M. R., Schwalm, E. L., and Booker, S. J. (2015). Mechanistic diversity of radical S-adenosylmethionine (SAM)-dependent methylation. *J. Biol. Chem.* 290, 3995–4002. doi:10.1074/jbc.R114.607044.

Bayram, O., Krappmann, S., Ni, M., Bok, J. W., Helmstaedt, K., Valerius, O., et al. (2008). VelB/VeA/LaeA complex coordinates light signal with fungal development and secondary metabolism. *Science* 320, 1504–6. doi:10.1126/science.1155888.

Boente, M. I. P., Kirby, G. W., Patrick, G. L., and Robins, D. J. (1991). Biosynthesis of Hyalodendrin and Didethiobis(methylthio)hyalodendrin, Sulphur-containing 2,5-Dioxopiperazines of the 3S,6S Series. 8, 1283–1290.

Bohle, K., Jungebloud, A., Göcke, Y., Dalpiaz, A., Cordes, C., Horn, H., et al. (2007). Selection of reference genes for normalisation of specific gene quantification data

of Aspergillus niger. *J. Biotechnol.* 132, 353–8. doi:10.1016/j.jbiotec.2007.08.005.

Bok, J. W., and Keller, N. P. (2004). LaeA, a regulator of secondary metabolism in Aspergillus spp. *Eukaryot. Cell* 3, 527–35. doi:10.1128/EC.3.2.527-535.2004.

Bok, J. W., Noordermeer, D., Kale, S. P., and Keller, N. P. (2006). Secondary metabolic gene cluster silencing in Aspergillus nidulans. *Mol. Microbiol.* 61, 1636–45. doi:10.1111/j.1365-2958.2006.05330.x.

Braaksma, M., Martens-Uzunova, E. S., Punt, P. J., and Schaap, P. J. (2010). An inventory of the Aspergillus niger secretome by combining in silico predictions with shotgun proteomics data. *BMC Genomics* 11, 584. doi:10.1186/1471-2164-11-584.

Bradshaw, R. E., Bird, D. M., Brown, S., Gardiner, R. E., and Hirst, P. (2001). Cytochrome c is not essential for viability of the fungus Aspergillus nidulans. *Mol. Genet. Genomics* 266, 48–55.

Brisco, P. R., and Kohlhaw, G. B. (1990). Regulation of yeast LEU2. Total deletion of regulatory gene LEU3 unmasks GCN4-dependent basal level expression of LEU2. *J. Biol. Chem.* 265, 11667–75.

Broekhuijsen, M. P., Mattern, I. E., Contreras, R., Kinghorn, J. R., and van den Hondel, C. A. (1993). Secretion of heterologous proteins by Aspergillus niger: production of active human interleukin-6 in a protease-deficient mutant by KEX2-like processing of a glucoamylase-hIL6 fusion protein. *J. Biotechnol.* 31, 135–45.

Brown, D. W., Yu, J. H., Kelkar, H. S., Fernandes, M., Nesbitt, T. C., Keller, N. P., et al. (1996). Twenty-five coregulated transcripts define a sterigmatocystin gene cluster in Aspergillus nidulans. *Proc. Natl. Acad. Sci. U. S. A.* 93, 1418–22.

Brzywczy, J., Natorff, R., Sieńko, M., and Paszewski, A. (2007). Multiple fungal enzymes possess cysteine synthase activity in vitro. *Res. Microbiol.* 158, 428–36. doi:10.1016/j.resmic.2007.03.002.

Brzywczy, J., Sieńko, M., Kucharska, A., and Paszewski, A. (2002). Sulphur amino acid synthesis in Schizosaccharomyces pombe represents a specific variant of sulphur metabolism in fungi. *Yeast* 19, 29–35. doi:10.1002/yea.798.

Burr, M. L., van den Boomen, D. J. H., Bye, H., Antrobus, R., Wiertz, E. J., and Lehner, P. J. (2013). MHC class I molecules are preferentially ubiquitinated on endoplasmic reticulum luminal residues during HRD1 ubiquitin E3 ligase-mediated dislocation. *Proc. Natl. Acad. Sci. U. S. A.* 110, 14290–5. doi:10.1073/pnas.1303380110.

Cantarel, B. I., Coutinho, P. M., Rancurel, C., Bernard, T., Lombard, V., and Henrissat,

B. (2009). The Carbohydrate-Active EnZymes database (CAZy): An expert resource for glycogenomics. *Nucleic Acids Res.* 37, 233–238. doi:10.1093/nar/gkn663.

Carberry, S., Molloy, E., Hammel, S., O'Keeffe, G., Jones, G. W., Kavanagh, K., et al. (2012). Gliotoxin effects on fungal growth: mechanisms and exploitation. *Fungal Genet. Biol.* 49, 302–12. doi:10.1016/j.fgb.2012.02.003.

Carman, A. J., Vylkova, S., and Lorenz, M. C. (2008). Role of acetyl coenzyme A synthesis and breakdown in alternative carbon source utilization in Candida albicans. *Eukaryot. Cell* 7, 1733–41. doi:10.1128/EC.00253-08.

Carvalho, N. D. S. P., Arentshorst, M., Kooistra, R., Stam, H., Sagt, C. M., van den Hondel, C. a. M. J. J., et al. (2011). Effects of a defective ERAD pathway on growth and heterologous protein production in Aspergillus niger. *Appl. Microbiol. Biotechnol.* 89, 357–373. doi:10.1007/s00253-010-2916-5.

Carvalho, N. D. S. P., Jørgensen, T. R., Arentshorst, M., Nitsche, B. M., van den Hondel, C. a. M. J. J., Archer, D. B., et al. (2012). Genome-wide expression analysis upon constitutive activation of the HacA bZIP transcription factor in Aspergillus niger reveals a coordinated cellular response to counteract ER stress. *BMC Genomics* 13, 350. doi:10.1186/1471-2164-13-350.

Carvalho, P., Goder, V., and Rapoport, T. a. (2006). Distinct Ubiquitin-Ligase Complexes Define Convergent Pathways for the Degradation of ER Proteins. *Cell* 126, 361–373. doi:10.1016/j.cell.2006.05.043.

Chamilos, G., Lewis, R. E., Lamaris, G. a, Albert, N. D., and Kontoyiannis, D. P. (2008). Genomewide screening for genes associated with gliotoxin resistance and sensitivity in Saccharomyces cerevisiae. *Antimicrob. Agents Chemother.* 52, 1325–9. doi:10.1128/AAC.01393-07.

Chang, S.-L., Chiang, Y.-M., Yeh, H.-H., Wu, T.-K., and Wang, C. C. C. (2013). Reconstitution of the early steps of gliotoxin biosynthesis in Aspergillus nidulans reveals the role of the monooxygenase GliC. *Bioorg. Med. Chem. Lett.* 23, 2155–7. doi:10.1016/j.bmcl.2013.01.099.

Chaudhuri, B., Ingavale, S., and Bachhawat, A. K. (1997). apd1+, a gene required for red pigment formation in ade6 mutants of Schizosaccharomyces pombe, encodes an enzyme required for glutathione biosynthesis: a role for glutathione and a glutathione-conjugate pump. *Genetics* 145, 75–83.

Coiner, H., Schröder, G., Wehinger, E., Liu, C.-J., Noel, J. P., Schwab, W., et al. (2006). Methylation of sulfhydryl groups: a new function for a family of small molecule plant O-methyltransferases. *Plant J.* 46, 193–205. doi:10.1111/j.1365-313X.2006.02680.x.

Coleman, J. J., Ghosh, S., Okoli, I., and Mylonakis, E. (2011). Antifungal activity of microbial secondary metabolites. *PLoS One* 6, e25321. doi:10.1371/journal.pone.0025321.

Copping, V. M. S., Barelle, C. J., Hube, B., Gow, N. A. R., Brown, A. J. P., and Odds, F. C. (2005). Exposure of Candida albicans to antifungal agents affects expression of SAP2 and SAP9 secreted proteinase genes. *J. Antimicrob. Chemother.* 55, 645–54. doi:10.1093/jac/dki088.

d'Enfert, C., and Fontaine, T. (1997). Molecular characterization of the Aspergillus nidulans treA gene encoding an acid trehalase required for growth on trehalose. *Mol. Microbiol.* 24, 203–16.

Dagenais, T. R. T., and Keller, N. P. (2009). Pathogenesis of Aspergillus fumigatus in invasive aspergillosis. *Clin. Microbiol. Rev.* 22, 447–465. doi:10.1128/CMR.00055-08.

Damveld, R. a., Arentshorst, M., VanKuyk, P. a., Klis, F. M., Van Den Hondel, C. a M. J. J., and Ram, a. F. J. (2005). Characterisation of CwpA, a putative glycosylphosphatidylinositol-anchored cell wall mannoprotein in the filamentous fungus Aspergillus niger. *Fungal Genet. Biol.* 42, 873–885. doi:10.1016/j.fgb.2005.06.006.

Däschner, K., Couée, I., and Binder, S. (2001). The mitochondrial isovaleryl-coenzyme a dehydrogenase of arabidopsis oxidizes intermediates of leucine and valine catabolism. *Plant Physiol.* 126, 601–12.

Davis, C., Carberry, S., Schrettl, M., Singh, I., Stephens, J. C., Barry, S. M., et al. (2011). The role of glutathione S-transferase GliG in gliotoxin biosynthesis in Aspergillus fumigatus. *Chem. Biol.* 18, 542–52. doi:10.1016/j.chembiol.2010.12.022.

Debeaupuis, J. P., Sarfati, J., Chazalet, V., and Latgé, J. P. (1997). Genetic diversity among clinical and environmental isolates of Aspergillus fumigatus. *Infect. Immun.* 65, 3080–5.

Deng, Y., Srivastava, R., and Howell, S. (2013). Endoplasmic Reticulum (ER) Stress Response and Its Physiological Roles in Plants. *Int. J. Mol. Sci.* 14, 8188–8212. doi:10.3390/ijms14048188.

Dhingra, S., Andes, D., and Calvoa, A. M. (2012). VeA regulates conidiation, gliotoxin production, and protease activity in the opportunistic human pathogen Aspergillus fumigatus. *Eukaryot. Cell* 11, 1531–1543. doi:10.1128/EC.00222-12.

Dolan, S. K., O'Keeffe, G., Jones, G. W., and Doyle, S. (2015). Resistance is not futile: gliotoxin biosynthesis, functionality and utility. *Trends Microbiol.* In Press,

10.1016/j.tim.2015.02.005. doi:10.1016/j.tim.2015.02.005.

Dolan, S. K., Owens, R. A., O'Keeffe, G., Hammel, S., Fitzpatrick, D. A., Jones, G. W., et al. (2014). Regulation of nonribosomal peptide synthesis: bis-thiomethylation attenuates gliotoxin biosynthesis in Aspergillus fumigatus. *Chem. Biol.* 21, 999–1012. doi:10.1016/j.chembiol.2014.07.006.

Domingo, M. P., Colmenarejo, C., Martínez-Lostao, L., Müllbacher, A., Jarne, C., Revillo, M. J., et al. (2012). Bis(methyl)gliotoxin proves to be a more stable and reliable marker for invasive aspergillosis than gliotoxin and suitable for use in diagnosis. *Diagn. Microbiol. Infect. Dis.* 73, 57–64. doi:10.1016/j.diagmicrobio.2012.01.012.

Dorgan, K. M., Wooderchak, W. L., Wynn, D. P., Karschner, E. L., Alfaro, J. F., Cui, Y., et al. (2006). An enzyme-coupled continuous spectrophotometric assay for S-adenosylmethionine-dependent methyltransferases. *Anal. Biochem.* 350, 249–55. doi:10.1016/j.ab.2006.01.004.

Dufresne, S. F., Datta, K., Li, X., Dadachova, E., Staab, J. F., Patterson, T. F., et al. (2012). Detection of urinary excreted fungal galactomannan-like antigens for diagnosis of invasive aspergillosis. *PLoS One* 7, e42736. doi:10.1371/journal.pone.0042736.

Dunlevy, J. D., Soole, K. L., Perkins, M. V, Dennis, E. G., Keyzers, R. A., Kalua, C. M., et al. (2010). Two O-methyltransferases involved in the biosynthesis of methoxypyrazines: grape-derived aroma compounds important to wine flavour. *Plant Mol. Biol.* 74, 77–89. doi:10.1007/s11103-010-9655-y.

Dunn-Coleman, N. S., Bloebaum, P., Berka, R. M., Bodie, E., Robinson, N., Armstrong, G., et al. (1991). Commercial levels of chymosin production by Aspergillus. *Biotechnology. (N. Y).* 9, 976–81.

Duran, R. M., Gregersen, S., Smith, T. D., Bhetariya, P. J., Cary, J. W., Harris-Coward, P. Y., et al. (2014). The role of Aspergillus flavus veA in the production of extracellular proteins during growth on starch substrates. *Appl. Microbiol. Biotechnol.* 98, 5081–94. doi:10.1007/s00253-014-5598-6.

von Eiff, M., Roos, N., Schulten, R., Hesse, M., Zühlsdorf, M., and van de Loo, J. (1995). Pulmonary aspergillosis: early diagnosis improves survival. *Respiration.* 62, 341–7.

Elkins, J. G., Raman, B., and Keller, M. (2010). Engineered microbial systems for enhanced conversion of lignocellulosic biomass. *Curr. Opin. Biotechnol.* 21, 657–62. doi:10.1016/j.copbio.2010.05.008.

Etxebeste, O., Garzia, A., Espeso, E. A., and Ugalde, U. (2010). Aspergillus nidulans asexual development: making the most of cellular modules. *Trends Microbiol.*

18, 569–76. doi:10.1016/j.tim.2010.09.007.

Fahey, R. C. (2013). Glutathione analogs in prokaryotes. *Biochim. Biophys. Acta* 1830, 3182–98. doi:10.1016/j.bbagen.2012.10.006.

Farooqui, J. Z., Tuck, M., and Paik, W. K. (1985). Purification and characterization of enzymes from Euglena gracilis that methylate methionine and arginine residues of cytochrome c. *J. Biol. Chem.* 260, 537–545.

Ferreira de Oliveira, J. M. P., van Passel, M. W. J., Schaap, P. J., and de Graaff, L. H. (2010). Shotgun proteomics of Aspergillus niger microsomes upon D-xylose induction. *Appl. Environ. Microbiol.* 76, 4421–9. doi:10.1128/AEM.00482-10.

Fitzpatrick, J., Kricka, W., James, T. C., and Bond, U. (2014). Expression of three Trichoderma reesei cellulase genes in Saccharomyces pastorianus for the development of a two-step process of hydrolysis and fermentation of cellulose. *J. Appl. Microbiol.* 117, 96–108. doi:10.1111/jam.12494.

Flipphi, M., Sun, J., Robellet, X., Karaffa, L., Fekete, E., Zeng, A.-P., et al. (2009). Biodiversity and evolution of primary carbon metabolism in Aspergillus nidulans and other Aspergillus spp. *Fungal Genet. Biol.* 46, S19–S44. doi:10.1016/j.fgb.2008.07.018.

Flipphi, M., van de Vondervoort, P. J. I., Ruijter, G. J. G., Visser, J., Arst, H. N., and Felenbok, B. (2003). Onset of carbon catabolite repression in Aspergillus nidulans. Parallel involvement of hexokinase and glucokinase in sugar signaling. *J. Biol. Chem.* 278, 11849–57. doi:10.1074/jbc.M209443200.

Fox, E. M., and Howlett, B. J. (2008). Biosynthetic gene clusters for epipolythiodioxopiperazines in filamentous fungi. *Mycol. Res.* 112, 162–9. doi:10.1016/j.mycres.2007.08.017.

Fox, M., Gray, G., Kavanagh, K., Lewis, C., and Doyle, S. (2004). Detection of Aspergillus fumigatus mycotoxins: immunogen synthesis and immunoassay development. *J. Microbiol. Methods* 56, 221–230. doi:10.1016/j.mimet.2003.10.009.

Fraser, C. M., and Chapple, C. (2011). The phenylpropanoid pathway in Arabidopsis. *Arabidopsis Book* 9, e0152. doi:10.1199/tab.0152.

Frisvad, J. C., Rank, C., Nielsen, K. F., and Larsen, T. O. (2009). Metabolomics of Aspergillus fumigatus. *Med. Mycol.* 47 Suppl 1, S53–71. doi:10.1080/13693780802307720.

Fujimoto, H., Sumino, M., Okuyama, E., and Ishibashi, M. (2004). Immunomodulatory Constituents from an Ascomycete, Chaetomium seminudum. *J. Nat. Prod.* 67, 98–102. doi:10.1021/np0302201.

Gallagher, L., Owens, R. A., Dolan, S. K., Keeffe, G. O., Schrettl, M., Kavanagh, K., et al. (2012). The Aspergillus fumigatus Protein GliK Protects against Oxidative Stress and Is Essential for Gliotoxin Biosynthesis. 11, 1226–1238. doi:10.1128/EC.00113-12.

Gan, S. D., and Patel, K. R. (2013). Enzyme immunoassay and enzyme-linked immunosorbent assay. *J. Invest. Dermatol.* 133, e12. doi:10.1038/jid.2013.287.

Ganz, T. (2009). Iron in innate immunity: starve the invaders. *Curr. Opin. Immunol.* 21, 63–7. doi:10.1016/j.coi.2009.01.011.

Gardiner, D. M., Waring, P., and Howlett, B. J. (2005). The epipolythiodioxopiperazine (ETP) class of fungal toxins: Distribution, mode of action, functions and biosynthesis. *Microbiology* 151, 1021–1032. doi:10.1099/mic.0.27847-0.

Gerke, J., Bayram, Ö., and Braus, G. H. (2012). Fungal S-adenosylmethionine synthetase and the control of development and secondary metabolism in Aspergillus nidulans. *Fungal Genet. Biol.* 49, 443–454. doi:10.1016/j.fgb.2012.04.003.

Gonçalves, E., Bucher, J., Ryll, A., Niklas, J., Mauch, K., Klamt, S., et al. (2013). Bridging the layers: towards integration of signal transduction, regulation and metabolism into mathematical models. *Mol. Biosyst.* 9, 1576–83. doi:10.1039/c3mb25489e.

Goto, D. B., and Nakayama, J. (2012). RNA and epigenetic silencing: insight from fission yeast. *Dev. Growth Differ.* 54, 129–41. doi:10.1111/j.1440-169X.2011.01310.x.

Gremel, G., Dorrer, M., and Schmoll, M. (2008). Sulphur metabolism and cellulase gene expression are connected processes in the filamentous fungus Hypocrea jecorina (anamorph Trichoderma reesei). *BMC Microbiol.* 8, 174. doi:10.1186/1471-2180-8-174.

Grüning, N.-M., Lehrach, H., and Ralser, M. (2010). Regulatory crosstalk of the metabolic network. *Trends Biochem. Sci.* 35, 220–7. doi:10.1016/j.tibs.2009.12.001.

Grynberg, M., Piotrowska, M., Pizzinini, E., Turner, G., and Paszewski, A. (2001). The Aspergillus nidulans metE gene is regulated by a second system independent from sulphur metabolite repression. *Biochim. Biophys. Acta - Gene Struct. Expr.* 1519, 78–84. doi:10.1016/S0167-4781(01)00224-X.

Guillemette, T., van Peij, N. N. M. E., Goosen, T., Lanthaler, K., Robson, G. D., van den Hondel, C. a M. J. J., et al. (2007). Genomic analysis of the secretion stress response in the enzyme-producing cell factory Aspergillus niger. *BMC Genomics*

8, 158. doi:10.1186/1471-2164-8-158.

Haraguchi, H., Hamatani, Y., and Hamada, M. (1996). Effect of gliotoxin on growth and branched-chain amino acid biosynthesis in plants. 42, 645–648.

Harris, S. D., Turner, G., Meyer, V., Espeso, E. A., Specht, T., Takeshita, N., et al. (2009). Morphology and development in Aspergillus nidulans: a complex puzzle. *Fungal Genet. Biol.* 46 Suppl 1, S82–S92.

Hartmann, M., Heinrich, G., and Braus, G. H. (2001). Regulative fine-tuning of the two novel DAHP isoenzymes aroFp and aroGp of the filamentous fungus Aspergillus nidulans. *Arch. Microbiol.* 175, 112–121. doi:10.1007/s002030000242.

Hendricks, C. L., Ross, J. R., Pichersky, E., Noel, J. P., and Zhou, Z. S. (2004). An enzyme-coupled colorimetric assay for S-adenosylmethionine-dependent methyltransferases. *Anal. Biochem.* 326, 100–5. doi:10.1016/j.ab.2003.11.014.

Hinnebusch, A. G. (2005). Translational regulation of GCN4 and the general amino acid control of yeast. *Annu. Rev. Microbiol.* 59, 407–50. doi:10.1146/annurev.micro.59.031805.133833.

Hissen, A. H. T., Chow, J. M. T., Pinto, L. J., and Moore, M. M. (2004). Survival of Aspergillus fumigatus in serum involves removal of iron from transferrin: the role of siderophores. *Infect. Immun.* 72, 1402–8.

Hissen, A. H. T., Wan, A. N. C., Warwas, M. L., Pinto, L. J., and Moore, M. M. (2005). The Aspergillus fumigatus siderophore biosynthetic gene sidA, encoding L-ornithine N5-oxygenase, is required for virulence. *Infect. Immun.* 73, 5493–503. doi:10.1128/IAI.73.9.5493-5503.2005.

Hoehamer, C. F., Cummings, E. D., Hilliard, G. M., and Rogers, P. D. (2010). Changes in the proteome of Candida albicans in response to azole, polyene, and echinocandin antifungal agents. *Antimicrob. Agents Chemother.* 54, 1655–64. doi:10.1128/AAC.00756-09.

van den Hombergh, J. P. T. ., van de Vondervoort, P. J. ., Fraissinet-Tachet, L., and Visser, J. (1997). Aspergillus as a host for heterologous protein production: the problem of proteases. *Trends Biotechnol.* 15, 256–263. doi:10.1016/S0167-7799(97)01020-2.

Hope, W. W., Walsh, T. J., and Denning, D. W. (2005). Laboratory diagnosis of invasive aspergillosis. *Lancet Infect. Dis.* 5, 609–622. doi:10.1016/S1473-3099(05)70238-3.

Hotta, K., Keegan, R. M., Ranganathan, S., Fang, M., Bibby, J., Winn, M. D., et al. (2014). Conversion of a disulfide bond into a thioacetal group during

echinomycin biosynthesis. *Angew. Chemie - Int. Ed.* 53, 824–828. doi:10.1002/anie.201307404.

Huyer, G., Piluek, W. F., Fansler, Z., Kreft, S. G., Hochstrasser, M., Brodsky, J. L., et al. (2004). Distinct Machinery Is Required in Saccharomyces cerevisiae for the Endoplasmic Reticulum-associated Degradation of a Multispanning Membrane Protein and a Soluble Luminal Protein. *J. Biol. Chem.* 279, 38369–38378. doi:10.1074/jbc.M402468200.

Hynes, M. J., and Murray, S. L. (2010). ATP-citrate lyase is required for production of cytosolic acetyl coenzyme A and development in Aspergillus nidulans. *Eukaryot. Cell* 9, 1039–1048. doi:10.1128/EC.00080-10.

Irmer, H., Tarazona, S., Sasse, C., Olbermann, P., Loeffler, J., Krappmann, S., et al. (2015). RNAseq analysis of Aspergillus fumigatus in blood reveals a just wait and see resting stage behavior. *BMC Genomics* 16, 640. doi:10.1186/s12864-015-1853-1.

Jakubowski, H. (2006). Pathophysiological consequences of homocysteine excess. *J. Nutr.* 136, 1741S–1749S.

Johansson, M. J. O., and Byström, A. S. (2002). Dual function of the tRNA(m(5)U54)methyltransferase in tRNA maturation. *RNA* 8, 324–335. doi:10.1017/S1355838202027851.

Johnson, G., Ferrini, A., Dolan, S. K., Nolan, T., Agrawal, S., Doyle, S., et al. (2014). Biomarkers for invasive aspergillosis: the challenges continue. *Biomark. Med.* 8, 429–51. doi:10.2217/bmm.13.129.

Kale, S. P., Milde, L., Trapp, M. K., Frisvad, J. C., Keller, N. P., and Bok, J. W. (2008). Requirement of LaeA for secondary metabolism and sclerotial production in Aspergillus flavus. *Fungal Genet. Biol.* 45, 1422–9. doi:10.1016/j.fgb.2008.06.009.

Kanai, M., Masuda, M., Takaoka, Y., Ikeda, H., Masaki, K., Fujii, T., et al. (2013). Adenosine kinase-deficient mutant of Saccharomyces cerevisiae accumulates S-adenosylmethionine because of an enhanced methionine biosynthesis pathway. *Appl. Microbiol. Biotechnol.* 97, 1183–90. doi:10.1007/s00253-012-4261-3.

Karaffa, L., and Kubicek, C. P. (2003). Aspergillus niger citric acid accumulation: do we understand this well working black box? *Appl. Microbiol. Biotechnol.* 61, 189–96. doi:10.1007/s00253-002-1201-7.

Karimi Aghcheh, R., Németh, Z., Atanasova, L., Fekete, E., Paholcsek, M., Sándor, E., et al. (2014). The VELVET A Orthologue VEL1 of Trichoderma reesei Regulates Fungal Development and Is Essential for Cellulase Gene Expression. *PLoS One* 9, e112799. doi:10.1371/journal.pone.0112799.

Karimi-Aghcheh, R., Bok, J. W., Phatale, P. A., Smith, K. M., Baker, S. E., Lichius, A., et al. (2013). Functional Analyses of Trichoderma reesei LAE1 Reveal Conserved and Contrasting Roles of This Regulator. *G3: Genes|Genomes|Genetics* 3, 369–378. doi:10.1534/g3.112.005140.

Kazakov, A. E., Rodionov, D. a., Alm, E., Arkin, A. P., Dubchak, I., and Gelfand, M. S. (2009). Comparative genomics of regulation of fatty acid and branched-chain amino acid utilization in proteobacteria. *J. Bacteriol.* 91, 52–64. doi:10.1128/JB.01175-08.

Kirby, B. G. W., and Sefton, M. a (1980). Biosynthesis of Bisdethiobis(methylthio)gliotoxin, a New Metabolite of Gliocladium delisquescens. 119–121.

Kohlhaw, G. B. (2003). Leucine biosynthesis in fungi: entering metabolism through the back door. *Microbiol. Mol. Biol. Rev.* 67, 1–15.

Korennykh, A., and Walter, P. (2012). Structural basis of the unfolded protein response. *Annu. Rev. Cell Dev. Biol.* 28, 251–77. doi:10.1146/annurev-cellbio-101011-155826.

Krijgsheld, P., Bleichrodt, R., van Veluw, G. J., Wang, F., Müller, W. H., Dijksterhuis, J., et al. (2013). Development in Aspergillus. *Stud. Mycol.* 74, 1–29. doi:10.3114/sim0006.

Krishnan, K., and Askew, D. S. (2014). The fungal UPR. *Virulence* 5, 334–340. doi:10.4161/viru.26571.

Krishnan, K., Feng, X., Powers-Fletcher, M. V., Bick, G., Richie, D. L., Woollett, L. a., et al. (2013). Effects of a Defective Endoplasmic Reticulum-Associated Degradation Pathway on the Stress Response, Virulence, and Antifungal Drug Susceptibility of the Mold Pathogen Aspergillus fumigatus. *Eukaryot. Cell* 12, 512–519. doi:10.1128/EC.00319-12.

Kuang, H., Wang, W., Xu, L., Ma, W., Liu, L., Wang, L., et al. (2013). Monoclonal antibody-based sandwich ELISA for the detection of staphylococcal enterotoxin A. *Int. J. Environ. Res. Public Health* 10, 1598–608. doi:10.3390/ijerph10041598.

Kubicek, C. P. (2013). Systems biological approaches towards understanding cellulase production by Trichoderma reesei. *J. Biotechnol.* 163, 133–142. doi:10.1016/j.jbiotec.2012.05.020.

DE LA HABA, G., and CANTONI, G. L. (1959). The enzymatic synthesis of S-adenosyl-L-homocysteine from adenosine and homocysteine. *J. Biol. Chem.* 234, 603–8.

Lakowski, T. M., and Frankel, A. (2008). A kinetic study of human protein arginine N-methyltransferase 6 reveals a distributive mechanism. *J. Biol. Chem.* 283, 10015–25. doi:10.1074/jbc.M710176200.

Lam, K. C., Ibrahim, R. K., Behdad, B., and Dayanandan, S. (2007). Structure, function, and evolution of plant O-methyltransferases. *Genome* 50, 1001–13. doi:10.1139/g07-077.

Latgé, J. P., Kobayashi, H., Debeaupuis, J. P., Diaquin, M., Sarfati, J., Wieruszeski, J. M., et al. (1994). Chemical and immunological characterization of the extracellular galactomannan of Aspergillus fumigatus. *Infect. Immun.* 62, 5424–33.

Latge, J.-P. (1999). Aspergillus fumigatus and Aspergillosis. *Clin. Microbiol. Rev.* 12, 310–350.

Lee, J., Hao, Y., Blair, P. M., Melby, J. O., Agarwal, V., Burkhart, B. J., et al. (2013). Structural and functional insight into an unexpectedly selective N-methyltransferase involved in plantazolicin biosynthesis. *Proc. Natl. Acad. Sci. U. S. A.* 110, 12954–9. doi:10.1073/pnas.1306101110.

Lee, S. C., Ni, M., Li, W., Shertz, C., and Heitman, J. (2010). The evolution of sex: a perspective from the fungal kingdom. *Microbiol. Mol. Biol. Rev.* 74, 298–340. doi:10.1128/MMBR.00005-10.

Lehmann, P. F., and Reiss, E. (1978). Invasive aspergillosis: antiserum for circulating antigen produced after immunization with serum from infected rabbits. *Infect. Immun.* 20, 570–2.

Lessing, F., Kniemeyer, O., Wozniok, I., Loeffler, J., Kurzai, O., Haertl, A., et al. (2007). The Aspergillus fumigatus transcriptional regulator AfYap1 represents the major regulator for defense against reactive oxygen intermediates but is dispensable for pathogenicity in an intranasal mouse infection model. *Eukaryot. Cell* 6, 2290–302. doi:10.1128/EC.00267-07.

Lewis, R. E., Wiederhold, N. P., Lionakis, M. S., Prince, R. A., and Kontoyiannis, D. P. (2005). Frequency and Species Distribution of Gliotoxin-Producing Aspergillus Isolates Recovered from Patients at a Tertiary-Care Cancer Center. 43, 6120–6122. doi:10.1128/JCM.43.12.6120.

Li, B., Forseth, R. R., Bowers, A. A., Schroeder, F. C., and Walsh, C. T. (2012a). A backup plan for self-protection: S-methylation of holomycin biosynthetic intermediates in Streptomyces clavuligerus. *Chembiochem* 13, 2521–6. doi:10.1002/cbic.201200536.

Li, B., and Walsh, C. T. (2011). Streptomyces clavuligerus HlmI is an intramolecular disulfide-forming dithiol oxidase in holomycin biosynthesis. *Biochemistry* 50,

4615–22. doi:10.1021/bi200321c.

Li, L., Li, D., Luan, Y., Gu, Q., and Zhu, T. (2012b). Cytotoxic metabolites from the antarctic psychrophilic fungus oidiodendron truncatum. *J. Nat. Prod.* 75, 920–927. doi:10.1021/np3000443.

Lin, S. J., Schranz, J., and Teutsch, S. M. (2001). Aspergillosis case-fatality rate: systematic review of the literature. *Clin. Infect. Dis.* 32, 358–66. doi:10.1086/318483.

Liscombe, D. K., Louie, G. V., and Noel, J. P. (2012). Architectures, mechanisms and molecular evolution of natural product methyltransferases. *Nat. Prod. Rep.* 29, 1238. doi:10.1039/c2np20029e.

Ljungdahl, P. O., and Daignan-Fornier, B. (2012). Regulation of amino acid, nucleotide, and phosphate metabolism in Saccharomyces cerevisiae. *Genetics* 190, 885–929. doi:10.1534/genetics.111.133306.

Lo, S., Hamer, L., and Hamer, J. E. (2002). Molecular characterization of a cystathionine β-synthase gene, CBS1 in *Magnaporthe grisea*. *Eukaryot. Cell* 1, 311–314. doi:10.1128/EC.1.2.311.

Lu, X., Sun, J., Nimtz, M., Wissing, J., Zeng, A.-P., and Rinas, U. (2010). The intra- and extracellular proteome of Aspergillus niger growing on defined medium with xylose or maltose as carbon substrate. *Microb. Cell Fact.* 9, 23. doi:10.1186/1475-2859-9-23.

De Lucca, A. J. (2007). Harmful fungi in both agriculture and medicine. *Rev. Iberoam. Micol.* 24, 3–13.

MacKenzie, D., and Guillemette, T. (2005). UPR-independent dithiothreitol stress-induced genes in Aspergillus niger. *Mol. Genet. ...* 274, 410–418. doi:10.1007/s00438-005-0034-3.

Maggio-Hall, L. A., Lyne, P., Wolff, J. A., and Keller, N. P. (2008). A single acyl-CoA dehydrogenase is required for catabolism of isoleucine, valine and short-chain fatty acids in Aspergillus nidulans. *Fungal Genet. Biol.* 45, 180–9. doi:10.1016/j.fgb.2007.06.004.

Malanovic, N., Streith, I., Wolinski, H., Rechberger, G., Kohlwein, S. D., and Tehlivets, O. (2008). S-adenosyl-L-homocysteine hydrolase, key enzyme of methylation metabolism, regulates phosphatidylcholine synthesis and triacylglycerol homeostasis in yeast: implications for homocysteine as a risk factor of atherosclerosis. *J. Biol. Chem.* 283, 23989–99. doi:10.1074/jbc.M800830200.

Malavazi, I., Savoldi, M., Di Mauro, S. M. Z., Menck, C. F. M., Harris, S. D.,

Goldman, M. H. de S., et al. (2006). Transcriptome analysis of Aspergillus nidulans exposed to camptothecin-induced DNA damage. *Eukaryot. Cell* 5, 1688–704. doi:10.1128/EC.00167-06.

Marous, D. R., Lloyd, E. P., Buller, A. R., Moshos, K. A., Grove, T. L., Blaszczyk, A. J., et al. (2015). Consecutive radical S-adenosylmethionine methylations form the ethyl side chain in thienamycin biosynthesis. *Proc. Natl. Acad. Sci. U. S. A.* 112, 10354–8. doi:10.1073/pnas.1508615112.

Marr, K. A., Laverdiere, M., Gugel, A., and Leisenring, W. (2005). Antifungal therapy decreases sensitivity of the Aspergillus galactomannan enzyme immunoassay. *Clin. Infect. Dis.* 40, 1762–9. doi:10.1086/429921.

Martinez, D., Berka, R. M., Henrissat, B., Saloheimo, M., Arvas, M., Baker, S. E., et al. (2008). Genome sequencing and analysis of the biomass-degrading fungus Trichoderma reesei (syn. Hypocrea jecorina). *Nat. Biotechnol.* 26, 553–60. doi:10.1038/nbt1403.

Marty, A. J., Broman, A. T., Zarnowski, R., Dwyer, T. G., Bond, L. M., Lounes-Hadj Sahraoui, A., et al. (2015). Fungal Morphology, Iron Homeostasis, and Lipid Metabolism Regulated by a GATA Transcription Factor in Blastomyces dermatitidis. *PLOS Pathog.* 11, e1004959. doi:10.1371/journal.ppat.1004959.

Marzluf, G. a (1997). Molecular genetics of sulfur assimilation in filamentous fungi and yeast. *Annu. Rev. Microbiol.* 51, 73–96. doi:10.1146/annurev.micro.51.1.73.

Mathieu, M., Nikolaev, I., Scazzocchio, C., and Felenbok, B. (2005). Patterns of nucleosomal organization in the alc regulon of Aspergillus nidulans: Roles of the AlcR transcriptional activator and the CreA global repressor. *Mol. Microbiol.* 56, 535–548. doi:10.1111/j.1365-2958.2005.04559.x.

Mattern, I. E., van Noort, J. M., van den Berg, P., Archer, D. B., Roberts, I. N., and van den Hondel, C. A. (1992). Isolation and characterization of mutants of Aspergillus niger deficient in extracellular proteases. *Mol. Gen. Genet.* 234, 332–6.

McDonagh, A., Fedorova, N. D., Crabtree, J., Yu, Y., Kim, S., Chen, D., et al. (2008). Sub-telomere directed gene expression during initiation of invasive aspergillosis. *PLoS Pathog.* 4, e1000154. doi:10.1371/journal.ppat.1000154.

Mello-de-Sousa, T. M., Rassinger, A., Pucher, M. E., dos Santos Castro, L., Persinoti, G. F., Silva-Rocha, R., et al. (2015). The impact of chromatin remodelling on cellulase expression in Trichoderma reesei. *BMC Genomics* 16, 588. doi:10.1186/s12864-015-1807-7.

Mendoza-Cózatl, D., Loza-Tavera, H., Hernández-Navarro, A., and Moreno-Sánchez, R. (2005). Sulfur assimilation and glutathione metabolism under cadmium stress

in yeast, protists and plants. *FEMS Microbiol. Rev.* 29, 653–671. doi:10.1016/j.femsre.2004.09.004.

Mennink-Kersten, M. A. S. H., Donnelly, J. P., and Verweij, P. E. (2004). Detection of circulating galactomannan for the diagnosis and management of invasive aspergillosis. *Lancet. Infect. Dis.* 4, 349–57. doi:10.1016/S1473-3099(04)01045-X.

Meyer, V., Damveld, R. a., Arentshorst, M., Stahl, U., Van Den Hondel, C. a M. J. J., and Ram, a. F. J. (2007). Survival in the presence of antifungals: Genome-wide expression profiling of aspergillus niger in response to sublethal concentrations of caspofungin and fenpropimorph. *J. Biol. Chem.* 282, 32935–32948. doi:10.1074/jbc.M705856200.

Meyer, V., Fiedler, M., Nitsche, B., and King, R. (2015). The Cell Factory Aspergillus Enters the Big Data Era: Opportunities and Challenges for Optimising Product Formation. *Adv. Biochem. Eng. Biotechnol.* 149, 91–132. doi:10.1007/10_2014_297.

Meyer, V., Wanka, F., van Gent, J., Arentshorst, M., van den Hondel, C. a. M. J. J., and Ram, a. F. J. (2011). Fungal Gene Expression on Demand: an Inducible, Tunable, and Metabolism-Independent Expression System for Aspergillus niger. *Appl. Environ. Microbiol.* 77, 2975–2983. doi:10.1128/AEM.02740-10.

Meyer, V., Wu, B., and Ram, A. F. J. (2010). Aspergillus as a multi-purpose cell factory: current status and perspectives. *Biotechnol. Lett.* 33, 469–476. doi:10.1007/s10529-010-0473-8.

Minic, Z. (2015). Proteomic Studies of the Effects of Different Stress Conditions on Central Carbon Metabolism in Microorganisms. *J. Proteomics Bioinform.* 08, 80–90. doi:10.4172/jpb.1000355.

Mohanram, S., Amat, D., Choudhary, J., Arora, A., and Nain, L. (2013). Novel perspectives for evolving enzyme cocktails for lignocellulose hydrolysis in biorefineries. *Sustain. Chem. Process.* 1, 15. doi:10.1186/2043-7129-1-15.

Mulder, H. J., Saloheimo, M., Penttilä, M., and Madrid, S. M. (2004). The transcription factor HACA mediates the unfolded protein response in Aspergillus niger, and up-regulates its own transcription. *Mol. Genet. Genomics* 271, 130–40. doi:10.1007/s00438-003-0965-5.

Mull, L., Ebbs, M. L., and Bender, J. (2006). A histone methylation-dependent DNA methylation pathway is uniquely impaired by deficiency in Arabidopsis S-adenosylhomocysteine hydrolase. *Genetics* 174, 1161–71. doi:10.1534/genetics.106.063974.

Müllbacher, A., Moreland, A. F., Waring, P., Sjaarda, A., and Eichner, R. D. (1988).

Prevention of graft-versus-host disease by treatment of bone marrow with gliotoxin in fully allogeneic chimeras and their cytotoxic T cell repertoire. *Transplantation* 46, 120–5.

Müllbacher, A., Waring, P., and Eichner, R. D. (1985). Identification of an agent in cultures of Aspergillus fumigatus displaying anti-phagocytic and immunomodulating activity in vitro. *J. Gen. Microbiol.* 131, 1251–8.

Müllbacher, A., Waring, P., Tiwari-Palni, U., and Eichner, R. D. (1986). Structural relationship of epipolythiodioxopiperazines and their immunomodulating activity. *Mol. Immunol.* 23, 231–5.

van Munster, J. M., Daly, P., Delmas, S., Pullan, S. T., Blythe, M. J., Malla, S., et al. (2014). The role of carbon starvation in the induction of enzymes that degrade plant-derived carbohydrates in Aspergillus niger. *Fungal Genet. Biol.* 72, 34–47. doi:10.1016/j.fgb.2014.04.006.

van Munster, J. M., Nitsche, B. M., Akeroyd, M., Dijkhuizen, L., van der Maarel, M. J. E. C., and Ram, A. F. J. (2015). Systems Approaches to Predict the Functions of Glycoside Hydrolases during the Life Cycle of Aspergillus niger Using Developmental Mutants ΔbrlA and ΔflbA. *PLoS One* 10, e0116269. doi:10.1371/journal.pone.0116269.

Natorff, R., Balińska, M., and Paszewski, A. (1993). At least four regulatory genes control sulphur metabolite repression in Aspergillus nidulans. *Mol. Gen. Genet.* 238, 185–92.

Natorff, R., Piotrowska, M., and Paszewski, A. (1998). The Aspergillus nidulans sulphur regulatory gene sconB encodes a protein with WD40 repeats and an F-box. *Mol. Gen. Genet.* 257, 255–63.

Natorff, R., Sieńko, M., Brzywczy, J., and Paszewski, A. (2003). The Aspergillus nidulans metR gene encodes a bZIP protein which activates transcription of sulphur metabolism genes. *Mol. Microbiol.* 49, 1081–1094. doi:10.1046/j.1365-2958.2003.03617.x.

Niide, O., Suzuki, Y., Yoshimaru, T., Inoue, T., Takayama, T., and Ra, C. (2006). Fungal metabolite gliotoxin blocks mast cell activation by a calcium- and superoxide-dependent mechanism: implications for immunosuppressive activities. *Clin. Immunol.* 118, 108–16. doi:10.1016/j.clim.2005.08.012.

Nitsche, B. M., Jørgensen, T. R., Akeroyd, M., Meyer, V., and Ram, A. F. (2012). The carbon starvation response of Aspergillus niger during submerged cultivation: Insights from the transcriptome and secretome. *BMC Genomics* 13, 380. doi:10.1186/1471-2164-13-380.

Nouri, M. A., Al-Halbosiy, M. M. F., Dheeb, B. I., and Hashim, A. J. (2015).

Cytotoxicity and genotoxicity of gliotoxin on human lymphocytes in vitro. *J. King Saud Univ. - Sci.* 27, 193–197. doi:10.1016/j.jksus.2014.12.005.

O'Gorman, C. M., Fuller, H. T., and Dyer, P. S. (2009). Discovery of a sexual cycle in the opportunistic fungal pathogen Aspergillus fumigatus. *Nature* 457, 471–4. doi:10.1038/nature07528.

O'Keeffe, G., Hammel, S., Owens, R. a, Keane, T. M., Fitzpatrick, D. a, Jones, G. W., et al. (2014). RNA-seq reveals the pan-transcriptomic impact of attenuating the gliotoxin self-protection mechanism in Aspergillus fumigatus. *BMC Genomics* 15, 894. doi:10.1186/1471-2164-15-894.

O'Keeffe, G., Jöchl, C., Kavanagh, K., and Doyle, S. (2013). Extensive proteomic remodeling is induced by eukaryotic translation elongation factor 1Bγ deletion in Aspergillus fumigatus. *Protein Sci.* 22, 1612–22. doi:10.1002/pro.2367.

Otzen, C., Bardl, B., Jacobsen, I. D., Nett, M., and Brock, M. (2014). Candida albicans utilizes a modified ??-oxidation pathway for the degradation of toxic propionyl-CoA. *J. Biol. Chem.* 289, 8151–8169. doi:10.1074/jbc.M113.517672.

Owens, R. A., O'Keeffe, G., Smith, E. B., Dolan, S. K., Hammel, S., Sheridan, K. J., et al. (2015). Interplay between Gliotoxin Resistance, Secretion and the Methyl/Methionine Cycle in Aspergillus fumigatus. *Eukaryot. Cell*. doi:10.1128/EC.00055-15.

Paik, W. K., Paik, D. C., and Kim, S. (2007). Historical review: the field of protein methylation. *Trends Biochem. Sci.* 32, 146–52. doi:10.1016/j.tibs.2007.01.006.

Palmer, J. M., Theisen, J. M., Duran, R. M., Grayburn, W. S., Calvo, A. M., and Keller, N. P. (2013). Secondary Metabolism and Development Is Mediated by LlmF Control of VeA Subcellular Localization in Aspergillus nidulans. *PLoS Genet.* 9, e1003193. doi:10.1371/journal.pgen.1003193.

Paoletti, M., Seymour, F. A., Alcocer, M. J. C., Kaur, N., Calvo, A. M., Archer, D. B., et al. (2007). Mating Type and the Genetic Basis of Self-Fertility in the Model Fungus Aspergillus nidulans. *Curr. Biol.* 17, 1384–1389. doi:10.1016/j.cub.2007.07.012.

Park, H.-S., Man Yu, Y., Lee, M.-K., Jae Maeng, P., Chang Kim, S., and Yu, J.-H. (2015). Velvet-mediated repression of β-glucan synthesis in Aspergillus nidulans spores. *Sci. Rep.* 5, 10199. doi:10.1038/srep10199.

Patananan, A. N., Palmer, J. M., Garvey, G. S., Keller, N. P., and Clarke, S. G. (2013). A novel automethylation reaction in the Aspergillus nidulans LaeA protein generates S-methylmethionine. *J. Biol. Chem.* 288, 14032–45. doi:10.1074/jbc.M113.465765.

Patron, N. J., Waller, R. F., Cozijnsen, A. J., Straney, D. C., Gardiner, D. M., Nierman, W. C., et al. (2007). Origin and distribution of epipolythiodioxopiperazine (ETP) gene clusters in filamentous ascomycetes. *BMC Evol. Biol.* 7, 174. doi:10.1186/1471-2148-7-174.

van Peij, N. N. M. ., Gielkens, P. M. ., de Vries, R. P., Visser, J., and Graaff, L. H. De (1998a). The Transcriptional Activator XlnR Regulates Both Xylanolytic and Endoglucanase Gene Expression in Aspergillus niger The Transcriptional Activator XlnR Regulates Both Xylanolytic and Endoglucanase Gene Expression in Aspergillus niger. *Appl. Environ. Microbiol.* 64, 3615–3619.

van Peij, N. N. M. E., Visser, J., and de Graaff, L. H. (1998b). Isolation and analysis of xln R, encoding a transcriptional activator co-ordinating xylanolytic expression in Aspergillus niger. *Mol. Microbiol.* 27, 131–142. doi:10.1046/j.1365-2958.1998.00666.x.

Pel, H. J., de Winde, J. H., Archer, D. B., Dyer, P. S., Hofmann, G., Schaap, P. J., et al. (2007a). Genome sequencing and analysis of the versatile cell factory Aspergillus niger CBS 513.88. *Nat. Biotechnol.* 25, 221–231. doi:10.1038/nbt1282.

Pel, H. J., de Winde, J. H., Archer, D. B., Dyer, P. S., Hofmann, G., Schaap, P. J., et al. (2007b). Genome sequencing and analysis of the versatile cell factory Aspergillus niger CBS 513.88. *Nat. Biotechnol.* 25, 221–31. doi:10.1038/nbt1282.

Perrin, R. M., Fedorova, N. D., Bok, J. W., Cramer, R. A., Wortman, J. R., Kim, H. S., et al. (2007). Transcriptional regulation of chemical diversity in Aspergillus fumigatus by LaeA. *PLoS Pathog.* 3, e50. doi:10.1371/journal.ppat.0030050.

Person, A. K., Chudgar, S. M., Norton, B. L., Tong, B. C., and Stout, J. E. (2010). Aspergillus niger: an unusual cause of invasive pulmonary aspergillosis. *J. Med. Microbiol.* 59, 834–8. doi:10.1099/jmm.0.018309-0.

Petersen, K. L., Lehmbeck, J., and Christensen, T. (1999). A new transcriptional activator for amylase genes in Aspergillus. *Mol. Gen. Genet.* 262, 668–76.

Peth, A., Nathan, J. a., and Goldberg, A. L. (2013). The ATP costs and time required to degrade ubiquitinated proteins by the 26 S proteasome. *J. Biol. Chem.* 288, 29215–29222. doi:10.1074/jbc.M113.482570.

Petrik, M., Haas, H., Dobrozemsky, G., Lass-Flörl, C., Helbok, A., Blatzer, M., et al. (2010). 68Ga-siderophores for PET imaging of invasive pulmonary aspergillosis: proof of principle. *J. Nucl. Med.* 51, 639–45. doi:10.2967/jnumed.109.072462.

Piłsyk, S., Natorff, R., Sieńko, M., Skoneczny, M., Paszewski, A., and Brzywczy, J. (2015). The Aspergillus nidulans metZ gene encodes a transcription factor

involved in regulation of sulfur metabolism in this fungus and other Eurotiales. *Curr. Genet.* 61, 115–125. doi:10.1007/s00294-014-0459-5.

Piotrowska, M., Natorff, R., Paszewski, a, and Paper, O. (2000). *sconC*, a gene involved in the regulation of sulphur metabolism in *Aspergillus nidulans*, belongs to the SKP1 gene family. *Mol. Gen. Genet.* 264, 276–82.

Plaine, A., Walker, L., Da Costa, G., Mora-Montes, H. M., McKinnon, A., Gow, N. a R., et al. (2008). Functional analysis of Candida albicans GPI-anchored proteins: Roles in cell wall integrity and caspofungin sensitivity. *Fungal Genet. Biol.* 45, 1404–1414. doi:10.1016/j.fgb.2008.08.003.

Pócsi, I., Miskei, M., Karányi, Z., Emri, T., Ayoubi, P., Pusztahelyi, T., et al. (2005). Comparison of gene expression signatures of diamide, H2O2 and menadione exposed Aspergillus nidulans cultures--linking genome-wide transcriptional changes to cellular physiology. *BMC Genomics* 6, 182. doi:10.1186/1471-2164-6-182.

Pócsi, I., Prade, R. A., and Penninckx, M. J. (2004). Glutathione, altruistic metabolite in fungi. *Adv. Microb. Physiol.* 49, 1–76. doi:10.1016/S0065-2911(04)49001-8.

Pollegioni, L., Molla, G., Sacchi, S., Rosini, E., Verga, R., and Pilone, M. S. (2008). Properties and applications of microbial D-amino acid oxidases: current state and perspectives. *Appl. Microbiol. Biotechnol.* 78, 1–16. doi:10.1007/s00253-007-1282-4.

Praseuth, A. P., Wang, C. C. C., and Watanabe, K. (2008). Complete sequence of Biosynthetic Gene Cluster Responsible for Producing Triosin A and Evaluation of Quinomycin-Type antibiotics from Streptpmyces triostinicus. 1226–1231. doi:10.1021/bp.34.

Priegnitz, B.-E., Brandt, U., Pahirulzaman, K. A. K., Dickschat, J. S., and Fleißner, A. (2015). The AngFus3 Mitogen-Activated Protein Kinase Controls Hyphal Differentiation and Secondary Metabolism in Aspergillus niger. *Eukaryot. Cell* 14, 602–15. doi:10.1128/EC.00018-15.

Punt, P. J., van Biezen, N., Conesa, A., Albers, A., Mangnus, J., and van den Hondel, C. (2002). Filamentous fungi as cell factories for heterologous protein production. *Trends Biotechnol.* 20, 200–206. doi:10.1016/S0167-7799(02)01933-9.

Punt, P. J., and van den Hondel, C. A. (1992). Transformation of filamentous fungi based on hygromycin B and phleomycin resistance markers. *Methods Enzymol.* 216, 447–57.

Puri, A., Ahmad, A., and Panda, B. P. (2009). Development of an HPTLC-based diagnostic method for invasive aspergillosis. *Biomed. Chromatogr.*, n/a–n/a. doi:10.1002/bmc.1382.

Pusztahelyi, T., Klement, É., Szajli, E., Klem, J., Miskei, M., Karányi, Z., et al. (2011). Comparison of transcriptional and translational changes caused by long-term menadione exposure in Aspergillus nidulans. *Fungal Genet. Biol.* 48, 92–103. doi:10.1016/j.fgb.2010.08.006.

Pusztahelyi, T., Molnár, Z., Emri, T., Klement, E., Miskei, M., Kerékgyárto, J., et al. (2006). Comparative studies of differential expression of chitinolytic enzymes encoded by chiA, chiB, chiC and nagA genes in Aspergillus nidulans. *Folia Microbiol. (Praha).* 51, 547–54.

Ragauskas, A. J., Williams, C. K., Davison, B. H., Britovsek, G., Cairney, J., Eckert, C. A., et al. (2006). The path forward for biofuels and biomaterials. *Science* 311, 484–9. doi:10.1126/science.1114736.

Rahman, I., Kode, A., and Biswas, S. K. (2006). Assay for quantitative determination of glutathione and glutathione disulfide levels using enzymatic recycling method. *Nat. Protoc.* 1, 3159–3165. doi:10.1038/nprot.2006.378.

Ramos, C., and Calderón, I. L. (1994). Biochemical evidence that the Saccharomyces cerevisiae THR4 gene encodes threonine synthetase. *FEBS Lett.* 351, 357–9.

Rapoport, T. A. (2007). Protein translocation across the eukaryotic endoplasmic reticulum and bacterial plasma membranes. *Nature* 450, 663–9. doi:10.1038/nature06384.

Reiser, K., Davis, M. a., and Hynes, M. J. (2010). AoxA is a major peroxisomal long chain fatty acyl-CoA oxidase required for ??-oxidation in A. nidulans. *Curr. Genet.* 56, 139–150. doi:10.1007/s00294-009-0286-2.

Reyes-Dominguez, Y., Bok, J. W., Berger, H., Shwab, E. K., Basheer, a, Gallmetzer, a, et al. (2010). Heterochromatic marks are associated with the repression of secondary metabolism clusters in Aspergillus nidulans. *Mol Microbiol* 76, 1376–1386. doi:10.1111/j.1365-2958.2010.07051.x.

Rhodes, J. C. (2006). Aspergillus fumigatus: growth and virulence. *Med. Mycol.* 44 Suppl 1, S77–81. doi:10.1080/13693780600779419.

Richter, L., Wanka, F., Boecker, S., Storm, D., Kurt, T., Vural, Ö., et al. (2014). Engineering of Aspergillus niger for the production of secondary metabolites. *Fungal Biol. Biotechnol.* 1, 4. doi:10.1186/s40694-014-0004-9.

Rodríguez, J. M., Ruíz-Sala, P., Ugarte, M., and Peñalva, M. Á. (2004). Fungal Metabolic Model for 3-Methylcrotonyl-CoA Carboxylase Deficiency. *J. Biol. Chem.* 279, 4578–4587. doi:10.1074/jbc.M310055200.

Rodriguez, P. L., and Carrasco, L. (1992). Gliotoxin: inhibitor of poliovirus RNA synthesis that blocks the viral RNA polymerase 3Dpol. *J. Virol.* 66, 1971–6.

Roeder, S., Dreschler, K., Wirtz, M., Cristescu, S. M., Van Harren, F. J. M., Hell, R., et al. (2009). SAM levels, gene expression of SAM synthetase, methionine synthase and ACC oxidase, and ethylene emission from N. suaveolens flowers. *Plant Mol. Biol.* 70, 535–546. doi:10.1007/s11103-009-9490-1.

Roehrl, M. H. A., Croft, W. J., Liao, Q., Wang, J. Y., and Kradin, R. L. (2007). Hemorrhagic pulmonary oxalosis secondary to a noninvasive Aspergillus niger fungus ball. *Virchows Arch.* 451, 1067–73. doi:10.1007/s00428-007-0487-3.

Rokas, a., Payne, G., Fedorova, N. D., Baker, S. E., Machida, M., Yu, J., et al. (2007). What can comparative genomics tell us about species concepts in the genus Aspergillus? *Stud. Mycol.* 59, 11–17. doi:10.3114/sim.2007.59.02.

Rokas, A. (2013). Aspergillus. *Curr. Biol.* 23, R187–8. doi:10.1016/j.cub.2013.01.021.

Rouillon, A., Barbey, R., Patton, E. E., Tyers, M., and Thomas, D. (2000). Feedback-regulated degradation of the transcriptional activator Met4 is triggered by the SCFMet30 complex. *EMBO J.* 19, 282–294. doi:10.1093/emboj/19.2.282.

Roze, L. V, Chanda, A., Laivenieks, M., Beaudry, R. M., Artymovich, K. a, Koptina, A. V, et al. (2010). Volatile profiling reveals intracellular metabolic changes in Aspergillus parasiticus: veA regulates branched chain amino acid and ethanol metabolism. *BMC Biochem.* 11, 33. doi:10.1186/1471-2091-11-33.

Ruepp, A., Zollner, A., Maier, D., Albermann, K., Hani, J., Mokrejs, M., et al. (2004). The FunCat, a functional annotation scheme for systematic classification of proteins from whole genomes. *Nucleic Acids Res.* 32, 5539–5545. doi:10.1093/nar/gkh894.

Ruggiano, a., Foresti, O., and Carvalho, P. (2014). Quality control: ER-associated degradation: Protein quality control and beyond. *J. Cell Biol.* 204, 869–879. doi:10.1083/jcb.201312042.

Saint-Macary, M. E., Barbisan, C., Gagey, M. J., Frelin, O., Beffa, R., Lebrun, M. H., et al. (2015). Methionine Biosynthesis is Essential for Infection in the Rice Blast Fungus Magnaporthe oryzae. *PLoS One* 10, e0111108. doi:10.1371/journal.pone.0111108.

Sarikaya Bayram, O., Bayram, O., Valerius, O., Park, H. S., Irniger, S., Gerke, J., et al. (2010). LaeA control of velvet family regulatory proteins for light-dependent development and fungal cell-type specificity. *PLoS Genet.* 6, e1001226. doi:10.1371/journal.pgen.1001226.

Sarikaya-Bayram, Ã., Palmer, J. M., Keller, N., Braus, G. H., and Bayram, Ã. (2015). One Juliet and four Romeos: VeA and its methyltransferases. *Front. Microbiol.* 6, 1–7. doi:10.3389/fmicb.2015.00001.

Sarikaya-Bayram, Ö., Bayram, Ö., Feussner, K., Kim, J.-H., Kim, H.-S., Kaever, A., et al. (2014). Membrane-Bound Methyltransferase Complex VapA-VipC-VapB Guides Epigenetic Control of Fungal Development. *Dev. Cell* 29, 406–420. doi:10.1016/j.devcel.2014.03.020.

Sauter, M., Moffatt, B., Saechao, M. C., Hell, R., and Wirtz, M. (2013). Methionine salvage and S-adenosylmethionine: essential links between sulfur, ethylene and polyamine biosynthesis. *Biochem. J.* 451, 145–54. doi:10.1042/BJ20121744.

Scharf, D. H., Habel, A., Heinekamp, T., Brakhage, A. a, and Hertweck, C. (2014). Opposed Effects of Enzymatic Gliotoxin N- and S-Methylations. *J. Am. Chem. Soc.*, 2–7. doi:10.1021/ja5033106.

Scharf, D. H., Remme, N., Habel, A., Chankhamjon, P., Scherlach, K., Heinekamp, T., et al. (2011). A dedicated glutathione S -transferase mediates carbon-sulfur bond formation in gliotoxin biosynthesis. *J. Am. Chem. Soc.* 133, 12322–12325. doi:10.1021/ja201311d.

Scharf, D. H., Remme, N., Heinekamp, T., Hortschansky, P., Brakhage, A. a, and Hertweck, C. (2010). Transannular disulfide formation in gliotoxin biosynthesis and its role in self-resistance of the human pathogen Aspergillus fumigatus. *J. Am. Chem. Soc.* 132, 10136–41. doi:10.1021/ja103262m.

Schrettl, M., Beckmann, N., Varga, J., Heinekamp, T., Jacobsen, I. D., Jöchl, C., et al. (2010a). HapX-Mediated adaption to iron starvation is crucial for virulence of Aspergillus fumigatus. *PLoS Pathog.* 6. doi:10.1371/journal.ppat.1001124.

Schrettl, M., Bignell, E., Kragl, C., Joechl, C., Rogers, T., Arst, H. N., et al. (2004). Siderophore biosynthesis but not reductive iron assimilation is essential for Aspergillus fumigatus virulence. *J. Exp. Med.* 200, 1213–9. doi:10.1084/jem.20041242.

Schrettl, M., Bignell, E., Kragl, C., Sabiha, Y., Loss, O., Eisendle, M., et al. (2007). Distinct roles for intra- and extracellular siderophores during Aspergillus fumigatus infection. *PLoS Pathog.* 3, 1195–207. doi:10.1371/journal.ppat.0030128.

Schrettl, M., Carberry, S., Kavanagh, K., Haas, H., Jones, G. W., O'Brien, J., et al. (2010b). Self-protection against gliotoxin--a component of the gliotoxin biosynthetic cluster, GliT, completely protects Aspergillus fumigatus against exogenous gliotoxin. *PLoS Pathog.* 6, e1000952. doi:10.1371/journal.ppat.1000952.

Schrettl, M., and Haas, H. (2011). Iron homeostasis--Achilles' heel of Aspergillus fumigatus? *Curr. Opin. Microbiol.* 14, 400–5. doi:10.1016/j.mib.2011.06.002.

Schrettl, M., Ibrahim-Granet, O., Droin, S., Huerre, M., Latgé, J.-P., and Haas, H.

(2010c). The crucial role of the Aspergillus fumigatus siderophore system in interaction with alveolar macrophages. *Microbes Infect.* 12, 1035–41. doi:10.1016/j.micinf.2010.07.005.

Schubert, H. L., Blumenthal, R. M., and Cheng, X. (2003). Many paths to methyltransfer: a chronicle of convergence. *Trends Biochem. Sci.* 28, 329–35. doi:10.1016/S0968-0004(03)00090-2.

Schumacher, J., Simon, A., Cohrs, K. C., Traeger, S., Porquier, A., Dalmais, B., et al. (2015). The VELVET Complex in the Gray Mold Fungus Botrytis cinerea: Impact of BcLAE1 on Differentiation, Secondary Metabolism, and Virulence. *Mol. Plant. Microbe. Interact.* 28, 659–74. doi:10.1094/MPMI-12-14-0411-R.

Schuster, E., Dunn-Coleman, N., Frisvad, J. C., and Van Dijck, P. W. M. (2002). On the safety of Aspergillus niger--a review. *Appl. Microbiol. Biotechnol.* 59, 426–35. doi:10.1007/s00253-002-1032-6.

Seiboth, B., Karimi, R. A., Phatale, P. a., Linke, R., Hartl, L., Sauer, D. G., et al. (2012). The putative protein methyltransferase LAE1 controls cellulase gene expression in Trichoderma reeseimm. *Mol. Microbiol.* 84, 1150–1164. doi:10.1111/j.1365-2958.2012.08083.x.

Sengupta, S., Banerjee, S., Lahiri, S., Dutta, T., Dhar, T. K., and Ghosh, A. K. (2014). Purification, characterization, sequencing and molecular cloning of a novel cysteine methyltransferase that regulates trehalose-6-phosphate synthase from Saccharomyces cerevisiae. *Biochim. Biophys. Acta - Gen. Subj.* 1840, 1861–1871. doi:10.1016/j.bbagen.2014.01.005.

Sewall, T. C., Mims, C. W., and Timberlake, W. E. (1990). abaA controls phialide differentiation in Aspergillus nidulans. *Plant Cell* 2, 731–9. doi:10.1105/tpc.2.8.731.

Sharma, R., Katoch, M., Srivastava, P. S., and Qazi, G. N. (2009). Approaches for refining heterologous protein production in filamentous fungi. *World J. Microbiol. Biotechnol.* 25, 2083–2094. doi:10.1007/s11274-009-0128-x.

Sheridan, K. J., Dolan, S. K., and Doyle, S. (2015). Endogenous cross-talk of fungal metabolites. *Front. Microbiol.* 5, 1–11. doi:10.3389/fmicb.2014.00732.

Shi, L., Li, F., Huang, M., Lu, J., Kong, X., Wang, S., et al. (2012a). Immunoproteomics based identification of thioredoxin reductase GliT and novel Aspergillus fumigatus antigens for serologic diagnosis of invasive aspergillosis. *BMC Microbiol.* 12, 11. doi:10.1186/1471-2180-12-11.

Shi, L., Li, F., Lu, J., Kong, X., Wang, S., Huang, M., et al. (2012b). Antibody specific to thioredoxin reductase as a new biomarker for serodiagnosis of invasive aspergillosis in non-neutropenic patients. *Clin. Chim. Acta* 413, 938–943.

doi:10.1016/j.cca.2012.02.011.

Shoseyov, O., Shani, Z., and Levy, I. (2006). Carbohydrate binding modules: biochemical properties and novel applications. *Microbiol. Mol. Biol. Rev.* 70, 283–95. doi:10.1128/MMBR.00028-05.

Sieńko, M., Natorff, R., Owczarek, S., Olewiecki, I., and Paszewski, A. (2009). Aspergillus nidulans genes encoding reverse transsulfuration enzymes belong to homocysteine regulon. *Curr. Genet.* 55, 561–570. doi:10.1007/s00294-009-0269-3.

Sieńko, M., Natorff, R., Skoneczny, M., Kruszewska, J., Paszewski, A., and Brzywczy, J. (2014). Regulatory mutations affecting sulfur metabolism induce environmental stress response in Aspergillus nidulans. *Fungal Genet. Biol.* 65, 37–47. doi:10.1016/j.fgb.2014.02.001.

Singh, O. V, and Kumar, R. (2007). Biotechnological production of gluconic acid: future implications. *Appl. Microbiol. Biotechnol.* 75, 713–22. doi:10.1007/s00253-007-0851-x.

Sohn, M. J., Yoo, S. J., Oh, D.-B., Kwon, O., Lee, S. Y., Sibirny, A. A., et al. (2014). Novel Cysteine-Centered Sulfur Metabolic Pathway in the Thermotolerant Methylotrophic Yeast Hansenula polymorpha. *PLoS One* 9, e100725. doi:10.1371/journal.pone.0100725.

de Souza, W. R., de Gouvea, P. F., Savoldi, M., Malavazi, I., de Souza Bernardes, L. a, Goldman, M. H. S., et al. (2011). Transcriptome analysis of Aspergillus niger grown on sugarcane bagasse. *Biotechnol. Biofuels* 4, 40. doi:10.1186/1754-6834-4-40.

de Souza, W. R., Maitan-Alfenas, G. P., de Gouvêa, P. F., Brown, N. A., Savoldi, M., Battaglia, E., et al. (2013). The influence of Aspergillus niger transcription factors AraR and XlnR in the gene expression during growth in D-xylose, L-arabinose and steam-exploded sugarcane bagasse. *Fungal Genet. Biol.* 60, 29–45. doi:10.1016/j.fgb.2013.07.007.

Steinbach, W. J. (2013). Are we There Yet? Recent Progress in the Molecular Diagnosis and Novel Antifungal Targeting of Aspergillus fumigatus and Invasive Aspergillosis. *PLoS Pathog.* 9. doi:10.1371/journal.

Strauss, J., and Reyes-Dominguez, Y. (2011). Regulation of secondary metabolism by chromatin structure and epigenetic codes. *Fungal Genet. Biol.* 48, 62–69. doi:10.1016/j.fgb.2010.07.009.

Stynen, D., Goris, A., Sarfati, J., and Latgé, J. P. (1995). A new sensitive sandwich enzyme-linked immunosorbent assay to detect galactofuran in patients with invasive aspergillosis. *J. Clin. Microbiol.* 33, 497–500.

Sugui, J. A., Pardo, J., Chang, Y. C., Zarember, K. A., Nardone, G., Galvez, E. M., et al. (2007). Gliotoxin is a virulence factor of Aspergillus fumigatus: gliP deletion attenuates virulence in mice immunosuppressed with hydrocortisone. *Eukaryot. Cell* 6, 1562–9. doi:10.1128/EC.00141-07.

Sun, X., Tan, Y., Yang, Z., Li, S., and Hoffman, R. M. (2005). A rapid HPLC method for the measurement of ultra-low plasma methionine concentrations applicable to methionine depletion therapy. *Anticancer Res.* 25, 59–62.

Sun, Y., Takada, K., Takemoto, Y., Yoshida, M., Nogi, Y., Okada, S., et al. (2012). Gliotoxin analogues from a marine-derived fungus, Penicillium sp., and their cytotoxic and histone methyltransferase inhibitory activities. *J. Nat. Prod.* 75, 111–4. doi:10.1021/np200740e.

Szilágyi, M., Miskei, M., Karányi, Z., Lenkey, B., Pócsi, I., and Emri, T. (2013). Transcriptome changes initiated by carbon starvation in Aspergillus nidulans. *Microbiology* 159, 176–90. doi:10.1099/mic.0.062935-0.

Taheri-Talesh, N., Horio, T., Araujo-Bazán, L., Dou, X., Espeso, E. A., Peñalva, M. A., et al. (2008). The tip growth apparatus of Aspergillus nidulans. *Mol. Biol. Cell* 19, 1439–49. doi:10.1091/mbc.E07-05-0464.

Takahashi, S., Furukawara, M., Omae, K., Tadokoro, N., Saito, Y., Abe, K., et al. (2014). A Highly Stable D-Amino Acid Oxidase of the Thermophilic Bacterium Rubrobacter xylanophilus. *Appl. Environ. Microbiol.* 80, 7219–29. doi:10.1128/AEM.02193-14.

Talebnia, F., Karakashev, D., and Angelidaki, I. (2010). Production of bioethanol from wheat straw: An overview on pretreatment, hydrolysis and fermentation. *Bioresour. Technol.* 101, 4744–4753. doi:10.1016/j.biortech.2009.11.080.

Tekaia, F., and Latgé, J.-P. (2005). Aspergillus fumigatus: saprophyte or pathogen? *Curr. Opin. Microbiol.* 8, 385–392. doi:10.1016/j.mib.2005.06.017.

Thibault, G., and Ng, D. T. W. (2012). The Endoplasmic Reticulum-Associated Degradation Pathways of Budding Yeast. *Cold Spring Harb. Perspect. Biol.* 4, a013193–a013193. doi:10.1101/cshperspect.a013193.

Thomas, D., Becker, a., and Surdin-Kerjan, Y. (2000). Reverse methionine biosynthesis from S-adenosylmethionine in eukaryotic cells. *J. Biol. Chem.* 275, 40718–40724. doi:10.1074/jbc.M005967200.

Thomas, D., and Surdin-Kerjan, Y. (1997). Metabolism of sulfur amino acids in Saccharomyces cerevisiae. *Microbiol. Mol. Biol. Rev.* 61, 503–32.

Trof, R. J., Beishuizen, A., Debets-Ossenkopp, Y. J., Girbes, A. R. J., and Groeneveld, A. B. J. (2007). Management of invasive pulmonary aspergillosis in non-

neutropenic critically ill patients. *Intensive Care Med.* 33, 1694–703. doi:10.1007/s00134-007-0791-z.

Uthus, E. O. (2003). Simultaneous detection of S-adenosylmethionine and S-adenosylhomocysteine in mouse and rat tissues by capillary electrophoresis. *Electrophoresis* 24, 1221–1226. doi:10.1002/elps.200390157.

Valkonen, M., Ward, M., Wang, H., Penttila, M., and Saloheimo, M. (2003). Improvement of Foreign-Protein Production in Aspergillus niger var. awamori by Constitutive Induction of the Unfolded-Protein Response. *Appl. Environ. Microbiol.* 69, 6979–6986. doi:10.1128/AEM.69.12.6979-6986.2003.

Vashist, S., and Ng, D. T. W. (2004). Misfolded proteins are sorted by a sequential checkpoint mechanism of ER quality control. *J. Cell Biol.* 165, 41–52. doi:10.1083/jcb.200309132.

Vembar, S. S., and Brodsky, J. L. (2008). One step at a time: endoplasmic reticulum-associated degradation. *Nat. Rev. Mol. Cell Biol.* 9, 944–957. doi:10.1038/nrm2546.

Verma, R., Oania, R. S., Kolawa, N. J., and Deshaies, R. J. (2013). Cdc48/p97 promotes degradation of aberrant nascent polypeptides bound to the ribosome. *Elife* 2013, 1–17. doi:10.7554/eLife.00308.

Verweij, P. E., Weemaes, C. M., Curfs, J. H., Bretagne, S., and Meis, J. F. (2000). Failure to detect circulating Aspergillus markers in a patient with chronic granulomatous disease and invasive aspergillosis. *J. Clin. Microbiol.* 38, 3900–1.

Vogt, K., Bhabhra, R., Rhodes, J. C., and Askew, D. S. (2005). Doxycycline-regulated gene expression in the opportunistic fungal pathogen Aspergillus fumigatus. *BMC Microbiol.* 5, 1. doi:10.1186/1471-2180-5-1.

Voit, E. O. (2003). Biochemical and genomic regulation of the trehalose cycle in yeast: review of observations and canonical model analysis. *J. Theor. Biol.* 223, 55–78. doi:10.1016/S0022-5193(03)00072-9.

Vu, B. V., Pham, K. T. M., and Nakayashiki, H. (2013). Substrate-Induced Transcriptional Activation of the MoCel7C Cellulase Gene Is Associated with Methylation of Histone H3 at Lysine 4 in the Rice Blast Fungus Magnaporthe oryzae. *Appl. Environ. Microbiol.* 79, 6823–6832. doi:10.1128/AEM.02082-13.

Wang, D.-N., Toyotome, T., Muraosa, Y., Watanabe, A., Wuren, T., Bunsupa, S., et al. (2014). GliA in Aspergillus fumigatus is required for its tolerance to gliotoxin and affects the amount of extracellular and intracellular gliotoxin. *Med. Mycol.* 52, 506–18. doi:10.1093/mmy/myu007.

Wartenberg, D., Vödisch, M., Kniemeyer, O., Albrecht-Eckardt, D., Scherlach, K., Winkler, R., et al. (2012). Proteome analysis of the farnesol-induced stress response in Aspergillus nidulans--The role of a putative dehydrin. *J. Proteomics* 75, 4038–49. doi:10.1016/j.jprot.2012.05.023.

Watanabe, K., Hotta, K., Praseuth, A. P., Koketsu, K., Migita, A., Boddy, C. N., et al. (2006). Total biosynthesis of antitumor nonribosomal peptides in Escherichia coli. *Nat. Chem. Biol.* 2, 423–8. doi:10.1038/nchembio803.

Welch, T. R., and Williams, R. M. (2014). Epidithiodioxopiperazines. occurrence, synthesis and biogenesis. *Nat. Prod. Rep.* 31, 1376–1404. doi:10.1039/c3np70097f.

Wellen, K. E., Hatzivassiliou, G., Sachdeva, U. M., Bui, T. V, Cross, J. R., and Thompson, C. B. (2009). ATP-citrate lyase links cellular metabolism to histone acetylation. *Science* 324, 1076–1080. doi:10.1126/science.1164097.

Wild, C. P. (2007). Aflatoxin exposure in developing countries: the critical interface of agriculture and health. *Food Nutr. Bull.* 28, S372–80.

Winterberg, B., Du Fall, L. A., Song, X., Pascovici, D., Care, N., Molloy, M., et al. (2014). The necrotrophic effector protein SnTox3 re-programs metabolism and elicits a strong defence response in susceptible wheat leaves. *BMC Plant Biol.* 14, 215. doi:10.1186/s12870-014-0215-5.

Withers, J. M., Swift, R. J., Wiebe, M. G., Robson, G. D., Punt, P. J., van den Hondel, C. A., et al. (1998). Optimization and stability of glucoamylase production by recombinant strains of Aspergillus niger in chemostat culture. *Biotechnol. Bioeng.* 59, 407–18.

Wullschleger, S., Loewith, R., and Hall, M. N. (2006). TOR signaling in growth and metabolism. *Cell* 124, 471–84. doi:10.1016/j.cell.2006.01.016.

Xu, X. M., and Møller, S. G. (2011). Iron-sulfur clusters: biogenesis, molecular mechanisms, and their functional significance. *Antioxid. Redox Signal.* 15, 271–307. doi:10.1089/ars.2010.3259.

Yamashita, N., Sakamoto, K., Yamada, O., Akita, O., and Nishimura, A. (2007). The promoter activity of isovaleryl-CoA dehydrogenase-encoding gene (ivdA) from Aspergillus oryzae is strictly repressed by glutamic acid. *Biosci. Biotechnol. Biochem.* 71, 1561–1563. doi:10.1271/bbb.60712.

Yamazaki, H., Tanaka, A., Kaneko, J., Ohta, A., and Horiuchi, H. (2008). Aspergillus nidulans ChiA is a glycosylphosphatidylinositol (GPI)-anchored chitinase specifically localized at polarized growth sites. *Fungal Genet. Biol.* 45, 963–72. doi:10.1016/j.fgb.2008.02.008.

Yang, Q., Ding, X., Liu, X., Liu, S., Sun, Y., Yu, Z., et al. (2014). Differential proteomic profiling reveals regulatory proteins and novel links between primary metabolism and spinosad production in Saccharopolyspora spinosa. *Microb. Cell Fact.* 13, 27. doi:10.1186/1475-2859-13-27.

Yang, Q., Li, Y., Yang, H., Rang, J., Tang, S., He, L., et al. (2015). Proteomic insights into metabolic adaptation to deletion of metE in Saccharopolyspora spinosa. *Appl. Microbiol. Biotechnol.* 99, 8629–41. doi:10.1007/s00253-015-6883-8.

Ye, Y. (2003). Function of the p97-Ufd1-Npl4 complex in retrotranslocation from the ER to the cytosol: dual recognition of nonubiquitinated polypeptide segments and polyubiquitin chains. *J. Cell Biol.* 162, 71–84. doi:10.1083/jcb.200302169.

Yuan, X. L., Van Der Kaaij, R. M., Van Den Hondel, C. a M. J. J., Punt, P. J., Van Der Maarel, M. J. E. C., Dijkhuizen, L., et al. (2008). Aspergillus niger genome-wide analysis reveals a large number of novel alpha-glucan acting enzymes with unexpected expression profiles. *Mol. Genet. Genomics* 279, 545–561. doi:10.1007/s00438-008-0332-7.

Zhang, W., Li, F., and Nie, L. (2010). Integrating multiple “omics” analysis for microbial biology: application and methodologies. *Microbiology* 156, 287–301. doi:10.1099/mic.0.034793-0.

Zhao, N., Ferrer, J. L., Moon, H. S., Kapteyn, J., Zhuang, X., Hasebe, M., et al. (2012). A SABATH Methyltransferase from the moss Physcomitrella patens catalyzes S-methylation of thiols and has a role in detoxification. *Phytochemistry* 81, 31–41. doi:10.1016/j.phytochem.2012.06.011.

Zheng, C. J., Kim, C. J., Bae, K. S., Kim, Y. H., and Kim, W. G. (2006). Bionectins A-C, epidithiodioxopiperazines with anti-MRSA activity, from Bionectra byssicola F120. *J. Nat. Prod.* 69, 1816–1819. doi:10.1021/np060348t.

Zhou, J. Z., Waszkuc, T., Garbis, S., and Mohammed, F. (2002). Liquid chromatographic determination of S-adenosyl-L-methionine in dietary supplement tablets. *J. AOAC Int.* 85, 901–5.

Znad, H., Markoš, J., and Baleš, V. (2004). Production of gluconic acid from glucose by Aspergillus niger: growth and non-growth conditions. *Process Biochem.* 39, 1341–1345. doi:10.1016/S0032-9592(03)00270-X.

Chapter 9

Appendix I

9 Appendix I

See electronic resource.